Transport and Dispersion of Fluorescent Tracer Particles for the Dune-Bed Condition, Atrisco Feeder Canal near Bernalillo, New Mexico

GEOLOGICAL SURVEY PROFESSIONAL PAPER 1037

Transport and Dispersion of Fluorescent Tracer Particles for the Dune-Bed Condition, Atrisco Feeder Canal near Bernalillo, New Mexico

By R. E. RATHBUN *and* V. C. KENNEDY

GEOLOGICAL SURVEY PROFESSIONAL PAPER 1037

An experimental study of the rates of transport and dispersion of sediment particles of various diameters and specific gravities for a dune-bed condition of alluvial-channel flow

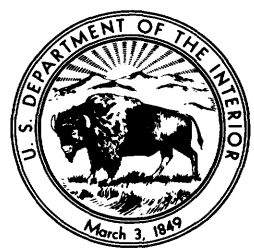

UNITED STATES GOVERNMENT PRINTING OFFICE, WASHINGTON : 1978

UNITED STATES DEPARTMENT OF THE INTERIOR

CECIL D. ANDRUS, *Secretary*

GEOLOGICAL SURVEY

H. William Menard, *Director*

Library of Congress Cataloging in Publication Data
Rathbun, R. E.
Transport and dispersion of fluorescent tracer particles for the dune-bed condition, Atrisco Feeder Canal near Bernalillo, New Mexico.
(Geological Survey Professional Paper 1037)
Bibliography: 78 p.
Supt. of Docs. no.: I 19.16:1037
1. Sediment transport—New Mexico—Atrisco Feeder Canal. 2. Radioisotopes in hydrology.
3. Sediments (Geology)—New Mexico—Atrisco Feeder Canal.
I. Kennedy, Vance Clifford 1923, joint author
II. Title: Transport and dispersion of fluorescent tracer particles for the dune-bed condition...
III. Series: United States Geological Survey Professional Paper 1037.
GB1225.N6R28 551.3'03 77-608063

For sale by the Superintendent of Documents, U.S. Government Printing Office
Washington, D. C. 20402
Stock Number 024-001-03075-6

CONTENTS

ILLUSTRATIONS

TABLES

[Tables 12 -31 and 46 -48 follow "References Cited"]

CONVERSION TABLE

Metric	Multiply by	English
Millimeters (mm)	0.03937	Inches (in).
Meters (m)	3.281	Feet (ft).
Meters per second (m/s)	3.281	Feet per second (ft/s).
Meters per hour (m/h)	3.281	Feet per hour (ft/h).
Meters per day (m/d)	3.281	Feet per day (ft/d).
Square meters (m^2)	10.76	Square feet (ft^2).
Square meters per meter (m^2/m)	3.281	Square feet per foot (ft^2/ft).
Square meters per hour (m^2/h)	10.76	Square feet per hour (ft^2/h).
Cubic meters per second (m^3/s)	35.31	Cubic feet per second (ft^3/s).
Grams per gram (g/g)	.002205	Pounds per gram (lb/g).
Kilograms (kg)	2.205	Pounds (lb).
Kilograms per cubic meter (kg/m^3)	.06250	Pounds per cubic foot (lb/ft^3).
Tonnes per day (t/d)	1.102	Tons per day (tons/d).

SYMBOLS

a Constant in the relation between velocity and median particle diameter, in meters per hour (feet per hour).

A_m Area under the measured longitudinal distribution curve of fluorescent tracers, in gram-meter per gram (pound-foot per pound); i subscript indicates i th sieve class.

A_t Area under the theoretical longitudinal distribution curve of fluorescent tracers which is the value that A_m would have if sampling and analysis procedures were perfect, in gram-meter per gram (pound-foot per pound); i subscript indicates i th sieve class.

b Exponent on median particle diameter in the relation between velocity and diameter.

B Width of the channel, in meters (feet).

C Concentration for a sieve class of fluorescent tracer in a core sample, determined by extrapolating or truncating the vertical tracer distribution to or at the mean depth of mixing, in grams of tracer per gram of total material; i subscript indicates i th sieve class, overbar indicates mean over the width of the channel.

C_b Background concentration, which is the concentration for a sieve class of fluorescent tracer naturally present in the material in transport, in grams of tracer per gram of total material.

C_C Concentration for a sieve class of fluorescent tracer at the centerline of the channel, in grams of tracer per gram of total material.

C_f Final concentration for a sieve class of fluorescent tracer in the study reach at the end of the experiment, in grams of tracer per gram of total material.

C_L Concentration for a sieve class of fluorescent tracer at the left quarter point of the channel, in grams of tracer per gram of total material.

C_0 Maximum concentration of fluorescent tracer of sieve class i for a lateral distribution, in grams of tracer per gram of total material.

$C_r(z)$ Relative concentration for a sieve class of fluorescent tracer at lateral position z, equal to the concentration at z divided by the area under the lateral distribution curve, in meters^{-1} (feet^{-1}).

$C_{r_{MAX}}$ Maximum relative concentration of a lateral distribution of fluorescent tracers, equal to the maximum concentration divided by the area under the lateral distribution curve, in meters^{-1} (feet^{-1}).

C_R Concentration for a sieve class of fluorescent tracer at the right quarter point of the channel, in grams of tracer per gram of total material.

$\overline{C}(t)$ Mean concentration for a sieve class of fluorescent tracer over the width of the channel at time t, in grams of tracer per gram of total material.

C_V Coefficient of variation, equal to the standard deviation divided by the mean, dimensionless.

$C(z,t)$ Concentration for a sieve class of fluorescent tracer at lateral position z at time t, in grams of tracer per gram of total material.

C_1 Concentration for a sieve class of fluorescent tracer in the injected material, in grams of tracer per gram of total injected material.

C_2 Equilibrium concentration for a sieve class of fluorescent tracer which is constant with time and uniform across the channel at the measurement cross section, in grams of tracer per gram of total material in transport.

$\overline{C_2}$ Mean equilibrium concentration for a sieve class of fluorescent tracer over the width of the channel at the measurement cross section, in grams of tracer per gram of total material in transport; i subscript indicates i th sieve class.

$\overline{d}$ Mean value of the centroid depth of the fluorescent tracers in the bed, measured relative to the mean bed-surface elevation, in meters (feet).

d_c Depth of mixing computed by the Crickmore (1967) procedure, in meters (feet).

d_k Distance from the top of the core sample to the center of the k th segment, in meters (feet).

d_m Distance from the top of the core sample to the lowest point in the sample where fluorescent tracers are found, in meters (feet); j subscript indicates j th core sample.

$\overline{d_m}$ Mean value of the depth of mixing of fluorescent tracers in the bed, measured relative to the mean bed-surface elevation, in meters (feet); i subscript indicates i th sieve class.

d_{m_i} Depth of mixing of fluorescent tracers for the i th subsection of the reach, equivalent to the minimum trough elevation for the i th subsection, Sayre and Hubbell (1965) procedure; in meters (feet).

d_{16} Particle diameter for which 16 percent by weight of the size distribution is finer, in millimeters (inches).

d_{50} Median particle diameter, in millimeters (inches).

d_{84} Particle diameter for which 84 percent by weight of the size distribution is finer, in millimeters (inches).

$\overline{D}$ Mean depth of flow, in meters (feet).

D_j Depth of flow at the point of collection of the j th core sample, in meters (feet).

$\overline{H}$ Mean dune height, in meters (feet).

i Indicates the i th sieve class or the i th subsection of the reach.

j Indicates the j th core sample.

k An integer from 1–5 indicating a particular segment of a core sample: 5 indicates the top 0.12-meter-thick (0.4-foot-thick) segment of the sample, 1 indicates the bottom 0.12-meter-thick (0.4-foot-thick) segment of the sample.

k_x Longitudinal dispersion coefficient for bed-material particles where the particles move by a combination of processes including movement along the bed surface, saltation, and suspension, in square meters per hour (square feet per hour).

k_z Lateral dispersion coefficient for bed-material particles where the particles move by a combination of processes including movement along the bed surface, saltation, and suspension, in square meters per hour (square feet per hour).

K_x Longitudinal dispersion coefficient for a dispersant in solution or in suspension, in square meters per hour (square feet per hour).

K_z Lateral dispersion coefficient for a dispersant in solution or in suspension, in square meters per hour (square feet per hour).

l_i Length of the i th subsection of the reach, in meters (feet).

L Length of the study reach, in meters (feet).

m Number of sieve classes.

n Number of core segments sieved.

n_k Number of fluorescent particles of a particular sieve class in the k th segment of a core sample.

n_s Number of subsections in the reach.

N Total number of core samples considered in the determination of the mean values of the depth of mixing and the centroid depth.

N_p Number of fluorescent particles per gram of fluorescent material.

p_i Fraction by weight of sieve class i in the bed material.

Q Water discharge, in cubic meters per second (cubic feet per second).

Q_s Transport rate of bed material load, in tonnes per day (tons per day); i subscript indicates i th sieve class.

Q_T Injection rate of fluorescent tracer plus any associated nontracer material, in kilograms per hour (pounds per hour); i subscript indicates i th sieve class.

$r_1, r_2, r_3,$ Radioactive tracer in segments 1, 2, 3 ..... of a core sample, Crickmore (1967) procedure, in counts per minute.

r_{MAX} Maximum radioactivity in any segment of the core sample, Crickmore (1967) procedure, in counts per minute.

R Ratio of the centroid depth to the depth of mixing, dimensionless.

RR Recovery ratio, equal to the ratio of the tracer actually recovered in the sample collection and analysis procedures to the amount that would be recovered if these procedures were perfect, dimensionless.

t Time, measured from the start of the injection of the fluorescent tracers, in hours or days.

t_1, t_2 Times, measured from the start of the injection of the fluorescent tracers, at which the centroids of the tracer masses are at the longitudinal positions $\bar{x}_1$ and $\bar{x}_2$, respectively; in days.

$\overline{U}$ Mean velocity of flow, in meters per second (feet per second).

U_* Shear velocity, equal to $\sqrt{g\overline{D}\,S}$, where g is the acceleration of gravity, S is the water-surface slope, and $\overline{D}$ is the mean depth of flow; in meters per second (feet per second).

V Velocity of the centroid of the fluorescent tracer mass, in meters per day (feet per day); i subscript indicates the ith sieve class.

V_L Velocity of the leading edge of the fluorescent tracer mass as determined from first arrival time at cross section 90, in meters per day (feet per day).

V_p Velocity of the fluorescent tracer particles, in meters per hour (feet per hour).

w_k Weight of all material in a specific sieve class in the kth segment of a core sample, in grams (pounds).

W Weight of fluorescent tracer injected in the study, in kilograms (pounds); i subscript indicates the ith sieve class.

x Longitudinal distance, measured from the injection point of the fluorescent tracers, in meters (feet).

$\bar{x}$ Longitudinal position of the centroid of the tracer mass, measured from the injection point of the fluorescent tracers, in meters (feet); subscripts 1 and 2 indicate centroid positions at times t_1 and t_2, respectively.

x_B Longitudinal position, measured from the injection point of the fluorescent tracers, at which a significant quantity of tracer reaches the banks of the channel, in meters (feet).

x_U Longitudinal position, measured from the injection point of the fluorescent tracers, at which the tracers become distributed approximately uniformly across the channel, in meters (feet).

y Vertical distance, measured from the mean bed-surface elevation, in meters (feet).

z Lateral distance, measured from the left bank of the channel, in meters (feet).

$\bar{z}$ Mean lateral position or centroid of the lateral distribution of fluorescent materials, measured from the left bank of the channel, in meters (feet).

α Significance level for statistical tests.

Δy Thickness of a core sample segment, Crickmore (1967) procedure, in meters (feet).

Δz Width increment of the channel over which $C(z,t)$ or $C_r(z)$ is assumed to be the concentration of fluorescent tracer, in meters (feet).

γ_s Specific weight of the bed material, in kilograms per cubic meter (pounds per cubic foot).

λ Porosity of the bed or the fraction of the volume of the bed not occupied by the particles, dimensionless.

ν_1 Number of degrees of freedom of the between-classes sum of squares, analysis of variance procedure.

ν_2 Number of degrees of freedom of the within-classes sum of squares, analysis of variance procedure.

σ A measure of the gradation of sediment mixtures, equal to $\frac{1}{2}(d_{84}/d_{50} + d_{50}/d_{16})$.

σ_y Standard deviation of the bed-surface elevation, in meters (feet).

σ_t^2 Variance of a concentration versus time curve, in square hours.

σ_x^2 Variance of a concentration versus distance downstream curve, in square meters (square feet).

σ_z^2 Variance of a concentration versus lateral distance curve, in square meters (square feet).

Σ Indicates summation.

TRANSPORT AND DISPERSION OF FLUORESCENT TRACER PARTICLES FOR THE DUNE-BED CONDITION, ATRISCO FEEDER CANAL NEAR BERNALILLO, NEW MEXICO

By R. E. RATHBUN and V. C. KENNEDY

ABSTRACT

A tracer technique in which mineral particles were coated with fluorescent dyes was used to study the rates of transport and dispersion of sediment particles of various diameters and specific gravities for a dune-bed condition in an alluvial channel. The experiment was conducted in the Atrisco Feeder Canal near Bernalillo, N. Mex., between May 1 and July 14, 1967. A continuous point source of tracers, approximated by injections at 5- or 10-minute intervals, was maintained for 7 days so that the steady-dilution procedure could be used to calculate the transport rate of bed material. After termination of the injection process, the spatial-integration procedure was used to follow the movement of the tracers downstream and to calculate the transport rate. Samples of the bed material in transport and the accompanying tracers moving along the surface of the dune bed were obtained periodically throughout the study with the "dustpan" sampler especially designed for fluorescent tracer studies. In addition, the spatial distributions of the tracers in the dune bed were determined three times during the study by core sampling.

The total transport rate of bed material measured by the steady-dilution procedure was within the range of total transport rates computed by the modified Einstein procedure. Comparisons showed that the measured rates for each of the 0.125- to 0.177-mm, 0.177- to 0.250-mm, and 0.250- to 0.350-mm sieve classes were within the range of computed rates. Measured rates for the larger particles exceeded the computed rates because of the failure to achieve plateau concentrations for these sieve classes. The total transport rate measured by the spatial-integration procedure for the time interval from May 1 to May 8 was within the range of the rates computed by the modified Einstein procedure. Only qualitative comparisons of measured and computed rates were possible for the periods from May 8 to June 6 and from June 6 to July 14. For the period from May 8 to June 6, the comparison was good, but for the June 6 to July 14 period, the spatial-integration result was too small. This discrepancy was attributed to burial of some of the tracers and to transport of large numbers of the small tracer particles beyond the study reach.

Comparison of dispersion parameters for the lateral concentration distributions showed that results from "dustpan" and core samples at the end of the injection period were approximately the same. This comparison suggests that the characteristics of a dune bed can be determined using only samples of the material moving along the bed surface, provided that a continuous tracer source is used and that sufficient time is allowed for vertical mixing to be established.

The variance of the lateral distributions of concentration increased with particle size at a particular cross section, and the rate of change of the variance with distance downstream increased with size, indicating that lateral dispersion increased with increase in particle size.

The variance of the longitudinal distributions of concentration and the rate of change of the variance with time decreased with increase in particle size, indicating that longitudinal dispersion decreased with increase in particle size.

The velocities of the tracer particles decreased with increase in particle size. Velocities of the leading edges of the tracer masses for the small tracer particles varied inversely with the 7.9 power of the fall diameter of the sieve class, whereas velocities for the large particles varied inversely with the 0.86 power of the fall diameter. Velocities of the centroids of the tracer masses varied inversely with the 1.1 power of the fall diameter.

Particle velocities, variances of the concentration distributions, and rates of change of the variances with distance and (or) time were comparable for tracer particles having the same fall diameter but different specific gravities. The smaller tracer particles, which moved predominantly in suspension, appeared to be more nearly hydraulically equivalent than were the large particles, which moved predominantly by surface creep. The scatter in the data, however, precluded any definite conclusions regarding hydraulic equivalence of the tracer particles.

Tracers were found at greater depths in the dune bed than had been expected on the basis of the sizes of the dunes in the channel; further study of the core-sampling procedure and the depth of mixing parameter is needed to explain this anomaly. The depth of mixing enters directly into the computation of the transport rate by the spatial-integration procedure and the areas under the longitudinal distribution curves; however, an incorrect depth of mixing does not affect the other parameters derived from the distributions of concentrations because concentration ratios are involved.

The fluorescent tracer technique is a valuable tool for studying the rates of transport and dispersion of groups of particles for the dune-bed condition of alluvial-channel flow. Improvements in technique are needed, however.

INTRODUCTION

In streams and rivers some pollutants, such as pesticides, herbicides, heavy metals, and radioisotopes, exhibit strong tendencies to absorb on the surface of sediment particles, and other solid pollutants move as sediment particles. In addition, sediment itself is often considered to be a pollutant because of its adverse effect on the use of waterways and on the facilities in and on waterways. To control such pollutants, knowledge of the transport and dispersion characteristics of sediment particles under various conditions is essential.

In 1966 and 1967 the U.S. Geological Survey conducted two field investigations to evaluate a fluorescent tracer technique as a means of determining the

transport and dispersion characteristics of sand-size particles in alluvial streams.

The first investigation was a study of the transport and dispersion of sediment particles of various sizes and specific gravities for a high-velocity flat-bed condition in the Rio Grande conveyance channel near Bernardo, N. Mex., in December 1966. Details and results of that work were described by Rathbun, Kennedy, and Culbertson (1971). The second investigation was a study of the transport and dispersion of sediment particles of various sizes and specific gravities for a low-velocity dune-bed condition. This report describes the procedures and results of this work.

The experiment began on May 1, 1967, and ended July 14, 1967; it was conducted in the Atrisco Feeder Canal near Bernalillo, N. Mex. Four materials of different specific gravity were each coated with a different color of fluorescent dye. The materials and the colors of dye used were quartz, yellow; garnet, green; monazite, red; and lead, blue. Each material contained a range of particle sizes with the quartz particles ranging from 0.125 to 1.00 mm, the garnet and monazite particles from 0.125 to 0.707 mm, and the lead particles ranging from 0.125 to 0.500 mm.

ACKNOWLEDGMENT

The study was the joint effort of U.S. Geological Survey personnel from Denver, Colo., Albuquerque, N. Mex., and Fort Collins, Colo. V. C. Kennedy originated and coordinated the project with the assistance of F. C. Ames. J. K. Culbertson and C. H. Scott, of the Albuquerque, N. Mex., Field Research Unit, provided extensive logistic support for the fieldwork and helped in the supervision of the experiment and in the collection of the data. F. C. Ames, C. F. Nordin, and W. W. Sayre assisted in the supervision of the experiment and helped with the data collection. Personnel from the New Mexico district who assisted with the collection of the data included B. M. Delaney, J. D. Dewey, D. E. Funderburg, V. W. Norman, and David Ortiz. Personnel from Fort Collins, Colo., who assisted with the data collection included J. P. Bennett and W. E. Gaskill. Graduate students from Colorado State University who prepared the fluorescent materials and assisted with the analysis of the samples included N. S. Grigg, C. H. Neuhauser, Ziad Mughrabi, and C. A. Ramirez. Mrs. Lois Niemann and M. R. Karlinger wrote the computer programs used in the analysis of the data and assisted with the data analysis. T. C. Demlow assisted with the data analysis and the preparation of the graphs.

DESIGN OF THE EXPERIMENT

The specific purposes of the experiment were to evaluate the steady-dilution and spatial-integration procedures for calculating the bed-material transport rate and to obtain information on the longitudinal and lateral dispersion characteristics of particles of several specific gravities and various diameters in the sand-size range for a low-velocity dune-bed condition of alluvial-channel flow.

SELECTION OF SITE

The site chosen for the study was a reach of the Atrisco Feeder Canal near Bernalillo, N. Mex. Figure 1 is a location map for the canal. The 880-m (2900-ft) section of the canal indicated in figure 1 was used for the experiment. Figure 2 is a photograph of the study reach, viewed downstream from the point of injection of the fluorescent tracers. Mean width of the canal was about 17 m (55 ft).

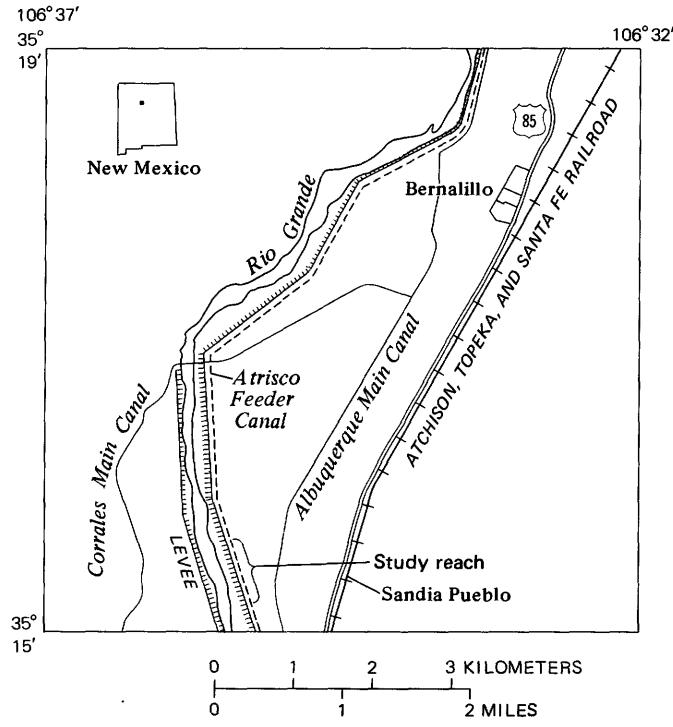

FIGURE 1. — Study area.

TYPE OF INJECTION

A continuous point-source method of injection was chosen for the study. A point injection provides data on the lateral dispersion characteristics of the particles. A continuous injection provides data so that the sediment transport rate can be calculated by the steady-dilution procedure. The steady-dilution equation, which is based on the conservation of mass, is

$$Q_T C_1 + Q_s C_b = (Q_T + Q_s) C_2, \quad (1)$$

FIGURE 2. — Study reach viewed in a downstream direction from the point of injection of the fluorescent tracers.

where Q_T is the injection rate of tracer material plus any associated nontracer material, Q_s is the sediment transport rate, C_1 is the concentration of tracer particles in the injected material, C_b is the background concentration of tracer particles that occurs naturally in the material in transport, and C_2 is the equilibrium concentration of tracer particles which is constant with time and uniform across the channel at the measurement section. The equilibrium concentration is assumed to be the concentration of tracer particles throughout the part of the bed at the measurement section where particles are subject to transport.

Usually, the injected material is totally tracer particles; hence, $C_1 = 1.0$. Also the background concentration, C_b, is generally zero, and Q_T should be negligible with respect to Q_s. With these conditions, equation 1 reduces to

$$Q_T = Q_s C_2, \tag{2}$$

where the concentration, C_2, is expressed as weight of tracer particles per weight of bed material in transport. Figure 3 is a definition sketch of the steady-dilution method according to equation 1.

The injection process should be continued until the concentration at the measurement section, C_2, is independent of time, t, and lateral position in the cross section, z. Because the rate of sediment transport for the dune-bed condition is small, a long time may be necessary for the tracer particles to move far enough downstream to achieve such a uniform concentration. The time required can be shortened by terminating the injection when a concentration distribution that is not varying appreciably with time but is nonuniform laterally is obtained at the measurement section. The equilibrium concentration is then an average of the concentration distribution

$$\bar{C}_2 = \frac{1}{B}\int_0^B C(z)dz, \tag{3}$$

where B is the channel width, and $C(z)$ is the concentration of fluorescent tracer at lateral position z. Inherent in the use of equation 3 is the assumption that the sediment transport rate is relatively constant across the width of the channel.

Equations 1 and 2 are written as applying to the sediment transport process as a whole. However, in general, the size distribution of the tracer material will match only approximately the size distribution of the bed material in transport. Hence, the usual procedure is to break the samples into size classes by sieving, apply equation 2 to each size class, and sum the results to obtain the total sediment transport rate.

After the injection process ends, the spatial-integration procedure can be used to follow the movement of the tracer mass downstream and to calculate the sediment transport rate. The only requirement of the procedure is an instantaneous determination of the spatial distribution of the tracer mass in the study reach at two or more times. An instantaneous determination is assumed to have been obtained provided the change of the position of the centroid of the tracer mass during the sampling period is negligible with respect to the change in centroid position between samplings. Figure 4 is a definition sketch of the spatial-integration method.

The position of the centroid of the tracer mass, $\bar{x}_1$, at time t_1 is given by

$$\bar{x}_1 = \left.\frac{\int_0^\infty \bar{C}\,x\,dx}{\int_0^\infty \bar{C}\,dx}\right|_{t=t_1}, \tag{4}$$

where x is the longitudinal displacement from the injection point, and $\bar{C}$ is the mean tracer concentration at a specific longitudinal position in the part of the bed where particles are subject to transport. The velocity of the centroid, V, is given by the change of the position of the centroid with time

$$V = \frac{\bar{x}_2 - \bar{x}_1}{t_2 - t_1}. \tag{5}$$

The sediment transport rate is given by

$$Q_s = V\bar{d}_m\gamma_s(1-\lambda)B, \tag{6}$$

where γ_s is the specific weight of the bed material, λ is the fraction of the volume of the bed not occupied by the

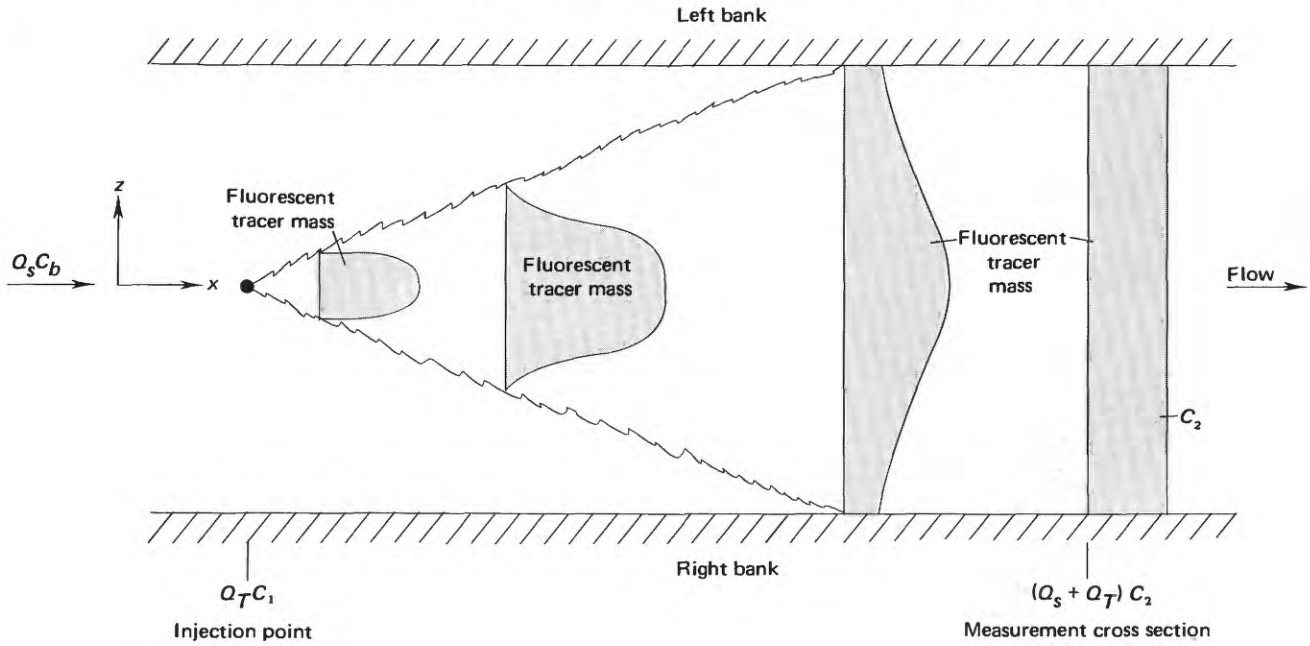

FIGURE 3. — Steady-dilution procedure according to equation 2.

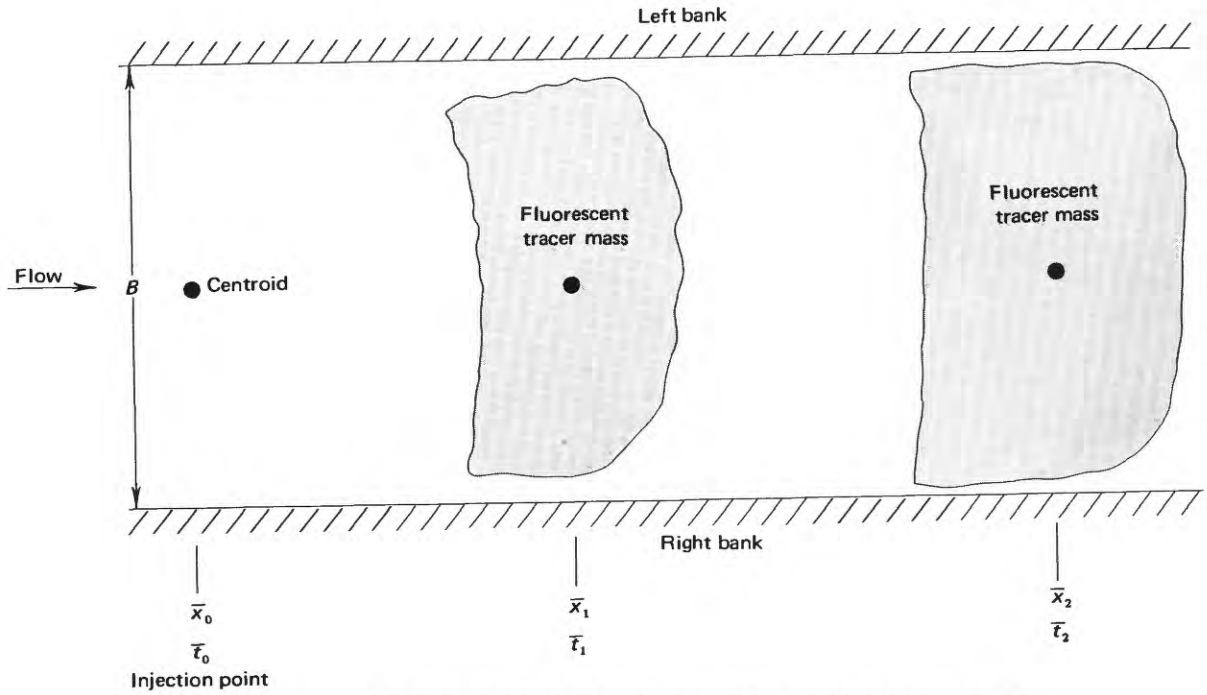

FIGURE 4. — Spatial-integration procedure according to equation 4.

particles, and $\bar{d}_m$ is the mean value of the depth of mixing. The depth of mixing is the mean thickness of the layer of the bed in which the tracer particles are mixed. It can be determined from analysis of sonic depth-sounding records of the bed by the method of Sayre and Hubbell (1965) or from an analysis of core samples.

Equations 4, 5, and 6 in general are applied to each size class of importance, and the results are summed to obtain the total sediment transport rate.

QUANTITY OF FLUORESCENT MATERIAL

The quantity of tracer material injected must be small enough that the natural sediment transport process is not appreciably disturbed; but it also must be large enough that statistically significant numbers of tracer particles are obtained in the samples. The quantity of fluorescent material needed was estimated in two ways — one based on the steady-dilution procedure

and the other based on the spatial-integration procedure.

The tracer injection rate for the steady-dilution experiment was estimated from equation 2. The sediment-transport rate for the Atrisco Feeder Canal was estimated by using the procedure of Colby (1964, fig. 26) and the mean hydraulic conditions and bed material properties observed in the canal by Fischer (1967). For a mean velocity of 0.67 m/s (2.2 ft/s), a mean depth of flow of 0.67 m (2.2 ft), a median bed-material diameter of 0.24 mm, and a mean channel width of 17 m (55 ft), the transport rate was estimated to be 268 t/d (295 tons/d). The temperature correction was small, and therefore, was neglected. Because approximately 30 percent of the bed material was in the 0.250- to 0.350-mm size class, the transport rate for that size class was estimated as 80 t/d (88 tons/d). If the equilibrium tracer concentration, $\overline{C}_2$, is to be on the order of 10^{-3} to 10^{-4}, then the injection rate for the 0.250- to 0.350-mm quartz tracer should be between about 3 and 0.3 kg/h (7 and 0.7 lb/h). The actual injection rate used for the 0.250- to 0.350-mm quartz material was 2.5 kg/h (5.6 lb/h). Injection rates for the other size classes of tracer material were estimated in the same manner.

The quantity of tracer material for the spatial-integration experiment was estimated by assuming that the injected tracer material was uniformly mixed throughout the study reach at the end of the study. Thus, the weight of tracer material, W_i, in sieve class i that must be injected to give a final concentration of C_f is —

$$W_i = LB\overline{d}_m\gamma_s(1-\lambda)C_f p_i, \tag{7}$$

where L is the length of the study reach, and p_i is the fraction by weight of sieve class i in the bed material. For a similar type of channel with similar hydraulic conditions, Sayre and Hubbell (1965) found that $\overline{d}_m$ was approximately 0.46 m (1.5 ft). If $\gamma_s(1-\lambda)$ is assumed to be 1600 kg/m^3 (100 lb/ft^3), L is 880 m (2900 ft), B is 17 m (55 ft), and p_i is 0.3 for the 0.250- to 0.350-mm sieve class, then for a C_f of 10^{-3}, equation 7 becomes W_i = (880)(17)(0.46)(1600)(10^{-3})(0.3) or 3300 kg (7300 lb); for a C_f of 10^{-4}, W_i is 330 kg (730 lb). The actual amount of quartz tracer injected for the 0.250-to 0.350-mm sieve class was 433 kg (955 lb)(table 4).

Because of the wide range of concentrations that can be determined with the fluorescent tracer technique, the estimation of the quantity of tracer to be injected need only be approximate. In the flat-bed study, Rathbun, Kennedy, and Culbertson (1971) found that concentrations for 500- to 800-gram (1.1- to 1.8-pound) samples ranged from about 0.1 to about 1 times 10^{-7}. Concentrations in the middle of this range appear to be the most advantageous from the point of view of ease and accuracy of analysis and economy of tracer materials.

SAMPLING

To define the spatial distribution of the tracer mass in a dune bed, it is necessary to sample to a depth below the mean elevation of the bed surface of at least the depth of movement of the tracers. This is done most conveniently with a piston-type core sampler. A sampler (fig. 5) to take cores of bed material 0.6 m (2.0 ft) in length was designed for this study. The handle of the sampler was scribed to facilitate dividing the core into increments of length as small as 0.03 m (0.1 ft).

FIGURE 5. — Sampler for obtaining cores of bed material 0.6 m (2.0 ft) long. The ruler is 305 mm (12 in) long.

The "dustpan" sampler used in the flat-bed study was also used in the dune-bed study to obtain samples of the material moving along the surface of the bed. Details of the design, construction, and operation of the "dustpan" sampler were presented by Rathbun, Kennedy, and Culbertson (1971).

EXPERIMENTAL PROCEDURE

PREPARATION OF THE FLUORESCENT MATERIALS

The materials for this study were coated with fluorescent dyes by the same procedure used in preparing the

TABLE 1. — *Size distributions of the fluorescent materials as determined by sieve analysis*

Mineral	Specific gravity	Percentage finer than the size (in millimeters) indicated						
		0.125	0.177	0.250	0.350	0.500	0.707	1.00
Quartz	2.64	2.05	12.3	31.8	51.7	81.8	99.0	100
Garnet	4.16	.20	2.56	17.4	59.4	96.2	100	100
Monazite	4.82	6.61	26.2	48.2	67.0	90.7	100	100
Lead flake	10.5	10.0	33.9	69.7	93.2	99.0	100	100
Lead shot	10.5	.18	.92	3.10	51.2	98.9	100	100

tracers for run 2 of the flat-bed study, and a description of the procedure was presented by Rathbun, Kennedy, and Culbertson (1971). The same colors of dye were used for the same minerals as in the flat-bed study — that is, yellow was used for quartz, green for garnet, red for monazite, and blue for lead. The garnet, monazite, and lead shot were obtained from the same sources as those used in the flat-bed study. Lead flakes which were predominantly smaller than 0.350 mm were used in addition to the lead shot which was predominantly larger than 0.250 mm. The quartz material was a composite of three materials: the flint shot and No. 17 silica grades of Ottawa quartz (Ottawa Silica Co., Ottawa, Ill.)[1] and a 0.19 mm sand used by Simons and Richardson (1966) and by Guy, Simons, and Richardson (1966). The Ottawa sands were clean well-rounded quartz particles and contained virtually no heavy minerals. The 0.19 mm sand was pure quartz sand from a decomposed sandstone deposit near Denver, Colo. The sandstone was run through a hammermill to break up large particles and washed to remove the clay binder (Guy, Simons, and Richardson, 1966). The three varieties of quartz were necessary to cover the range of particle sizes in the bed material of the Atrisco Feeder Canal.

The size distributions of the fluorescent materials were determined by sieving and are presented in table 1. The quartz distribution is for a sample consisting of 42.7 percent No. 17 silica, 33.0 percent 0.19 mm quartz, and 24.3 percent flint quartz by weight. These percentages are the proportions in which the three types of quartz were injected into the canal (table 3). Specific gravities of the coated materials were 2.64, 4.16, 4.82, and 10.5 for quartz, garnet, monazite, and lead, respectively.

The median fall diameter of the particles within each $\sqrt{2}$ sieve class for both the fluorescent materials and bed material from the canal was determined either by dropping single particles in a column of quiescent distilled water or by the visual accumulation-tube method (U.S. Inter-Agency Committee on Water Resources, 1957a). The visual accumulation-tube method was used to analyze the materials smaller than 0.350 mm, with the exception of the lead which was analyzed by the single-particle method. Fall velocities obtained from the single-particle method were converted to median fall diameters by means of table 2 of the U.S. Inter-Agency Committee on Water Resources (1957b). The median fall diameters are summarized in table 2.

TABLE 2. — *Median fall diameters of fluorescent materials and bed material for various sieve classes*

[Leaders (. . .) indicate no data available]

	Sieve class (mm)	Median fall diameter (mm)					
		Bed material	Quartz	Garnet	Monazite	Lead flake	Lead shot
(1)	0.125–0.177	. . . 0.159	0.144	0.228	0.250	0.392	. . .
(2)	0.177–0.250	207	.196	.304	.310	.522	0.772
(3)	0.250–0.350	286	.295	.395	.460	.722	1.16
(4)	0.350–0.500	386	.430	.506	.615	.868	1.30
(5)	0.500–0.707	506	.539	.584	.810	. . .	. . .
(6)	0.707–1.00	646	.728	. . .	. . .	. . .	. . .

The fall diameters presented in table 2 show the effect of shape and specific gravity on fall diameter. Fall diameters for the three size classes of lead shot are 48, 61, and 50 percent larger than fall diameters for lead flakes of the same sieve diameter. The effect of specific gravity on fall diameter is shown by the fact that the fall diameters for garnet, monazite, and lead tracer particles are, in general, larger than the sieve diameters.

Photomicrographs of one sieve class each of Ottawa quartz, garnet, monazite, and lead shot were presented by Rathbun, Kennedy, and Culbertson (1971), and a photograph of the 0.19 mm quartz was presented by Guy, Simons, and Richardson (1966). These photographs show the general shapes of the tracer materials used in the dune-bed study.

INJECTION OF THE FLUORESCENT MATERIALS

A continuous point-source method of injection was used. The point of injection was the centerline of the canal at the upstream end of the study reach. A continuous injection was approximated by a series of injections at discrete intervals of time.

To facilitate the injection at the centerline of the canal, a wooden walkway was constructed from the bank out over the water. The walkway was supported on a boat tied to the bank of the canal. An injection tube was attached to the end of the walkway so that the bottom of the tube was about 0.15 m (0.5 ft) above the bed

[1] The use of any brand or company name in this report is for identification purposes only and does not imply endorsement by the U.S. Geological Survey.

FIGURE 6. — Walkway and injection tube used for injecting the fluorescent tracers at the center of the channel.

surface. Figure 6 is a photograph of the walkway and the injection tube. The tube had a 0.1-m (4-in) inside diameter and the top was expanded to a diameter of about 0.3 m (12 in) to form a funnel. A water slurry of the appropriate quantities of each of the fluorescent materials (table 3) was prepared, and a small quantity of detergent was added to counteract the nonwetting property of the fluorescent coating. The nonwetting property of the fluorescent coatings was discussed by Rathbun, Kennedy, and Culbertson (1971). This slurry was washed down the injection tube with a stream of water from a garden-type pressure sprayer.

TABLE 3. — *Injection rates and total quantities injected for the various fluorescent materials*

Mineral	Injection rate (kg/h)	Total injected (kg)
Flint quartz	3.12	529
No. 17 silica quartz .	5.49	928
0.19-mm quartz	4.22	717
Garnet	3.35	568
Monazite	3.12	530
Lead shot	.599	102
Lead flake	1.25	213
Total	21.1	3587

Approximately 2 kg (4 lb) of a mixture of the tracer materials were injected at 5-minute intervals beginning at 1320 hours on May 1, 1967. This procedure was continued until 0200 hours on May 3, 1967, when a schedule of about 4 kg (8 lb) of tracer material at 10-minute intervals was begun. Injection was stopped at 1500 hours on May 8, 1967. The injection rates and the total quantities injected for the various fluorescent materials are summarized in table 3 and the breakdown by sieve class of the quantities of each mineral injected is summarized in table 4.

TABLE 4. — *Total quantities of fluorescent materials injected for each sieve class*

[Leaders (. . .) indicate no data available]

	Sieve class (mm)	Quantity injected (kg)			
		Quartz	Garnet	Monazite	Lead
(1)	0.125 – 0.177	222	13.4	104	51.7
(2)	0.177 – 0.250	424	84.4	116	78.5
(3)	0.250 – 0.350	433	239	99.8	98.9
(4)	0.350 – 0.500	655	209	125	60.8
(5)	0.500 – 0.707	374	21.3	47.2	...
(6)	0.707 – 1.00	21.0	...	...	...
	Total	2129	567	492	290

The totals in table 4 are slightly less than the totals in table 3 because of the presence of small quantities of material in the ends of the size distributions, that is, larger than 1.00 mm and smaller than 0.125 mm. Particles smaller than 0.125 mm were not considered in the analysis of the samples because of the difficulty of distinguishing between actual fluorescent particles and chips or flakes of dye from large particles.

SAMPLING PROCEDURE

Sampling with "dustpan" samplers was begun at cross sections 90 and 180 just prior to the start of the injection of the fluorescent materials to obtain background samples. The numbers used to designate cross sections in this report are the distances, in meters, downstream from the point of injection of the fluorescent tracers. These samples were used to check the bed material in the study reach for naturally fluorescent materials which might be mistaken for fluorescent tracers. The "dustpan" sampler, which was designed primarily for the flat-bed condition (Rathbun and others, 1971), was found to work satisfactorily for the dune-bed condition with two qualifications. First, a longer sampling period was necessary because of the much slower rates of sediment movement for the dune-bed condition. Second, the person sampling had to be careful not to push or dig the sampler into the soft surface of the dune because the "dustpan" sampler is designed for sampling only the material moving along the surface of the bed. The length of time required to obtain a sample large enough for analysis varied, depending upon position on the dune form. In general, a 2- to 5-minute sampling period was required to obtain a 0.1- to 0.3-kg (0.2- to 0.7-lb) sample.

After the start of the injection, "dustpan" samples were obtained at 1.5-m (5-ft) intervals across the channel at cross sections 90 and 180 at approximately 15-

minute intervals for 1 hour, then at 6-hour intervals for the remainder of the injection period. When the 6-hour interval sampling was started, sampling at 1.5-m (5-ft) intervals across the channel at cross section 360 was started. On the final day of injection (May 8), "dustpan" samples were obtained at 1.5-m (5-ft) intervals across the channel at cross sections 15, 60, 270, 450, and 540; in addition, samples were obtained at the 0.75-m (2.5-ft) interval points across the center third of the channel for cross section 15. Following the completion of the injection of the tracers, "dustpan" samples were obtained, all at 1.5-m (5-ft) intervals across the channel, at cross sections 90, 360, and 540 on May 9 and at cross sections 90, 180, 360, and 540 on May 11, 13, 15, 19, 23, and 26. The procedure for sampling with the "dustpan" sampler was described by Rathbun, Kennedy, and Culbertson (1971).

Core samples 0.6 m (2 ft) in length were collected with the sampler shown in figure 5. The sampling procedure consisted of placing the sampler on the bed surface, determining the depth of flow at the sample point from calibration markings on the sampler, pushing the barrel of the sampler into the bed as the piston was held stationary with respect to the bed, lifting the core from the bed, and extruding the core from the sampler in 0.12 m (0.4-ft) long segments. Each segment was placed in an appropriately marked sample bag with the segments numbered from bottom (No. 1) to top (No. 5). Figure 7 is a photograph of the core-sampling process.

FIGURE 7. — Core-sampling to determine the distribution of fluorescent tracers in the study reach.

Core samples were obtained at various positions in the study reach on May 2, 3, and 5. These samples and the "dustpan" samples were inspected under an ultraviolet light in a closed trailer at the field site to estimate qualitatively how the tracer particles were distributed. This information was used to determine when to terminate the injection of the tracer material. It was also used in the design of the sampling grid for determining the spatial distribution of the tracers in the study reach at the conclusion of the injection process on May 8. Core samples to define the spatial distributions of the tracers within the study reach were obtained also on June 6 and July 14.

Core samples were collected at the following locations in the study reach:

May 8:
(a) At the centerline of the channel at cross sections 1.5, 3, 4.5, 6, 7.5, 15, 22.5, 30, 45, 60, and 75.
(b) At 30-m (100-ft) intervals along the centerline of the channel from cross section 90 through cross section 600.
(c) At 1.5-m (5-ft) intervals across the channel at cross sections 15, 30, 60, 90, 180, 270, 360, 450, and 540; also at 0.75-m (2.5-ft) intervals across the center half of the channel at cross section 7.5.

June 6: At 30-m (100-ft) intervals along the centerline, left, and right quarter points of the channel from cross section 30 through 870.

July 14: At 60-m (200-ft) intervals along the centerline, left, and right quarter points of the channel from cross section 30 through 870.

ANALYSIS OF THE SAMPLES

The "dustpan" and core samples were analyzed for fluorescent tracers by the same procedure used in the study of the flat-bed condition, and details of the procedure were presented by Rathbun, Kennedy, and Culbertson (1971). Briefly, the procedure consisted of drying the sample, sieving the sample into the various sieve classes, counting a specific number of fluorescent particles of each color in a split of each sieve class, and converting the number of fluorescent particles to concentrations. The concentration of a fluorescent tracer is the ratio of the weight of tracer material in a given sieve class to the total weight of all material in that sieve class of the sample.

The number of fluorescent particles of each color in each sieve class was converted to a weight by dividing by the appropriate number of fluorescent particles per gram of fluorescent material, which was determined by the same procedure as was used for the flat-bed study. (See Rathbun and others, 1971.) The conversion factors are presented in table 5.

Differences between the values in table 5 and the values for the flat-bed study (Rathbun and others,

TABLE 5. — *Number of fluorescent particles per gram of fluorescent material*

[Leaders (. . .) indicate no data available]

Sieve class (mm)	Particles per gram			
	Quartz	Garnet	Monazite	Lead
0.125 – 0.177	133 000	73 500	76 300	26 200
0.177 – 0.250	55 600	29 600	32 000	11 500
0.250 – 0.350	19 100	11 900	9 930	5 110
0.350 – 0.500	6 770	5 470	3 290	2 910
0.500 – 0.707	2 760	3 370	1 740	. . .
0.707 – 1.00	1 300	. . .	. . .	. . .

1971, table 6) are large for some size classes. The differences for the quartz and lead are not unexpected because different types or combinations of materials were used in the two studies. The differences for the garnet were not great; however, the differences for the monazite were not expected because the same source material was used in both studies. These differences may have been the result of errors in the counting and weighing process. However, a comparison of the replicate counts for each sieve class, where large differences occurred, showed that in general all replicate counts for this study were outside the range of replicate counts for the flat-bed study, indicating that the differences were real. Apparently, either the source materials must have actually been different for the two studies or the samples of the pure fluorescent materials that were analyzed were not representative of the whole. The latter condition is a distinct possibility in the dune-bed study because the sample analyzed consisted of a composite of a small grab sample from each 45-kg (100-lb) batch of fluorescent material prepared.

Possible errors in the particles per gram factors, however, will affect the results of only part of the experiment for the following reason. In the calculation of the means and variances of the lateral and longitudinal distributions, the data are normalized by dividing by the area under the curve. Hence, because the concentration appears in both the numerator and the denominator, the particles per gram factor cancels. The only place where an error would result because of an incorrect particles per gram factor is in the calculation of the sediment transport rate by the steady dilution procedure (eq 2). Here, a concentration, C_2, appears by itself rather than in a ratio. Only the quartz tracers are used for the calculation of the sediment transport rate, and it is assumed that heavy minerals constitute an insignificant fraction of the material in transport.

Ideally, the relative number of particles per gram for a particular sieve class should be inversely proportional to the specific gravity. In reality, the particle counts are also affected by the shape of the particles and the distribution of particle sizes within a sieve class. The quartz particles generally had a higher sphericity than the garnet and monazite particles and, hence, would be expected to have fewer particles per gram if specific gravity and size distribution were the same. At the extremes of the size distributions of the minerals, the size distribution within the sieve classes may by highly asymmetric, thus giving higher or lower particle counts than would be expected for these sieve classes. The fact that the 0.500- to 0.707-mm size class of garnet has more particles per gram than the lighter quartz of the same sieve size demonstrates the effects of particle shape and the asymmetry of the size distribution within the sieve class on the number of particles per gram. A similar situation occurs for the 0.125- to 0.177-mm and the 0.177- to 0.250-mm sieve classes of garnet and monazite.

PRESENTATION AND DISCUSSION OF RESULTS

The basic information obtained in this study consisted of hydraulic and sediment data for the reach, fluorescent tracer concentrations as a function of time from "dustpan" samples at cross section 90, lateral distributions of the fluorescent tracers on May 8 from core samples and "dustpan" samples, and longitudinal distributions of the fluorescent tracers on May 8, June 6, and July 14, 1967, from core samples.

HYDRAULIC AND SEDIMENT MEASUREMENTS

Hydraulic and sediment data were collected a number of times during the study. The hydraulic data which included water-surface slope, water temperature, and water-discharge measurements at cross section 180 are presented in table 6. Also shown in table 6 for five dates is a mean depth of flow for the study reach determined during core sampling for fluorescent materials. During the period of injection of the tracers (May 1–8), the water discharge ranged from 7.82 to 10.6 m^3/s (276 to 373 ft^3/s) and averaged 8.81 m^3/s (311 ft^3/s). During the period from May 9 to July 14, the discharge was measured only on May 16 and discharges for the other dates were estimated from the stage-discharge relation for the canal (table 6). In general, the discharge decreased with time and reached a minimum of 5.30 m^3/s (187 ft^3/s) on July 14. The water temperature showed a diurnal variation and ranged from 11° or 12° during the early morning hours to 16° or 17°C during the afternoon hours of the period May 1 to 8. Mid-day water temperatures, in general, increased with time (table 6).

In addition to obtaining measurements of hydraulic variables, depth-integrated samples of the suspended sediment and 0.1-m (4-in) long core samples of the bed material were collected at cross section 180. Also, 0.6-m-long (2-ft-long) core samples of the bed material were collected at various lateral and longitudinal posi-

TABLE 6. — *Water-discharge measurement, water-surface slope, temperature, and mean depth of flow data for the study reach*

[Leaders (...) indicate no data available]

Date	Time (24-hour clock time)	Water-discharge measurement at cross section 180				Water-surface slope (m/m)	Water temperature (°C)	Mean depth for reach (m)
		Discharge (m^3/s)	Width (m)	Mean depth (m)	Mean velocity (m/s)			
5-1-67	1325	8.55	17.4	0.771	0.640	...	10.0	...
5-2-67	1115	9.63	17.7	.756	.719	0.00056	...	...
5-3-67	1350	10.6	18.0	.786	.747	.000 55	11.1	...
5-4-67	0920	8.69	17.7	.695	.710	.000 60	...	...
5-5-67	1245	7.82	17.5	.704	.634	.000 59	12.8	0.76
5-6-67	1035	8.38	17.5	.716	.668	...	12.2	...
5-7-67	1050	[1]8.27	...	...	...	.000 56	...	...
5-8-67	0955	8.52	17.4	.710	.689	...	13.9	.79
5-9-67	1400	[1]8.27	...	...	...	...	...	...
5-15-67	1645	[1]6.94	...	...	...	...	12.8	...
5-16-67	1020	6.37	17.4	.567	.646	...	...	.61
5-19-67	0830	[1]7.08	...	...	...	...	...	...
5-23-67	...	[1]8.16	...	...	...	...	...	...
5-26-67	...	[1]7.87	...	...	...	...	...	...
6-6-67	...	[1]7.56	...	...	...	...	...	.73
7-14-67	...	[1]5.30	...	...	...	...	...	.52

[1] Estimated from stage-discharge relation

TABLE 7. — *Suspended-sediment concentrations and discharges, water discharges, and size distributions of suspended sediment determined by the visual accumulation-tube procedure*

Date	Time (24-hour clock time)	Water discharge (m^3/s)	Suspended-sediment concentration (mg/L)		Measured suspended-sediment discharge (tonnes/day)		Percentage finer than the size (in millimeters) indicated						
			<0.0625 mm	>0.0625 mm	<0.0625 mm	>0.0625 mm	0.0625	0.088	0.125	0.177	0.250	0.350	0.500
5-1-67	1330	8.55	159	249	118	184	1.0	7.0	29.8	63.8	91.8	100	100
5-2-67	2000	[1]10.2	171	254	151	224	1.3	8.0	30.2	61.1	94.9	100	100
5-3-67	1420	10.6	133	274	122	250	0.3	5.6	23.3	58.2	87.7	100	100
5-6-67	1115	8.38	1030	208	747	151	2.3	12.0	39.2	70.2	97.9	100	100
5-16-67	1111	6.37	443	166	244	91.6	3.3	24.9	52.0	70.1	95.0	100	100

[1] Estimated from stage-discharge relations.

tions in the study reach on May 8, June 6, and July 14 for the determination of the distributions of the fluorescent tracer particles.

Size distributions of the measured suspended sediment, measured suspended-sediment concentrations, and measured suspended-sediment discharges are presented in table 7. Size distributions were determined by the visual accumulation-tube procedure (U.S. Inter-Agency Committee on Water Resources, 1957b). The suspended-sediment discharge was also measured on May 8, the last day of the injection process. However, the median diameter of the sampled sediment was 0.231 mm, which is more characteristic of bed material than of suspended sediment. Also, the measured suspended-sediment discharge was about three times larger than any of the other measured discharges. Hence, it seems probable that the sampler inadvertently was pushed into the bed during sampling. Data from the May 8 measurement are not included in table 7.

The measured suspended-sand discharges (>0.0625 mm) ranged from 91.6 to 250 t/d (101 to 276 tons/d) and averaged 180 t/d (199 tons/d). The median fall diameter of the measured suspended sand ranged from 0.122 to 0.162 mm, averaged 0.146 mm, and had a mean geometric standard deviation of 1.47. The geometric standard deviation, σ, is defined as $\sigma = {}^1/_2(d_{84}/d_{50} + d_{50}/d_{16})$, where d is the diameter for which 84, 50, or 16 percent, respectively, of the size distribution, by weight, is finer. The mean discharge of sediment finer than 0.0625 mm was 276 t/d (304 tons/d). The large variations in the discharge are assumed the result of variations in the upstream supply of this sediment.

Size distributions and parameters of the distributions of the bed-material samples obtained with the 0.1-m-long (4-in-long) core-sampler are presented in table 8. These distributions were determined by the visual accumulation-tube procedure (U.S. Inter-Agency Committee on Water Resources, 1957b). The mean median fall diameter of the three bed-material samples was 0.242 mm, and the mean geometric standard deviation was 1.34.

Mean values of the d_{16}, d_{50}, d_{84}, and σ parameters of the size distributions of bed-material samples obtained with the 0.6-m-long (2-ft-long) core sampler are presented in tables 9 and 10 for the May 8 and the June 6, July 14 samples, respectively. Not all segments of

TABLE 8. — *Size distributions and parameters of the distributions of bed material as determined by the visual accumulation-tube procedure; 0.1- m core samples*

Date	Time (24-hour clock time)	Percentage finer than size (in millimeters) indicated							d_{16} (mm)	d_{50} (mm)	d_{84} (mm)	σ
		0.0625	0.125	0.177	0.250	0.350	0.500	1.00				
5–1–67	1313	0.2	1.0	9.9	57.3	88.0	95.8	99.4	0.188	0.240	0.329	1.32
5–8–67	1110	.5	1.2	9.8	52.4	83.9	93.7	98.7	.189	.247	.351	1.36
5–16–67	1140	.4	1.9	12.0	57.1	88.7	97.9	100	.183	.239	.326	1.34

TABLE 9. — *Mean parameters of the size distributions of bed material from various cross sections as determined by sieve analysis; 0.6-m core samples, May 8*

Cross section	Cores in which all segments were sieved					Cores in which all segments were not sieved				
	Number of segments (n)	d_{16} (mm)	d_{50} (mm)	d_{84} (mm)	σ	Number of segments (n)	d_{16} (mm)	d_{50} (mm)	d_{84} (mm)	σ
7.5	40	0.213	0.310	0.492	1.52	51	0.212	0.307	0.488	1.52
15	45	.211	.310	.508	1.56	73	.206	.301	.492	1.55
30	30	.210	.310	.512	1.56	45	.206	.298	.492	1.55
60	10	.207	.299	.471	1.51	45	.197	.289	.460	1.53
90	15	.207	.292	.449	1.48	45	.197	.291	.460	1.53
180	10	.201	.288	.462	1.52	42	.202	.291	.453	1.50
270	20	.202	.289	.453	1.50	47	.199	.289	.458	1.52
360	10	.203	.290	.473	1.53	40	.189	.277	.433	1.51
450	35	.196	.293	.528	1.65	47	.194	.289	.492	1.60
540	5	.203	.304	.549	1.65	38	.198	.290	.483	1.56
Composite .	220	.207	.301	.492	1.56	473	.200	.295	.473	1.53

the May 8 samples were sieved because some of the bottom segments contained no fluorescent particles. Hence, the samples are divided into two categories, one in which all five segments of the core were sieved and one in which one or more of the segments were not sieved. The number of segments, n, sieved for each cross section or lateral position is also given in tables 9 and 10.

A comparison of the values presented in tables 9 and 10 shows that there is essentially no variation in the mean values of d_{16} and d_{50} with either location in the channel or with time. There appears to be slightly more variation in the d_{84} and σ values, mostly with respect to longitudinal location for the May 8 values. This variation could be the result of pumice which was found in several of the samples. Pumice has a very low specific gravity and will bias slightly distributions obtained by sieve analysis.

The mean values of the parameters in tables 9 and 10, however, are consistently larger than those for the 0.1-m-long (4-in-long) core samples given in table 8. There are several possible explanations for this difference. The 0.1-m-long (4-in-long) core samples were analyzed by the visual accumulation-tube procedure, whereas the 0.6-m-long (2-ft-long) core samples were sieved. Figure 7 of the U.S. Inter-Agency Committee on Water Resources (1957b) shows the difference between fall diameter and sieve diameter for naturally worn quartz particles of various shape factors. However, for particles to have a sieve diameter of 0.30 mm and a fall diameter of 0.24 mm,

TABLE 10. — *Mean parameters of the size distributions of bed material from lateral positions as determined by sieve analysis; 0.6-m core samples, June 6 and July 14*

Lateral position	Number of segments (n)	d_{16} (mm)	d_{50} (mm)	d_{84} (mm)	σ
		June 6, 1967			
Left quarter ..	145	0.202	0.300	0.490	1.56
Centerline	145	.211	.306	.469	1.54
Right quarter .	145	.202	.292	.468	1.52
Composite	435	.204	.299	.470	1.52
		July 14, 1967			
Left quarter ..	75	.201	.300	.478	1.54
Centerline	75	.211	.302	.461	1.48
Right quarter .	75	.199	.300	.478	1.55
Composite	225	.202	.300	.472	1.53

the shape factor would have to be less than 0.3; for the particles involved, such a shape factor would seem to be too small to be reasonable. Estimates of shape factors for the 0.125- to 0.177-mm, 0.177- to 0.250-mm, and 0.250- to 0.350-mm sieve classes of bed material from the geometric mean sieve size, the fall diameters presented in table 2, and figure 7 of the U.S. Inter-Agency Committee on Water Resources (1957b) are 0.8, 0.6, and 0.65, respectively. Probably a better explanation for the difference is that the 0.6-m-long (2-ft-long) cores contained particles from throughout the dune whereas, the 0.1-m-long (4-in.-long) cores consisted primarily of the finer topset material on the crests and backs of the dunes.

The bed of the canal consisted of dunes that moved slowly downstream. The dimensionless Chezy discharge coefficient, $C/\sqrt{g}$, where g is the acceleration of gravity and C is the Chezy coefficient, ranged from 10

TABLE 11. — *Hydraulic and bed-form data, June 1966*

[From Nordin (1971)]

Run	Date	Mean depth (m)	Mean velocity (m/s)	Water-surface slope (m/m)	Water temperature (°C)	Dune length		Dune height		σ_y (m)
						Length (m)	C_V	Height (m)	C_V	
1	6–23–66	0.671	0.658	0.000 55	19	1.85	0.533	0.113	0.643	0.0789
2	6–22–66	.701	.643	.000 55	20	1.87	.535	.112	.655	.0841
3	6–21–66	.698	.634	.000 58	20	1.61	.535	.124	.597	.0823

to 11. The corresponding Manning n values ranged from 0.027 to 0.030.

Profiles of the bed surface were obtained on May 1 and May 8 with a sonic depth sounder (Karaki and others, 1961). The May 8 record obtained along the centerline of the canal from the injection point to cross section 360 was divided into 30–m (100–ft) increments, and the mean bed elevation and the standard deviation of the bed elevation determined for each increment. The standard deviation varied from 0.0536 to 0.101 m (0.176 to 0.330 ft) with a mean standard deviation of 0.0783 m (0.257 ft). Additional statistical analysis of these two profiles according to the procedures of Nordin (1971) was not possible because of variations in the boat speed during the profiling. Nordin (1971) analyzed three centerline profiles obtained in the Atrisco Feeder Canal in June of 1966. Some of the results of this analysis together with the mean hydraulic conditions, which are essentially the same as those during the fluorescent tracer study, are presented in table 11. The mean dune length was measured from trough to trough, the mean dune height was measured from crest to trough, σ_y is the standard deviation of the bed-surface elevation, and C_V is the coefficient of variation. The mean dune length was about 2 m (6 ft), the mean dune height about 0.12 m (0.38 ft), and the mean standard deviation of bed-surface elevation was about 0.082 m (0.27 ft). The coefficients of variation (table 11) were computed from individual dune heights and lengths, whereas the standard deviation of the bed-surface elevation was determined from the complete profile.

"DUSTPAN" SAMPLES

"Dustpan" samples collected at cross section 90 at various times were used for two purposes; first, to evaluate the steady-dilution procedure for estimating the total transport rate of bed material for a dune-bed condition; and second, to obtain information on how sediment particles move and disperse downstream from a point source. Results of importance are the speed of movement of the particles and properties of the lateral distributions of the tracers, namely, the centroid and the variance. The centroid, in general, indicates the point at which the largest concentrations would be expected, and the variance indicates the extent that the particles are dispersed in the lateral direction about the centroid.

"Dustpan" samples collected at various cross sections at the termination of the injection process were used to obtain information on how the mean cross-sectional concentrations, the centroids, and the variances of the lateral distributions varied with distance downstream.

"DUSTPAN" SAMPLES AT CROSS SECTION 90

Of the many "dustpan" samples from cross section 90, the sets of cross section samples collected at 27 different times during the injection period and at 8 times after termination of injection were analyzed for fluorescent tracers. Concentrations for the various sieve classes of the four minerals are given in tables 12–31 at the end of this report.

Graphs of fluorescent tracer concentrations versus distance from the left bank are presented in figures 8–11 for selected sieve classes of quartz, garnet, and monazite for several times during the study. Data for lead particles are not included because significant quantities of this tracer were found in only a few samples (tables 28–31). Consideration of the graphs shows how the concentrations of tracers increase with time at various points in the cross section, and how the lateral distributions develop as tracer material is injected continuously.

STEADY-DILUTION PROCEDURE

The steady-dilution procedure requires a steady, uniform concentration at the measurement cross section. The results presented in tables 12–31 and figures 8–11 show that a steady uniform concentration, illustrated in figure 3, was not obtained for any of the tracers at cross section 90. Thus, the injection period may not have been of sufficient duration or the cross section may not have been far enough downstream from the injection point to ever have a uniform distribution for the existing hydraulic conditions.

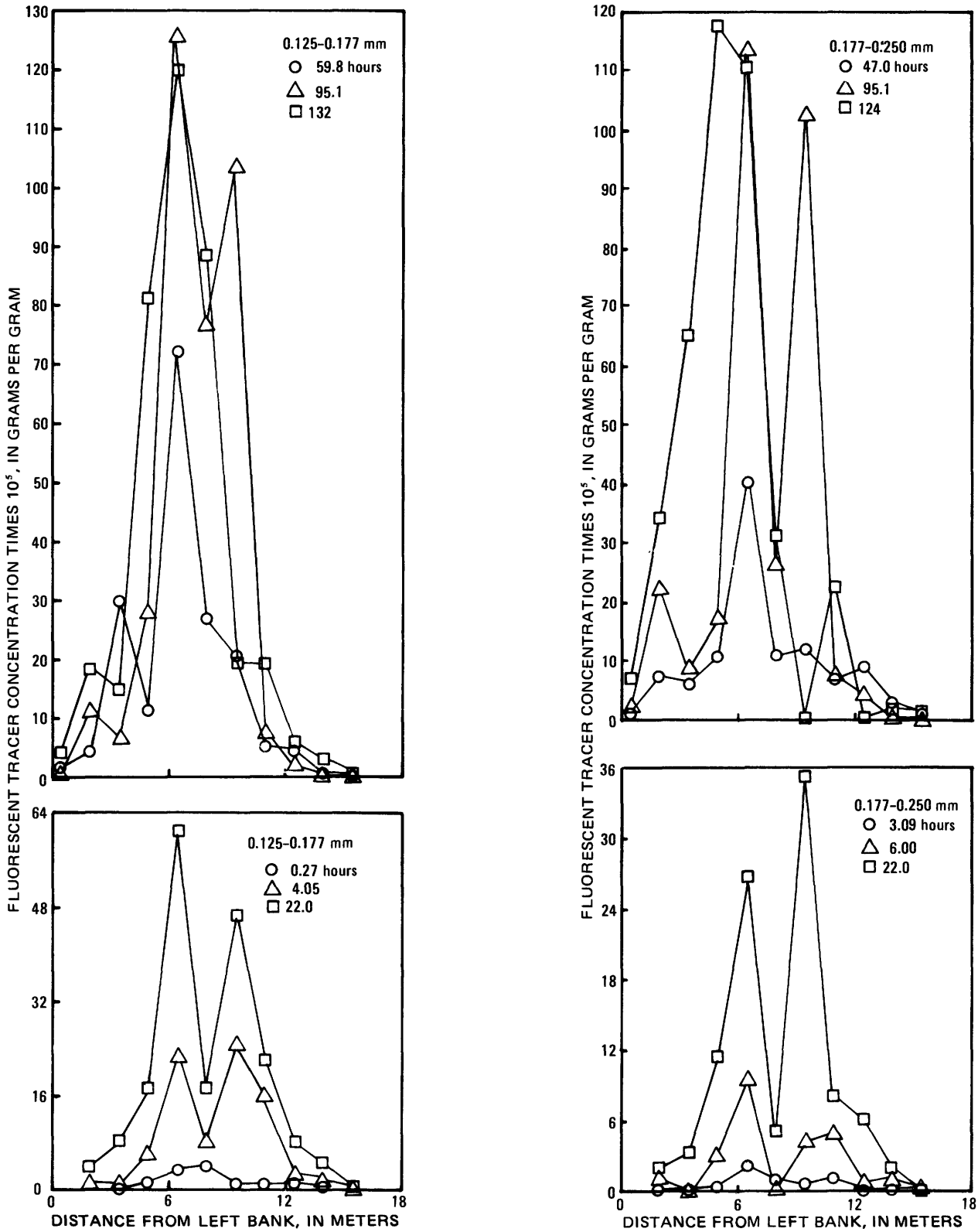

FIGURE 8. — Lateral concentration distributions of quartz in the 0.125- to 0.177-mm and 0.177- to 0.250-mm sieve classes as defined by "dustpan" samples collected at cross section 90 for various times measured from the start of injection of the fluorescent tracers.

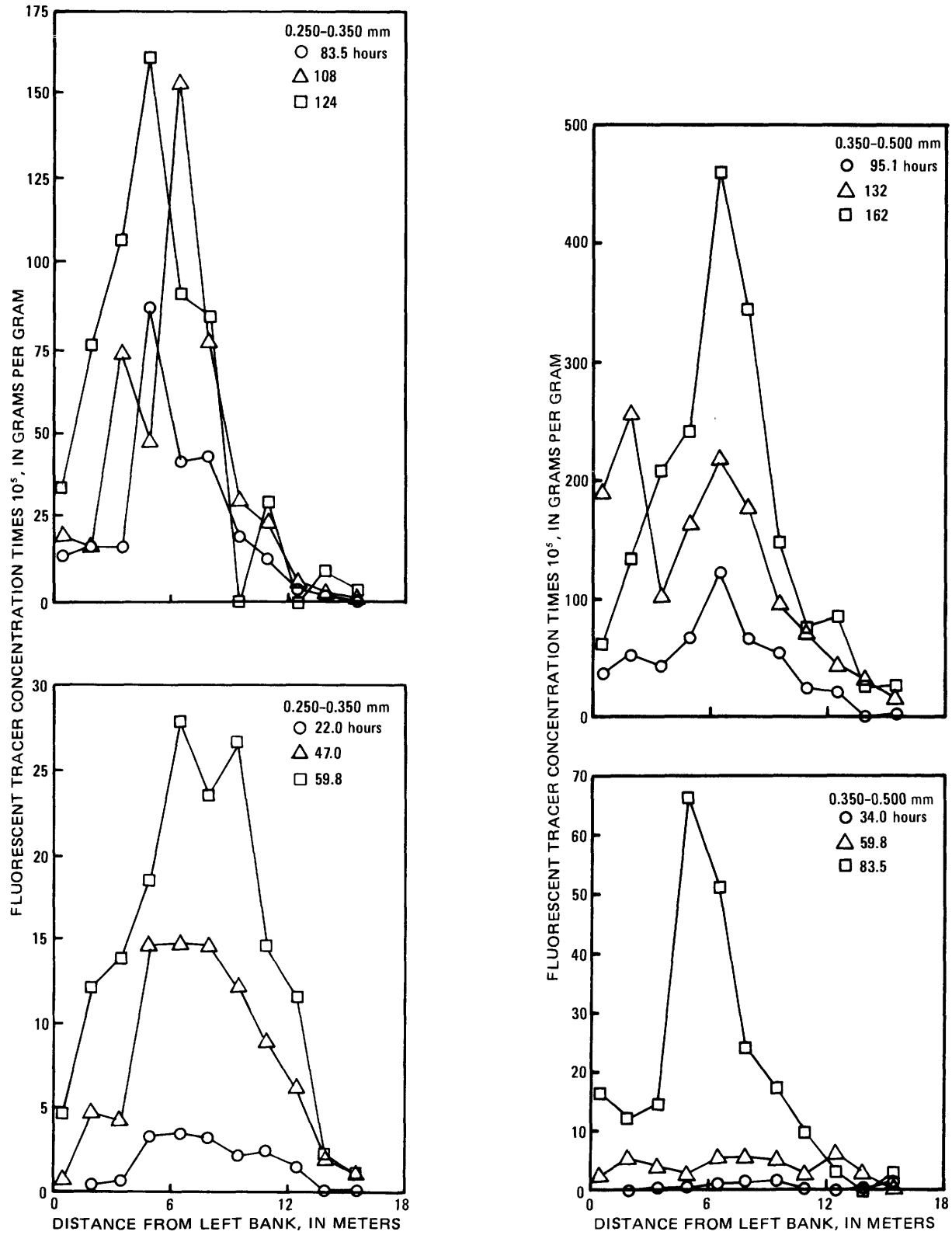

FIGURE 9. — Lateral concentration distributions of quartz in the 0.250- to 0.350-mm and 0.350- to 0.500-mm sieve classes as defined by "dustpan" samples collected at cross section 90 for various times measured from the start of injection of the fluorescent tracers.

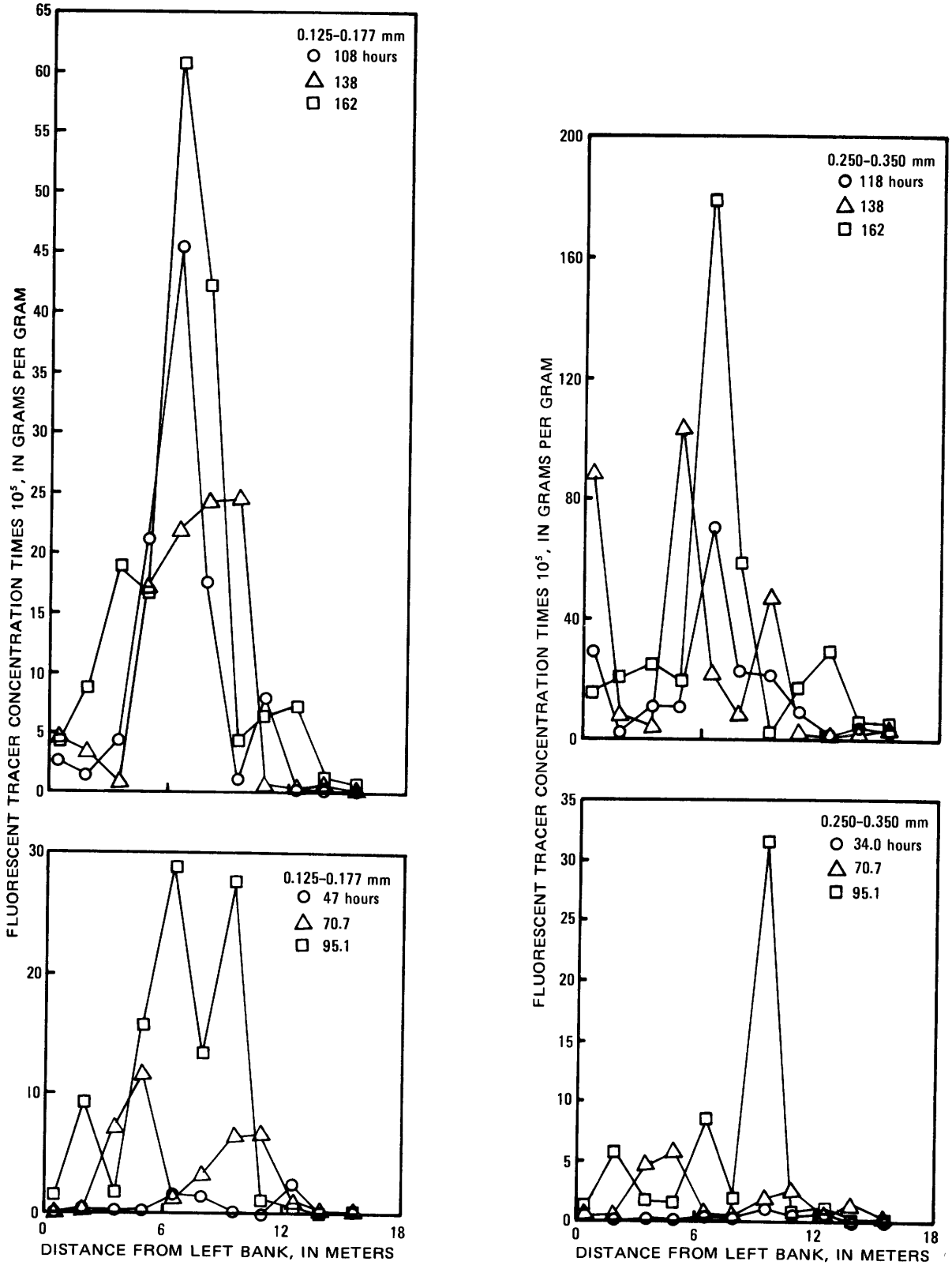

FIGURE 10. — Lateral concentration distributions of garnet in the 0.125- to 0.177-mm and 0.250- to 0.350-mm sieve classes as defined by "dustpan" samples collected at cross section 90 for various times measured from the start of injection of the fluorescent tracers.

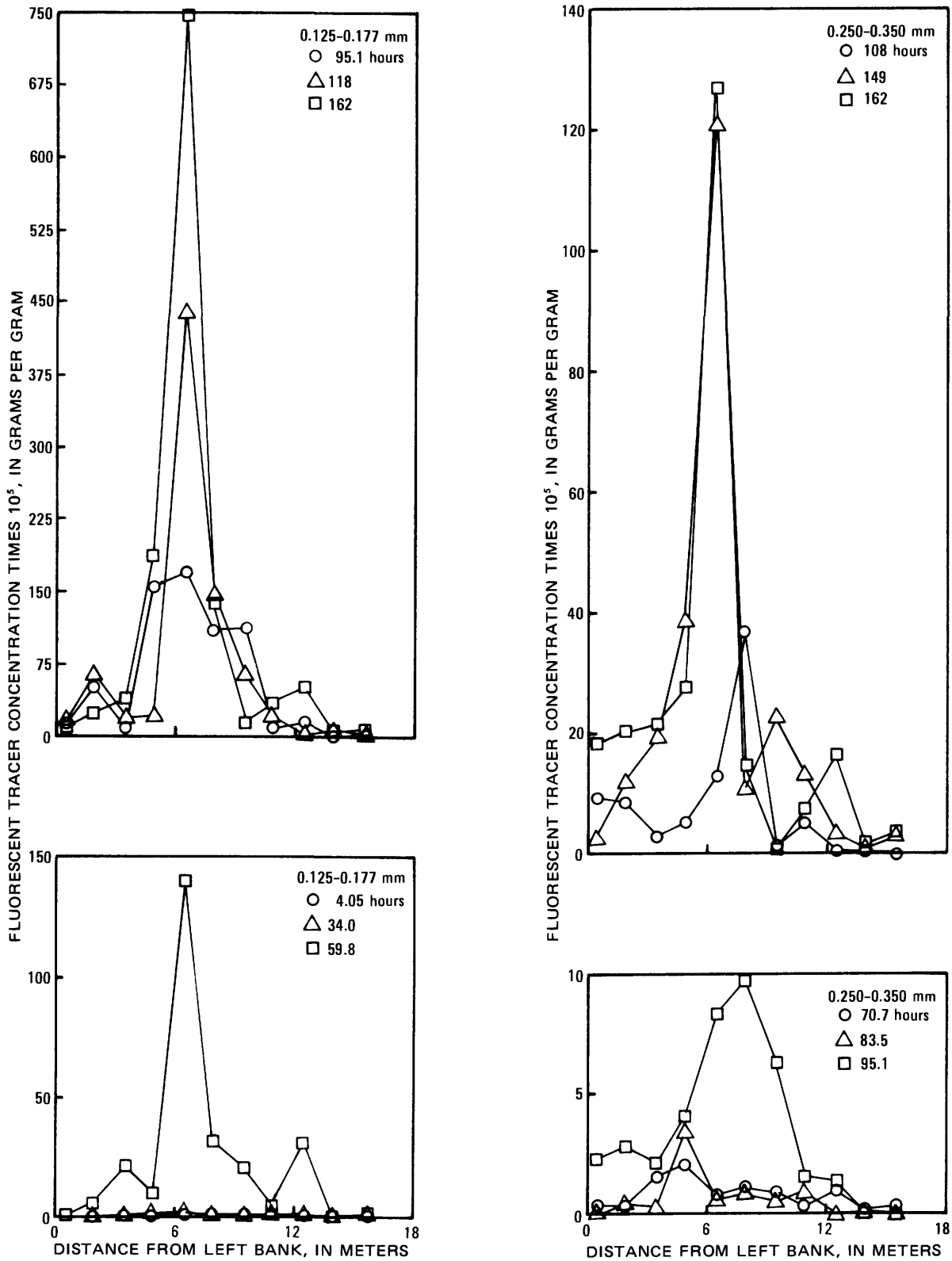

FIGURE 11. — Lateral concentration distributions of monazite in the 0.125- to 0.177-mm and 0.250- to 0.350-mm sieve classes as defined by "dustpan" samples collected at cross section 90 for various times measured from the start of injection of the fluorescent tracers.

Because a steady uniform concentration distribution was not attained, the alternative of using the mean concentration for the cross section defined by equation 3 was applied. A summation approximation of equation 3 was used to calculate the mean tracer concentration for each sample time for each sieve class of the four minerals. This approximation is

$$\bar{C}(t) = \frac{\sum_{z=0}^{z=B} C(z,t)\,\Delta z}{B}, \tag{8}$$

where $\bar{C}$ (t) is the mean fluorescent tracer concentration for the cross section at time t, $C(z,t)$ is the concentration at time t at lateral position z, and Δz is the width increment over which $C(z,t)$ is assumed to be the concentration. The lateral position, z, was measured from the left bank of the channel (facing downstream) and time, t, was measured from the start of the injection of the fluorescent tracers.

The mean concentration data are plotted versus time from the start of the injection of the tracers in figures 12–16. Each graph is broken into two sections with different time scales to facilitate presenting all data for a specific sieve class of a mineral on one graph. The first section corresponds to the injection period, and the second section, to the period after the termination of the injection process. The vertical dashed line indicates the time of 170 hours, when injection of tracers was stopped. To aid in comparing the two sections, the last point of the first section was repeated as the first point of the second section.

Figure 12 shows that the 0.125- to 0.177-mm sieve class of quartz tracer particles appeared at cross section 90 almost immediately after the start of injection and that an approximately constant plateau concentration developed at about 120 hours. When the injection was stopped, the mean concentration decreased rapidly until 429 hours, when a large quantity of these tracer particles appeared. This large concentration was not the result of a single sample because large concentrations were found at several points in the cross section (table 12). These large concentrations suggest that a quantity of tracer material probably was buried and then reexposed at a later time.

The 0.177- to 0.250-mm quartz tracer particles appear to have reached a plateau near the end of injection, although the plateau is not as well defined as for the 0.125- to 0.177-mm quartz tracer particles. The concentration decreased rapidly when injection was stopped. The 0.250- to 0.350-mm quartz tracer particles did not appear to reach a plateau because the concentration continued to increase for a short time after termination of the injection. Thereafter, however, the concentration decreased with time.

Figure 13 shows that the 0.350- to 0.500-mm, 0.500- to 0.707-mm, and 0.707- to 1.00-mm quartz tracer particles did not reach plateau concentrations during injection. As a result, large concentrations of these tracers were observed at cross section 90 after injection was stopped, as the tracer material accumulated between the injection point and cross section 90 continued to feed downstream parts of the channel.

Figure 14 suggests that plateau concentrations were not reached for any of the sieve classes of garnet tracer particles. The 0.125- to 0.177-mm, 0.177- to 0.250-mm, and 0.250- to 0.350-mm garnet concentrations began to decrease as soon as injection was stopped, whereas the concentrations for the 0.350- to 0.500-mm sieve class oscillated between increasing and decreasing. The concentration for the 0.500- to 0.707-mm sieve class increased to a maximum at 339 hours and then decreased slowly.

Figure 15 suggests that plateau concentrations were not reached for any of the sieve classes of monazite tracer particles. The concentration for the 0.125- to 0.177-mm sieve class decreased rapidly when injection was stopped, and the concentration for the 0.177- to 0.250-mm sieve class increased for a short time after injection was stopped, then decreased rapidly also. The concentrations for the 0.250- to 0.350-mm, 0.350- to 0.500-mm, and 0.500- to 0.707-mm sieve classes in general decreased more slowly.

Figure 16 shows that significant concentrations of the lead tracer particles were found only at 193 hours, the first sample time following termination of injection. Tables 28 through 31 show that these large concentrations resulted from large concentrations at several points in the cross section and were not from isolated samples.

The total sediment transport rate was calculated from the results of the steady-dilution study by using the mean quartz tracer concentrations for the cross section, applying equation 2 to each sieve class of importance, and summing the results according to

$$Q_s = \sum_{i=1}^{m} Q_{s_i} = \sum_{i=1}^{m} Q_{T_i} / \bar{C}_{2_i}, \tag{9}$$

where the subscript i indicates the i th sieve class, and m is the number of sieve classes. The analysis for fluorescent tracer concentrations was limited to particle sizes larger than 0.125 mm because of the difficulty of differentiating between chips or flakes of dye from large particles and actual fluorescent particles in the small-diameter sieve classes. The concentrations used for $\bar{C}_{2_i}$ for the 0.125- to 0.177-mm and 0.177- to 0.250-mm sieve classes were averages over the time period for

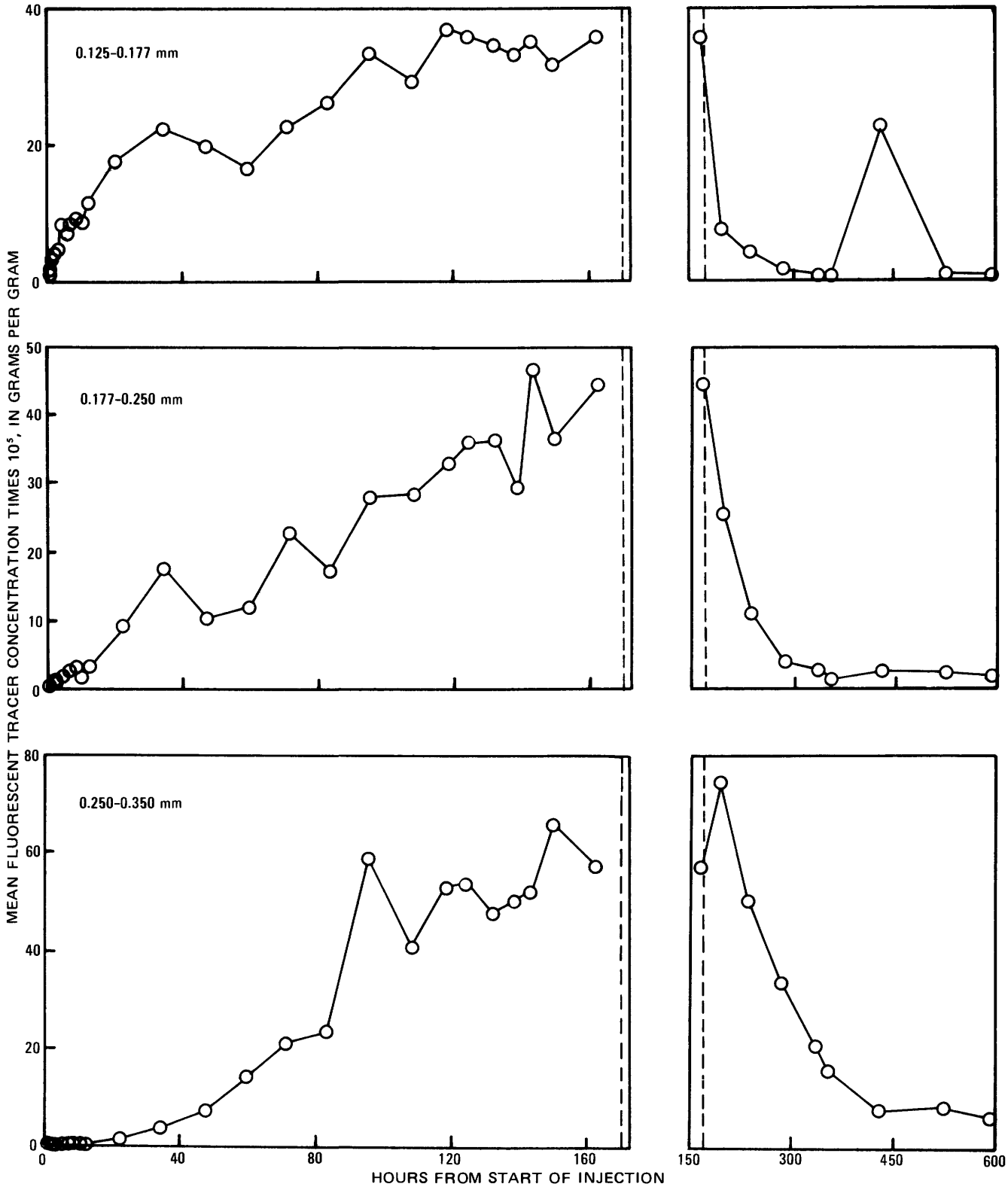

FIGURE 12. — Variation with time in the mean concentration of the 0.125- to 0.177-mm, 0.177- to 0.250-mm, and 0.250- to 0.350-mm sieve classes of quartz tracer as defined by "dustpan" samples collected at cross section 90; the vertical dashed line indicates the time of 170 hours, when injection of tracers was stopped.

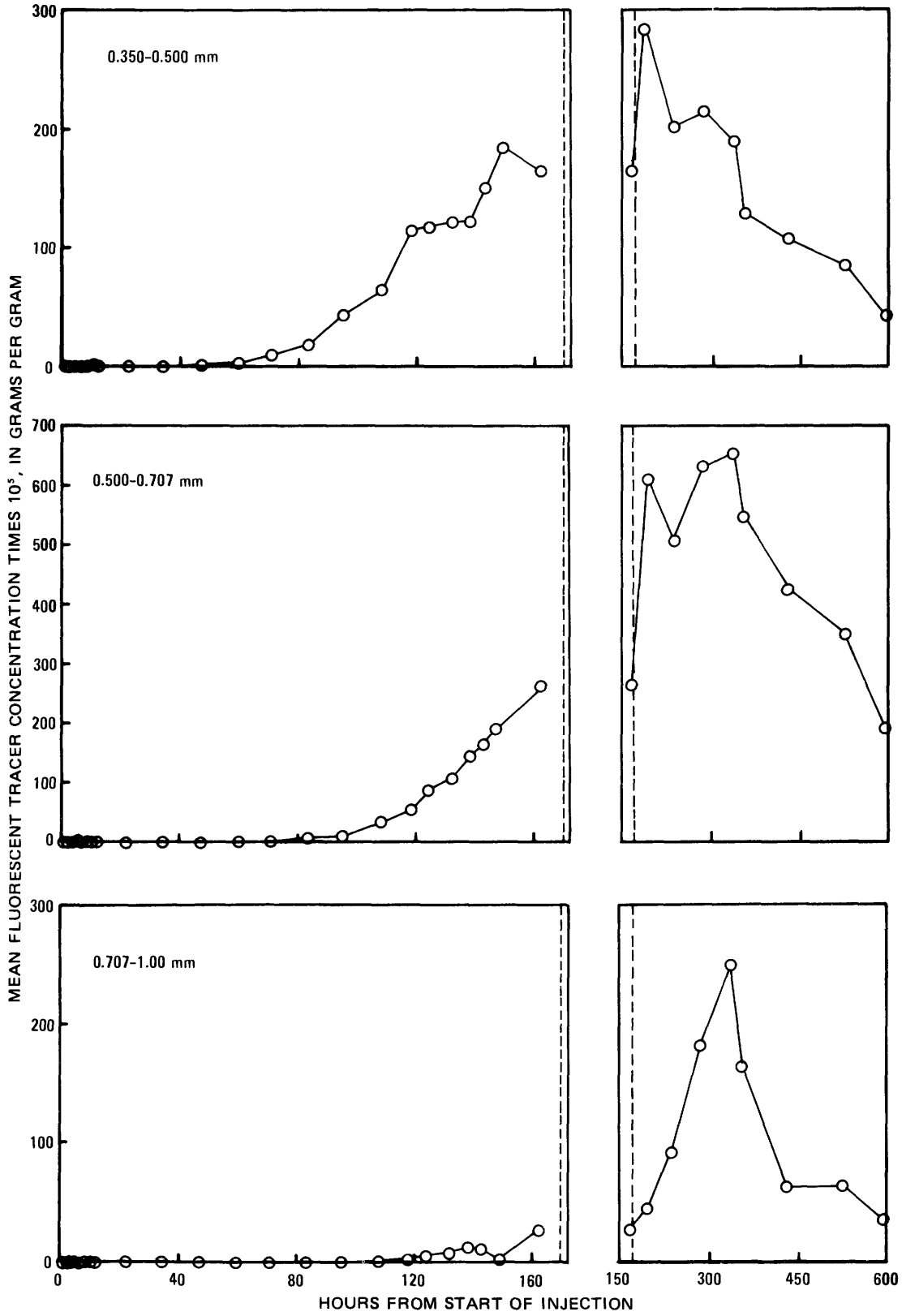

FIGURE 13. — Variation with time in the mean concentration of the 0.350- to 0.500-mm, 0.500- to 0.707-mm, and 0.707- to 1.00-mm sieve classes of quartz tracer as defined by "dustpan" samples collected at cross section 90; the vertical dashed line indicates the time of 170 hours, when injection of tracers was stopped.

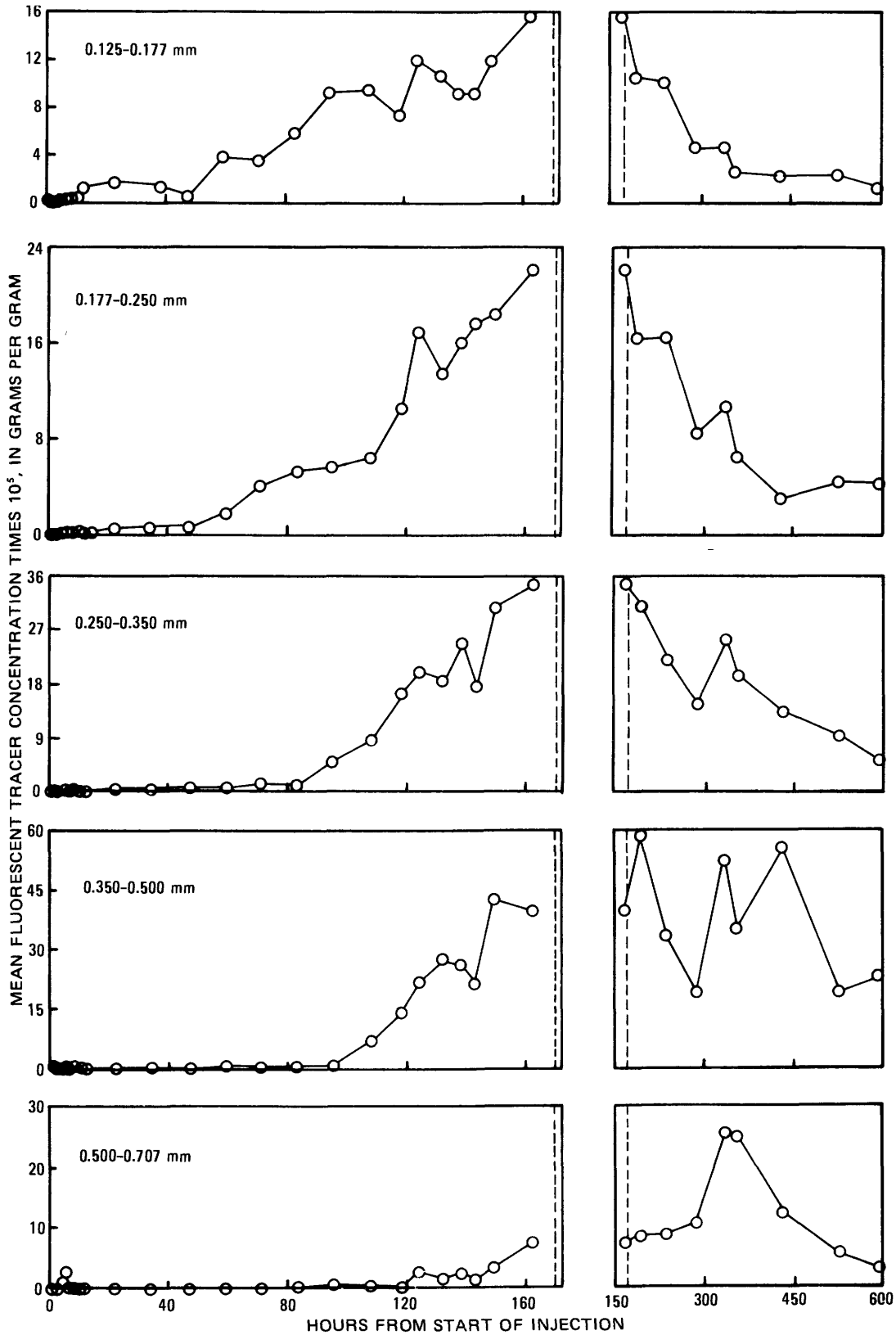

FIGURE 14. — Variation with time in the mean concentration of the 0.125- to 0.177-mm, 0.177- to 0.250-mm, 0.250- to 0.350-mm, 0.350-to 0.500-mm, and 0.500- to 0.707-mm sieve classes of garnet tracer as defined by "dustpan" samples collected at cross section 90; the vertical dashed line indicates the time of 170 hours, when injection of tracers was stopped.

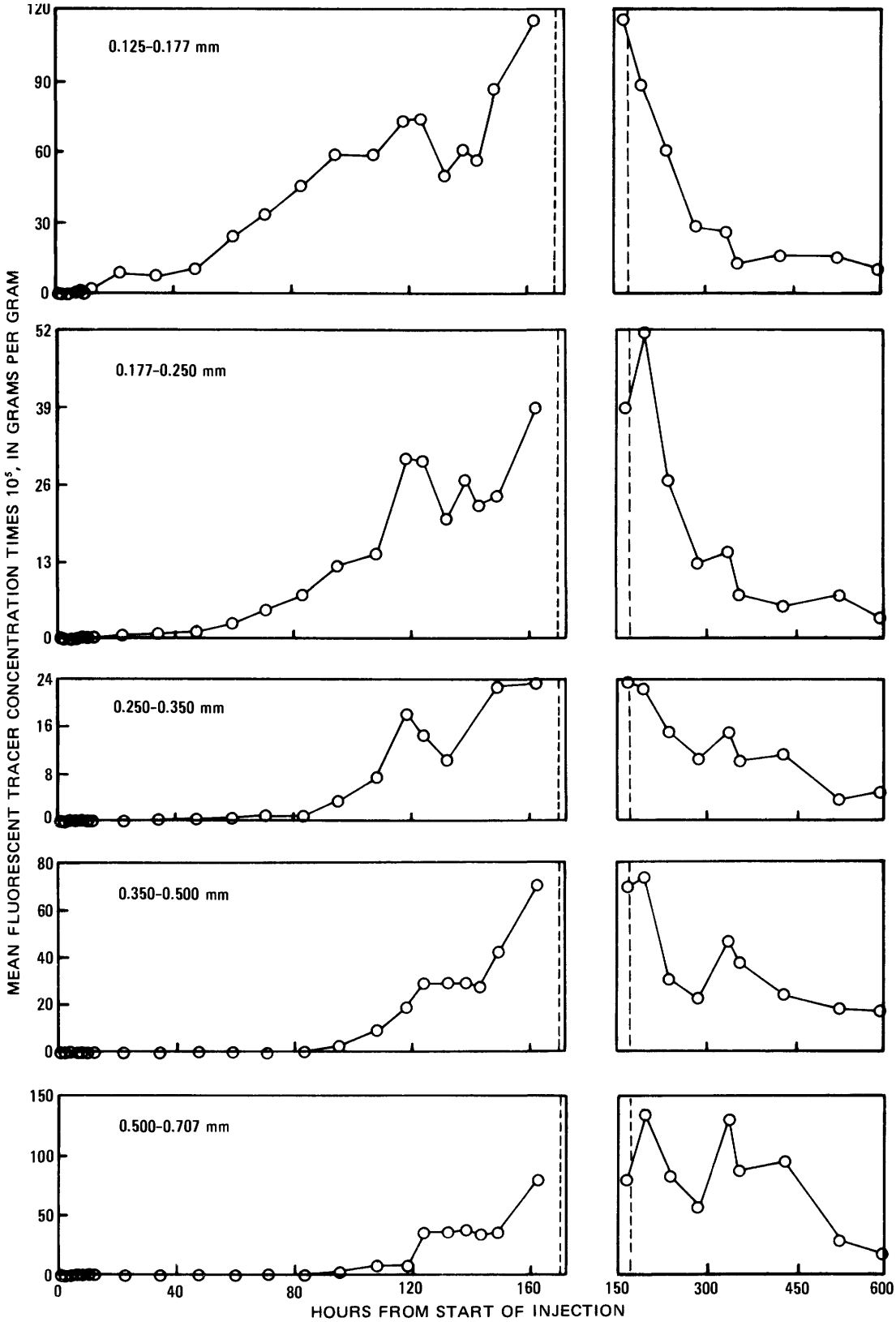

FIGURE 15. — Variation with time in the mean concentration of the 0.125- to 0.177-mm, 0.177- to 0.250-mm, 0.250- to 0.350-mm, 0.350- to 0.500-mm, and 0.500- to 0.707-mm sieve classes of monazite tracer as defined by "dustpan" samples collected at cross section 90; the vertical dashed line indicates the time of 170 hours, when injection of tracers was stopped.

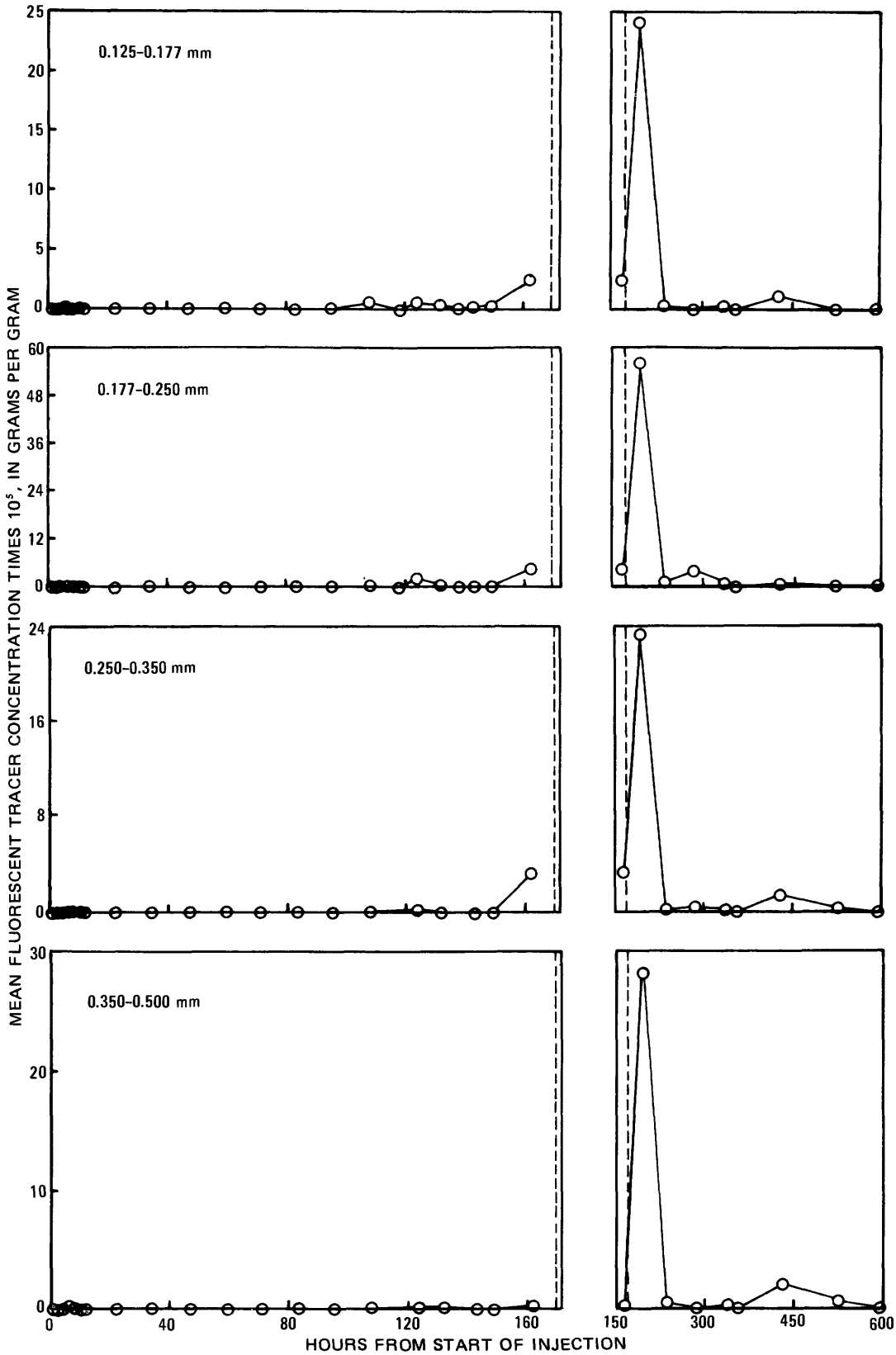

FIGURE 16. — Variation with time in the mean concentration of the 0.125- to 0.177-mm, 0.177- to 0.250-mm, 0.250- to 0.350-mm, and 0.350- to 0.500-mm sieve classes of lead tracer as defined by "dustpan" samples collected at cross section 90; the vertical dashed line indicates the time of 170 hours, when injection of tracers was stopped.

TABLE 32. — *Sediment transport rates calculated from the steady-dilution study*

Sieve class (mm)	Injection rate (kg/h)	$\overline{C}_{2_i}$ times 10^6 (g/g)	Q_{s_i} (t/d)
0.125–0.177 ...	1.31	34.8	90.1
0.177–0.250 ...	2.50	41.6	144.2
0.250–0.350 ...	2.55	≥ 76.3	≤ 80.4
0.350–0.500 ...	3.86	≥ 290	≤ 32.0
0.500–0.707 ...	2.20	≥ 675	≤ 7.8
0.707–1.00 ...	.12	≥ 250	≤ 1.2
		$Q_s = \Sigma Q_{s_i}$	= ≤ 355.7

which the concentration appeared to be at a plateau. For the large particle sieve classes that did not reach plateau concentrations, the largest concentration observed between termination of injection and termination of the experiment was rounded upward and arbitrarily used as the $\overline{C}_{2_i}$ value. Because these $\overline{C}_{2_i}$ values were too small, the calculated transport rates for the large sizes are too large. Results of the steady-dilution calculations are summarized in table 32.

Because facilities were not available in the Atrisco Feeder Canal for measuring the total sediment discharge, it was necessary to compare the transport rate determined from the steady-dilution procedure with calculated sediment transport rates. Of the many calculation procedures available, the Task Committee of the American Society of Civil Engineers (1971) recommended that the modified Einstein procedure be used when the necessary hydraulic characteristics and suspended-sediment concentrations for the stream are available. Details of the modified Einstein procedure were described by Colby and Hembree (1955), and nomographs allowing a graphical solution of the modified Einstein procedure were presented by Colby and Hubbell (1961). Results of the modified Einstein calculations for four dates for which suspended-sediment concentrations were measured are presented in table 33. The water discharge is also shown in table 33 to indicate the hydraulic conditions at the time of sampling. The discharge shown for the steady-dilution procedure is the average discharge for the period during which the tracers were injected.

TABLE 33. — *Sediment transport rates calculated by the steady-dilution and modified Einstein procedures*

Sieve class (mm)	Calculated sediment-transport rate, in tonnes/day				
	Steady-dilution procedure	Modified Einstein procedure			
		5-1-67	5-2-67	5-3-67	5-6-67
0.125–0.177 ..	90.1	76.2	85.7	108	59.9
0.177–0.250 ..	144.2	126	163	191	125
0.250–0.350 ..	≤80.4	52.1	86.2	85.6	65.9
0.350–0.500 ..	≤32.0	8.7	15.7	16.5	15.5
0.500–0.707 ..	≤ 7.8	2.3	4.5	4.7	7.0
0.707–1.00 ..	≤ 1.2	.2	.9	1.0	1.1
Total ...	≤356	266	356	407	274
Water (m^3/s)	[1]8.81	8.55	9.63	10.6	8.38

[1] Average discharge for tracer injection period.

Comparison of the results presented in table 33 shows that the transport rates computed from the steady-dilution procedure for the 0.125- to 0.177-mm, 0.177- to 0.250-mm, and 0.250- to 0.350-mm sieve classes are within the range of the transport rates calculated from the modified Einstein procedure. For the 0.350- to 0.500-mm sieve class, the steady-dilution result is almost twice the largest rate calculated for this sieve class by the modified Einstein procedure. For the 0.500- to 0.707-mm and 0.707- to 1.00-mm sieve classes, the steady-dilution results are slightly larger than the largest of the rates computed for these sieve classes by the modified Einstein procedure. These latter two size classes, however, constitute only a small percentage of the total transport rate. The total transport rate computed from the steady-dilution procedure is within the range of the total transport rates calculated by the modified Einstein procedure.

In evaluating these comparisons, the characteristics of both the steady-dilution and the modified Einstein procedures must be considered. The steady-dilution procedure gives calculated results that are too large for sieve classes that do not reach plateau concentrations. This characteristic undoubtedly explains why the steady-dilution result for the 0.350- to 0.500-mm sieve class was almost 2 times larger than the largest of the modified Einstein results for this sieve class. The modified Einstein procedure was developed by Colby and Hembree (1955) and was checked on several sand-channel streams in western Nebraska. These streams have characteristics similar to the Atrisco Feeder Canal, although they are somewhat larger in size. Evaluation of the modified Einstein procedure by Colby and Hembree (1955) showed that the calculated total sediment discharge ranged from 56 to 187 percent and averaged 97 percent of the measured total sediment discharges for the Niobrara River in Nebraska. Similarly, Hubbell and Matejka (1959) found for the Middle Loup River in Nebraska that the calculated total sediment discharges ranged from 64 to 166 percent and averaged 112 percent of the measured total sediment discharges. Thus, on the basis of these considerations and the results presented in table 33, it was concluded that the steady-dilution procedure based on a mean concentration for the cross section is a satisfactory procedure for measuring the sediment-transport rates for a dune-bed condition, such as existed for this study in the Atrisco Feeder Canal. The major disadvantage in using the technique for a low-transport dune-bed condition is the long time interval needed to attain plateau concentrations at the measurement cross section.

The sediment transport rate was also computed from the results of the steady-dilution study by another procedure. This procedure was based on the observation that the lateral distributions of tracers at cross section

90 near the end of the injection period were approximately Gaussian. Lean and Crickmore (1966) showed that if the lateral distributions of tracers are Gaussian, then

$$Q_s = \sum_{i=1}^{m} Q_{s_i} = \sum_{i=1}^{m} \left[\frac{Q_{T_i} B}{C_{0_i} \sqrt{(2\pi \sigma_{z_i}^2)}} \right], \quad (10)$$

where C_{0_i} is the concentration of fluorescent tracer of sieve class i along the centerline of the channel, which generally is the maximum concentration of the distribution, and $\sigma_{z_i}^2$ is the variance of the lateral distribution. Equation 10 assumes that the lateral concentration distributions do not vary with time and that the sediment discharge per unit of width is constant across the channel. This procedure is basically another way of correcting for the fact that a steady uniform concentration, illustrated in figure 3, was not obtained for any of the tracers at cross section 90.

For each lateral distribution of tracer particles, determined from "dustpan" samples collected at cross section 90, the variance was calculated from

$$\sigma_z^2 = \frac{\sum_{z=0}^{z=B} z^2 C(z,t)\,\Delta z}{\sum_{z=0}^{z=B} C(z,t)\,\Delta z} - (\bar{z})^2, \quad (11)$$

where $\bar{z}$ is the mean lateral position of the lateral distribution, calculated from

$$\bar{z} = \frac{\sum_{z=0}^{z=B} zC(z,t)\,\Delta z}{\sum_{z=0}^{z=B} C(z,t)\,\Delta z}. \quad (12)$$

The variances with the corresponding centerline concentrations of tracer particles were used in equation 10 to calculate the sediment transport rates for six times near the end of the injection period. Results are presented in table 34, together with transport rates calculated by the modified Einstein procedure for May 1, May 2, May 3, and May 6.

The sediment-transport rates calculated from equation 10 for the 0.125- to 0.177-mm and 0.177- to 0.250-mm sieve classes are generally within the range of transport rates computed for these sieve classes from the modified Einstein procedure. The results from equation 10 for the 0.250- to 0.350-mm sieve class are generally slightly larger and the results for the 0.350- to 0.500-mm, 0.500- to 0.707-mm, and 0.707- to 1.00-mm sieve classes are considerably larger than the rates computed from the modified Einstein procedure for these sieve classes. Because the latter three sieve classes contribute only a relatively small percentage to the total rate, the total transport rates computed by the two procedures agree reasonably well. There is a tendency, however, for the differences to be largest for the earliest times. This tendency is attributed to the fact that the lateral distributions for the large particles were not fully developed at the end of the injection period. Hence, the variance and particularly the maximum concentration values were less than the true values for fully developed lateral distributions.

PARTICLE VELOCITIES

Figures 12 and 13 show the effect of particle size on the rate of movement of the quartz tracer particles. The 0.125- to 0.177-mm particles appeared almost immediately at cross section 90, whereas the 0.707- to 1.00-mm particles began to appear only after about 110 hours. Similar variations in the arrival times at cross section 90 were observed for the other sieve classes and specific gravities of tracers. The velocities of the various types of tracer particles were compared using first arrival times at cross section 90. The first arrival time for a particular type of tracer particle was taken as that time at which the concentration began to increase rapidly and (or) continuously (figs. 12–16). First arrival times were difficult to estimate because the concentrations for most of the tracer particles tended to vary somewhat with time before increasing rapidly. The 0.125- to 0.177-mm and 0.177- to 0.250-mm sieve classes of quartz tracers behaved differently from most of the other tracer particles in that the concentration

TABLE 34. — *Sediment transport rates calculated from equation 10 and the modified Einstein procedure*

Sieve class (mm)	Calculated sediment transport rate, in tonnes/day									
	Modified Einstein procedure				Equation 10 for times, in hours, of					
	5-1-67	5-2-67	5-3-67	5-6-67	124	132	138	143	149	162
0.125–0.177	76.2	85.7	108	59.9	83.0	73.6	72.9	56.7	105	69.5
0.177–0.250	126	163	191	125	137	152	188	79.6	122	101
0.250–0.350	52.1	86.2	85.6	65.9	89.1	108	95.3	81.7	69.9	78.0
0.350–0.500	8.7	15.7	16.5	15.5	71.8	62.8	52.3	51.0	44.9	41.8
0.500–0.707	2.3	4.5	4.7	7.0	46.0	53.0	17.7	24.9	24.1	17.9
0.707–1.00	.2	.9	1.0	1.1	36.3	10.3	13.9	10.9	54.1	5.0
Total	266	356	407	274	463	460	440	305	420	313

first increased at a rapid rate, then at a somewhat slower rate. The 0.125- to 0.177-mm sieve classes of the garnet and monazite tracers also tended to behave in this manner.

The first arrival times and the corresponding velocities are presented in table 35 and the velocities are plotted in figure 17 as a function of the median fall diameter of the sieve class. Some of the arrival times and velocities for the different minerals and sieve classes were identical because of the limited number of sample times and the manner in which the arrival times were determined. This tended to aline the velocities and thus introduced scatter that might not have been present, had more frequent sampling been possible. Significant quantities of the lead tracers appeared at cross section 90 only for one short period of the experiment, hence, the velocities for all four sieve classes were identical.

The vertical dashed lines in figure 17 give the size limits of the sieve classes used in the analysis of the samples, and the number next to each point indicates the sieve class number given in table 35. The median fall diameters for the different sieve classes of garnet and monazite are in general displaced to the next larger sieve class.

TABLE 35. — *First arrival times and velocities of the leading edges of the tracer masses as determined from "dustpan" samples collected at cross section 90*

Mineral	Sieve class (mm)	First arrival time (hours from start of injection)	Velocity (m/h)
Quartz	(1) 0.125–0.177	0.067	1370
	(2) 0.177–0.250	.50	183
	(3) 0.250–0.350	10	9.1
	(4) 0.350–0.500	47	1.9
	(5) 0.500–0.707	71	1.3
	(6) 0.707–1.00	118	.77
Garnet	(1) 0.125–0.177	10	9.1
	(2) 0.177–0.250	47	1.9
	(3) 0.250–0.350	84	1.1
	(4) 0.350–0.500	95	.96
	(5) 0.500–0.707	118	.77
Monazite	(1) 0.125–0.177	10	9.1
	(2) 0.177–0.250	47	1.9
	(3) 0.250–0.350	84	1.1
	(4) 0.350–0.500	84	1.1
	(5) 0.500–0.707	95	.96
Lead	(1) 0.125–0.177	162	.56
	(2) 0.177–0.250	162	.56
	(3) 0.250–0.350	162	.56
	(4) 0.350–0.500	162	.56

The velocities are plotted against the fall diameters of the sieve classes because the concept of hydraulic equivalence (Rubey, 1933; Rittenhouse, 1943) suggests that particles having equal fall diameters tend to be of equivalent hydraulic value.

Figure 17 shows that the velocity values tend to be divided into two groups, each with a very different dependence on fall diameter. Least-squares regression lines were computed for these groups according to

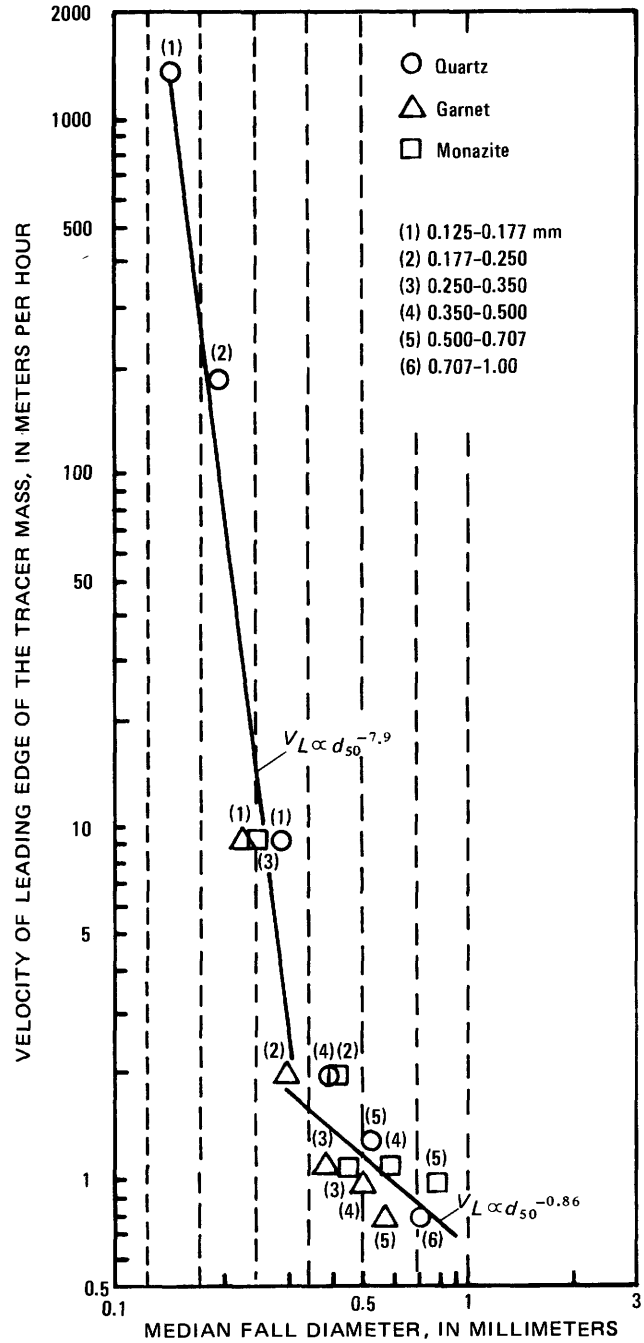

FIGURE 17. — Variation in the velocity of the leading edge of the tracer masses with median fall diameter as defined by "dustpan" samples collected at cross section 90.

$$V_L = a\, d_{50}^{b}, \tag{13}$$

where a and b are constants. The velocities for the small particles were found to vary inversely with the 7.9 power of the median fall diameter, whereas the velocities for the large particles varied inversely with

the 0.86 power of the fall diameter. The velocities for the lead tracer particles were not considered in the determination of the relation for the large particles.

The difference in behavior is presumed to be the result of differences in the ways in which the particles moved in the channel. The small particles moved predominantly in suspension, intermediate particles moved alternatively in suspension and by creep along the bed surface, and the larger particles moved almost exclusively by creep along the bed surface. The change in dependence on diameter in figure 17 appeared to occur at a diameter in the range between 0.25 and 0.30 mm, which is just slightly larger than the median diameter of the bed material in the channel (table 8).

Kennedy and Kouba (1970) determined first arrival times for sand-size (0.18 to 0.99 mm) tracer particles in a gravel-bed stream. They found that the velocities varied inversely with the 2.0 power of the diameter. Observed velocities were within the range of velocities presented in figure 17 for the small particles. Rathbun, Kennedy, and Culbertson (1971) determined the diameter dependence of sand-size particles for the flat-bed condition and found that the diameter dependence was U-shaped with the smallest and largest particles having the largest velocities. Observed velocities also were within the range of velocities presented in figure 17 for the small particles. Thus, there are few similarities between the results of these prior studies and the present study. However, considering the different flow and bed conditions, none should probably be expected.

The scatter of the data in figure 17 prevents any definite conclusions regarding the hydraulic equivalence of the tracer particles. However, it appeared that the smaller particles, moving predominantly in suspension, were more nearly hydraulically equivalent than were the large particles which move predominantly by surface creep.

The determination of particle velocities was limited to those based on first arrival times because most of the sizes and specific gravities of tracer particles did not reach plateau concentrations during the injection period. Had plateau concentrations been achieved, then the time required to reach half the plateau concentration could have been taken as a mean time of travel and then a mean velocity could have been computed. However, as discussed previously, only the 0.125- to 0.177-mm and 0.177- to 0.250-mm sieve classes of quartz tracer appeared to reach plateau concentrations during the injection period.

MEAN LATERAL POSITIONS AND VARIANCES

As discussed in previous paragraphs, mean lateral positions and variances were calculated from equations 12 and 11, respectively, for each lateral distribution of tracer particles determined from "dustpan" samples collected at cross section 90. Consideration of these mean lateral positions and variances gives general information about the lateral dispersion characteristics of the tracers.

Consideration of the mean lateral positions shows that the lateral distributions of the 0.125- to 0.177-mm and 0.177- to 0.250-mm sieve classes of quartz tracers were established very rapidly with little variation with time of the mean lateral positions. The $\bar{z}$ values for the other sieve classes of quartz tracers and for the garnet and monazite tracers oscillated considerably during the initial 22 hours of injection, with most of the values lying to the right of the channel centerline. After establishment of the lateral distributions, the $\bar{z}$ values gradually shifted to a position 0.9 to 1.5 m (3 to 5 ft) to the left of the channel centerline during the experiment. Aside from the fact that the lateral distributions for the small quartz particles were established more rapidly than for the other tracer particles, there were no obvious effects of either size or specific gravity on the variation with time of the mean lateral positions of the tracer masses.

Figure 18 shows the variances of the lateral distributions for the last two sampling times of the injection period as a function of the median fall diameter of the sieve class. The line represents a least-squares fit of the data points. The very large value for the 0.707- to 1.00-mm sieve class of quartz was the result of a bimodal distribution produced by detectable tracer concentrations in the left half of the channel, three sample points with zero concentration to the right of centerline, and relatively large concentrations near the right bank (table 17). On the other hand, the small σ_z^2 value for the 0.500- to 0.707-mm sieve class of garnet is the result of tracer concentrations at only 3 of the 11 sample points in the cross section (table 22). Much of the apparently random behavior, particularly for the large sizes, is the result of the fact that steady-state concentration distributions were not obtained at cross section 90. Although there is considerable scatter in the data, the general trend is for the variances of the lateral distributions to increase with the fall diameter of the tracer particles.

The variances of the lateral distributions of the different sizes of tracer particles used in this study, the larger of which move predominantly as bed load and the smaller of which move alternately in suspension and as bed load, were compared with the variances for a dissolved dispersant. A dispersion study using a water-soluble fluorescent dye was conducted on another section of the Atrisco Feeder Canal under approximately the same hydraulic conditions (Fischer, 1967). From the results of that study, it is estimated that for a dis-

TABLE 36. — *Mean concentrations of fluorescent tracers as defined by "dustpan" samples collected at various cross sections on May 8*

Mineral	Sieve class (mm)	Mean concentration times 10^5 at cross section: 15	60	90	180	270	[1]360	450	540
Quartz	0.125–0.177	17.4	29.7	36.2	37.5	44.3	25.8	41.0	33.0
	0.177–0.250	35.3	38.1	44.5	36.3	29.2	18.1	12.1	8.24
	0.250–0.350	110	90.0	57.6	24.0	5.11	1.25	.371	.232
	0.350–0.500	518	387	166	3.42	0.426	1.00	.334	.102
	0.500–0.707	1220	1050	265	0.0	.583	1.04	.114	0
	0.707–1.00	294	212	27.7	0	0	0	0	0
Garnet	0.125–0.177	24.6	18.8	15.4	11.1	2.37	1.98	.999	1.69
	0.177–0.250	66.0	22.9	22.5	11.6	1.38	1.11	.597	.895
	0.250–0.350	99.7	43.8	34.8	7.07	.437	.0719	.147	.0461
	0.350–0.500	280	87.6	40.2	.138	.0752	.0334	.0342	0
	0.500–0.707	45.3	19.1	7.42	0	.384	0	.0935	0
Monazite ...	0.125–0.177	233	182	116	36.2	15.3	6.62	4.03	6.63
	0.177–0.250	109	63.4	39.8	4.68	1.71	.686	.188	.246
	0.250–0.350	66.4	38.2	23.4	.324	.226	.251	.0796	.233
	0.350–0.500	219	75.4	70.4	.0708	.439	.139	.0306	.834
	0.500–0.707	216	251	80.4	0	.630	1.11	.218	0
Lead	0.125–0.177	30.4	0.528	2.59	.385	0	0	.0631	.0223
	0.177–0.250	22.2	.158	1.47	.0307	0	0	.0614	0
	0.250–0.350	10.2	.231	3.39	0	0	.0190	.0207	0
	0.350–0.500	51.0	.580	.122	0	0	0	0	0

[1] Collected on May 9.

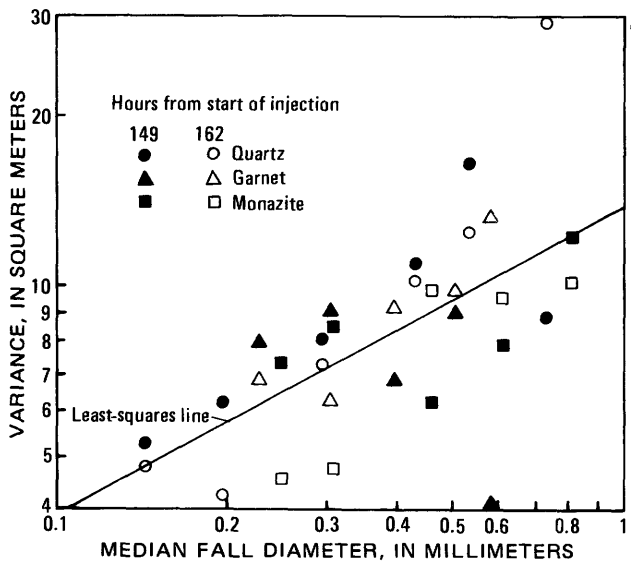

FIGURE 18. — Variation with median fall diameter in the variances of the lateral concentration distributions as defined "dustpan" samples collected at cross section 90 for the last two sampling times of the injection period on May 8.

tribution 90 m (300 ft) downstream from a point source at the channel centerline, the variance of a lateral distribution of dye would be about 2.8 m^2 (30 ft^2). If the line in figure 18 is extended, this variance would correspond to a fall diameter of about 0.05 mm, a size which would be transported completely in suspension.

The effect of size on lateral mixing can also be seen from the data presented in tables 12 through 31. For example, for $t = 149$ hours, the concentrations for the 0.125- to 0.177-mm sieve class of quartz for the two sampling points nearest the left and right banks are 0.38 and 0.76 percent, respectively, of the maximum concentration for the cross section, whereas for the 0.500- to 0.707-mm sieve class of quartz, the corresponding concentrations are 51 and 19 percent, respectively, of the maximum concentration. Similar results are obtained for the other minerals. The examples of the lateral distributions presented in figures 8–11 show graphically the same effect.

"DUSTPAN" SAMPLES AT VARIOUS CROSS SECTIONS

The mean cross-sectional concentrations for the "dustpan" samples collected at various cross sections near the end of the injection period are presented in table 36. These samples were collected on May 8, with the exception of those for cross section 360, which were collected on May 9. The data show that the mean concentration for the 0.125- to 0.177-mm sieve class of quartz tracer was essentially uniformly distributed longitudinally over the 540-m (1800-ft) section of the reach that was sampled. The mean concentrations for the other five sieve classes of quartz tracer decreased with distance downstream, and the rate of decrease increased with size. Large concentrations of the lead tracers were found only at cross section 15.

The mean lateral positions, $\bar{z}$, and the variances, σ_z^2, of the lateral distributions were calculated from equations 12 and 11, respectively. Most of the mean lateral positions were slightly to the left of the channel centerline; however, there was no large shift away from the centerline such as occurred in the flat-bed study (Rathbun and others, 1971).

The variances of the lateral distributions are plotted in figure 19 as a function of distance downstream from

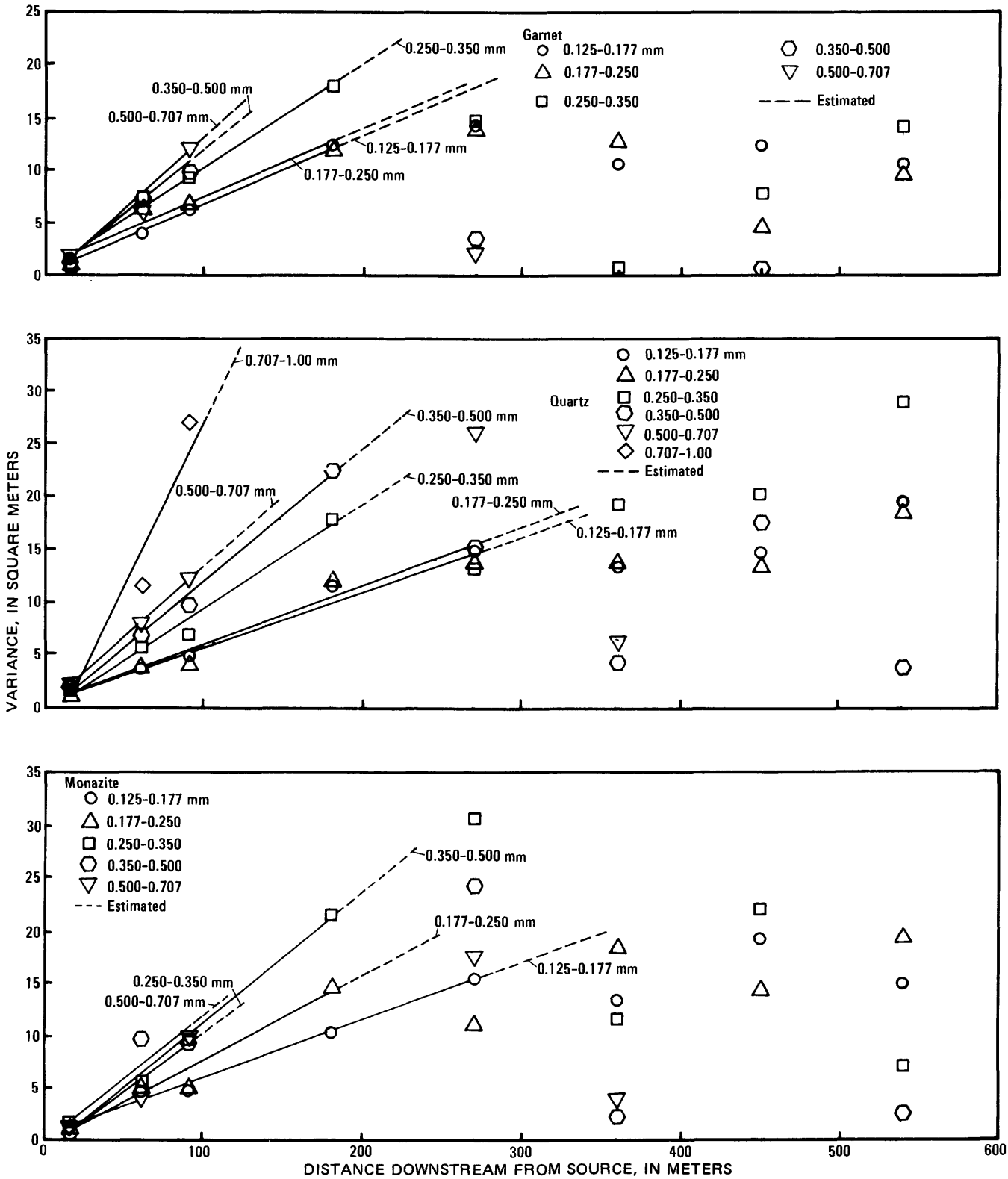

FIGURE 19. — Variation with distance downstream in the variances of the lateral distributions of the quartz, garnet, and monazite tracers as defined by "dustpan" samples collected at various cross sections on May 8.

the injection point. The lead values are not presented because large quantities of the lead tracer were found only at cross section 15. Variances for some cross sections for some sieve classes of the quartz, garnet, and monazite tracers were either zero or indeterminate because of the very small or zero concentrations of tra-

cers. The variances plotted in figure 19 were determined by the method of moments as defined by equation 11.

Two trends are evident in figure 19. First, the variances increase approximately linearly with distance for several points, then tend to fall away from the linear relation. There are at least two possible explanations for this behavior. First, reflection of the tracer particles by the banks of the channel tends to give smaller variance values than would have been obtained had the banks not been there. (See figure 7 of Lean and Crickmore (1966) for an example of this effect.) Second, the lateral distributions at the downstream cross sections were not fully developed at the time of sampling. This second explanation is supported by the fact that, with the exception of the 0.125- to 0.177-mm and 0.177- to 0.250-mm sieve classes of quartz tracer particles, the cross section at which the deviation begins corresponds to the cross section at which the mean concentration first was small. (Compare fig. 19 and table 36.) Sayre and Chang (1968) pointed out that, for lateral distributions that are approximately Gaussian, the variance can be calculated from

$$\sigma_z^2 = \frac{1}{2\pi(C_{r_{MAX}})^2}, \tag{14}$$

where $C_{r_{MAX}}$ is the maximum relative concentration for the distribution. Equation 14 has the advantage that calculated variances are not affected by the banks until the reflected tracer reaches the centerline of the channel whereas the variances calculated by the method of moments (eq. 11) are affected as soon as significant quantities of tracer reach the banks. Variances were calculated for the 0.125- to 0.177-mm and 0.177- to 0.250-mm sieve classes of quartz tracer using equation 14; the same behavior as shown in figure 19 was found, thus supporting the explanation that the downstream distributions were not fully developed.

The second trend evident in figure 19 is the tendency for the variance at a particular cross section to increase with size and, consequently, for the rate of change of the variance with distance to increase with size.

The Fickian diffusion theory (Sayre and Chang, 1968) of the dispersion of dissolved dispersants defines a lateral dispersion coefficient, K_z, as the product of a velocity and the rate of change of the variance. The recommended procedure (Sayre and Chang, 1968) for calculating K_z for dispersion from a continuous point source is

$$K_z = \frac{\overline{U}}{2}\frac{d\sigma_z^2}{dx}, \tag{15}$$

where $\overline{U}$ is the mean flow velocity, and $d\sigma_z^2/dx$ is the rate of change of the variance of the lateral distribution of the tracer with distance downstream. Analogously, a dispersion coefficient for bed-material dispersion may be defined as

$$k_z = \frac{V_p}{2}\frac{d\sigma_z^2}{dx}, \tag{16}$$

where V_p is the velocity of the tracer particles. This dispersion coefficient is for the net effect of all processes by which the particles move — that is, movement along the bed surface, saltation, and suspension, provided the particles spend at least a finite part of the time moving along the bed surface where the samples were collected.

Least-squares lines were calculated for the approximately linear range of the data for each sieve class presented in figure 19, and the slopes of these lines, $d\sigma_z^2/dx$, are presented in table 37. Also given in table 37 are the number of cross sections considered in each of the least-squares calculations. To convert the $d\sigma_z^2/dx$ values to k_z values with equation 16 requires particle velocities. The velocity values presented previously (table 35) were used for this purpose, and the calculated k_z values are summarized in table 37. The k_z values show approximately the same behavior as the velocity data plotted in figure 17 — that is, a large dependence on size for the small tracer particles and relatively little dependence for the large particles. This behavior, however, is not strictly the result of effect of the velocities because the $d\sigma_z^2/dx$ values increased considerably with the size of the tracer particles.

TABLE 37. — *Lateral dispersion parameters of the fluorescent-tracer particles determined from concentration distributions defined by "dustpan" samples collected on May 8 and 9*

Mineral	Sieve class (mm)	Number of cross sections	$d\sigma_z^2/dx$ (m^2/m)	k_z (m^2/h)	x_B (m)	x_U (m)
Quartz	0.125–0.177	5	0.0546	37.4	103	1540
	0.177–0.250	5	.0533	4.9	105	1580
	0.250–0.350	4	.100	.46	56	843
	0.350–0.500	4	.127	.12	44	664
	0.500–0.707	3	.134	.087	42	629
	0.707–1.00	3	.323	.12	17	261
Garnet	0.125–0.177	4	.0658	.30	85	1280
	0.177–0.250	4	.0637	.061	88	1320
	0.250–0.350	4	.100	.055	56	843
	0.350–0.500	3	.116	.055	48	727
	0.500–0.707	3	.133	.051	42	634
Monazite ...	0.125–0.177	5	.0549	.25	102	1540
	0.177–0.250	4	.0805	.076	70	1050
	0.250–0.350	4	123	.068	46	685
	0.350–0.500	3	.123	.068	46	685
	0.500–0.707	3	.111	.053	51	759

Sayre and Chang (1968) showed that the point at which significant tracer reaches the bank is estimated by

$$x_B \simeq 0.01\ \frac{\overline{U}B^2}{K_z}, \tag{17}$$

and the point where the tracer becomes distributed approximately uniformly across the channel is estimated by

$$x_U \simeq 0.15 \frac{\bar{U}B^2}{K_z}. \quad (18)$$

Combining equations 17 and 18 with equation 15 gives

$$x_B = 0.02\, B^2 \Big/ (d\sigma_z^2/dx), \quad (19)$$

and

$$x_U = 0.30\, B^2 \Big/ (d\sigma_z^2/dx), \quad (20)$$

These values of x are presented in table 37 also. According to these estimates, none of the sieve classes of tracer particles should have attained a uniform distribution at cross section 90. On the other hand, the x_B values indicate that significant quantities of the larger tracer particles should have reached the banks at cross section 90. This was observed, as discussed previously and as shown by the data presented in tables 12 through 31.

The x_B and x_U values show that the distances required for significant quantities of tracer to reach the bank and for uniform distributions, respectively, decreased as the size of the tracer particles increased. This indicates that the small tracer particles dispersed in the lateral direction the least amount, and the large particles the most, for the conditions prevailing for the tracer study.

The lateral dispersion coefficient is usually made nondimensional by dividing by the product of the depth of flow and the shear velocity. The mean depth of flow was 0.735 m (2.41 ft), and the shear velocity for the mean flow conditions was 0.0640 m/s (0.210 ft/s). Hence, $k_z/\bar{D}U_*$ was 0.22 for the 0.125- to 0.177-mm sieve class of quartz tracer, in good agreement with the value of 0.24 found by Fischer (1967) for the lateral dispersion of dye in the same channel for essentially the same hydraulic conditions. The nondimensional lateral dispersion parameter for the larger particles, which move predominantly by creep along the bed surface, was more than two orders of magnitude smaller. Using a mean of the k_z values for the three sieve classes of the largest quartz tracer particles and the four sieve classes each of the largest garnet and monazite tracer particles, $k_z/\bar{D}U_*$ was 0.00044.

Comparison of the two factors used in the calculation of k_z shows that the rate of change of the variance with distance for the dye was about 0.03 m²/m (0.1 ft²/ft) (Fischer, 1967, fig. 5), whereas this value for the larger tracer particles ranged from about 0.06 to 0.32 m²/m and averaged 0.13 m²/m (0.21 to 1.05 ft²/ft and averaged 0.43 ft²/ft); the mean water velocity for the dye study was 0.64 m/s (2.1 ft/s), whereas the velocities for the large tracer particles ranged from 0.77 to 1.9 m/h and averaged 1.25 m/h (2.5 to 6.2 ft/h and averaged 4.1 ft/h). Hence, the big difference in the dimensionless lateral dispersion coefficients is largely the result of the differences in velocity.

APPLICABILITY OF THE "DUSTPAN" SAMPLER TO DUNE BEDS

The correctness of sampling only the layer of material moving along the surface of the bed, when the depth of particle movement for the dune-bed form is approximately one-half the dune height, may be questioned. The "dustpan" sampler originally was designed for sampling the flat-bed condition, where most of the material in transport is concentrated in a thin layer near the bed surface (Rathbun and others, 1971). The efficiency of the sampler is not important; the significant factor is the ratio of the number of fluorescent particles of a given size to the number of nonfluorescent particles of the same size.

The conceptual models commonly used to describe the dune-bed form consider the individual particles to move in a series of steps and rest periods. The particles travel up the back of a dune and avalanche down the face into the trough, where most are buried. These particles remain buried until the dune moves by, and the particles are re-exposed; at which time, they move up the back of the dune that has just moved past, and the process is repeated. The important point, though, is that the dominant process in the movement of the dune forms is the movement of the individual particles along the surface of the dune back and down its face. A schematic diagram of this process has been presented by Grigg (1970).

The continued suspension, transport downstream, and deposition of the small sand-size particles also contributes to the downstream movement of the dune forms. These particles, however, also spend some small part of the time moving as bed load along the backs of the dunes and, hence, would be sampled by the "dustpan" sampler.

Consideration of the factors involved in the movement of dune forms suggests that sampling for fluorescent tracers in the material moving along the surface of the bed should be valid, provided that two conditions are fulfilled — (1) a continuous injection is used, and (2) enough time has elapsed that an equilibrium condition is established with respect to mixing of the particles in the depth of flow over the bed and mixing to the depth of particle movement within the bed. The previously noted agreement between sediment transport rates calculated by the steady-dilution and modified Einstein procedures supports the suggestion that the "dustpan" sampler can be used for the dune-bed condition.

CORE SAMPLES

The 0.6-m-long (2-ft-long) core samples collected during the study were used for several purposes. First, the distributions of the tracer particles among the five segments of each core sample were used to obtain information on the vertical distributions of the tracers within the dune bed. Also determined was the manner in which these distributions changed with time and position in the reach during the course of the experiment. Second, the distributions of the tracers among the segments of each sample were used to estimate the mean value of the depth of mixing, that is, the distance from the mean bed-surface elevation to the lower limit of the zone of particle movement. The distributions were also used to compute the mean centroid depth — that is, the distance from the mean bed-surface elevation to the centroid of the vertical tracer distribution. Third, the core samples collected on May 8 were used to obtain information on the lateral dispersion characteristics of the tracers. Finally, the core samples were used to determine the longitudinal distributions of the tracers on May 8, June 6, and July 14. These distributions, in turn, were used to estimate the total transport rate of bed material by the spatial-integration procedure, to compute the recovery ratios for the tracers, and to obtain information on the longitudinal dispersion characteristics of the tracers.

VERTICAL DISTRIBUTION

Vertical distributions of the tracer particles were determined for each sieve class and specific gravity of tracer material for each core sample analyzed. To demonstrate the effect of size, time, and longitudinal position on these distributions, the vertical distributions of the 0.125- to 0.177-mm, 0.250- to 0.350-mm, and 0.500- to 0.707-mm sieve classes of quartz tracers are presented on plate 1. The June 6 and July 14 samples are those from along the centerline of the channel; the May 8 samples are those nearest the channel centerline for each of the lateral distributions. In these figures, the lower abscissa is the distance downstream from the injection point for the tracers. In addition, each individual distribution has a separate abscissa to designate the concentrations of tracers. The scales of these abscissae were adjusted according to the concentrations of tracers in the segments of each sample. This procedure facilitates interpretation of the vertical distributions, but complicates somewhat the interpretation of the longitudinal distributions. However, for a discussion of the latter, the reader is referred to the section specifically concerned with the longitudinal distributions. The ordinates in these figures are the distance below the water surface. Thus, the ordinate value of the top of each distribution is the depth of flow at that particular sample point.

Plate 1*A* shows that the largest concentration of 0.125- to 0.177-mm quartz tracer particles in any one segment on May 8 was in the top segment of the sample at 60 m (200 ft) downstream from the injection point. Furthermore, all the May 8 distributions contained large concentrations of this size of quartz tracer in the upper two or three segments of the cores, with only very small concentrations in the bottom two or three segments. The large concentration in the upper segments tended to be approximately the same over the length of the reach sampled, with the exception of the sample at 450 m (1500 ft), which contained much smaller concentrations.

The largest concentration of 0.125- to 0.177-mm quartz tracer particles in any one segment on June 6 was in the fourth segment from the top in the sample at 180 m (600 ft). This concentration was somewhat less than half the largest concentration observed on May 8. Also, it was about twice the next largest concentration observed on June 6, suggesting that a large amount of the tracer had moved out of the study reach between May 8 and June 6.

The June 6 distributions between the injection point and 210 m (700 ft) show that the largest concentrations occurred in the lower segments of the cores, with relatively small concentrations in the upper segments. Downstream of 210 m (700 ft), the distributions tended to contain more tracer particles in the upper segments. However, with the exception of the sample at 420 m (1400 ft), these samples contained relatively smaller concentrations than those close to the injection point.

The largest concentration of 0.125- to 0.177-mm tracers on July 14 was in the middle segment of the sample at 390 m (1300 ft). The July 14 distributions tended to be more irregular than the June 6 distributions, with many of the former having large concentrations of tracers in only one or two segments.

Comparison of the distributions for May 8, June 6, and July 14 suggests that the general behavior of the 0.125- to 0.177-mm quartz tracer particles was to move rapidly down the channel during the injection period from May 1 to May 8, remaining largely in the upper layers of the bed. At the conclusion of the injection process, the tracers continued to move down the channel and to mix into the bed. But because of the rapid rate of movement of these tracers, a large part moved out of the study reach. Those tracers deposited at lower levels in the bed also continued to move down the channel but at a much slower rate. The result was vertical distributions that initially were weighted toward the top of the cores and final distributions that were weighted toward the center of the cores. Also, because of the random nature of the sediment movement, the vertical distributions tended to become more irregular with time.

Plate 1*B* shows that the largest concentration of 0.250- to 0.350-mm quartz tracer particles in any one segment on May 8 was in the top segment of the sample at 7.5 m (25 ft), which was the sample nearest the injection point. Furthermore, it is apparent that large concentrations of tracers were present only in the top one or two segments of the cores. An exception is the sample at 90 m (300 ft), where a large concentration was found in the middle segment. However, this sample was taken at a relatively high point in the channel, probably near a dune crest. It is also apparent that the tracer concentrations in the segments decreased rapidly downstream, with only relatively small concentrations occurring downstream from 270 m (900 ft).

On June 6 the largest concentration in any one segment was in the middle segment of the sample at 150 m (500 ft). This concentration was approximately one-tenth of the largest concentration observed on May 8. The large reduction was a result of movement downstream of the mass of tracers located between the source and 180 m (600 ft) on May 8. The June 6 distributions show that the tracer concentrations in the segments were relatively uniform down to about 600 m (2000 ft), at which point the concentrations tended to decrease. Also, the distributions between the injection point and 180 m (600 ft) contained relatively small concentrations in the upper segments with large concentrations occurring in the middle segments of the cores. At 210 and 240 m (700 and 800 ft) significant concentrations of tracers were found in all five segments. From 270 m (900 ft) to the end of the study reach at 870 m (2900 ft), the tracers again tended to be present in relatively large amounts only in the upper two or three segments of the core samples.

On July 14 the largest concentration in any one segment was in the fourth segment from the top of the sample at 90 m (300 ft). This concentration was actually slightly larger than the largest concentration observed on June 6. However, other segments of this sample contained only very small concentrations. The other July 14 distributions between the injection point and 210 m (700 ft) show the continuing depletion of the 0.250- to 0.350-mm quartz tracers in the upper segments of these samples. At 270, 330, and 390 m (900, 1100, and 1300 ft), the distributions tended to have the largest concentrations near the middle of the cores. However, from 450 m (1500 ft) to the end of the study reach, the tracers again tended to be concentrated in the upper two or three segments of the samples.

The general behavior of the 0.250- to 0.350-mm quartz tracer particles was similar to that of the 0.125- to 0.177-mm particles, with the important difference that changes occurred much more slowly for the 0.250- to 0.350-mm particles.

Plate 1*C* shows that on May 8 significant concentrations of the 0.500- to 0.707-mm quartz tracers were found only between the injection point and the point 90 m (300 ft) downstream. The largest concentration in any one segment was in the top segment of the core sample at 7.5 m (25 ft). Significant concentrations were found only in the top two or three segments of the cores.

On June 6 significant concentrations of the 0.500- to 0.707-mm quartz tracers were found between the injection point and the point 480 m (1600 ft) downstream. The largest concentration in any one segment was in the middle segment of the sample at 180 m (600 ft). This concentration was about one-tenth of the largest concentration observed on May 8. The general tendency was for the large concentrations of tracers to be in the upper two or three segments. This was particularly true for the samples downstream from 300 m (1000 ft). The samples at 30, 60, and 90 m (100, 200, and 300 ft) contained relatively few tracers in the top segment. The samples between 120 and 270 m (400 and 900 ft) contained tracers in most of the segments.

On July 14 the largest concentration in any one segment was in the middle segment of the sample at 30 m (100 ft), and, as for the 0.250- to 0.350-mm tracers, this concentration was larger than the largest concentration observed on June 6. The July 14 distributions show that the samples at 30 and 90 m (100 and 300 ft) contained essentially no tracers in the top two segments, that the samples at 150 and 210 m (500 and 700 ft) contained relatively large amounts in the top two segments, and that from this point on downstream large concentrations were found only in the top two or three segments.

The general behavior of the 0.500- to 0.707-mm quartz tracer particles was similar to that of the 0.250- to 0.350-mm particles except that changes occurred much more slowly for the 0.500- to 0.707-mm particles.

This discussion of the behavior of the three sizes of quartz tracer particles pointed out the tendency, particularly just downstream from the injection point, for the tracers to be concentrated initially in the upper layers of the bed, whereas in samples collected at later times, the large concentrations tended to be in the lower segments. There are at least two factors that could contribute to the development of these types of vertical distributions. The first factor is the slow rate of movement of sediment particles for the dune-bed form, with the result that the establishing of a vertical distribution that is in equilibrium with the flow conditions and injection rate may take an extremely long time. With the cessation of injection on May 8, those tracer particles in the upper more mobile layers of the bed moved on down the reach, whereas those in the lower layers moved at a slower rate. This is not to imply that there are two separate groups of particles; on the con-

trary, there is continual exchange of particles among all levels of the bed, and it is this exchange which is the essence of the movement of the dune-bed form. The large decrease in concentration between May 8 and June 6 suggests that vertical equilibrium had not been established, and this decrease probably was a result of the bulk of the tracers moving on downstream. Between June 6 and July 14 changes in concentration were considerably smaller, and in some instances increases actually occurred at specific locations, pointing to the stochastic nature of sediment movement.

The second factor is the possibility that decreasing flow conditions resulted in the entrapment of tracers in layers of the bed not in motion. As pointed out previously and as the data presented in table 6 show, the water discharge fluctuated during the injection period, then decreased steadily to the end of the experiment. Because the sediment-transport rate is dependent on the hydraulic conditions, some of the tracers may have been trapped by the decreasing transport conditions. Comparison of the June 6 and July 14 distributions at specific locations reveals no persistent layers of tracer material. This comparison, however, does not eliminate the possibility that burial of some of the tracers occurred at some time after June 6 and persisted until just before the sampling on July 14.

DEPTH OF MIXING

The vertical distributions of the tracers were used to estimate $\bar{d}_m$, the mean value of the depth of mixing of the tracer particles in the bed. This method and two other methods — one based on depth-sounding records of the bed and the other based on the conservation of the tracer particles — were used by Hubbell and Sayre (1964) for radioactive tracers. The same methods, with one qualification necessary for the method based on the conservation of the tracer particles, may be used for fluorescent particles.

The first method consists of looking at a large number of core samples that have been divided into segments and determining by inspection the maximum depth to which tracer particles have moved. Then the mean value of the depth of mixing with respect to the mean bed-surface elevation is given by

$$\bar{d}_m = \frac{1}{N} \sum_{j=1}^{N} (D_j + d_{m_j} - \bar{D}) , \qquad (21)$$

where D_j is the depth of flow at the sample point, $\bar{D}$ is the mean depth of flow for the study reach at the time of sampling, d_{m_j} is the maximum depth in the core sample to which tracer particles are mixed, and N is the total number of core samples considered.

Equation 21 was applied to each sieve class of each of the four minerals for each of three dates on which core samples were collected. The most difficult problem in using equation 21 was the determination of d_{m_j} from inspection of the particle counts for the five segments of each core sample. This determination was complicated by the fact that the distribution of tracers among the segments of the core samples was very irregular and in general had no continuous distribution pattern in the vertical direction. Similar results were found with radioactive tracers by Hubbell and Sayre (1964) and Crickmore (1967).

Two somewhat arbitrary decisions were necessary in determining the depth of mixing. First, it was necessary to decide if the sample contained a sufficient number of particles to permit a valid determination of d_{m_j}. In general, a sample was not considered if the five segments contained a total of less than 10 fluorescent particles of the sieve class and specific gravity under consideration, except when the 10 particles were all in one or two segments of the sample. Second, it was necessary to decide what the lower limit of mixing was for the fluorescent tracers. Because of the extreme sensitivity of the fluorescent tracer procedure, concentrations as small as 10^{-7} for the 0.125- to 0.177-mm sieve class are detectable for the size of samples obtained in this study. Hence, the procedure used was to neglect the lower of two adjacent segments when they had small counts with respect to the upper segments; for example, if the middle segment contained 300 fluorescent particles, the next segment 5, and the bottom 3 particles, then the 3 particles were disregarded in determining the depth of mixing. This procedure tends to make the d_{m_j} values smaller than they would be if all the fluorescent particles were considered.

Two other factors should be considered also. Because each core was divided into only five segments, the possibility exists that the lower limit of the tracer distribution may have been near the upper edge of the segment, thus giving a depth of mixing almost 0.12 m (0.40 ft) too great. In another sample, however, the lower limit of the distribution might be near the bottom of the segment, thus giving a nearly correct depth of mixing. Because a large number of samples was used in the determination of $\bar{d}_m$, one might expect these effects to be averaged, thus giving a $\bar{d}_m$ that is about 0.06 m (0.2 ft) too great. On the other hand, the lower limit of the tracer distributions in many of the samples, particularly on June 6 and July 14, was in the bottom core; hence, the possibility existed that the tracers may have been mixed to greater depths than those sampled. These two factors would tend to compensate for each other. Thus, it was decided to use the bottom of the deepest segment that contained a significant number of tracer particles as the depth of mixing for that particular sample.

Mean values of the depth of mixing for the various sieve classes and specific gravities of tracers and the

three sample dates are presented in table 38. To determine if significant differences existed among these mean values, the technique of analysis of variance and the F test (Bennett and Franklin, 1954) was used.

TABLE 38. — *Mean values of the depth of mixing for the various sieve classes of the quartz, garnet, monazite, and lead tracers as determined from core samples collected on May 8, June 6, and July 14*

Mineral	Sieve class (mm)	$\bar{d}_m$ (m) May 8	June 6	July 14
Quartz	0.125–0.177	0.52	0.58	0.58
	0.177–0.250	.52	.58	.58
	0.250–0.350	.49	.58	.58
	0.350–0.500	.49	.58	.58
	0.500–0.707	.49	.55	.55
	0.707–1.00	.43	.43	.43
Garnet	0.125–0.177	.43	.55	.55
	0.177–0.250	.46	.55	.55
	0.250–0.350	.46	.52	.55
	0.350–0.500	.49	.52	.49
	0.500–0.707	.46	.46	.52
Monazite	0.125–0.177	.46	.55	.55
	0.177–0.250	.46	.52	.55
	0.250–0.350	.46	.49	.49
	0.350–0.500	.43	.49	.49
	0.500–0.707	.46	.46	.43
Lead	0.125–0.177	.37	.43	.37
	0.177–0.250	.34	.43	.46
	0.250–0.350	.43	.46	.43
	0.350–0.500	.40	.46	.40

The procedure consisted of first testing the depth of mixing values of all the sieve classes for a specific mineral. If significant differences existed, then the value that was most different from the mean was excluded, and the test was repeated. Also tested were the depth of mixing values for various combinations of the minerals and sieve classes. Results of the analysis of variance are presented in table 39.

The depth of mixing values for the largest of the quartz and monazite tracers were significantly smaller than the values for the other sizes of these tracers. Similarly, the values for all four sieve classes of lead tracer were significantly smaller than the values for comparable sizes of the other tracers. Thus, the heavy and (or) large particles tended to move in layers that were thinner than were the layers for the quartz particles comprising most of the bed material in transport. These observations for the heavy particles are in qualitative agreement with the work of Brady and Jobson (1972) who studied, for the dune-bed condition in a laboratory flume, the movement of the magnetite in a natural river sand. They found that the magnetite tended to form patches of large concentrations on the backs and crests of the dunes, suggesting that the magnetite moved in the upper part of the zone of movement for the dune-bed form.

TABLE 39. — *Results of the analysis of variance of the depth of mixing values for the fluorescent tracers as defined by core samples collected on May 8, June 6, and July 14*

Date	Minerals and sieve classes included[a]	Variance ratio, F	$F_{\nu_1, \nu_2, \alpha}$ [b]
May 8	Q1–Q6	3.09	$F_{5,508,0.005} = 3.35$
	Q1–Q5	1.22	$F_{4,461,0.05} = 2.37$
	G1–G5	.67	$F_{4,407,0.05} = 2.37$
	M1–M5	.23	$F_{4,384,0.05} = 2.37$
	L1–L4	2.12	$F_{3,190,0.05} = 2.60$
	Q6, L1–L4	2.36	$F_{4,237,0.05} = 2.37$
	All except Q6	4.98	$F_{18,1442,0.005} = 2.06$
	Q1–Q5, G1–G5, M1–M5	2.29	$F_{14,1252,0.005} = 2.24$
	G1–G5, M1–M5	.40	$F_{9,791,0.05} = 1.88$
June 6	Q1–Q6	9.68	$F_{5,415,0.005} = 3.35$
	Q1–Q5	.97	$F_{4,383,0.05} = 2.37$
	G1–G5	2.30	$F_{4,354,0.05} = 2.37$
	M1–M5	4.45	$F_{4,342,0.005} = 3.72$
	M1–M4	2.45	$F_{3,298,0.05} = 2.60$
	L1–L4	.09	$F_{3,87,0.05} = 2.71$
	Q1–Q5, G1–G5, M1–M4, L1–L4	5.88	$F_{17,1122,0.005} = 2.10$
	Q1–Q5, G1–G2, M1–M2	2.52	$F_{7,639,0.01} = 2.64$
	Q6, G5, M5, L1–L4	.21	$F_{6,194,0.05} = 2.10$
July 14	Q1–Q6	7.74	$F_{5,247,0.005} = 3.35$
	Q1–Q5	.95	$F_{4,219,0.05} = 2.37$
	G1–G5	1.41	$F_{4,202,0.05} = 2.37$
	M1–M5	4.81	$F_{4,197,0.005} = 3.72$
	M1–M4	3.10	$F_{3,169,0.025} = 3.12$
	L1–L4	.67	$F_{3,60,0.05} = 2.76$
	Q1–Q5, G1–G3, M1, M2	1.56	$F_{9,439,0.05} = 1.88$
	Q6, M3–M5, L1–L4	1.30	$F_{7,197,0.05} = 2.01$
	Q6, G4, G5, M3–M5, L1–L4	2.07	$F_{9,267,0.025} = 2.11$

[a] Q, G, M, and L denote quartz, garnet, monazite, and lead, respectively; 1, 2, 3, 4, 5, and 6 denote the 0.125- to 0.177-mm, 0.177- to 0.250-mm, 0.250- to 0.350-mm, 0.350- to 0.500-mm, 0.500- to 0.707-mm, and 0.707- to 1.00-mm sieve classes, respectively.

[b] Values for $F_{\nu_1, \nu_2, \alpha}$ from table IV of Bennett and Franklin (1954).

The Student's *t* test (Bennett and Franklin, 1954) was used to determine whether significant differences existed among mean values of the depth of mixing for May 8, June 6, and July 14. Mean values for groups of sieve classes were compared in pairs and results are presented in table 40.

The May 8–June 6 and May 8–July 14 comparisons, with the exception of the May 8–July 14 comparison for the lead tracer particles, show that the mean depths of mixing for June 6 and July 14 were significantly larger than for May 8 at the 0.005 level of significance. The June 6–July 14 comparisons show that the mean depths for these dates were not significantly different at the 0.05 level of significance. Thus, the depth of mixing increased significantly between May 8 and June 6

TABLE 40. — *Results of the Student's t test of the mean values of the depth of mixing for the fluorescent tracers as defined by core samples collected on May 8, June 6, and July 14*

Dates, minerals, and sieve classes[a]	Confidence limits for difference of means[b]		Significance level
May 8, Q1–Q5: June 6, Q1–Q5	0.26	±0.086	0.005
May 8, Q1–Q5: July 14, Q1–Q5	0.26	±0.10	.005
June 6, Q1–Q5: July 14, Q1–Q5	0.0083	±0.066	.05
May 8, G1–G5: June 6, G1–G5	0.23	±0.10	.005
May 8, G1–G5: July 14, G1–G5	0.26	±0.12	.005
June 6, G1–G5: July 14, G1–G5	0.030	±0.078	.05
May 8, M1–M5: June 6, M1–M4	0.21	±0.11	.005
May 8, M1–M5: July 14, M1–M3	0.22	±0.15	.005
June 6, M1–M4: July 14, M1–M3	0.010	±0.090	.05
May 8, L1–L4: June 6, L1–L4	0.20	±0.21	.005
May 8, L1–L4: July 14, L1–L4	0.11	±0.17	.05
June 6, L1–L4: July 14, L1–L4	0.089	±0.21	.05
May 8, Q1–Q5: June 6, Q1–Q5, G1–G5: G1–G2, M1–M5: M1–M2	0.30	±0.063	.005
June 6, Q1–Q5: July 14, Q1–Q5, G1–G2: G1–G3, M1–M2: M1–M2	0.0051	±0.048	.05

[a] Q, G, M, and L denote quartz, garnet, monazite, and lead, respectively; 1, 2, 3, 4, 5, and 6 denote the 0.125- to 0.177-mm, 0.177- to 0.250-mm, 0.250- to 0.350-mm, 0.350- to 0.500-mm, 0.500- to 0.707-mm, and 0.707- to 1.00-mm sieve classes, respectively.

[b] Mean values are not significantly different at the indicated significance level if the confidence limits for the difference of the means include zero (Bennett and Franklin, 1954).

but did not change significantly between June 6 and July 14.

The second method for determining the depth of mixing, $\bar{d}_m$, is based on an analysis of a sonic depth-sounding record of the longitudinal profile of the bed surface. The record is divided into sections beginning at the upstream end. The first section l_1, extends from the first dune trough on the record to the next trough downstream that is at a lower bed elevation. The second section extends from this trough downstream to the next trough that is at a lower bed elevation and so on until the complete record is sectioned. The mean bed-surface elevation is determined for the total record, and the difference between the mean bed-surface elevation and the trough elevation gives the depth of mixing for that section. The mean value of the depth of mixing for the reach is the weighted average of the values for the sections given by

$$\bar{d}_m = \frac{1}{L} \sum_{i=1}^{n_s} l_i d_{m_i}, \qquad (22)$$

where L is the length of the reach, l_i is the length of the ith section, d_{m_i} is the depth of mixing for the ith section, and n_s is the number of sections. The number of bed profiles obtained during the fluorescent tracer study was limited and the quality was poor because of equipment difficulties. Only one record obtained on May 7 along the centerline between the injection point and cross section 360 was analyzed, and a depth of mixing of 0.31 m (1.02 ft) was obtained.

The third method for determining the depth of mixing, $\bar{d}_m$, is based on the conservation of the tracer particles. The equation is

$$\bar{d}_m = \frac{W}{B(1-\lambda)\gamma_s \int_0^\infty C dx}, \qquad (23)$$

where W is the weight of tracer particles injected, B is the channel width, λ is the fraction of the volume of the bed not occupied by the bed-material particles, γ_s is the specific weight of the bed material, and

$$\int_0^\infty \bar{C} dx$$

is the area under the longitudinal distribution curve for the tracer particles. This method differs for fluorescent and radioactive tracers. For radioactive tracers the integral term can be determined from in situ activity measurements with radiation detectors. For fluorescent tracers core samples are necessary to determine the integral term; hence, the mean value of the depth of mixing in effect must be known to permit determination of the concentrations.

The centroid depth, which is the distance from the mean bed-surface elevation to the centroid of the vertical distribution of the tracer material, was also determined from the vertical distributions of the tracers. The mean value of the centroid depth was calculated from

$$\bar{d} = \frac{1}{N}\left[\sum_{j=1}^{N} D_j - \bar{D} + \frac{\sum_{k=1}^{5} d_k n_k}{\sum_{k=1}^{5} n_k}\right], \qquad (24)$$

where d_k is the distance from the top of the core to the center of the kth segment, that is 0.06, 0.18, 0.30, 0.42, and 0.54 m (0.2, 0.6, 1.0, 1.4, and 1.8 ft), respectively, for the five 0.12-m-thick (0.4-ft-thick) segments, and n_k is the number of fluorescent particles in the kth segment.

The mean value of the centroid depth was calculated from equation 24 for each sieve class of each of the four minerals for May 8, June 6, and July 14. The basic raw data were used in these calculations — that is, small numbers of fluorescent particles in the bottom segments were not neglected as was done in the determination of the depth of mixing. This procedure was possible because the centroid depth is weighted with respect to the number of particles and hence small numbers do not contribute substantially to the summation in equation 24; on the other hand, the depth of mixing is based strictly on the presence or absence of particles in a specific segment of the sample.

Mean values of the centroid depth, $\bar{d}$, for the various sieve classes and specific gravities of tracers and the

three sample dates are presented in table 41. To determine if significant differences existed among these mean values, the technique of analysis of variance, as was used for the depth of mixing, was used.

Results of the analysis of variance of the centroid depths are presented in table 42. Few differences were found among the centroid depths for each of the three sampling dates. For May 8 it was necessary to exclude the depths for the 0.500-to 0.707-mm sieve class of garnet tracer and the 0.250- to 0.350-mm and 0.350- to 0.500-mm sieve classes of lead tracers to have no significant differences at the 0.05 level. For June 6 it was necessary to exclude the depths for the 0.125- to 0.177-mm sieve class of quartz tracer and the 0.250- to 0.350-mm and 0.350- to 0.500-mm sieve classes of lead tracers to have no significant differences at the 0.05 level. For July 14 it was necessary to exclude only the depth for the 0.125- to 0.177-mm sieve class of quartz tracer to have no significant differences at the 0.05 level.

TABLE 41. — *Mean values of the centroid depths of the vertical distributions of fluorescent tracers as defined by core samples collected on May 8, June 6, and July 14*

Mineral	Sieve class (mm)	$\bar{d}$ (m) May 8	June 6	July 14
Quartz	0.125–0.177	0.18	0.27	0.31
	0.177–0.250	.16	.24	.29
	0.250–0.350	.16	.21	.25
	0.350–0.500	.17	.23	.24
	0.500–0.707	.18	.22	.23
	0.707–1.00	.19	.23	.25
Garnet	0.125–0.177	.19	.24	.27
	0.177–0.250	.18	.22	.26
	0.250–0.350	.19	.22	.26
	0.350–0.500	.20	.25	.26
	0.500–0.707	.23	.25	.29
Monazite	0.125–0.177	.16	.20	.27
	0.177–0.250	.16	.20	.26
	0.250–0.350	.18	.23	.25
	0.350–0.500	.18	.23	.26
	0.500–0.707	.21	.24	.26
Lead	0.125–0.177	.18	.26	.25
	0.177–0.250	.18	.25	.28
	0.250–0.350	.25	.29	.28
	0.350–0.500	.26	.27	.27

TABLE 42. — *Results of the analysis of variance of the centroid depths of the vertical distributions of fluorescent tracers as defined by core samples collected on May 8, June 6, and July 14*

Date	Minerals and sieve classes included[a]	Variance ratio, F	$F_{\nu_1, \nu_2, \alpha}$[b]
May 8	Q1–Q6	0.90	$F_{5,508,0.05} = 2.21$
	G1–G5	1.64	$F_{4,407,0.05} = 2.37$
	M1–M5	1.93	$F_{4,389,0.05} = 2.37$
	L1–L4	5.67	$F_{3,190,0.005} = 4.28$
	L1, L2	.04	$F_{1,111,0.05} = 3.27$
	L3, L4	.09	$F_{1,79,0.05} = 3.96$
	Q1–Q6, G1–G5, M1–M5, L1, L2	1.67	$F_{17,1410,0.025} = 1.77$
	Q1–Q6, G1–G4, M1–M5, L1, L2	1.07	$F_{16,1357,0.05} = 1.64$
June 6	Q1–Q6	3.13	$F_{5,415,0.05} = 2.21$
	Q2–Q6	.91	$F_{4,329,0.05} = 2.37$
	G1–G5	1.23	$F_{4,354,0.05} = 2.37$
	M1–M5	1.78	$F_{4,342,0.05} = 2.37$
	L1–L4	.35	$F_{3,87,0.05} = 2.71$
	Q2–Q6, G1–G5, M1–M5, L1–L4	1.65	$F_{18,1112,0.025} = 1.60$
	Q2–Q6, G1–G5, M1–M5, L1, L2	1.29	$F_{16,1075,0.05} = 1.64$
July 14	Q1–Q6	2.81	$F_{5,247,0.01} = 3.02$
	Q2–Q6	1.38	$F_{4,205,0.05} = 2.37$
	G1–G5	.43	$F_{4,202,0.05} = 2.37$
	M1–M5	.20	$F_{4,197,0.05} = 2.37$
	L1–L4	.13	$F_{3,60,0.05} = 2.76$
	Q2–Q6, G1–G5, M1–M5, L1–L4	.55	$F_{18,662,0.05} = 1.60$

[a] Q, G, M, and L denote quartz, garnet, monazite, and lead, respectively; 1, 2, 3, 4, 5, and 6 denote the 0.125- to 0.177-mm, 0.177- to 0.250-mm, 0.250- to 0.350-mm, 0.350- to 0.500-mm, 0.500- to 0.707-mm, and 0.707- to 1.00-mm sieve classes, respectively.

[b] Values for $F_{\nu_1, \nu_2, \alpha}$ from table IV of Bennett and Franklin (1954).

The Student's *t* test (Bennett and Franklin, 1954) was used to determine if significant differences existed among mean values of the centroid depth for May 8, June 6, and July 14. Mean values for groups of sieve classes were compared in pairs and results are presented in table 43.

All the comparisons for the three sampling dates, with the exception of three comparisons for the lead tracers, showed significant differences at the 0.005 level. Thus, the results of the statistical tests show that the centroid depths for the quartz, garnet, and monazite tracers increased with time throughout the study. This is in contrast with the depths of mixing which increased between May 8 and June 6 but did not change significantly between June 6 and July 14. These observations suggest that the lower limit of particle movement essentially had been established prior to June 6, whereas the centroids of the vertical distributions of the tracer particles apparently were still moving downward at the end of the study on July 14.

Another explanation for the increase of the centroid depths between June 6 and July 14 is possible, however. The water discharge, and consequently the sediment transport rate, decreased considerably toward the end of the study. Thus, lower regions of the bed that previously had been involved in the transport process may no longer have been in motion. Because tracers were deposited in these regions of the bed by the higher flow and transport conditions, a layer of bed material con-

TABLE 43. — *Results of the Student's* t *test of the mean values of the centroid depths of the vertical distributions of fluorescent tracers as defined by core samples collected on May 8, June 6, and July 14*

Dates, minerals, and sieve classes[a]	Confidence limits for difference of means[b]	Significance level
May 8, Q1–Q6: June 6, Q2–Q6	0.17±0.067	0.005
May 8, Q1–Q6: July 14, Q2–Q6	0.26±0.081	.005
June 6, Q2–Q6: July 14, Q2–Q6	0.085±0.091	.005
May 8, G1–G5: June 6, G1–G5	0.12±0.076	.005
May 8, G1–G5: July 14, G1–G5	0.24±0.090	.005
June 6, G1–G5: July 14, G1–G5	0.11±0.090	.005
May 8, M1–M5: June 6, M1–M5	0.14±0.073	.005
May 8, M1–M5: July 14, M1–M5	0.28±0.088	.005
June 6, M1–M5: July 14, M1–M5	0.13±0.089	.005
May 8, L1–L2; June 6, L1–L4	0.28±0.17	.005
May 8, L1–L2: July 14, L1–L4	0.28±0.21	.005
June 6, L1–L4: July 14, L1–L4	0.01±0.17	.05
May 8, L3–L4: June 6, L1–L4	0.04±0.14	.05
May 8, L3–L4: July 14, L1–L4	0.04±0.16	.05
May 8, Q1–Q6: June 6, Q2–Q6, G1–G4: G1–G5, M1–M5: M1–M5, L1–L2: L1–L2	0.16±0.04	.005
May 8, Q1–Q6: July 14, Q2–Q6, G1–G4: G1–G5, M1–M5: M1–M5, L1–L2: L1–L4	0.27±0.05	.005
June 6, Q2–Q6: July 14, Q2–Q6, G1–G5: G1–G5. M1–M5, M1–M5: L1–L2; L1–L4	0.11±0.05	.005

[a] Q, G, M, and L denote quartz, garnet, monazite, and lead, respectively; 1, 2, 3, 4, 5, and 6 denote the 0.125- to 0.177-mm, 0.177- to 0.250-mm, 0.250- to 0.350-mm, 0.350- to 0.500-mm, 0.500- to 0.707-mm, and 0.707- to 1.00-mm sieve classes, respectively.

[b] Mean values are not significantly different at the indicated significance level if the confidence limits for the difference of the means include zero (Bennett and Franklin, 1954)

taining tracer particles, but which was no longer in motion, may have been formed. Under these circumstances, the depth of mixing as indicated by the core samples would not change, as was found (table 38); but the centroid depth would appear to increase because the tracer particles still in motion moved on down the channel and out of the study reach, whereas the layer of particles not in motion remained, lowering the centroid of the vertical distribution. This effect should be greatest for the small particles because they move the fastest (figure 44). A consideration of the increase of the $\bar{d}$ values between June 6 and July 14 shows that, with the exception of the lead particles, the increases in general are largest for the small particles, thus supporting the hypothesis.

The ratio, R, of the centroid depth to the depth of mixing was used as an index of the vertical concentration gradient by Hubbell and Sayre (1965). For a concentration distribution that is uniform, $R = 0.5$; for a concentration distribution that has the larger part of the tracers in the upper part of the sample, $R < 0.5$; and for a concentration distribution that has the larger part of the tracers in the bottom part of the sample, $R > 0.5$. Courtois and Sauzay (1966) computed values of the

TABLE 44. — *Values of the ratio* R *of the centroid depth to the depth of mixing for the vertical distributions of fluorescent tracers as defined by core samples collected on May 8, June 6, and July 14*

Mineral	Sieve class (mm)	R		
		May 8	June 6	July 14
Quartz	0.125–0.177	0.35	0.47	0.53
	0.177–0.250	.31	.41	.50
	0.250–0.350	.33	.36	.43
	0.350–0.500	.35	.40	.41
	0.500–0.707	.37	.40	.42
	0.707–1.00	.44	.53	.58
Garnet	0.125–0.177	.44	.44	.49
	0.177–0.250	.39	.40	.47
	0.250–0.350	.41	.42	.47
	0.350–0.500	.41	.48	.53
	0.500–0.707	.50	.54	.56
Monazite	0.125–0.177	.35	.36	.49
	0.177–0.250	.35	.38	.47
	0.250–0.350	.39	.47	.51
	0.350–0.500	.42	.47	.53
	0.500–0.707	.46	.52	.60
Lead	0.125–0.177	.49	.60	.68
	0.177–0.250	.53	.58	.61
	0.250–0.350	.58	.63	.65
	0.350–0.500	.65	.59	.68

ratio for five types of distributions and found that R was between 0.33 and 0.50 for all five. These five included a uniform distribution, a linear distribution decreasing from the maximum concentration at the surface of the bed, two types of parabolic distributions with the maximum concentration at the surface of the bed, and a parabolic distribution with the maximum concentration at some fraction of the depth of mixing below the bed surface. They suggested, therefore, that the depth of mixing could be replaced in the sediment transport equation by $2.5\,\bar{d}$, with a maximum error on the order of 25 percent. This procedure thereby circumvents the previously discussed difficulties that are involved in estimating the true lower limit of the zone of movement for determining the depth of mixing.

Values of the ratio for the various sieve classes of tracer and the three sample dates are presented in table 44. The ratio values in general increased with time, probably because the centroid depths increased with time. The quartz, garnet, and monazite ratios for May 8 ranged from 0.31 to 0.50, indicating that most of the distributions were weighted toward the bed surface. The ratios for June 6 and July 14 were larger and, in several instances, exceeded the 0.50 of a uniform distribution. Most of the ratios larger than 0.50 were for the lead particles and the largest of the quartz, garnet, and monazite particles. Thus, the vertical distributions for these particles tended to be weighted toward the bottom of the zone of movement — that is, concentrated in the lower regions, rather than uniformly distributed over the depth of movement. The ratio values for July 14 for the 0.125- to 0.177-mm and 0.177- to 0.250-mm sieve classes of quartz tracer were larger than might be expected in comparison with the values

for the other sieve classes. However, these values were probably large because the $\bar{d}$ values for these sieve classes were larger than for the other sieve classes, for reasons discussed previously.

CORE-SAMPLE CONCENTRATIONS

In previous sections, the vertical distributions of the tracers within the different core samples were discussed. From this point on, the variations with lateral and longitudinal positions and with time of the concentrations of the fluorescent tracers as determined from the core samples will be discussed.

Before computing concentrations of fluorescent tracers from the results of the analysis of the core samples, it is necessary first to consider the problem of how to treat the bottom limit of the cores. Because of the irregular nature of the dune bed and the constant 0.6-m (2-ft) length of the sampler (fig. 5), samples to varying depths below the mean bed elevation were obtained. The depth of flow at the sampling points for the 115 core samples collected on May 8 ranged from 0.6 to 1.1 m (2.0 to 3.6 ft) and averaged 0.79 m (2.6 ft). On June 6 the depth of flow at the sampling points for the 87 samples ranged from 0.52 to 1.0 m (1.7 to 3.3 ft) and averaged 0.73 m (2.4 ft). On July 14 the depth for the 45 samples collected ranged from 0.34 to 0.82 m (1.1 to 2.7 ft) and averaged 0.52 m (1.7 ft). The variation of the bed-surface elevation with longitudinal position may also be seen in the vertical concentration distributions presented on plate 1.

In theory, sampling depth should be just to the lower limit of the zone of particle movement. This lower limit, however, undoubtedly varies with time and position in the reach. However, in the calculations in this report, the lower limit of the zone of particle movement was assumed on the average to be a plane parallel to the water surface. This assumption should be valid so long as equilibrium flow conditions (as defined, for example, by Simons and Richardson, 1966, p. J3) exist in the channel.

To correct the core samples to the lower limit of the zone of movement, the following procedure was used. First, the depth of mixing was determined, as described previously, for each sieve class of each of the four minerals for each core sample analyzed. Second, the mean value of the depth of mixing was determined from the values obtained in step 1 for each of the three sampling dates (May 8, June 6, July 14). Third, the concentration distribution for each core sample was extrapolated or truncated to a distance below the mean bed-surface elevation equal to the mean value of the depth of mixing for the specific sieve class of mineral under consideration. The extrapolations and truncations were to the nearest 0.03 m (0.1 ft). Estimates of the weight of material in the truncated or extrapolated parts were on a proportional basis — that is, if a segment were truncated at the mid-point, the retained part was assumed to contain half the material; if the segment were extrapolated half the thickness of a segment, the extrapolated part was assumed to contain half as much material as was contained in the segment just above the extrapolated portion. Estimates of the number of tracer particles were made on the basis of the particle distributions in all the segments of the core sample above the truncated or extrapolated part.

The concentration of fluorescent tracers in each core sample was calculated from

$$C = \frac{1}{N_p} \frac{\sum_{k=1}^{k=5} n_k}{\sum_{k=1}^{k=5} w_k}, \tag{25}$$

where n_k is the number of fluorescent particles of a particular sieve class for a particular mineral in the k th segment of the core sample, w_k is the weight in grams of all material in that sieve class in the k th segment, and N_p is the particles per gram factor for that sieve class and mineral (table 5). The summation in equation 25 was generally not over precisely five segments because of the extrapolation or truncation of the concentration distributions of the core samples.

LATERAL DISTRIBUTIONS

Lateral distributions of the fluorescent tracers were determined from the May 8 core samples for cross sections 7.5, 15, 30, 60, 90, 180, 270, 360, 450, and 540. The distributions for the 0.125- to 0.177-mm sieve classes of quartz, garnet, and monazite are presented in figures 20, 21, and 22, respectively, as examples. The concentrations plotted in the figures are relative concentrations—that is, each concentration has been divided by the area under the lateral distribution curve. The defining equation is

$$C_r(z) = \frac{C(z)}{\int_0^B C(z)\, dz}, \tag{26}$$

Several trends are evident in figures 20–22. First, the distributions for the cross sections near the injection point were approximately Gaussian, whereas the distributions for the cross sections farther downstream tended to be more rounded and also more irregular. The increased irregularity was probably because the distributions at the downstream cross sections were not fully developed, whereas the increased roundness was a result of the increased lateral spread or dispersion of the particles with distance downstream. Second, the peak relative concentration decreased with distance

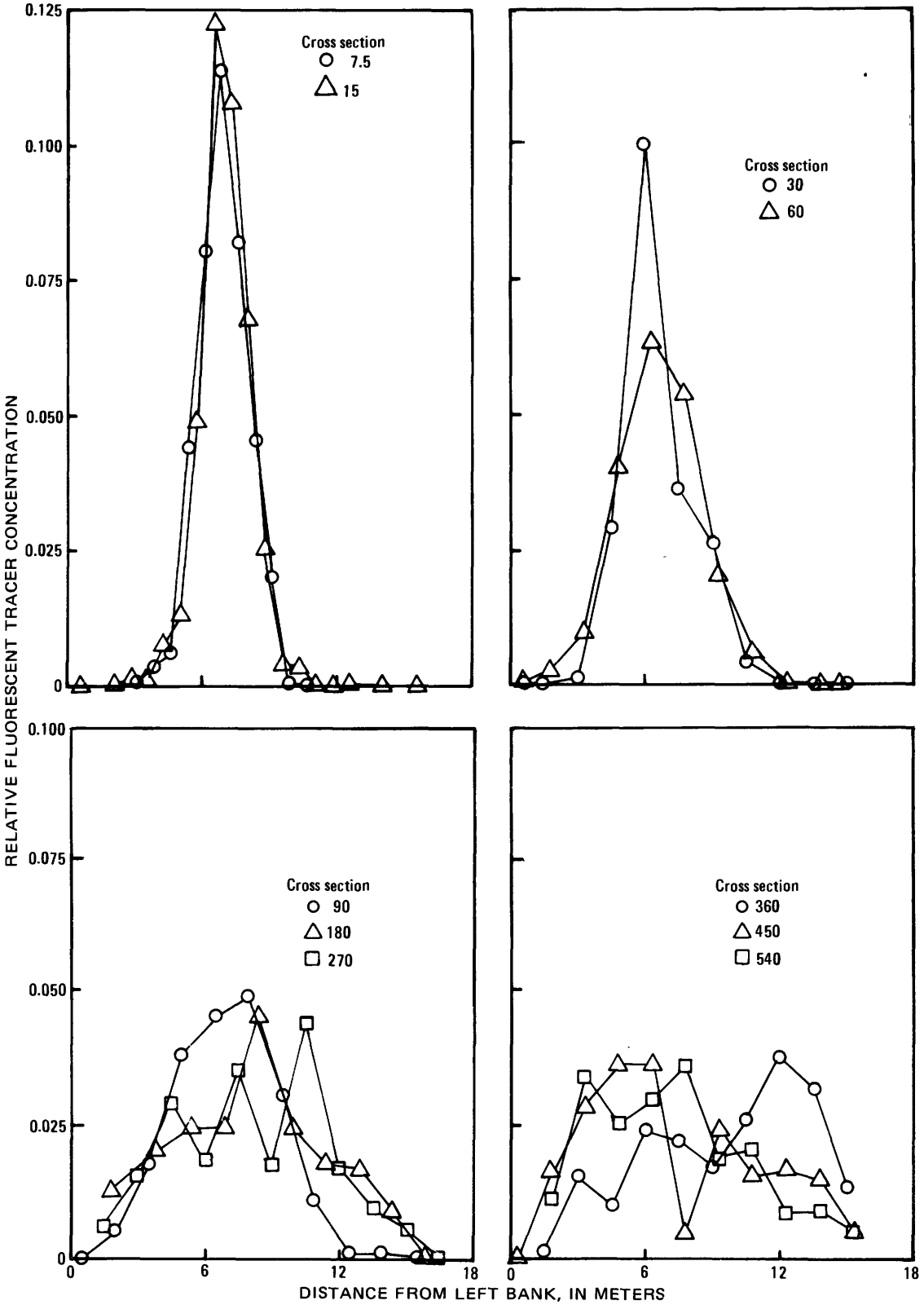

FIGURE 20. — Variation with distance downstream in the lateral distributions of relative concentrations of the 0.125- to 0.177-mm sieve class of quartz tracers as defined by core samples collected on May 8.

downstream because of the increased lateral spread. Third, the lateral distributions for the cross sections between the source and cross section 90 tended to have mean lateral positions 0.9 to 1.5 m (3 to 5 ft) to the left

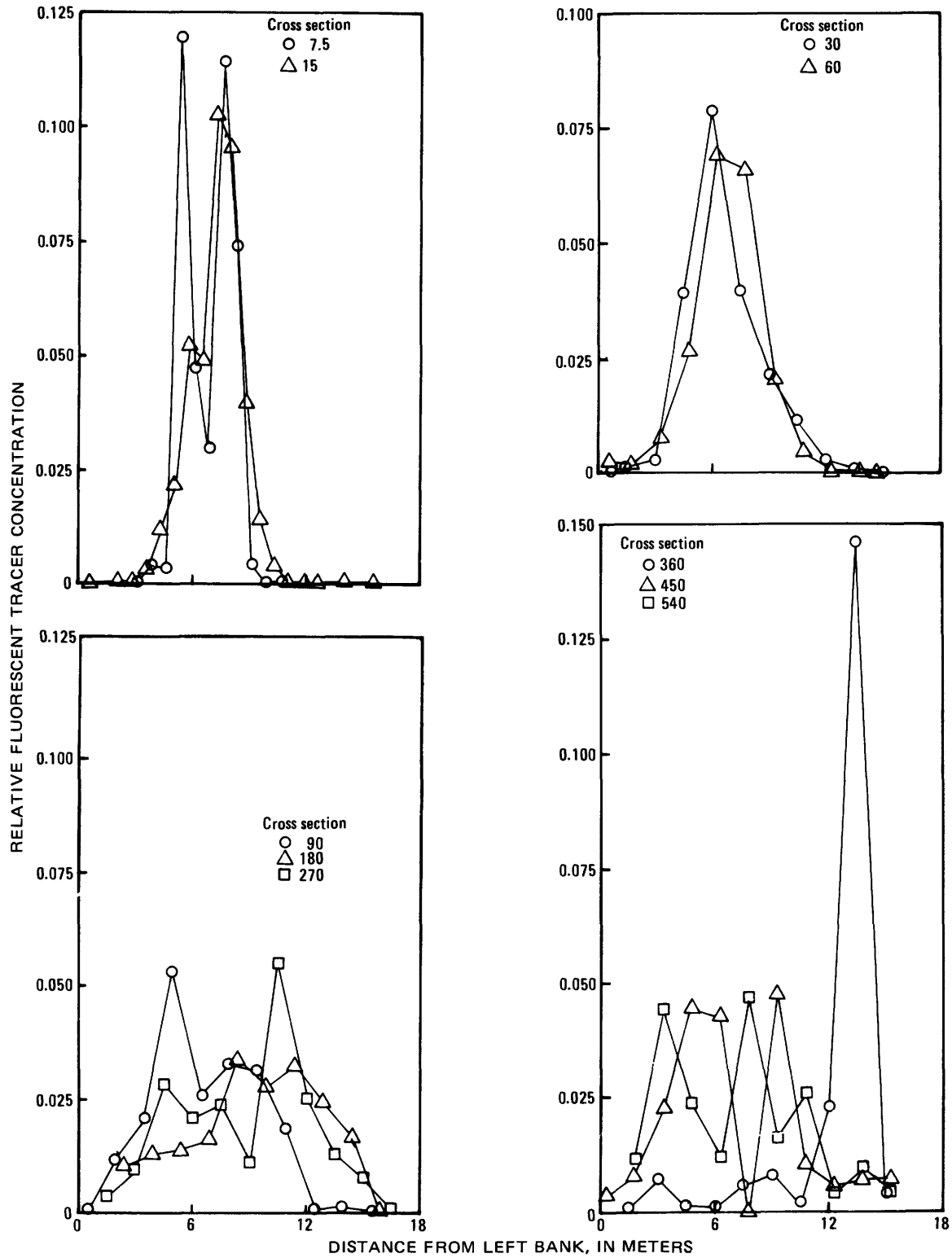

FIGURE 21. — Variation with distance downstream in the lateral distributions of relative concentrations of the 0.125- to 0.177-mm sieve class of garnet tracers as defined by core samples collected on May 8.

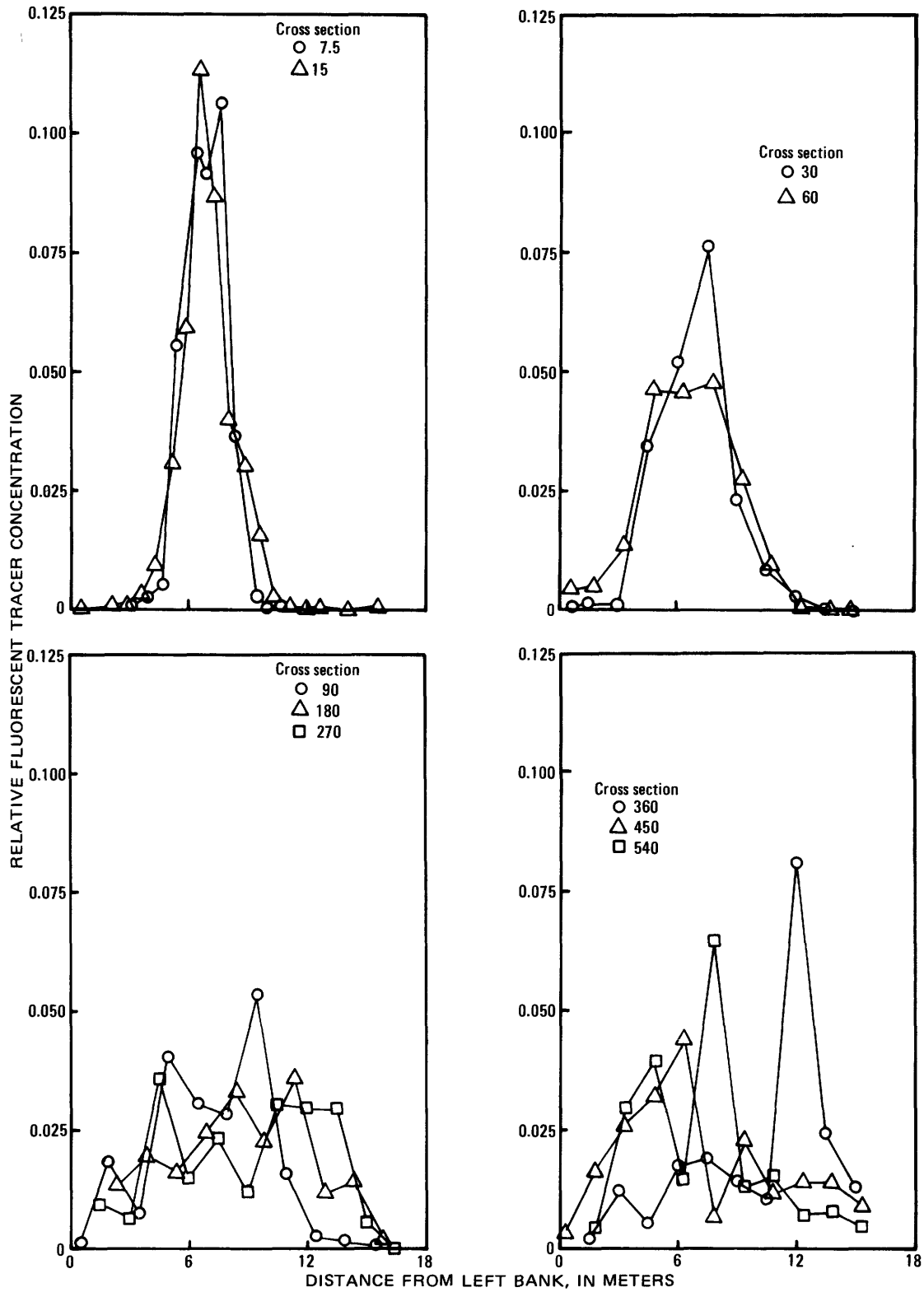

FIGURE 22. — Variation with distance downstream in the lateral distributions of relative concentrations of the 0.125- to 0.177-mm sieve class of monazite tracers as defined by core samples collected on May 8.

of centerline, whereas the distributions for the cross sections farther downstream tended to have mean lateral positions to the right of centerline.

MEAN LATERAL POSITIONS AND VARIANCES

The mean lateral positions, $\bar{z}$, of the lateral distributions were calculated from equation 12. The $\bar{z}$ values tended to shift toward the left bank for cross sections between the injection point and cross section 90. This was most evident for the large sizes of tracer particles. For cross sections farther downstream, the $\bar{z}$ values for the small particles were generally to the right of centerline, and the $\bar{z}$ values for the large particles varied considerably, presumably because these lateral distributions were not completely developed.

Comparison of the $\bar{z}$ values for the "dustpan" samples with the $\bar{z}$ values for the core samples showed that differences were small; when large differences in the $\bar{z}$ values did occur, they were almost always for the large particles and (or) downstream cross sections where the distributions probably were not completely developed at the time of sampling.

The variances of the lateral distributions were calculated from equation 11 and are plotted as a function of distance downstream in figures 23 and 24 for the quartz and garnet, and monazite and lead tracers, respectively. The variation of the variances was essentially the same as that shown in figure 19 for the variances determined from the "dustpan" samples, that is, the variances increased approximately linearly with distance for several points, then tended to fall away from the linear relation. Similarly, the variances at a particular cross section tended to increase with the size of the tracer particles as for the "dustpan" samples. Several variances exceeded the theoretical maximum for a uniform distribution of about 23 m² (250 ft²); but, as for the "dustpan" samples, these were for large particles at downstream cross sections where the lateral distributions were not fully developed but were bimodal or multimodal.

LATERAL DISPERSION COEFFICIENTS

Least-squares lines were calculated for the approximately linear range of the variance versus distance data, and these lines are shown in figures 23 and 24. The slopes of these lines, $d\sigma_z^2/dx$, and the number of cross sections considered in each of the least-squares calculations are presented in table 45. The $d\sigma_z^2/dx$ values increased with the size of the tracer particles for each mineral, suggesting that the rate of lateral dispersion, as indicated by the rate of change of the variance with distance, increased with particle size. Similar results were obtained for the "dustpan" samples (table 37).

TABLE 45. — *Rate of change of the variance with distance downstream,* $d\sigma_z^2/dx$, *and lateral dispersion coefficient* k_z *for fluorescent tracer particles as determined from concentration distributions defined by core samples collected on May 8*

Mineral	Sieve class (mm)	Number of cross sections	$d\sigma_z^2/dx$ (m²/m)	k_z (m²/h)
Quartz ...	0.125–0.177	6	0.0573	0.0460
	0.177–0.250	6	.0664	.0382
	0.250–0.350	6	.0646	.0157
	0.350–0.500	5	.109	.0151
	0.500–0.707	5	.123	.0140
	0.707–1.00	3	.174	.0170
Garnet ..	0.125–0.177	6	.0728	.0292
	0.177–0.250	6	.0710	.0142
	0.250–0.350	5	.0823	.0124
	0.350–0.500	5	.141	.0174
	0.500–0.707	4	.183	.0240
Monazite	0.125–0.177	6	.0716	.0218
	0.177–0.250	5	.0978	.0174
	0.250–0.500	4	.142	.0245
	0.350–0.500	4	.193	.0248
	0.500–0.707	4	.234	.0307
Lead	0.125–0.177	5	.150	.0082
	0.177–0.250	4	.145	.0092
	0.250–0.350	4	.106	.0097
	0.350–0.500	4	.436	.0223

Comparison of the $d\sigma_z^2/dx$ values for the core and "dustpan" samples showed that 11 of the core sample values were larger than the corresponding "dustpan" sample results and that 5 were smaller. The largest difference was for the 0.707- to 1.00-mm sieve class of quartz; however, only three cross sections were used in determining $d\sigma_z^2/dx$ for this size, and the small number of points undoubtedly contributed to the large difference observed. The mean $d\sigma_z^2/dx$ value of the 16 sieve classes (excluding the lead) was 0.118 m²/m (0.386 ft²/ft) compared with a mean of 0.110 m²/m (0.361 ft²/ft) for the "dustpan" samples.

The $d\sigma_z^2/dx$ values are plotted in figure 25 as a function of median fall diameter of the sieve class. The trend line through the data shows the increase of $d\sigma_z^2/dx$ with increase in the median fall diameter of the tracer particles. There did not appear to be any consistent differences between the $d\sigma_z^2/dx$ values determined from the core samples and those determined from the "dustpan" samples. The scatter of the data precluded any definite conclusions regarding hydraulic equivalence of the particles. It appeared, however, that the scatter increased with diameter, suggesting that the smaller particles of differing specific gravity, which move predominantly in suspension, were more nearly equivalent than the larger particles.

The velocities of the centroids of the tracer masses, to be discussed in the next section (table 49), were used to convert the $d\sigma_z^2/dx$ values to lateral dispersion coefficients with equation 16. The resulting k_z values are

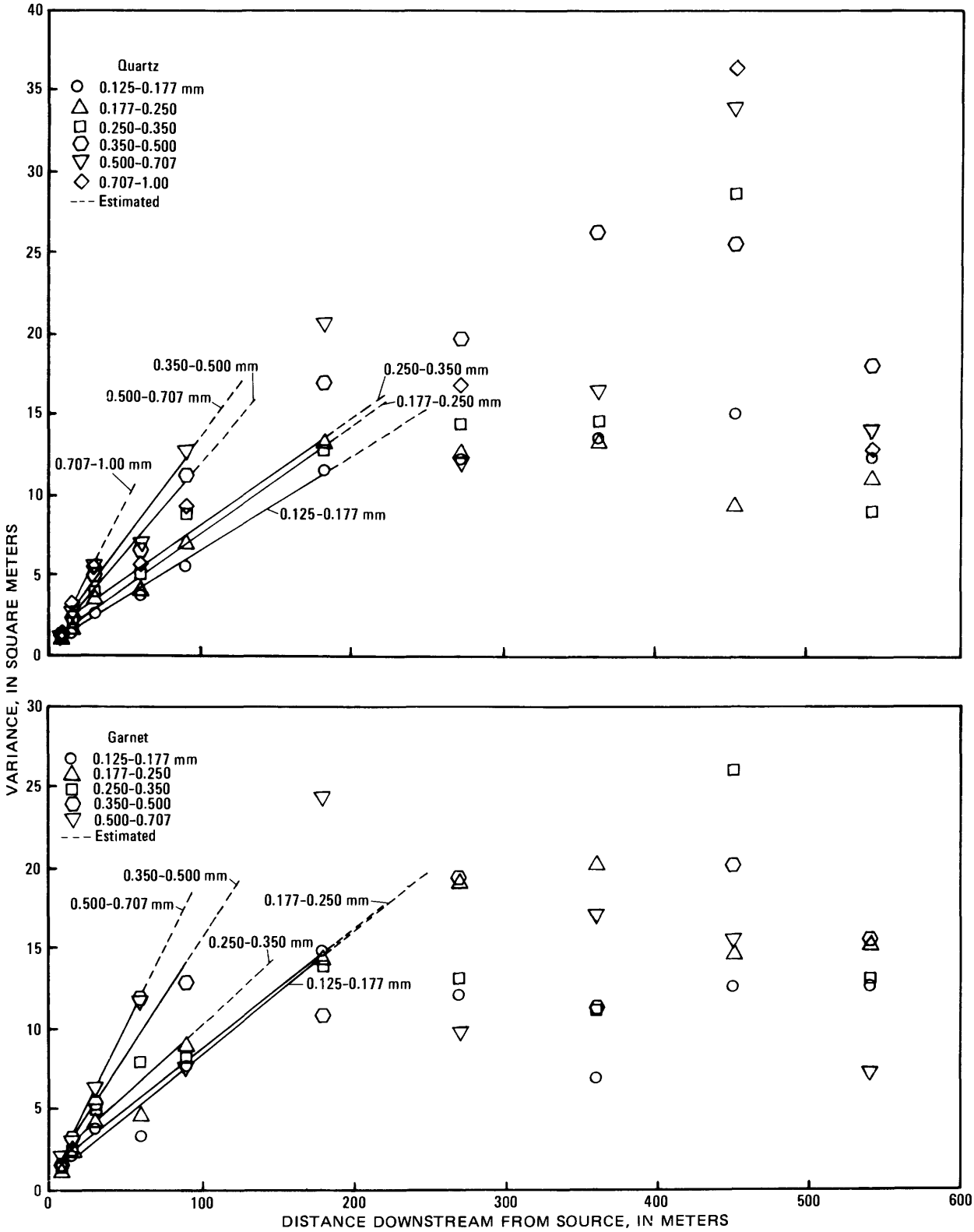

FIGURE 23. — Variation with distance downstream in the variances of the lateral distributions of the quartz and garnet tracers as defined by core samples collected on May 8.

presented in table 45. Because the $d\sigma_z^2/dx$ values increased with size of the tracer particles and the centroid velocities decreased with size, the tendency was for the k_z values to be approximately constant with

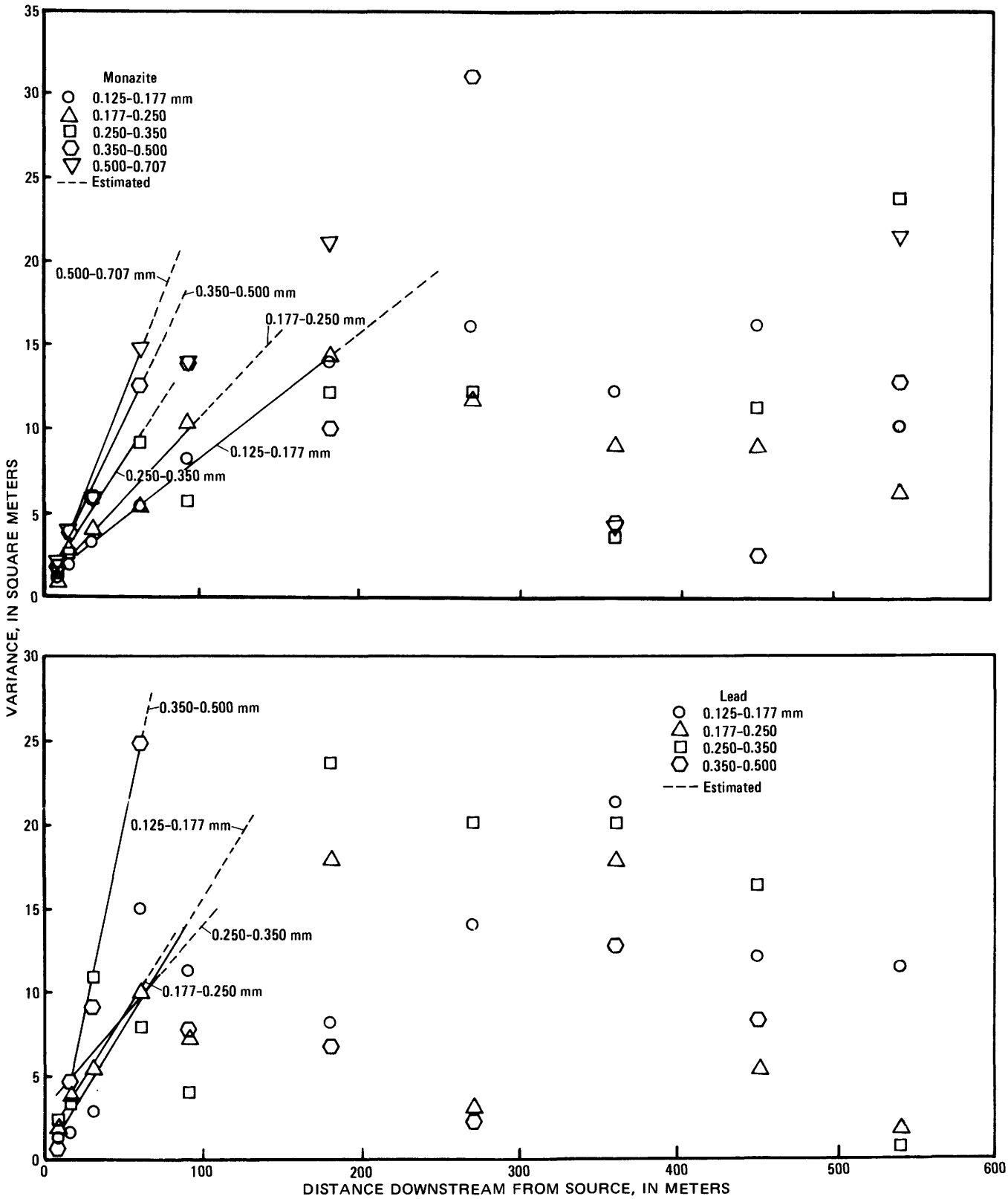

FIGURE 24. — Variation with distance downstream in the variances of the lateral distributions of monazite and lead tracers as defined by core samples collected on May 8.

respect to both the particle size and the specific gravity of the tracers. However, three of the four sieve classes of lead had k_z values considerably less than the overall mean of 0.0206 m²/h (0.222 ft²/h) for all 20 sieve classes.

The mean, excluding the lead tracer particles, was

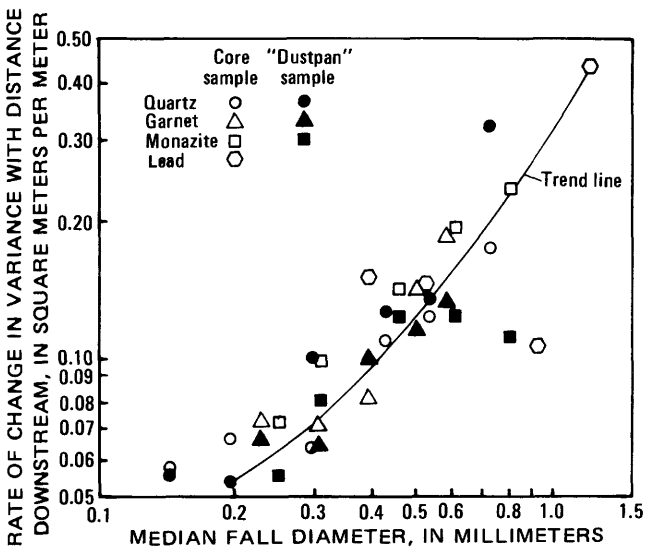

FIGURE 25. — Variation with median fall diameter in the rate of change in the variance with distance downstream, $d\sigma_z^2 / dx$, for lateral distributions of fluorescent tracers as defined by core and "dustpan" samples collected on May 8.

0.0227 m²/h (0.244 ft²/h). This is about a third of the mean k_z value for the larger tracer particles obtained from analysis of the "dustpan" samples (table 37). Because the $d\sigma_z^2/dx$ values were approximately comparable, the large difference is a result of differences in the particle velocities. Recall, however, that first arrival time velocities were used for the "dustpan" values, whereas centroid velocities were used for the core sample values. Because velocities based on first arrival times are characteristic of the smaller particles within the sieve class, it is not unreasonable that these velocities be larger than the velocities of the centroids of the tracer masses which are for tracer particles moving throughout the complete zone of movement of the dune bed. Also, the particles arriving first undoubtedly spent a greater than average amount of time moving in suspension and by saltation compared with the time spent moving throughout the complete zone of movement.

LONGITUDINAL DISTRIBUTIONS

Longitudinal distributions of the fluorescent tracers were determined for each of the sieve classes of the four tracer materials from the core samples collected on May 8, June 6, and July 14. Sampling in the lateral direction on June 6 and July 14 was limited to samples at the centerline and the right and left quarter points of the channel because it was believed that the tracers would be approximately uniformly distributed in the lateral direction at these times in the experiment. To facilitate comparing the results of the lateral distributions of the core samples obtained on May 8 with the longitudinal distributions of June 6 and July 14, the concentrations at the centerline and the right and left quarter points were determined, using linear interpolation between points of the lateral distributions. These concentrations are plotted in figures 26 and 27 for the six sieve classes of quartz tracer, in figure 28 for the five sieve classes of garnet tracer, in figure 29 for the five sieve classes of monazite tracer, and in figure 30 for the four sieve classes of lead tracer.

Significant quantities of only the 0.125- to 0.177-mm, 0.177- to 0.250-mm, and 0.250- to 0.350-mm sieve classes of quartz tracers were found downstream of cross section 180. The 0.125- to 0.177-mm and 0.177- to 0.250-mm sieve classes showed similar trends over the length of the reach sampled. The largest concentrations were along the centerline, and the smallest concentrations were along the right quarter points between the source and cross section 180; between cross sections 180 and 540 the concentrations were approximately uniform, in both the lateral and the longitudinal directions.

Between the source and cross section 180, the sieve classes of the four minerals generally had the largest concentrations along the centerline and the smallest concentrations along the right quarter point. The effect of size of the tracer particles on longitudinal dispersion — that is, the spreading out of the tracer masses in the downstream direction — was very evident; for example, the 0.125- to 0.177-mm sieve class of quartz tracer was almost uniformly distributed over the 540-m (1800-ft) section of the reach that was sampled, whereas the 0.707- to 1.00-mm sieve class of quartz tracer was found only in the reach between the source and cross section 90.

The longitudinal concentration distributions for the June 6 core samples are plotted in figures 31 and 32 for the six sieve classes of quartz tracer, in figure 33 for the five sieve classes of garnet tracer, in figure 34 for the five sieve classes of monazite tracer, and in figure 35 for the four sieve classes of lead tracer. The quartz and garnet tracers in general were approximately uniformly distributed across the channel — that is, the centerline and the right and left quarter-point concentrations were approximately the same at most cross sections. For the monazite tracers, there was considerable tendency, particularly in the first 240 m (800 ft) of the reach, for the centerline concentrations to exceed the right and left quarter-point concentrations. The centerline concentrations for the lead tracers greatly exceeded the right and left quarter-point concentrations, and the largest concentrations were found at cross section 30. Comparison for a particular size of

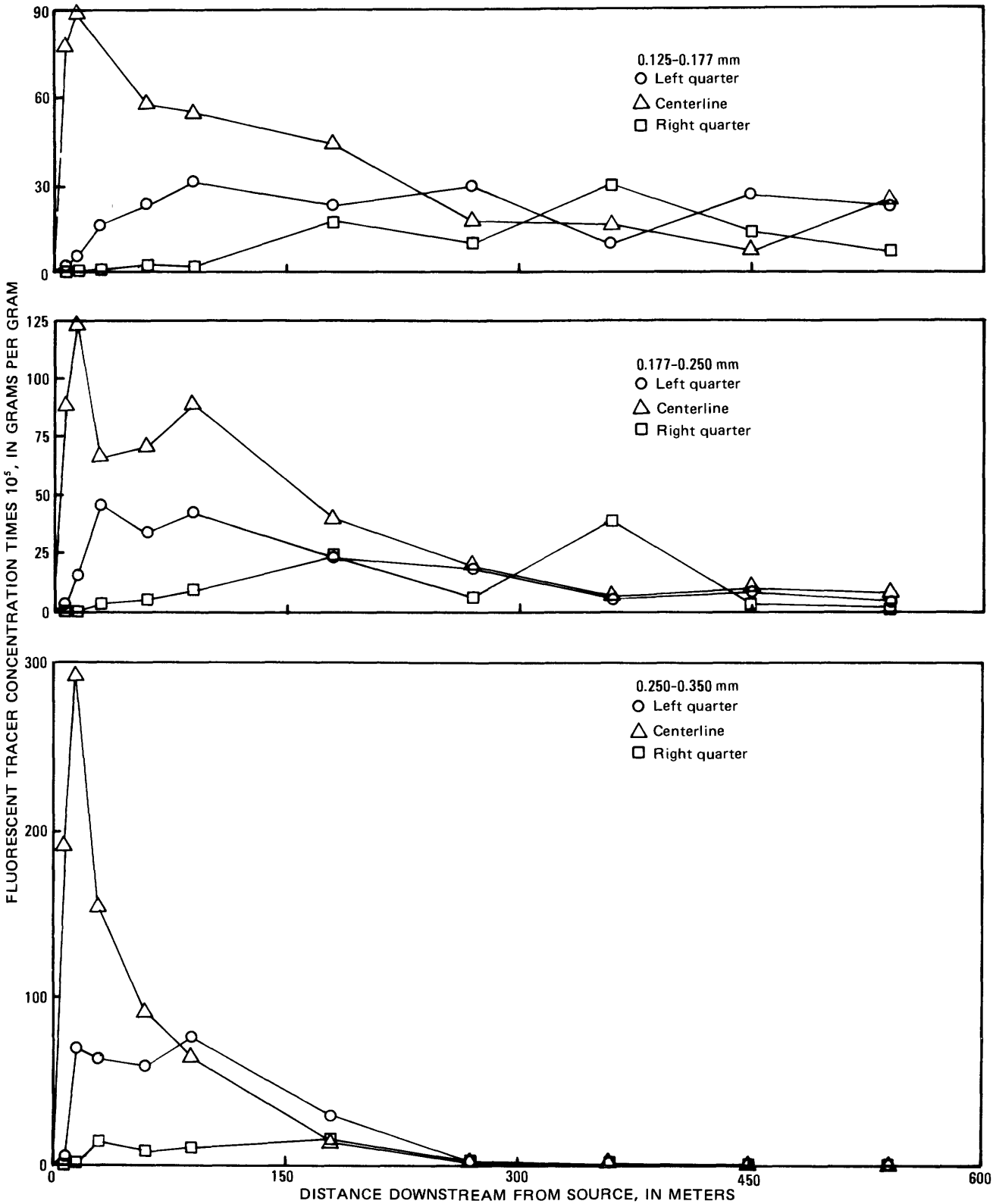

FIGURE 26. — Variation with distance downstream in the concentration of fluorescent tracers for the 0.125- to 0.177-mm, 0.177- to 0.250-mm, and 0.250- to 0.350-mm sieve classes of quartz tracers as defined by core samples collected on May 8.

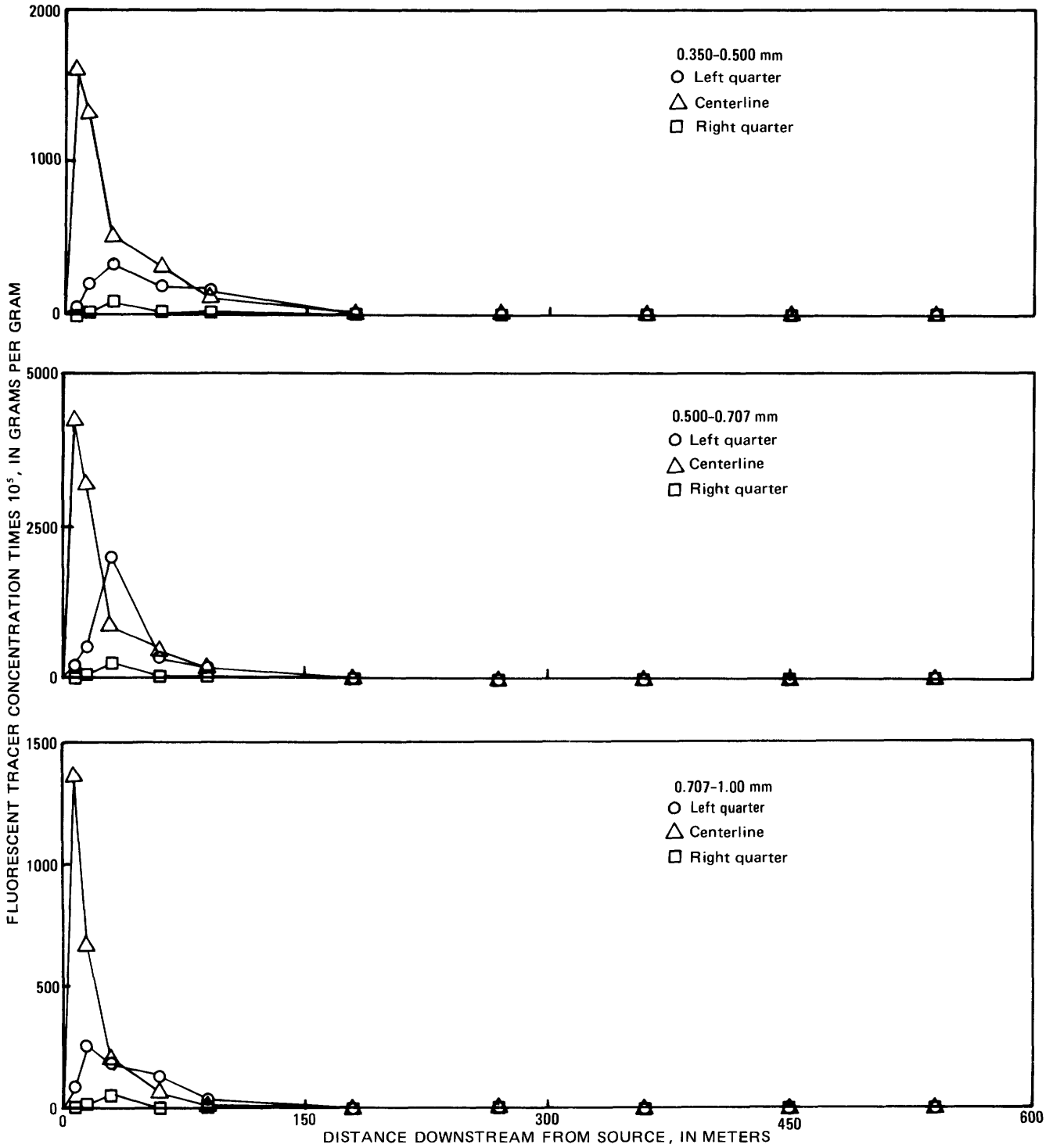

FIGURE 27. — Variation with distance downstream in the concentration of fluorescent tracers for the 0.350- to 0.500-mm, 0.500- to 0.707-mm, and 0.707- to 1.00-mm sieve classes of quartz tracers as defined by core samples collected on May 8.

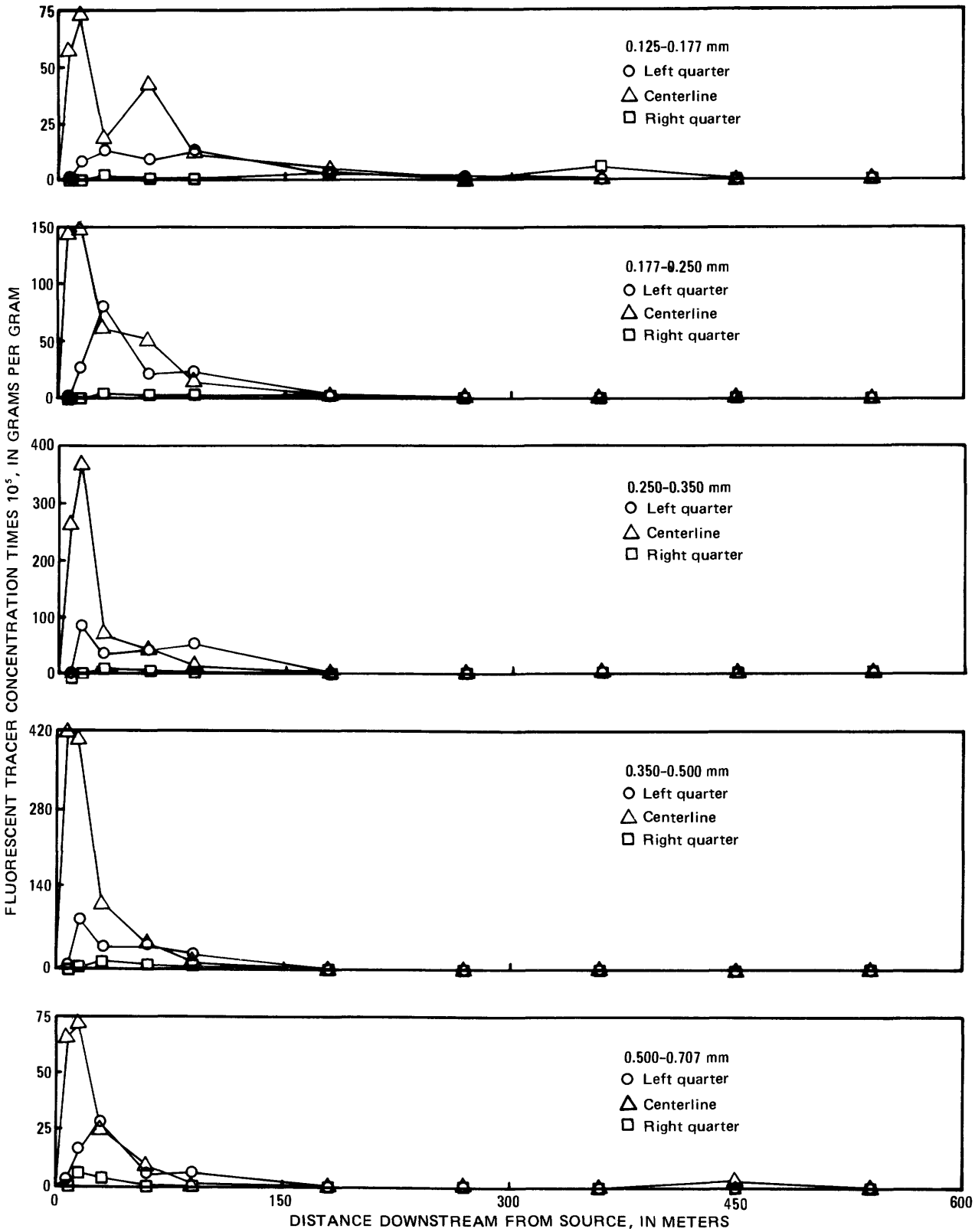

FIGURE 28. — Variation with distance downstream in the concentration of fluorescent tracers for the 0.125- to 0.177-mm, 0.177- to 0.250-mm, 0.250- to 0.350-mm, 0.350- to 0.500-mm, and 0.500- to 0.707-mm sieve classes of garnet tracers as defined by core samples collected on May 8.

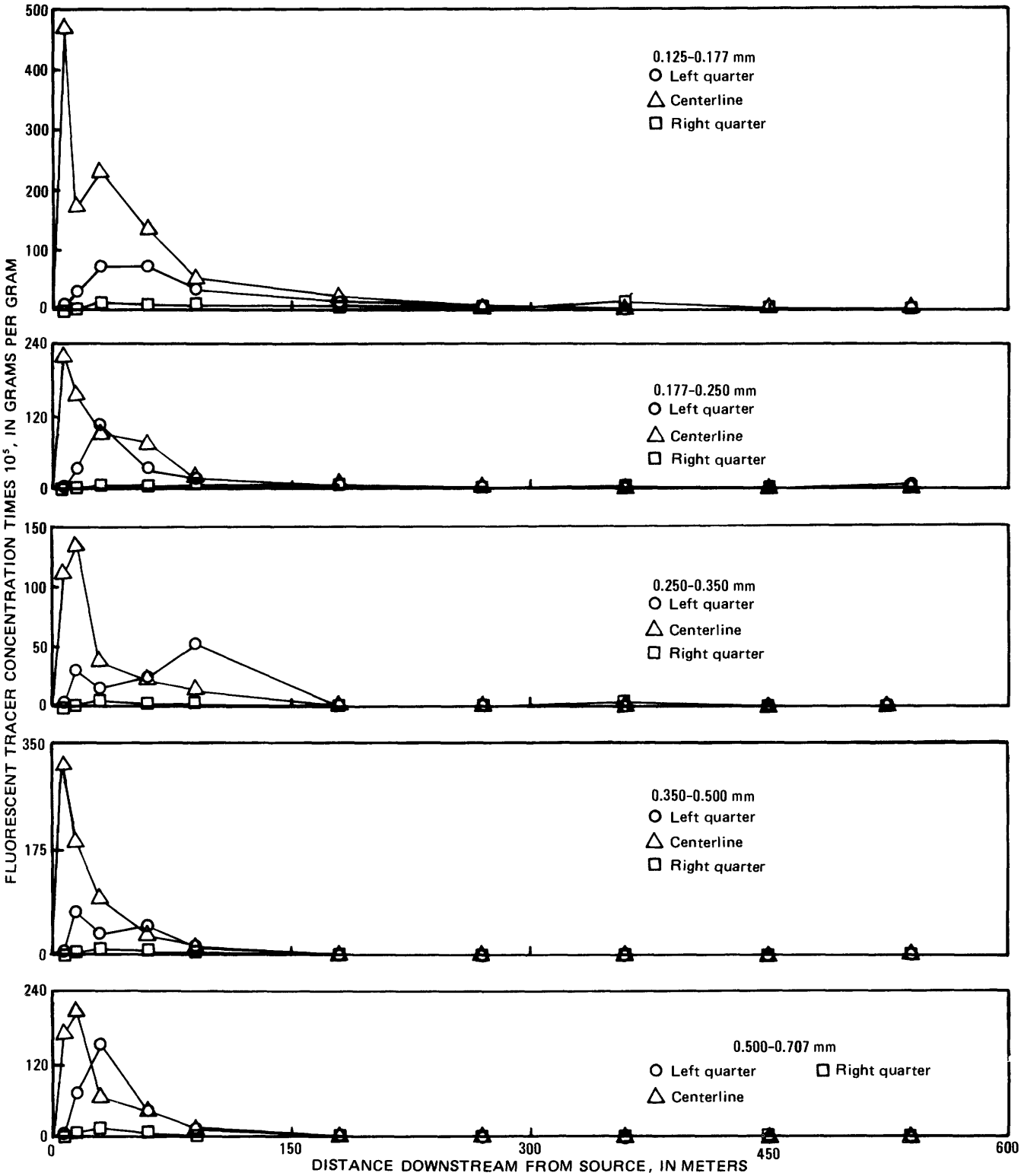

FIGURE 29. — Variation with distance downstream in the concentration of fluorescent tracers for the 0.125- to 0.177-mm, 0.177- to 0.250-mm, 0.250- to 0.350-mm, 0.350- to 0.500-mm, and 0.500- to 0.707-mm sieve classes of monazite tracers as defined by core samples collected on May 8.

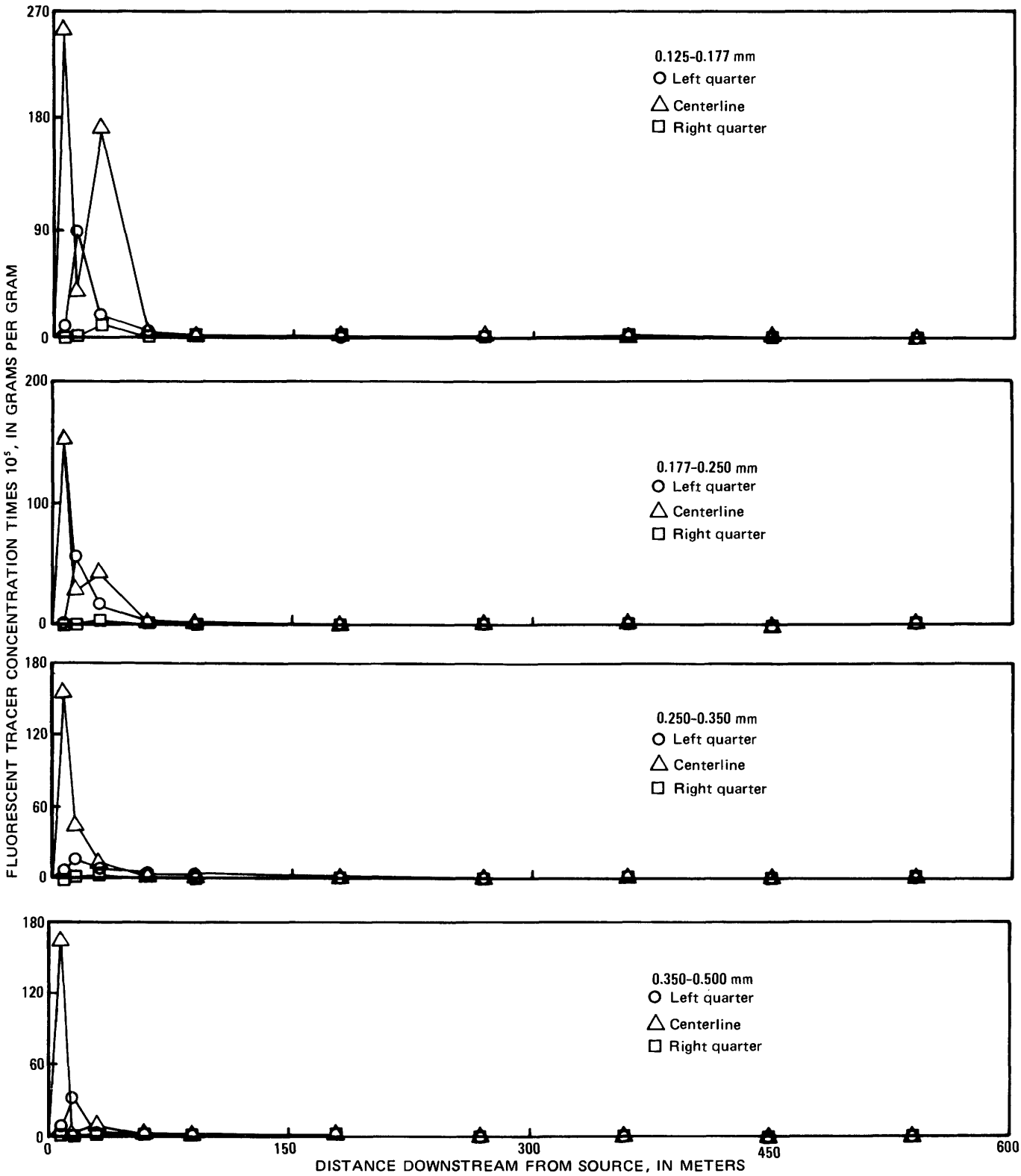

FIGURE 30. — Variation with distance downstream in the concentration of fluorescent tracers for the 0.125- to 0.177-mm, 0.177- to 0.250-mm, 0.250- to 0.350-mm, and 0.350- to 0.500-mm sieve classes of lead tracers as defined by core samples collected on May 8.

tracer particle of the May 8 and June 6 graphs shows the movement of the tracer masses downstream.

The longitudinal concentration distributions for the July 14 core samples are plotted in figures 36 and 37 for the six sieve classes of quartz tracer, in figure 38 for the five sieve classes of garnet tracer, in figure 39 for the five sieve classes of monazite tracer, and in figure 40 for the four sieve classes of lead tracer. The 0.125- to 0.177-mm and 0.177-to 0.250-mm sieve classes of quartz tracer were approximately uniformly distributed over the reach, in both the lateral and the longitudinal directions. The general trends of the longitudinal distributions for the other four sieve classes of quartz tracers are shown in figures 36 and 37. Somewhat surprising was the fact that large centerline concentrations for these four sieve classes of quartz tracer and for the five sieve classes of monazite tracer were found at either one or both of cross sections 30 and 90. These concentrations in some instances were larger than the corresponding June 6 concentrations (figs 31–34). This observation suggests probably that a quantity of tracer buried at some point between the source and cross section 30 was exposed and transported downstream during the latter part of the interval between June 6 and July 14.

Large centerline concentrations of lead tracer were found (fig. 40) but this was expected because of the large centerline concentrations found on May 8 (fig. 30) and June 6 (fig. 35). Comparison for a particular size of tracer particle of the longitudinal distributions for May 8, June 6, and July 14 shows the movement of the tracer mass downstream.

In the analysis of the longitudinal distributions for June 6 and July 14, it was assumed that sufficient time had elapsed since the injection that the tracers were approximately uniformly distributed across the channel. The graphs presented in figures 31 through 40 and the preceding discussion suggest that this assumption is in general valid, with the possible exception of some cross sections near the injection point. Hence, mean cross-sectional concentrations were calculated from equation 8, which for the June 6 and July 14 samples, reduces to:

$$\bar{C} = {}^3/_8(C_L + C_R) + {}^1/_4C_C, \qquad (27)$$

where the L, R, and C subscripts indicate the left quarter point, the right quarter point, and the centerline of the channel, respectively. For the May 8 longitudinal distributions, mean cross-sectional concentrations were calculated from equation 8 for each of the lateral distributions. The mean concentration data for the longitudinal distributions for May 8, June 6, and July 14 are presented in tables 46, 47, and 48.

VELOCITIES OF THE TRACER MASSES

The positions of the centroids of the tracer masses on May 8, June 6, and July 14 were calculated from equation 4 for the longitudinal distributions of tracers as described by the data tabulated in tables 46, 47, and 48. One of the problems in using equation 4 was the determination of the downstream points at which the concentrations of fluorescent tracers were zero. Because of the extreme sensitivity of the fluorescent tracer technique, it was possible to detect the leading edge of the tracer masses far downstream of the bulk of the tracers (figs. 26–40). These concentrations influence the calculation of the centroid positions and, in particular, affect the calculation of the variances of the distribution curves. To standardize the calculations, the point at which the concentration was assumed to be zero was taken as the longitudinal position at which the concentration decreased to 1.0 percent of the maximum concentration. This point in general was different for the various sieve classes and specific gravities of tracers. It was necessary to extrapolate several of the May 8 distributions, many of the June 6 distributions, and most of the July 14 distributions to reach this limiting concentration; in general, the extrapolations were performed such that the increases in areas under the distribution curves were minimized but at the same time such that extrapolations were consistent with the general trends of the curves. The integrals in equation 4 were evaluated by plotting $\bar{C}$ versus x and $\bar{C}x$ versus x and drawing straight lines between the points. The areas under the two curves were determined by summing the areas of the triangles and trapezoids thus formed.

The velocities of the centroids were determined from equation 5 for three time periods: the interval between the start of injection on May 1 and the end of injection on May 8 (7.1 days), the interval between May 8 and June 6 (29 days); and the interval between June 6 and July 14 (38 days). The velocities are presented in table 49 and are plotted as a function of median fall diameter of the sieve class in figures 41, 42, and 43 for the quartz, garnet, and monazite tracers, respectively. The velocities for the lead particles were not plotted because no consistent trends were evident in the data.

Figure 41 shows that the logarithm of the centroid velocity varied approximately linearly with the logarithm of the median fall diameter of the sieve class for the quartz tracer particles and that the dependence on size decreased somewhat with time. The change with

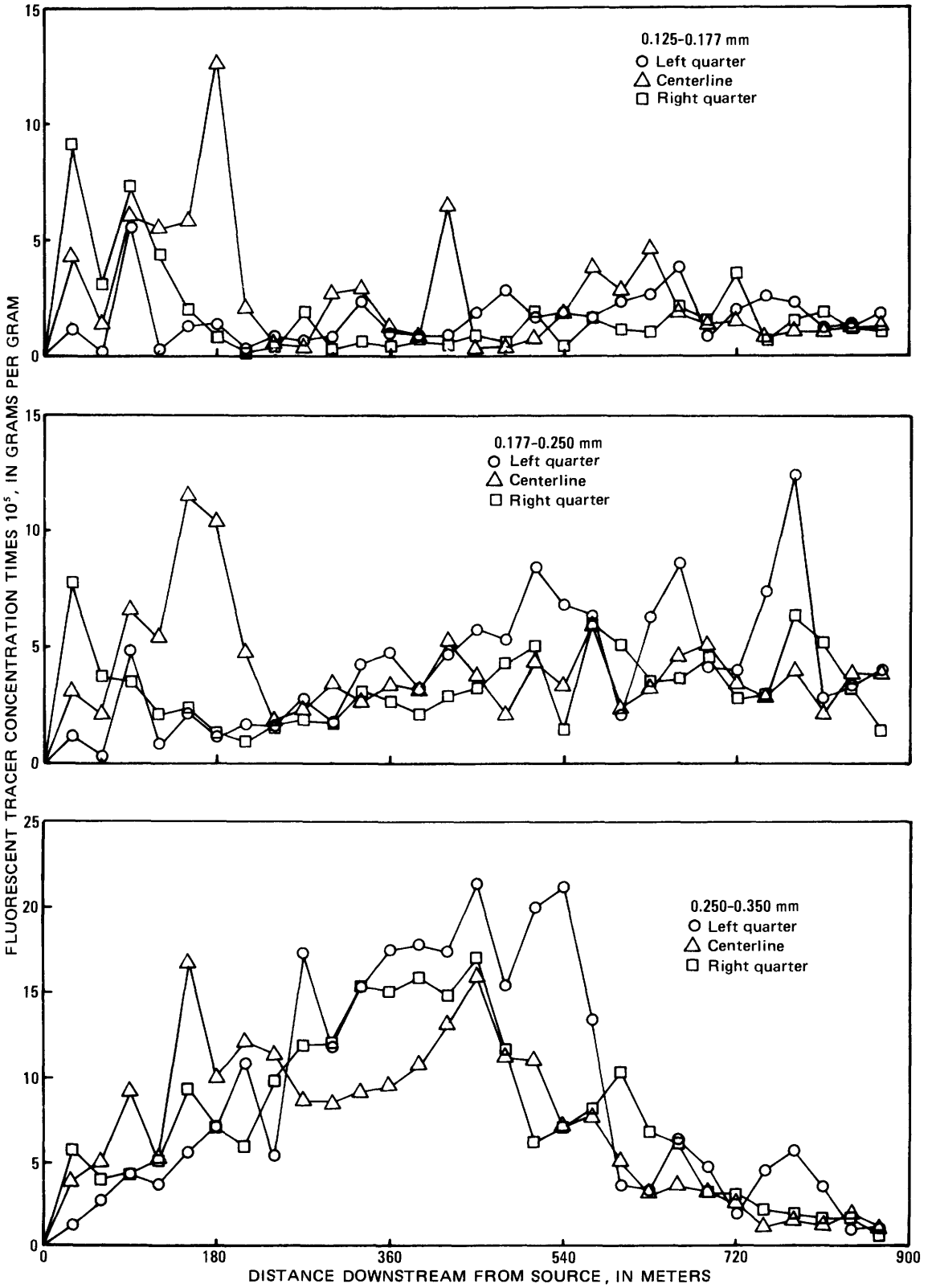

FIGURE 31. — Variation with distance downstream in the concentration of fluorescent tracers for the 0.125- to 0.177-mm, 0.177- to 0.250-mm, and 0.250- to 0.350-mm sieve classes of quartz tracers as defined by core samples collected on June 6.

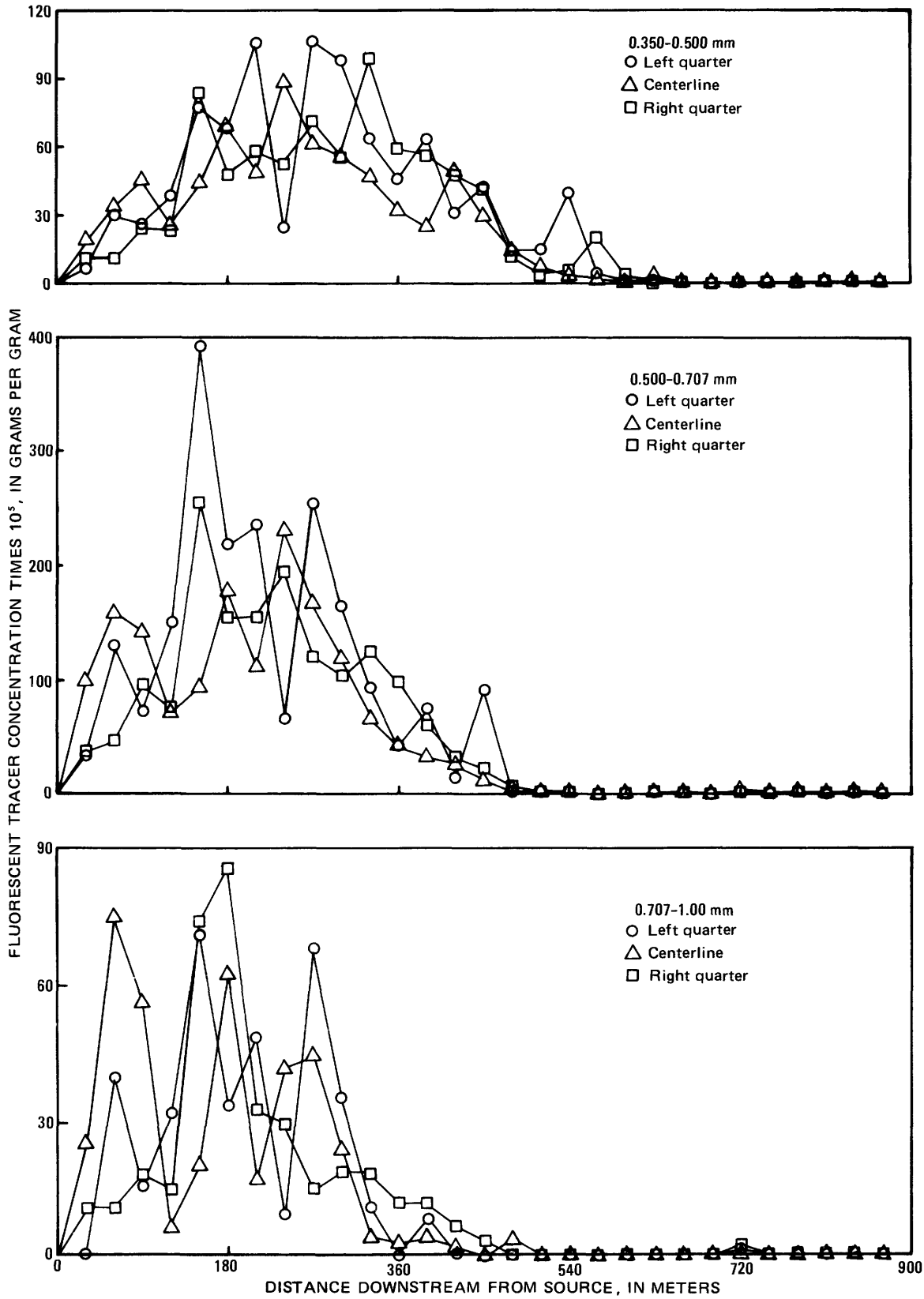

FIGURE 32. — Variation with distance downstream in the concentration of fluorescent tracers for the 0.350- to 0.500-mm, 0.500- to 0.707-mm, and 0.707- to 1.00-mm sieve classes of quartz tracers as defined by core samples collected on June 6.

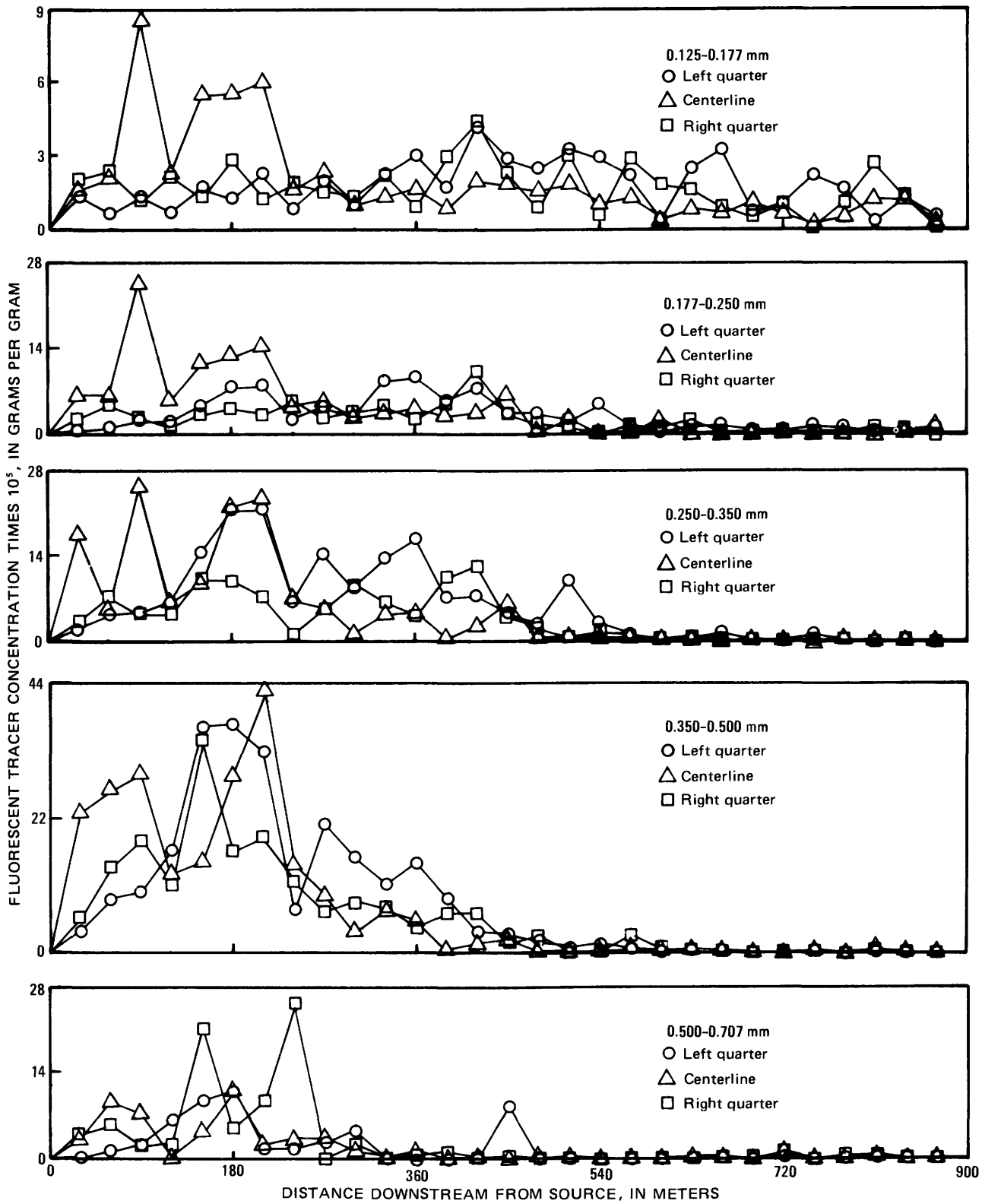

FIGURE 33. — Variation with distance downstream in the concentration of fluorescent tracers for the 0.125- to 0.177-mm, 0.177- to 0.250-mm, 0.250- to 0.350-mm, 0.350- to 0.500-mm, and 0.500- to 0.707-mm sieve classes of garnet tracers as defined by core samples collected on June 6.

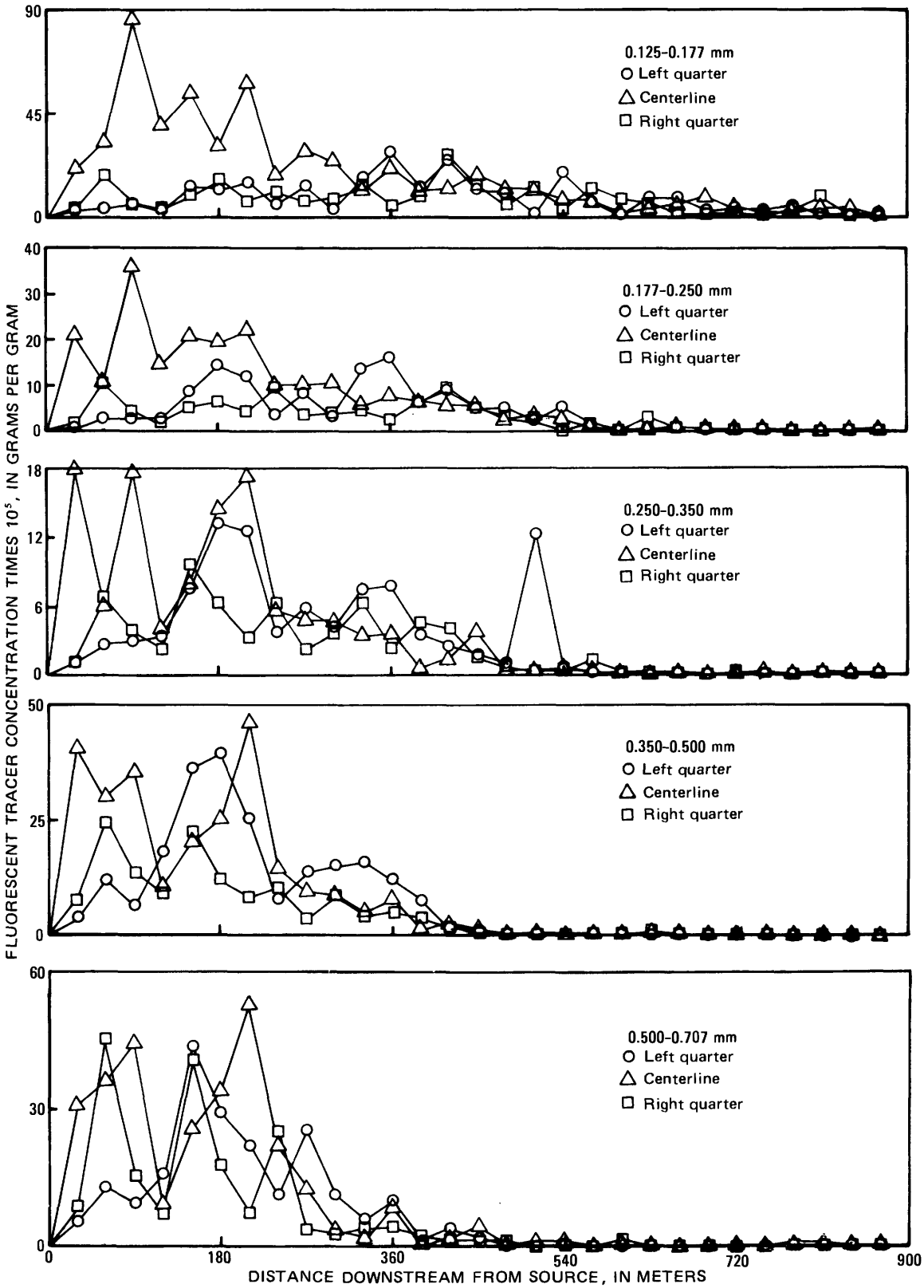

FIGURE 34. — Variation with distance downstream in the concentration of fluorescent tracers for the 0.125- to 0.177-mm, 0.177- to 0.250-mm, 0.250- to 0.350-mm, 0.350- to 0.500-mm, and 0.500- to 0.707-mm sieve classes of monazite tracers as defined by core samples collected on June 6.

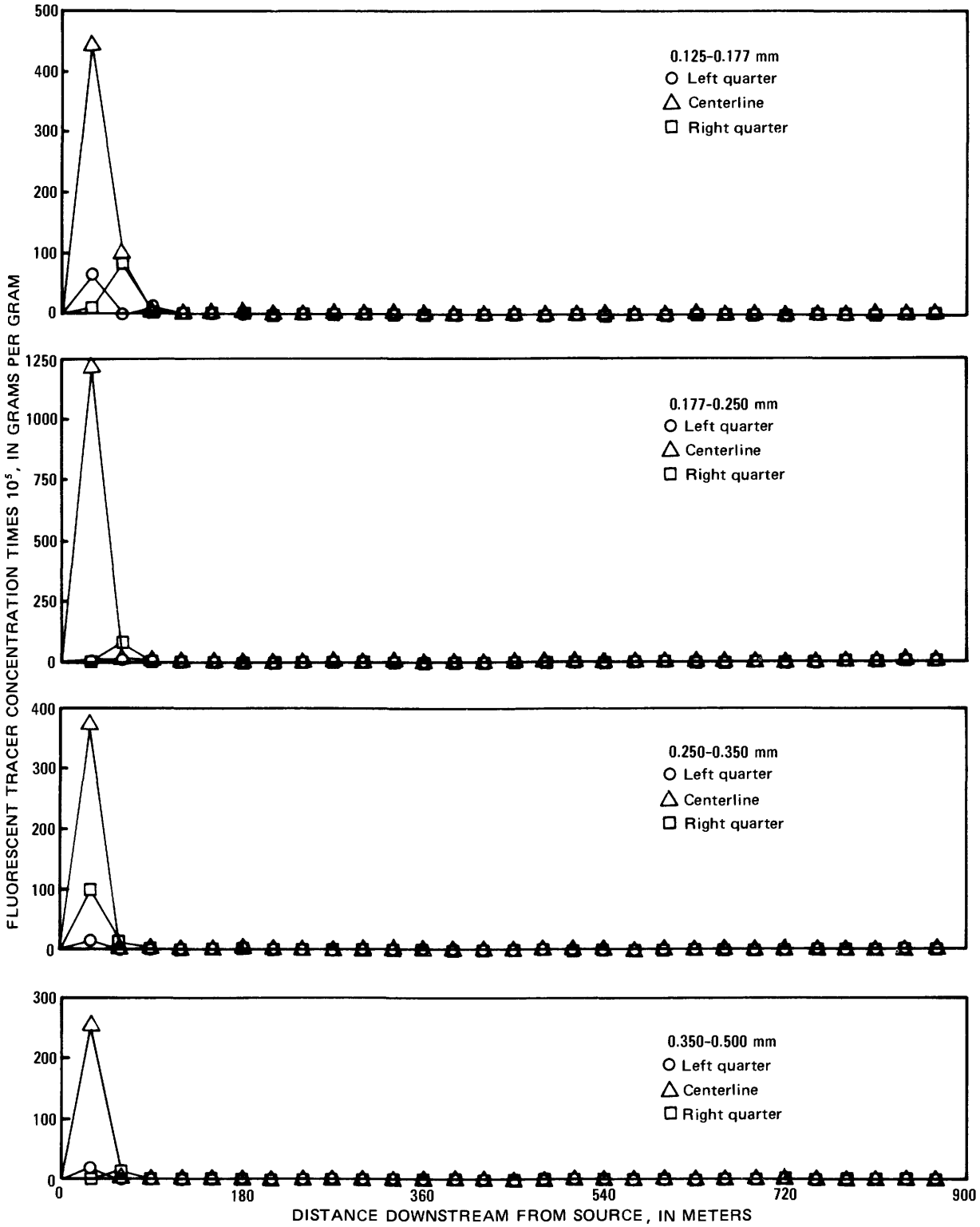

FIGURE 35. — Variation with distance downstream in the concentration of fluorescent tracers for the 0.125- to 0.177-mm, 0.177- to 0.250-mm, 0.250- to 0.350-mm, and 0.350- to 0.500-mm sieve classes of lead tracers as defined by core samples collected on June 6.

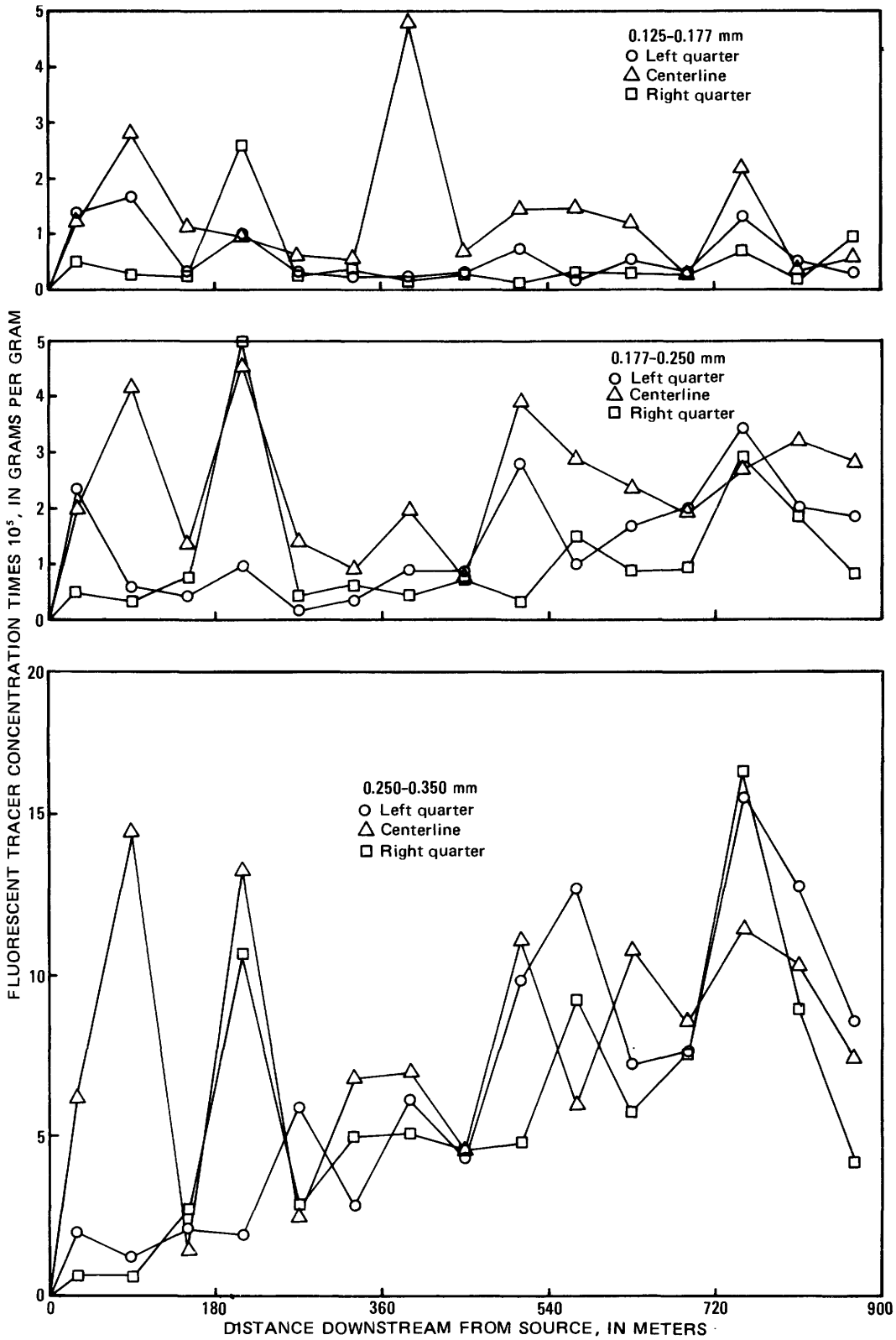

FIGURE 36. — Variation with distance downstream in the concentration of fluorescent tracers for the 0.125- to 0.177-mm, 0.177- to 0.250-mm, and 0.250- to 0.350-mm sieve classes of quartz tracers as defined by core samples collected on July 14.

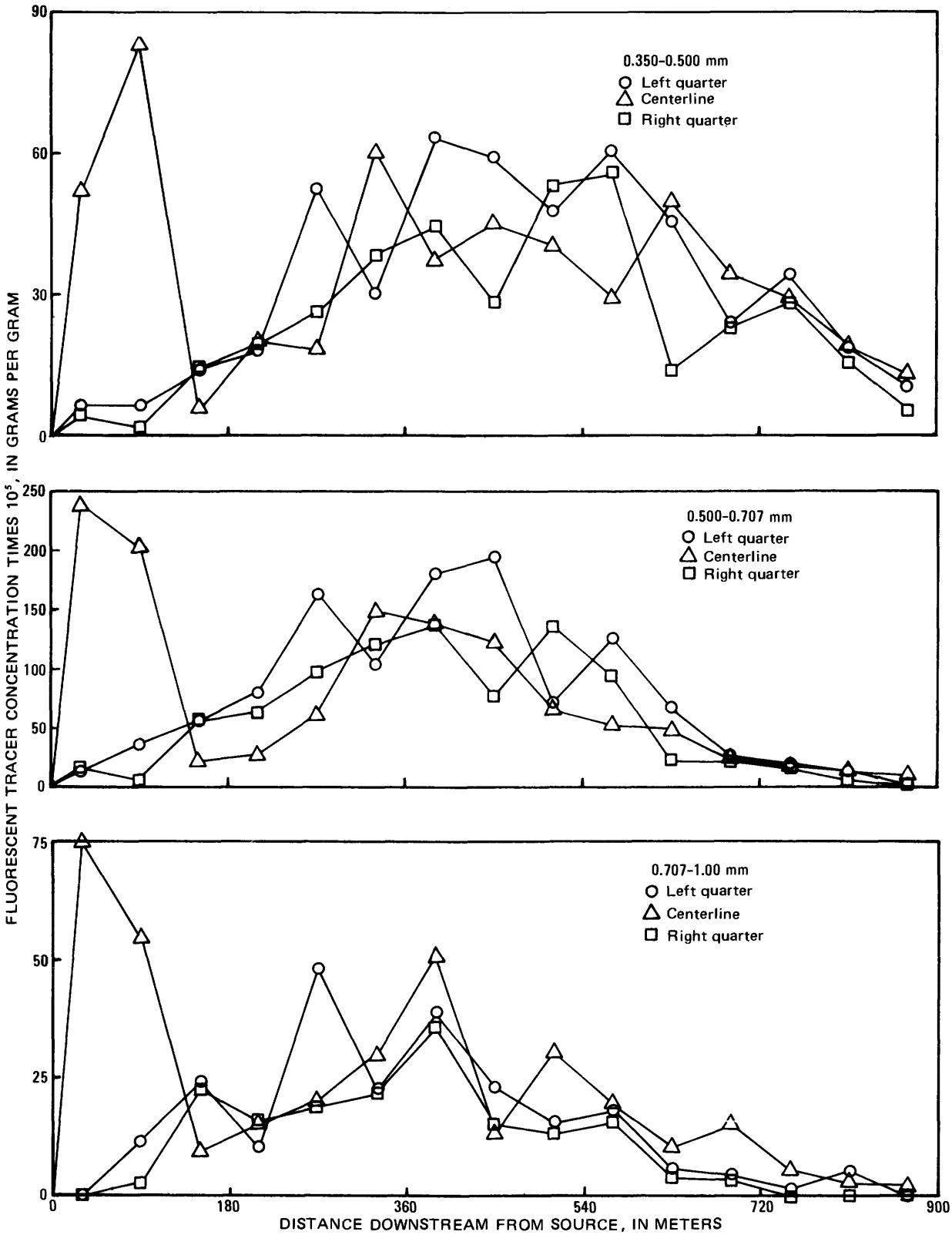

FIGURE 37. — Variation with distance downstream in the concentration of fluorescent tracers for the 0.350- to 0.500-mm, 0.500- to 0.707-mm, and 0.707- to 1.00-mm sieve classes of quartz tracers as defined by core samples collected on July 14.

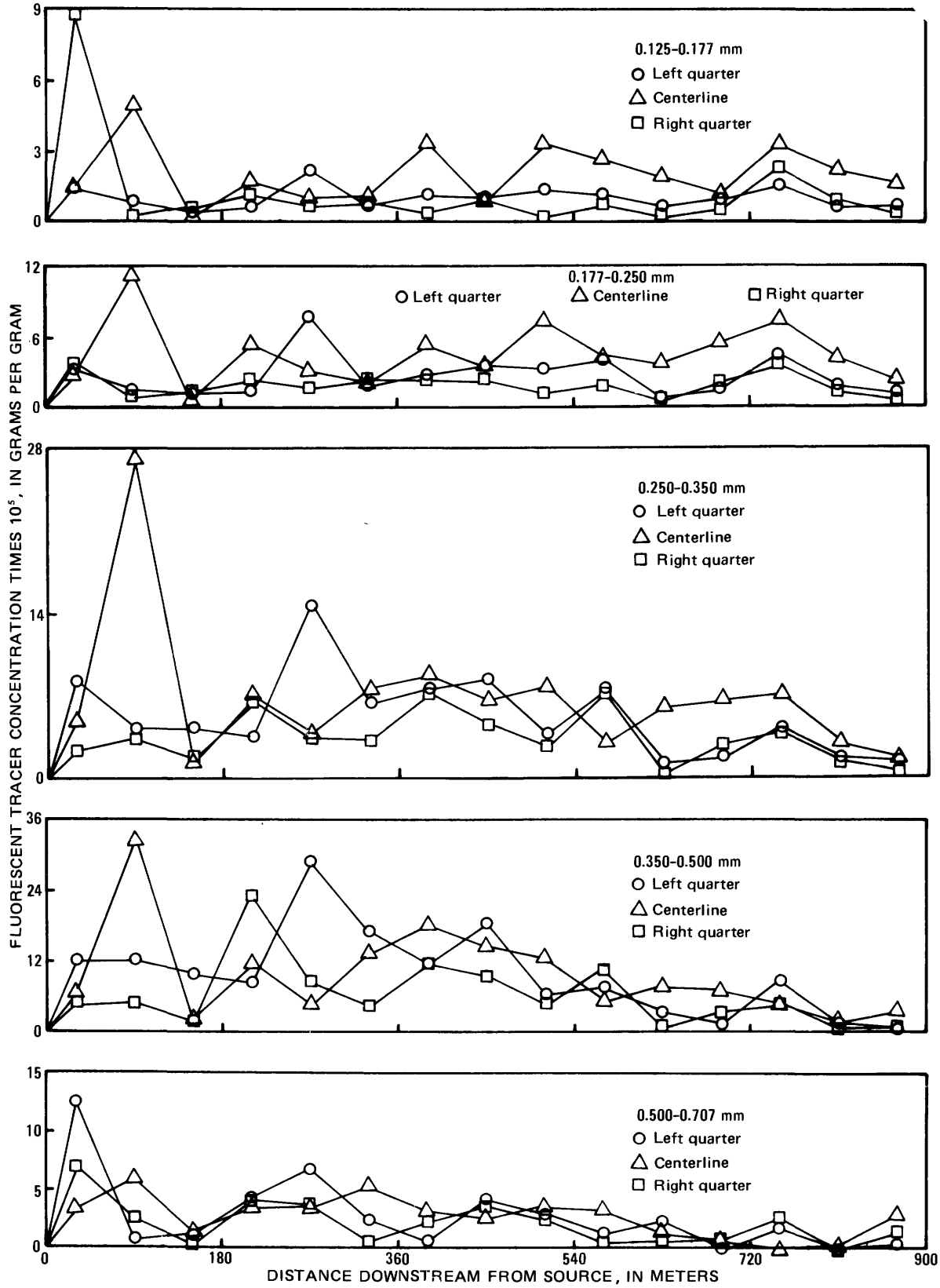

FIGURE 38. — Variation with distance downstream in the concentration of fluorescent tracers for the 0.125- to 0.177-mm, 0.177- to 0.250-mm, 0.250- to 0.350-mm, 0.350- to 0.500-mm, and 0.500- to 0.707-mm sieve classes of garnet tracers as defined by core samples collected on July 14.

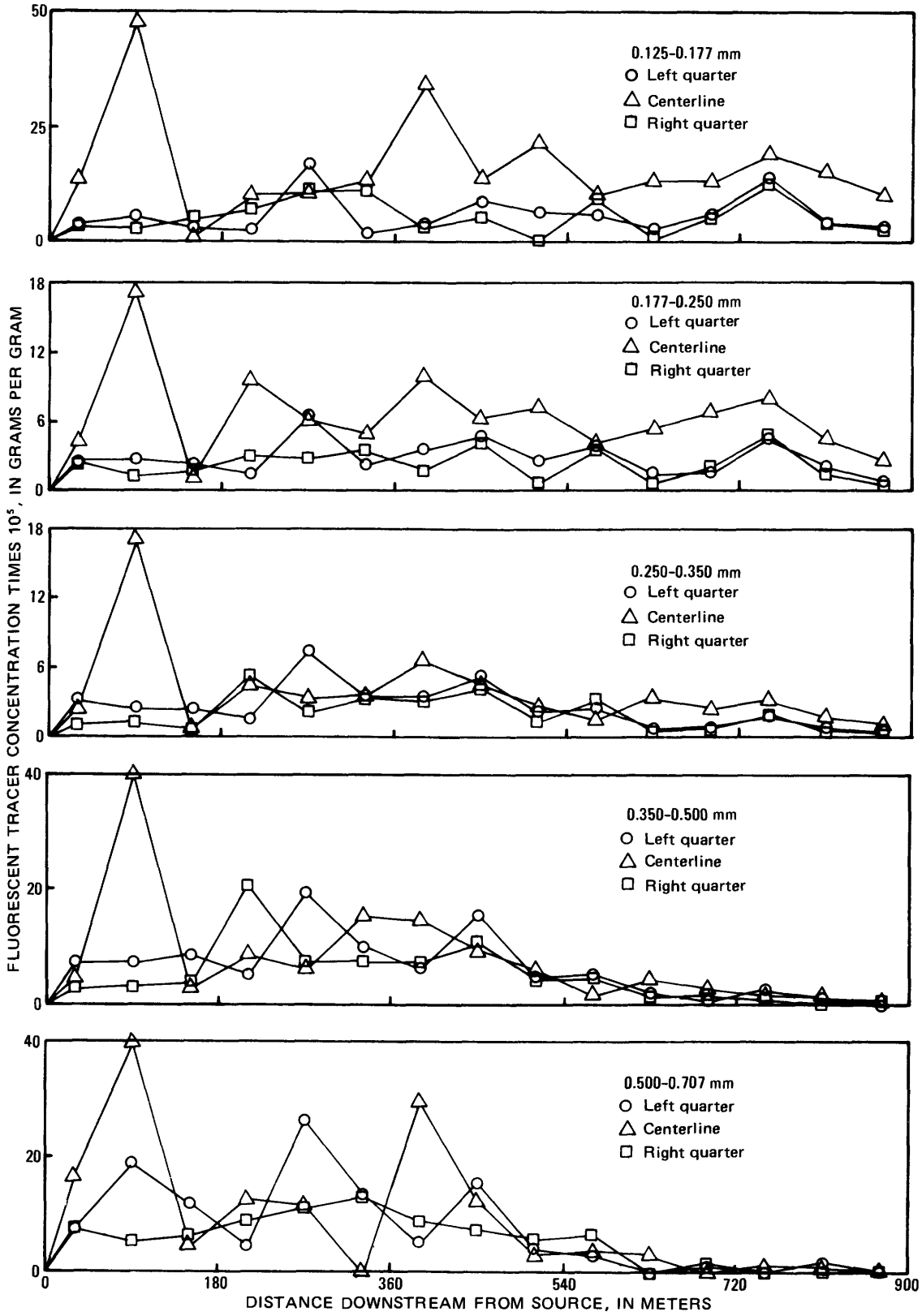

FIGURE 39. — Variation with distance downstream in the concentration of fluorescent tracers for the 0.125- to 0.177-mm, 0.177-to 0.250-mm, 0.250- to 0.350-mm, 0.350- to 0.500-mm, and 0.500- to 0.707-mm sieve classes of monazite tracers as defined by core samples collected on July 14.

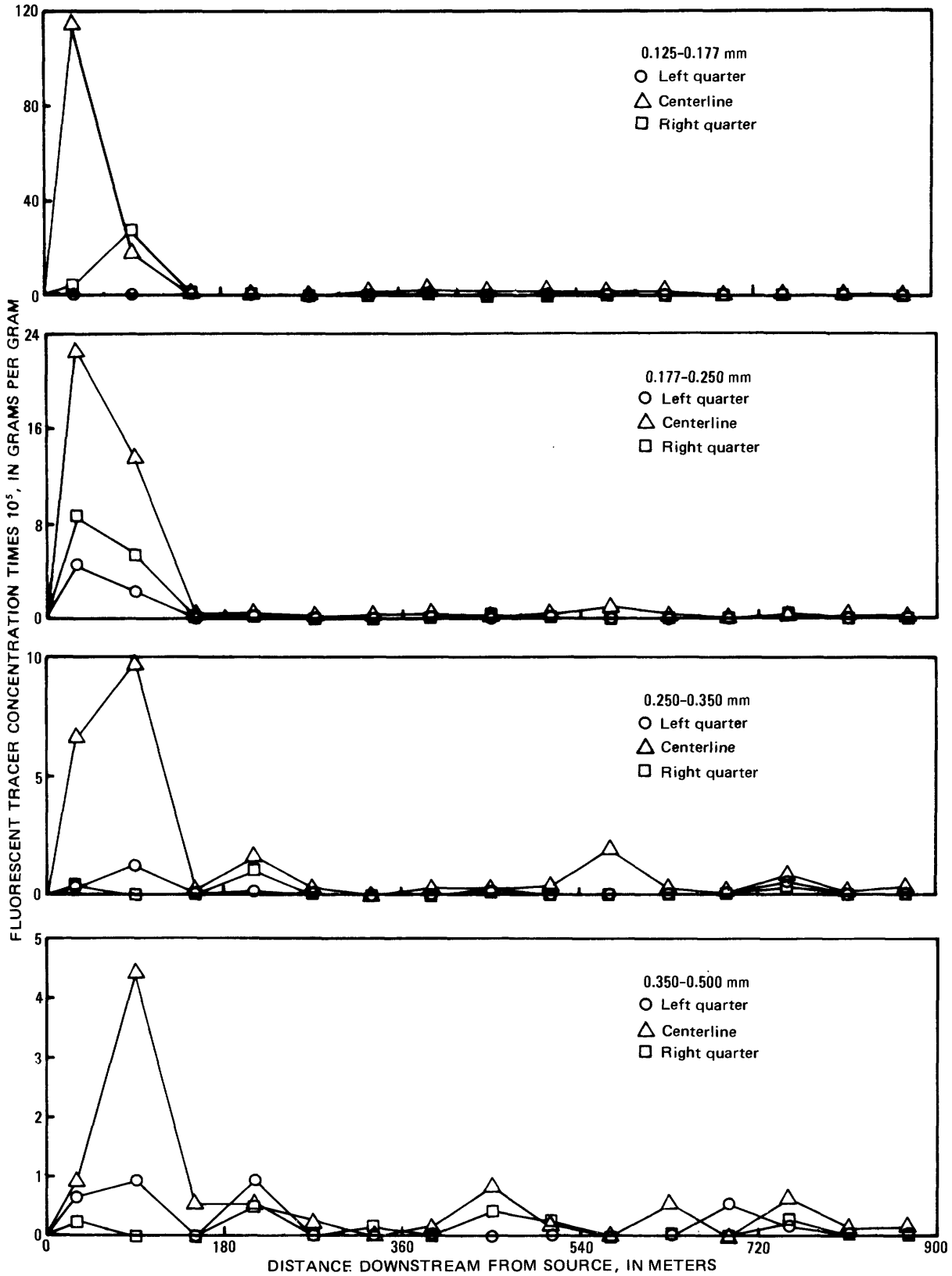

FIGURE 40. — Variation with distance downstream in the concentration of fluorescent tracers for the 0.125- to 0.177-mm, 0.177- to 0.250-mm, 0.250- to 0.350-mm, and 0.350- to 0.500-mm sieve classes of lead tracers as defined by core samples collected on July 14.

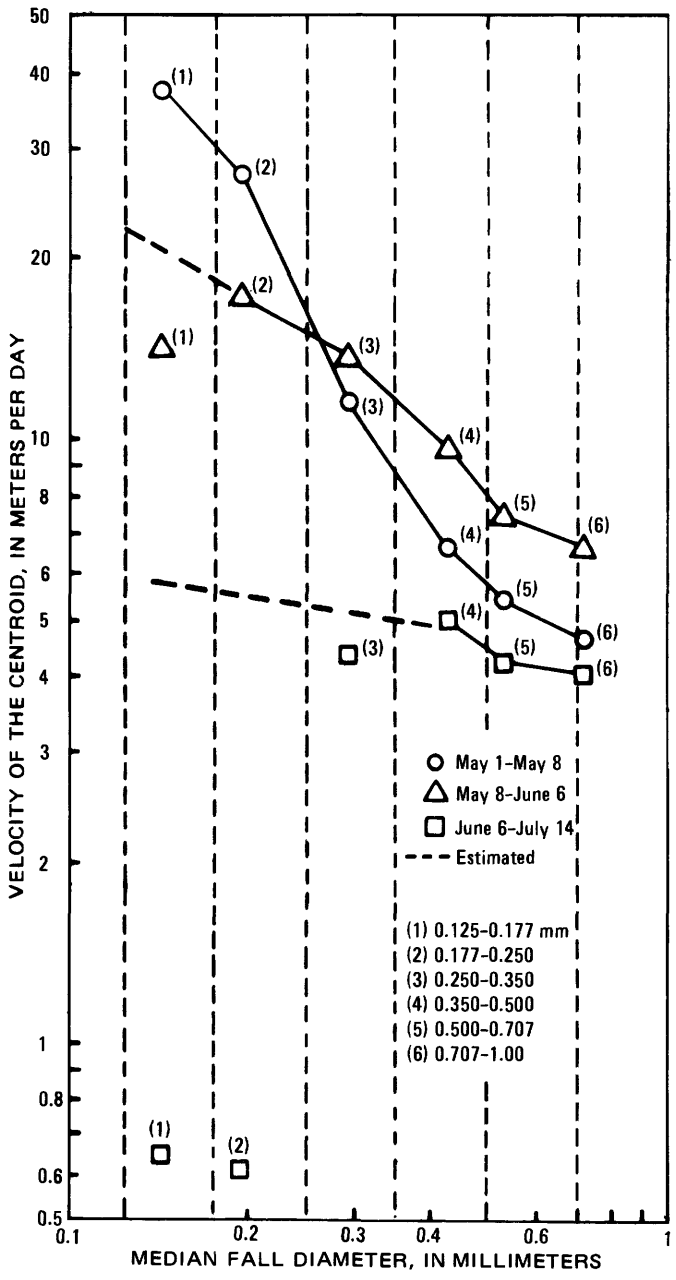

FIGURE 41. — Variation with fall diameter in the velocities of the centroids of the quartz tracer masses as defined by core samples collected on May 8, June 6, and July 14.

time of the dependence on size was probably a result of the fact that large quantities of the small quartz tracer particles had moved out of the study reach by June 6 and July 14. In particular, the V values for the 0.125- to 0.177-mm and 0.177- to 0.250-mm sieve classes for the June 6 to July 14 period were almost one order of magnitude less than what the velocities for the other sieve classes suggested they should be. Some attempt was made, as discussed previously, to correct for this movement beyond the downstream limit of the study reach by extrapolating the longitudinal distribution curve,

TABLE 49. — *Velocities of the centroids of the fluorescent tracer masses as defined by core samples collected on May 8, June 6, and July 14*

Mineral	Sieve class (mm)	V (m/d)		
		May 1–8	May 8–June 6	June 6–July 14
Quartz	(1) 0.125–0.177	38.4	14.3	0.658
	(2) 0.177–0.250	27.6	17.3	.619
	(3) 0.250–0.350	11.6	14.0	4.45
	(4) 0.350–0.500	6.64	9.78	5.03
	(5) 0.500–0.707	5.46	7.53	4.30
	(6) 0.707–1.00	4.69	6.68	4.08
Garnet	(1) 0.125–0.177	19.2	13.7	1.05
	(2) 0.177–0.250	9.63	10.9	3.57
	(3) 0.250–0.350	7.25	9.33	3.20
	(4) 0.350–0.500	5.91	7.19	3.99
	(5) 0.500–0.707	6.28	6.77	3.66
Monazite	(1) 0.125–0.177	14.6	11.6	3.41
	(2) 0.177–0.250	8.53	9.57	4.14
	(3) 0.250–0.350	8.26	8.32	3.54
	(4) 0.350–0.500	6.16	6.46	3.50
	(5) 0.500–0.707	6.28	6.07	2.90
Lead	(1) 0.125–0.177	2.62	1.55	.257
	(2) 0.177–0.250	3.05	1.19	.619
	(3) 0.250–0.350	4.39	1.37	1.53
	(4) 0.350–0.500	2.46	1.39	3.60

but this extrapolation was much too limited, as the following example shows. For the 0.125- to 0.177-mm sieve class to have a V of 6.1 m/d (20 ft/d) for the period between June 6 and July 14, the centroid on July 14 would have to be at about 630 m (2100 ft); for a uniform distribution, the downstream limit of the distribution would have to be at about 1300 m (4300 ft). An extrapolation of 420 m (1400 ft) to this point from the last sample point at 870 m (2900 ft) could not be done with confidence. This example assumed that the centroid position on June 6 was the true position, whereas data for the areas under the distribution curves to be presented shortly (table 52) showed that a significant quantity of the 0.125- to 0.177-mm quartz had already moved out of the study reach on June 6. In fact, even on May 8 some of the 0.125- to 0.177-mm quartz had moved beyond the 540-m (1800-ft) point. Thus, had the June 6 centroid position been moved downstream, the true July 14 centroid position would have been even farther downstream. Figure 41 suggests that the velocities for both the 0.125- to 0.177-mm and 0.177- to 0.250-mm sieve classes of quartz tracer particles for the May 8 to June 6 period probably had been significantly affected by movement of tracer out of the study reach. Also, the centroid velocity for the 0.125- to 0.177-mm sieve class of quartz for the period May 1–8 may have been affected slightly by this factor.

Another factor that probably contributed to the lack of dependence of centroid velocity on size for the June 6–July 14 period, neglecting the 0.125- to 0.177-mm and 0.177- to 0.250-mm sieve classes, was the possibility that quantities of the tracers were trapped in immobile layers near the lower limit of the zone of movement because of decreasing water discharge and

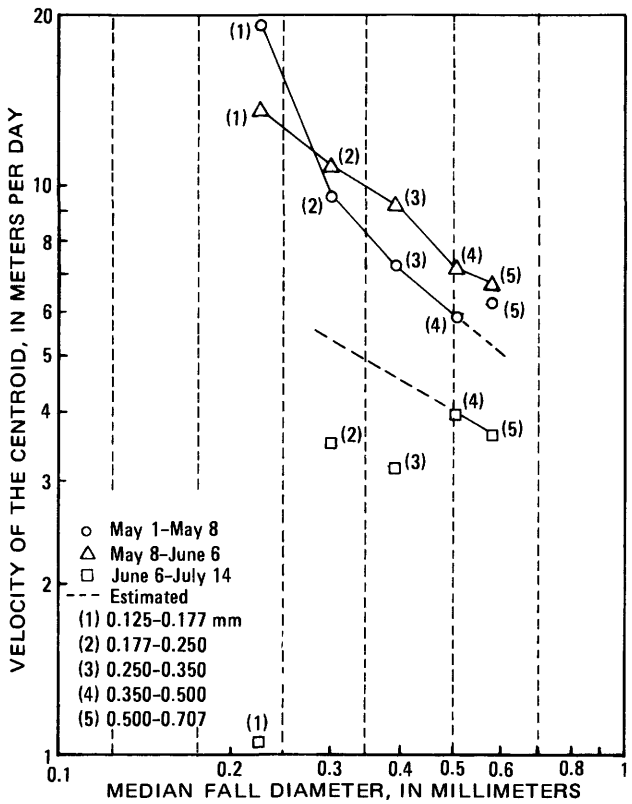

FIGURE 42. — Variation with fall diameter in the velocities of the centroids of the garnet tracer masses as defined by core samples collected on May 8, June 6, and July 14.

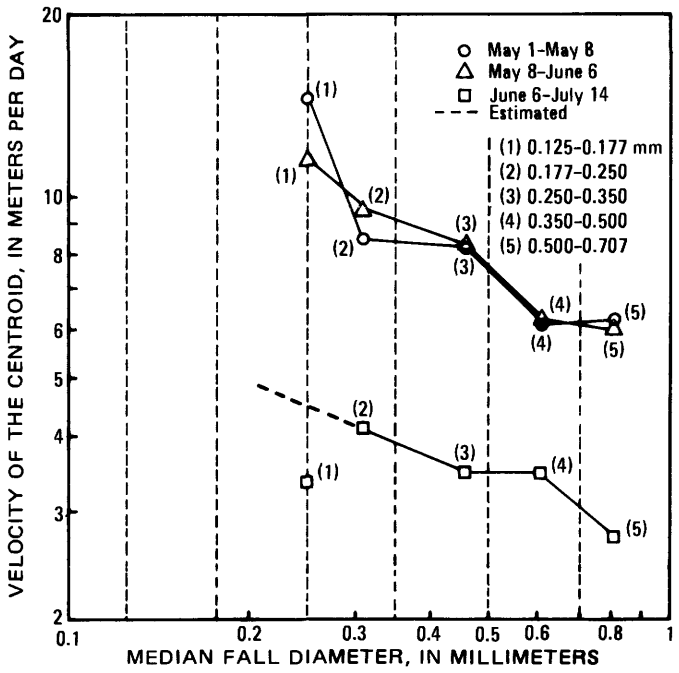

FIGURE 43. — Variation with fall diameter in the velocities of the centroids of the monazite tracer masses as defined by core samples collected on May 8, June 6, and July 14.

the decrease in the sediment transport rate. This possibility would explain not only the apparent decreased dependence on size but also the fact that the velocities for this period were less than for the other two periods. This latter observation is particularly true for the garnet and monazite tracers, as figures 42 and 43 show. These two tracers also showed the same relation of velocity to size that the quartz tracers showed for the June 6–July 14 period.

The centroid velocities for the May 1–8 period presented in table 49 are smaller than the velocities determined from the first-arrival times of the tracer particles at cross section 90 as defined by the "dustpan" samples (table 35). However, the centroid velocities are for tracer particles moving through the complete zone of movement of the dune bed, whereas first-arrival-time velocities are for the smaller particles within the sieve class, which spend a greater than average amount of time moving in suspension and by saltation.

Figures 41, 42, and 43 show that there was little difference between the velocities for the May 1–8 and the May 8–June 6 periods; the May 8–June 6 velocities were, in general, larger than the May 1–8 velocities for the large particles and smaller for the small particles; part of this latter effect, particularly for the quartz, was the result of movement of part of the tracer out of the study reach.

The velocity for the 0.125- to 0.177-mm sieve class of garnet for the June 6–July 14 period was low, probably because a significant quantity of the tracer moved out of the study reach (table 52); to increase this velocity to 4.0 m/d (13 ft/d) would require a July 14 centroid position of about 540 m (1800 ft) which would put the downstream limit at about 1060 m (3500 ft), for an approximately uniform distribution. The longitudinal distribution for this sieve class was truncated at about 1000 m (3300 ft); however, an additional 60-m (200-ft) extrapolation would not be unreasonable (figure 38).

All the quartz, garnet, and monazite velocities, with the exception of the several points that deviated considerably from the other points, are plotted together in figure 44 as a function of the median fall diameter of the sieve class. The scatter increased with fall diameter of the tracer particles. A least-squares regression analysis of the data points showed that the centroid velocity was inversely proportional to the 1.1 power of the fall diameter. This dependence is slightly larger than the 0.86 diameter dependence found for the velocities of the larger tracer particles as defined by the "dustpan" samples (fig. 17).

The considerable scatter of the data points precluded any definite conclusions as to the hydraulic equivalence of the tracer particles. However, because the scatter increased with fall diameter, the smaller particles of

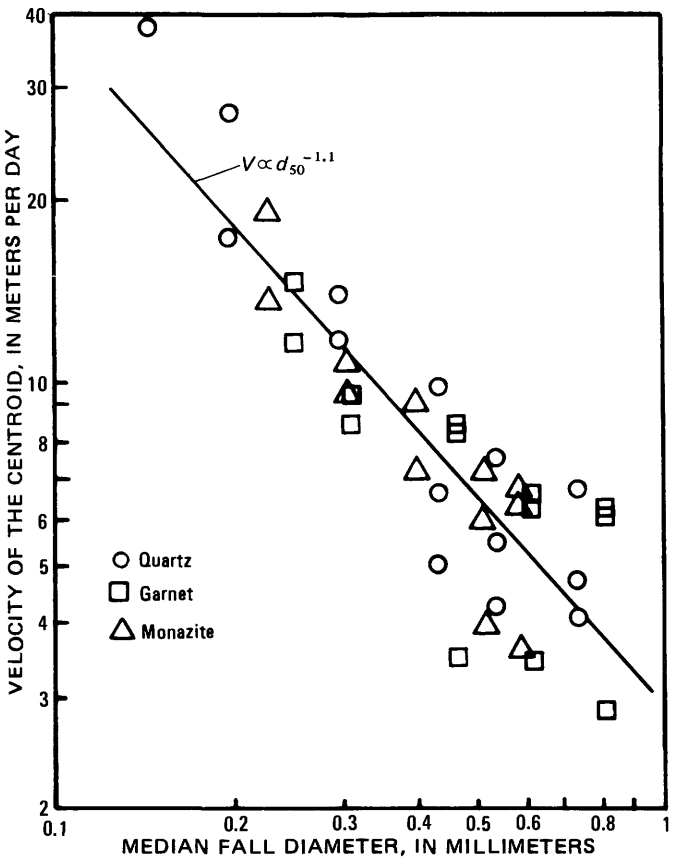

FIGURE 44. — Variation with fall diameter in the velocities of the centroids of the masses of the quartz, garnet, and monazite tracers as defined by core samples collected on May 8, June 6, and July 14.

differing specific gravity appear to be more nearly equivalent hydraulically than the larger particles. These smaller particles moved predominantly in suspension, whereas the larger particles moved predominantly along the bed surface.

SPATIAL-INTEGRATION PROCEDURE

The transport rate of bed material was calculated from the spatial-integration procedure by applying equation 6 to each sieve class of quartz tracer and summing the results.

The equation used was

$$Q_s = \sum_{i=1}^{m} Q_{s_i} = \sum_{i=1}^{m} V_i \bar{d}_{m_i} \gamma_s \ (1-\lambda) p_i B , \quad (28)$$

where m is the number of sieve classes, and p_i is the fraction by weight of bed material in sieve class i. Application of equation 28 was limited to sizes larger than 0.125 mm, for reasons discussed previously.

The mean channel width, B, for the 10 cross sections sampled on May 8 was 17 m (55 ft), and this value was assumed also for June 6 and July 14. The centroid velocities, V_i, were presented in table 49 and discussed in the previous section. The velocities for the 0.125- to 0.177-mm sieve class for the May 8–June 6 period and the 0.125- to 0.177-mm and 0.177- to 0.250-mm sieve classes for the June 6–July 14 period were estimated as 22.9, 5.8, and 5.4 m/d (75.0, 19.0, and 17.8 ft/d), respectively; the observed velocities for these sieve classes were too small, as discussed previously. The mean values of the depth of mixing were presented and discussed previously (table 38). Because the centroid velocities in equation 28 were determined from the change in the position of the centroid in a time period, equation 28 in a sense integrates over the changing flow and transport conditions during this period. Hence, the May 8 and June 6 values were averaged to obtain values of $\bar{d}_{m_i}$ for the May 8–June 6 period and similarly, the June 6 and July 14 values were averaged to obtain values for the June 6–July 14 period. The May 8 values were used for the initial period because it seemed unrealistic to average these values with zero for the start of the injection process.

The $\gamma_s\,(1-\lambda)$ factor was estimated in the laboratory from the volume, under wet conditions, of a known dry weight of sample and the specific weight of quartz. Three samples of bed material from the Atrisco Feeder Canal gave $\gamma_s\,(1-\lambda)$ values of 1676, 1697, and 1697 kg/m^3 (104.7, 106.0, and 106.0 lb/ft^3). These values tended to be maximum values because of the agitation and shaking used in settling the wet sand. Troxell and Davis (1956) suggested that $\gamma_s\,(1-\lambda)$ was 1360 to 1521 kg/m^3 (85 to 95 lb/ft^3) for damp loose sand, Gottschalk (1964) listed 1489 kg/m^3 (93 lb/ft^3) for reservoir deposits of sand under varying conditions of submergence, and Sayre and Hubbell (1965) used 1600 kg/m^3 (100 lb/ft^3) in their application of equation 28. It was decided from a consideration of these values to use 1600 kg/m^3 (100 lb/ft^3) in the present study.

Mean values of the p_i factors were determined from the three size distributions (table 8) of bed material that were used to determine transport rates by the modified Einstein procedure.

The transport rates of bed material calculated from equation 28 are summarized in table 50. Comparison of transport rates for the May 1–8 period and modified Einstein results (table 33) shows good agreement with the May 1 and the May 6 results, both with respect to total rate and the breakdown by sieve class. The May 2 and May 3 modified Einstein results, however, are larger than the rates calculated by the spatial-integration procedure. Further comparison shows that the spatial-integration results are −41.2, +13.3, −35.0, −45.8, −62.8, −20.0, and −15.0 percent different from a mean of the four modified Einstein computations for the 0.125- to 0.177-mm, 0.177- to 0.250-mm, 0.250- to 0.350-mm, 0.350- to 0.500-mm, 0.500- to 0.707-mm,

TABLE 50. — *Sediment transport rates calculated by the spatial-integration procedure*

Sieve class (mm)	Q_s (t/d)		
	May 1–8	May 8–June 6	June 6–July 14
0.125–0.177	48.4	30.8	8.3
0.177–0.250	171.6	116.1	38.7
0.250–0.350	47.1	62.5	22.0
0.350–0.500	7.6	12.2	6.9
0.500–0.707	1.6	2.6	1.6
0.707–1.00	.5	.8	.5
Total	276.8	225.0	78.0

0.707- to 1.00-mm sieve classes and the total transport rate, respectively. These mean modified Einstein results, however, tended to be weighted toward the high side because two of the four computations were for days on which the water discharge was considerably larger than the mean water discharge for the injection period (table 6). Thus, the spatial-integration results are, with one exception, less than the mean of the modified Einstein computations. The true percentage differences are probably less, and agreement, in general, is satisfactory.

Estimates of the water discharge from the stage-discharge relation for the period from May 8 to June 6 showed that the discharge decreased from 8.35 m^3/s (295 ft^3/s) on May 8 to a minimum of 6.17 m^3/s (218 ft^3/s) on May 16, increased to 8.16 m^3/s (288 ft^3/s) on May 23, and then decreased to 7.56 m^3/s (267 ft^3/s) on June 6. The mean discharge for this period was 7.59 m^3/s (268 ft^3/s). A least-squares regression of the logarithm of Q_s versus the logarithm of Q for the four sets of values given in table 33 plus a measured Q and a modified Einstein computed Q_s for May 16 gave an estimated Q_s of 236 t/d (260 tons/d) for a Q of 7.59 m^3/s (268 ft^3/s). This value agrees well with the 225 t/d (248 tons/d) obtained from the spatial-integration procedure.

No stage readings were obtained between June 6 and July 14; hence, it is known only that the discharge was 7.56 m^3/s (267 ft^3/s) on June 6 and 5.30 m^3/s (187 ft^3/s) on July 14. However, a stage-discharge record from the headworks of the canal for the period June 6 to June 25 showed that the decrease in discharge at that point approximately paralleled what the decrease in discharge would have been at the study section, if Q had decreased linearly with time from the June 6 value to the July 14 value. If this hypothesis is true, then the mean discharge for the period was 6.43 m^3/s (227 ft^3/s). The corresponding estimated Q_s was about 154 t/d (170 tons/d) or about two times the rate calculated from the spatial-integration procedure. This large difference for the June 6–July 14 period is not surprising, however, because of the aforementioned possibility that quantities of tracers were trapped during the decreasing flow and transport conditions in immobile layers below the sediment still being transported. These particles were not in motion but were nevertheless sampled and, thus, contributed to the determination of the centroids of the tracer masses. These particles in effect retarded the movement of the centroids downstream, and the calculated velocities were therefore less than the true velocities. Thus, while the spatial-integration procedure has the capability to integrate the effects of changing flow conditions, it would seem that this capability is limited to increasing transport conditions only.

An overall evaluation of the results of the spatial-integration procedure suggested that the calculated transport rates tended to be smaller than the rates estimated by the modified-Einstein procedure. This difference could be the result of modified-Einstein results that were too large, or spatial-integration procedure results that were too small. The first possibility was supported by Maddock (1972) who stated that the modified-Einstein procedure tended to overestimate transport rates. The second possibility results if any of the five factors in equation 28 or combinations of these factors are too small. The study reach was straight and uniform, as figure 2 shows; hence, the channel width was accurately known. The γ_s $(1-\lambda)$ factor was probably within ± 5 percent of the true value. The p_i factors, although by necessity summing to approximately unity, could affect the results. For example, when the p_i factors determined from the analyses of the 0.6-m (2-ft) core samples were used, the calculated total transport rates were less and the distribution of the rates with respect to sieve class was shifted toward the larger sizes. The manner in which bed material samples were obtained and analyzed could affect the results; however, it is expected that this effect should be small. The calculated centroid velocities may be too small if parts of the tracers become buried and stop moving or if the downstream edge of the distribution is truncated such that appreciable tracer is neglected. The last factor is the depth of mixing, and considerable interpretation of the tracer distributions in the different segments of the core samples was necessary, as discussed previously, in the determination of the $\bar{d}_m$ values. However, in view of the sizes of the dunes in the canal, it seems unlikely that the $\bar{d}_m$ values could be much larger than those given in table 38 and used in equation 28. In fact, the dune size and other considerations suggest that the $\bar{d}_m$ values presented in table 38 may be too large. This subject is discussed in detail in the section on the evaluation of the tracer technique.

The difficulties involved in the determination of the depth of mixing can be circumvented by using the centroid depth, which requires no arbitrary decision in its determination, and the procedure of Courtois and Sauzay (1966) to compute the sediment transport rate. Courtois and Sauzay (1966) found for five different types

of vertical distributions that $\bar{d}_m$ was always between two and three times $\bar{d}$. Hence, they concluded that the sediment transport rate could be computed from

$$Q_s = \sum_{i=1}^{m} Q_{s_i} = \sum_{i=1}^{m} 2.5\, V_i \bar{d}_i \gamma_s (1-\lambda) p_i B \qquad (29)$$

and that the actual sediment transport rate should be within 25 percent of the computed value.

Equation 29 was used to compute the sediment transport rates and the results are presented in table 51. Comparison of the results with the transport rates presented in table 50 shows that the rates computed using $\bar{d}$ are −18.1, −8.1, and +8.2 percent different from the rates computed using $\bar{d}_m$ for the May 1–8, May 8–June 6, and June 6–July 14 periods, respectively. Use of equation 29 has inherent in it the assumption that the actual experimental vertical distributions of tracers are similar to one or a combination of several of the five distributions considered by Courtois and Sauzay (1966). In general, experience has shown that vertical distributions of tracers tend to be irregular for the dune-bed configuration. Hence, it seems reasonable to expect that the range of distributions considered by Courtois and Sauzay (1966) would encompass most distributions observed experimentally.

Consideration of the ratio values presented in table 44, which are actually reciprocals of the ratios as used by Courtois and Sauzay, shows that most of the ratios for the quartz tracers for the three sample dates are between 0.50 and 0.33 (2 and 3 for the Courtois and Sauzay definition). Exceptions are the 0.125- to 0.177-mm sieve class on July 14, which has a d value believed to be too large, for reasons discussed previously; the 0.177- to 0.250-mm sieve class on May 8, which may have a $\bar{d}_m$ value too small because the tracer distributions were not fully developed on May 8; and the 0.707- to 1.00-mm sieve class on both June 6 and July 14. The latter tracer particles were found for the most part to be mixed to a significantly smaller depth in the bed than the other tracers, as discussed previously. This sieve class, however, contributed an insignificant amount to the total sediment transport rate. Therefore, it would appear, on the basis of the present study, that equation 29 can be used to avoid the difficulties involved in the determination from core samples of the lower limit of the zone of movement. Further verification is needed, however.

RECOVERY RATIOS

Recovery ratios were calculated for each of the sieve classes of tracers for the three dates on which the spatial distributions of the tracers were determined. The recovery ratio was defined by Sayre and Chang (1968) as the ratio of the amount of tracer actually recovered in the sample collection and analysis procedures to that which would be recovered if these procedures were perfect. Hence,

$$RR = \frac{A_m}{A_t} \qquad (30)$$

where A_m is the area under the measured longitudinal distribution curve and A_t is the area under the theoretical longitudinal distribution curve.

The area for sieve class i, A_{m_i}, is given by

$$A_{m_i} = \int_0^{\infty} \int_0^{B} \int_0^{d_{m_i}} C_i \, dy \, dz \, dx, \qquad (31)$$

where C_i is the tracer concentration of sieve class i at a point x, y, z, where x is distance in the downstream direction, z is distance in the lateral direction, and y is distance in the vertical direction. In practice, integration over the vertical direction was accomplished by extrapolating or truncating, relative to the mean bed elevation, the vertical distributions of tracers in the core sample to a distance equal to the mean value of the depth of mixing and calculating the concentration from equation 25; integration over the lateral direction was accomplished by averaging concentrations at several points in the cross section according to equation 8. Equation 31 then reduces to

$$A_{m_i} = \int_0^{\infty} \bar{C}_i \, dx, \qquad (32)$$

where $\bar{C}_i$ is the concentration of tracer of sieve class i at longitudinal position x as computed by equation 25, and the overbar indicates a mean with respect to z. The area, A_{t_i}, is given by

$$A_{t_i} = \frac{W_i}{\gamma_s (1-\lambda) B \bar{d}_{m_i} p_i}, \qquad (33)$$

where W_i is the weight of tracer of sieve class i injected for the experiment.

The W_i values are given in table 4 and the $\bar{d}_{m_i}$ values in table 38. A value of 1600 kg/m^3 (100 lb/ft^3) was used for $\gamma_s(1-\lambda)$, and a value of 17 m (55 ft) was used for the mean channel width, B. Means of the p_i values determined from the analyses of the many core samples were used. The A_{m_i} values defined by equation 32 are the denominators of equation 4, and the procedure used in the determination of these integrals was described pre-

TABLE 51. — *Sediment transport rates calculated by the Courtois-Sauzay modification of the spatial-integration procedure*

Sieve class (mm)	Q_s (t/d)		
	May 1–8	May 8–June 6	June 6–July 14
0.125–0.177	42.8	31.8	10.3
0.177–0.250	134.8	104.6	43.0
0.250–0.350	40.3	55.0	21.7
0.350–0.500	6.8	11.9	7.1
0.500–0.707	1.5	2.5	1.6
0.707–1.00	.6	1.0	.7
Total	226.8	206.8	84.4

TABLE 52. — *Areas under the measured longitudinal distribution curves (A_m) and recovery ratios (RR) for the fluorescent tracers as defined by core samples collected on May 8, June 6, and July 14*

Mineral	Sieve class (mm)	A_m, in gram-meter/gram			RR		
		May 8	June 6	July 14	May 8	June 6	July 14
Quartz ...	0.125–0.177	0.101	0.019 3	0.006 64	0.422	0.0846	0.0304
	0.177–0.250	.089 3	.035 4	.016 2	.691	.288	.132
	0.250–0.350	.079 6	.072 8	.065 5	.845	.972	.853
	0.350–0.500	.231	.251	.283	.785	1.14	1.32
	0.500–0.707	.500	.533	.637	1.12	1.37	1.67
	0.707–1.00	.115	.112	.142	1.90	1.82	2.27
Garnet ..	0.125–0.177	.019 6	.016 7	.012 5	1.17	1.13	.888
	0.177–0.250	.029 0	.029 2	.026 3	1.00	1.09	1.02
	0.250–0.350	.043 9	.044 8	.045 1	.800	.954	1.00
	0.350–0.500	.051 5	.065 2	.076 8	.547	.833	.966
	0.500–0.707	.012 2	.019 0	.022 3	.427	.722	.956
Monazite	0.125–0.177	.091 7	.101	.082 3	.738	.900	.754
	0.177–0.250	.035 1	.043 9	.033 2	.858	1.16	.901
	0.250–0.350	.024 1	.027 8	.025 0	1.05	1.37	1.14
	0.350–0.500	.044 5	.061 3	.057 6	.716	1.26	1.16
	0.500–0.707	.046 6	.068 3	.065 2	.754	1.13	1.04
Lead	0.125–0.177	.036 9	.065 2	.022 9	.469	.926	.287
	0.177–0.250	.010 2	.107	.008 81	.292	3.41	.297
	0.250–0.350	.007 56	.035 7	.003 29	.313	1.62	.138
	0.350–0.500	.007 01	.025 6	.002 04	.213	.978	.0715

viously in the section on the centroid velocities of the tracers.

The A_m values for May 8, June 6, and July 14 are presented in table 52. The areas under the measured longitudinal distribution curves for each sieve class of tracer should be identical for the three sample times if the sample collection and analysis procedures are perfect. Consideration of the A_m values in table 52 shows definite trends with both time and particle size. The areas for the 0.125- to 0.177-mm sieve classes of quartz and garnet and the 0.177- to 0.250-mm sieve class of quartz decreased with time. This decrease with time was probably the result of failure to extrapolate the leading edges of the concentration distributions far enough downstream. If the May 8 area is used as a basis, then only about 19 percent and 6.6 percent of the 0.125- to 0.177-mm quartz tracer remained in the study reach on June 6 and July 14, respectively; similarly for the 0.177- to 0.250-mm quartz, about 40 percent and 18 percent remained on June 6 and July 14, respectively. Stated another way, if the mean longitudinal concentrations observed in the study reach on June 6 and July 14 for the 0.125- to 0.177-mm sieve class of quartz were continued downstream, then the lengths of reach required to give an area equal to the area under the longitudinal distribution curve observed on May 8 would be 5420 and 15 200 m (17 800 and 49 800 ft), respectively; similarly, for the 0.177- to 0.250-mm sieve class of quartz, the reach lengths would be 2450 and 5890 m (8040 and 19 320 ft), respectively. These large reach lengths indicate that the centroid velocities for these sieve classes may have been considerably underestimated using the limited extrapolation procedures described previously.

The change in area with time for the 0.125- to 0.177-mm sieve class of garnet was not so large as for the quartz tracers. Using the May 8 area as a basis, the percentages remaining on June 6 and July 14 were about 85 and 64, respectively.

The area values for the four sieve classes of lead tracers varied considerably with time and showed no consistent trends except that the areas were largest for all four sieve classes on June 6. The large variations in the areas for the lead tracers were probably the result of a problem associated with counting the lead particles. A blue dye was used on the lead and the color of this dye's fluorescence resembled that of lint and fiber under the ultraviolet light. Hence, it was difficult to distinguish between actual lead tracer particles and extraneous materials.

The areas for some of the large particles increased with time. This is believed to be a result of the fact that on May 8 these tracers had, for the most part, moved only a short distance downstream. Hence, sample coverage was poor, and linear interpolation between the limited number of sample points probably resulted in large errors in the estimation of the areas. On the later dates, these particles had moved farther downstream, and sample coverage was improved.

The recovery ratios defined by equation 30 are presented in table 52 also. The ratios, in comparison with the theoretical value of 1.00, were satisfactory, with the exception of the June 6 and July 14 values for the 0.125- to 0.177-mm and 0.177- to 0.250-mm sieve classes of quartz tracer, the three values for the 0.707- to 1.00-mm sieve class of quartz tracer, and the values for the four sieve classes of lead tracer. The lead tracers have both the largest and the smallest of all the ratio values and by far the largest variability with time. This variability was not unexpected, in view of the large

variability of the A_m values presented in table 52 and the previously discussed problem in counting the lead particles. The decrease with time of the ratios for the two sieve classes of quartz tracer also was expected because of the aforementioned movement of these sizes of tracer out of the study reach and the associated decrease of the A_m values. The May 8 ratio suggests that only slightly more than 40 percent of the 0.125- to 0.177-mm sieve class of quartz tracer was recovered on this sample date; this means that the estimated extrapolations based on the May 8 areas, discussed in previous paragraphs, would be even longer than those presented. The explanation for the large values for the 0.707- to 1.00-mm sieve class of quartz tracers is unknown. Ratios larger than 1.00 indicate that more tracer material was recovered than was injected. A possible explanation is that the A_m values were too large as a result of the poor sample coverage discussed previously.

To analyze the calculation of the recovery ratios, consider the various factors contained in equations 32 and 33. The $\gamma_s(1-\lambda)$ and B factors were discussed in the section on the spatial-integration procedure and were considered to be known accurately. The p_i factors were determined from the analysis of a large member of 0.6-m (2-ft) core samples and thus were accurately known. The W_i factors were determined from the size distributions of the pure tracer materials (table 1) and the total amounts of tracer injected (table 3). The total amount injected was determined for each tracer from the injection rate and the length of the injection period. This amount was checked against the amount determined from the weights of tracers in each bag at the beginning of the experiment and the empty bags at the conclusion of the experiment; the differences for the various tracers were all less than 5 percent.

The mean value of the depth of mixing appears both in the denominator of equation 33 and inherently in equation 32 as the upper limit of integration over the vertical direction. To estimate the effect that an incorrect $\bar{d}_{m_i}$ value would have on the recovery ratio, recovery ratios were computed using a value of 0.6 m (2.0 ft).

It was found that a relatively large error in the depth of mixing had only a very small effect on the calculated values of the recovery ratios. The explanation for this may be seen at least qualitatively by considering again equations 30, 32, and 33. If $\bar{d}_{m_i}$ is overestimated, then the effect in equation 33 is to give an A_{t_i} value that is too small; the effect in equation 32 will be to include additional bed material containing zero or very small concentrations of tracer at the bottom of the core, thus producing concentrations that are too small and areas under the distribution curves that are too small; the net effect on the recovery ratio in equation 30 tends to cancel. It was concluded, therefore, that the computation of the recovery ratio is relatively insensitive to the value of the depth of mixing, at least for the conditions of the present study.

The final factor entering into the calculation of the recovery ratios is the integral term defined by equation 32. Numerous considerations enter into the accurate determination of these integrals, among which are obtaining sufficient samples across the channel and sampling to a sufficient depth to define accurately the cross sectional mean concentration; sieve analysis of the samples and counting of the number of fluorescent particles of each color in each sieve class; determining the particles per gram factors (table 5) for conversion of the number of particles to concentrations; determining the depth of mixing from the vertical distributions of the tracers; conversion of the cross sectional mean concentrations into longitudinal distributions; and extrapolating or truncating the leading edges of the longitudinal distributions to give a finite upper limit of integration for equation 32. The same procedures were used for all 20 sieve classes of tracer materials; thus, if there had been some consistent error in these procedures, one might expect that the recovery ratios would have all been similarly affected. However, the various sieve classes of tracers all moved with different velocities and dispersion rates, and, hence, the same procedure could result in different errors for the different sieve classes and specific gravities of tracers.

Mean values of the recovery ratios were calculated, neglecting the 0.125- to 0.177-mm and 0.177- to 0.250-mm sieve classes of quartz tracer for the June 6 and July 14 sample dates and the 0.707- to 1.00-mm sieve class for all three dates. Results are presented in table 53. The mean ratios increased from May 8 to June 6 but changed little between June 6 and July 14. In view of the large volume of bed material in which the tracers were mixed, the recovery ratios are considered satisfactory.

TABLE 53. — *Mean values of the recovery ratios for the fluorescent tracers as defined by core samples collected on May 8, June 6, and July 14*

Mineral	Mean recovery ratio			
	May 8	June 6	July 14	Mean
Quartz	0.772	1.16	1.28	1.02
Garnet	.789	.945	.966	.900
Monazite	.824	1.16	.999	.996
Mean	0.795	1.08	1.05	...
Overall mean	...	...	...	0.966

LONGITUDINAL DISPERSION COEFFICIENTS

The recommended procedure (Sayre and Chang, 1968) for calculating the longitudinal dispersion coefficient, K_x, of a dissolved dispersant is

$$K_x = \frac{\bar{U}^3}{2} \frac{d\sigma_t^2}{dx}, \qquad (34)$$

where $\bar{U}$ is the mean flow velocity, σ_t^2 is the variance of a concentration versus time curve, and x is the coordinate in the longitudinal direction. Fischer (1966) showed that an equivalent representation for K_x is

$$K_x = \frac{1}{2}\frac{d\sigma_x^2}{dt}, \tag{35}$$

where σ_x^2 is the variance of a concentration versus distance curve, and t is time. Furthermore, Fischer (1966) showed that these relations are independent of the initial distribution of tracers, after some initial period during which the one-dimensional diffusion equation does not apply. In equations 34 and 35 the variances are determined by the method of moments.

By analogy, then, the longitudinal dispersion coefficient for sediment tracer particles moving by a combination of transport along the bed surface, saltation, and suspension may be defined as

$$k_x = \frac{1}{2}\frac{d\sigma_x^2}{dt}, \tag{36}$$

Variances of the longitudinal distribution curves of the various sieve classes of tracers for May 8, June 6, and July 14 were calculated from

$$\sigma_x^2 = \frac{\int_0^{x_{0.01}} x^2\bar{C}\,dx}{\int_0^{x_{0.01}} \bar{C}\,dx} - \bar{x}^2 \tag{37}$$

where $\bar{x}$ is the position of the centroid, the calculation of which was described in the section on the velocities of the centroids of the tracer masses. The upper limit of integration is the longitudinal position at which the concentration decreased to 1.0 percent of the maximum concentration. The denominator is the area under the longitudinal distribution curve; these areas have been presented previously in table 52. The integral in the numerator was evaluated in the same manner as the integrals were evaluated in determining the velocities, that is, by plotting $x^2\bar{C}$ versus x and assuming that $x^2\bar{C}$ varied linearly with x between sample points. The area was determined by summing the areas of the trapezoids thus formed.

The variances of the longitudinal distribution curves are presented in table 54 and plotted as a function of the median fall diameter of the sieve class in figures 45, 46, and 47 for the quartz, garnet, and monazite tracers, respectively. The variances for the lead distributions were not plotted because they were considered to be less reliable than the quartz, garnet, and monazite values.

Figures 45, 46, and 47 show similar trends — that is, a very large dependence of σ_x^2 on fall diameter for the May 8 samples, less dependence on diameter for the June 6 samples, and least dependence on diameter for the July 14 samples. The vertical dashed lines in these figures represent the size limits of the sieve classes used in the analysis of the samples and the numbers next to each point are the sieve class number given in table 54. With the exception of the 0.500- to 0.707-mm sieve class of garnet on May 8 and July 14, the variances in general decrease with increasing particle size.

The variance, σ_x^2, represents the rate of spreading

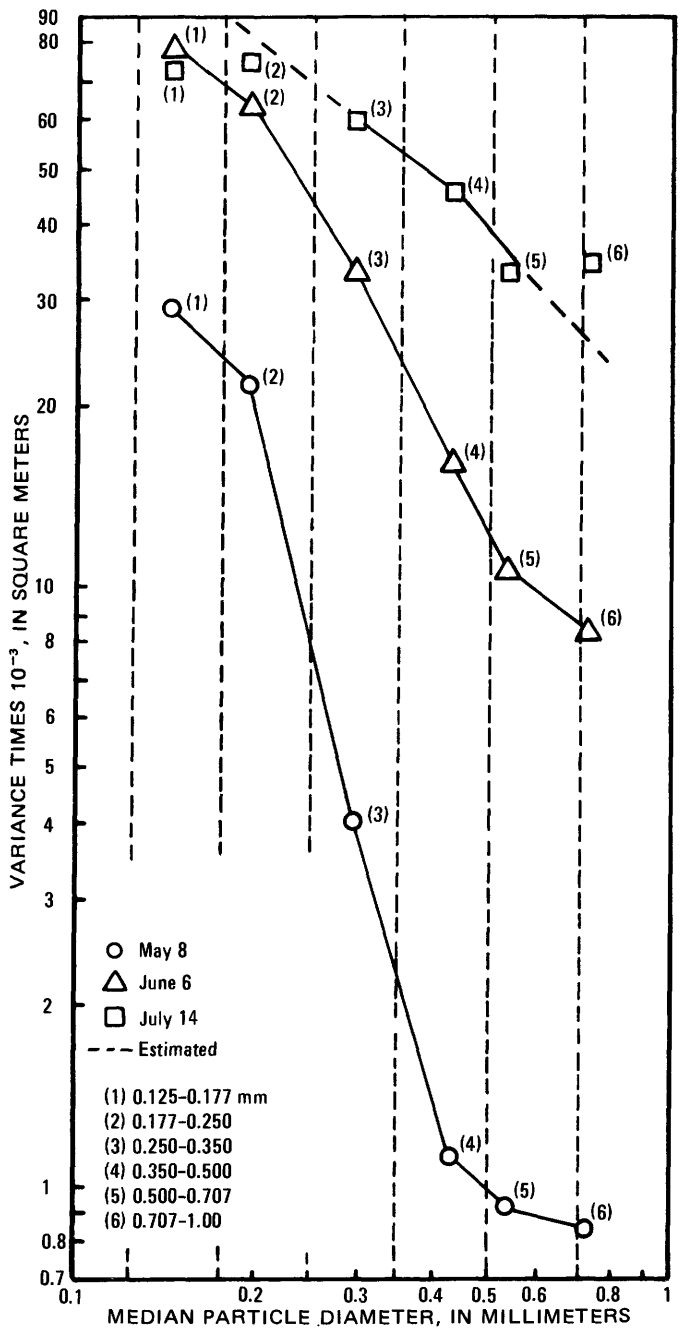

FIGURE 45. — Variation with fall diameter in the variances of the longitudinal distributions of the quartz tracers as defined by core samples collected on May 8, June 6, and July 14.

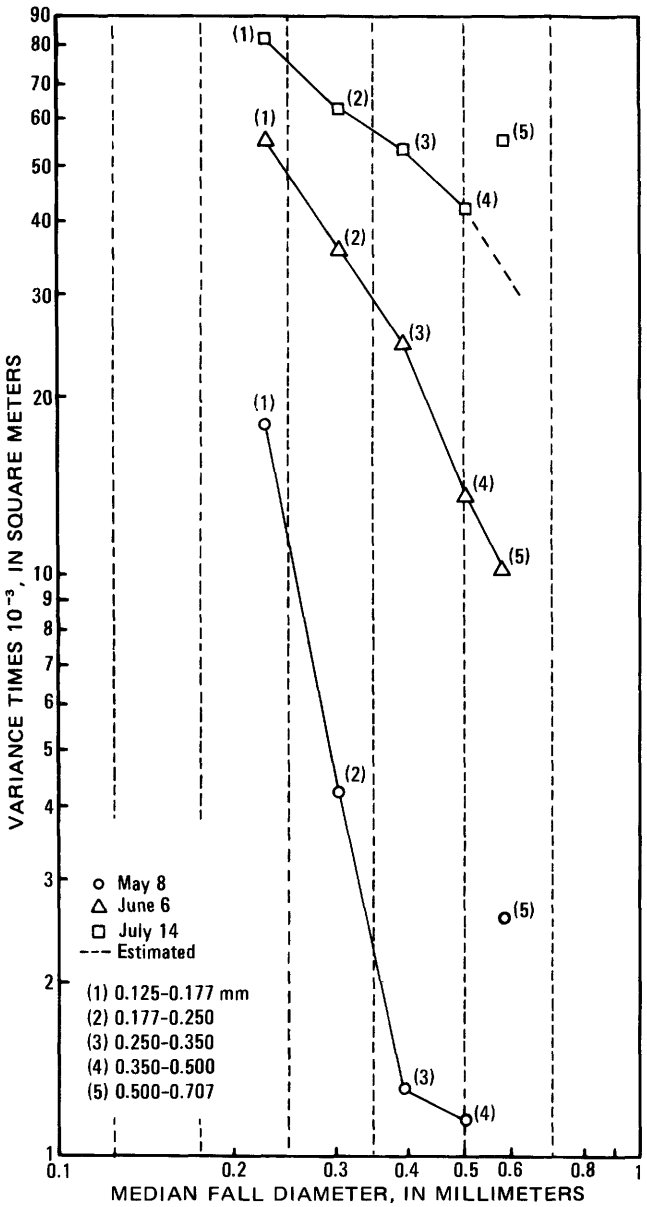

FIGURE 46. — Variation with fall diameter in the variances of the longitudinal distributions of the garnet tracers as defined by core samples collected on May 8, June 6, and July 14.

downstream. These variances and the longitudinal distribution curves from which they were derived (figs. 26–40) clearly show that the small particles moved and spread far downstream, whereas the large particles tended to move only a short distance downstream from the source.

The variance values presented in table 54 for the lead tracers in general show exactly the opposite effect — that is, σ_x^2 tended to increase with particle size. The reason for this is uncertain, but it probably reflects the generally less reliable nature of the lead results. Personnel counting fluorescent particles tended to ignore a few small blue particles because small pieces of lint and fiber looked much the same under the ultraviolet light.

TABLE 54. — *Variances of the longitudinal distributions of fluorescent tracers as defined by core samples collected on May 8, June 6, and July 14*

Mineral	Sieve class (mm)	σ_x^2 times 10^{-3} (m^2)		
		May 8	June 6	July 14
Quartz	(1) 0.125–0.177	29.4	80.7	73.5
	(2) 0.177–0.250	22.0	64.5	76.0
	(3) 0.250–0.350	4.04	33.8	60.8
	(4) 0.350–0.500	1.11	16.2	46.4
	(5) 0.500–0.707	.920	10.7	33.9
	(6) 0.707–1.00	.845	8.45	34.8
Garnet	(1) 0.125–0.177	18.0	55.2	82.5
	(2) 0.177–0.250	4.25	36.1	62.8
	(3) 0.250–0.350	1.31	24.9	53.2
	(4) 0.350–0.500	1.15	13.7	42.4
	(5) 0.500–0.707	2.56	10.2	55.3
Monazite ..	(1) 0.125–0.177	12.0	43.0	67.6
	(2) 0.177–0.250	2.40	28.3	61.3
	(3) 0.250–0.350	1.17	19.4	49.2
	(4) 0.350–0.500	1.11	11.2	33.4
	(5) 0.500–0.707	1.02	9.66	28.9
Lead	(1) 0.125–0.177	.186	.604	.910
	(2) 0.177–0.250	.316	.130	.948
	(3) 0.250–0.350	.929	.929	3.87
	(4) 0.350–0.500	.223	1.03	20.2

To test the concept of hydraulic equivalence, the σ_x^2 values in figures 45, 46, and 47 were plotted together in figure 48 as a function of the median fall diameter. The quartz points in figure 48 for each sample date were connected with straight lines. On each date, the garnet and monazite points tended to fall around the line; however, the scatter about the lines appeared to increase with increasing particle size. The scatter in the results and uncertainties introduced in extrapolating the longitudinal distributions beyond the end of the study reach precluded any definite conclusions regarding hydraulic equivalence of the tracer particles. It appeared, however, that the small particles, which moved predominantly in suspension, were approximately equivalent but that the large particles, which moved predominantly by surface creep, were not. Also, the results of the present study do not permit a distinction between transport along the back of a dune and transport from the crest of a dune to the trough but apply only to the net result of the transport over many dune forms.

The problem of extrapolating the longitudinal distribution curves for the 0.125- to 0.177-mm and 0.177- to 0.250-mm sieve classes of quartz tracer for the June 6 and July 14 sample dates was discussed previously. Because the extrapolations of these tracer distributions were very conservative and because the variances are extremely sensitive to the concentrations in the area of the leading edge of the distribution curves, the calculated variances for the 0.125- to 0.177-mm and 0.177- to 0.250-mm sieve classes were expected to be much too

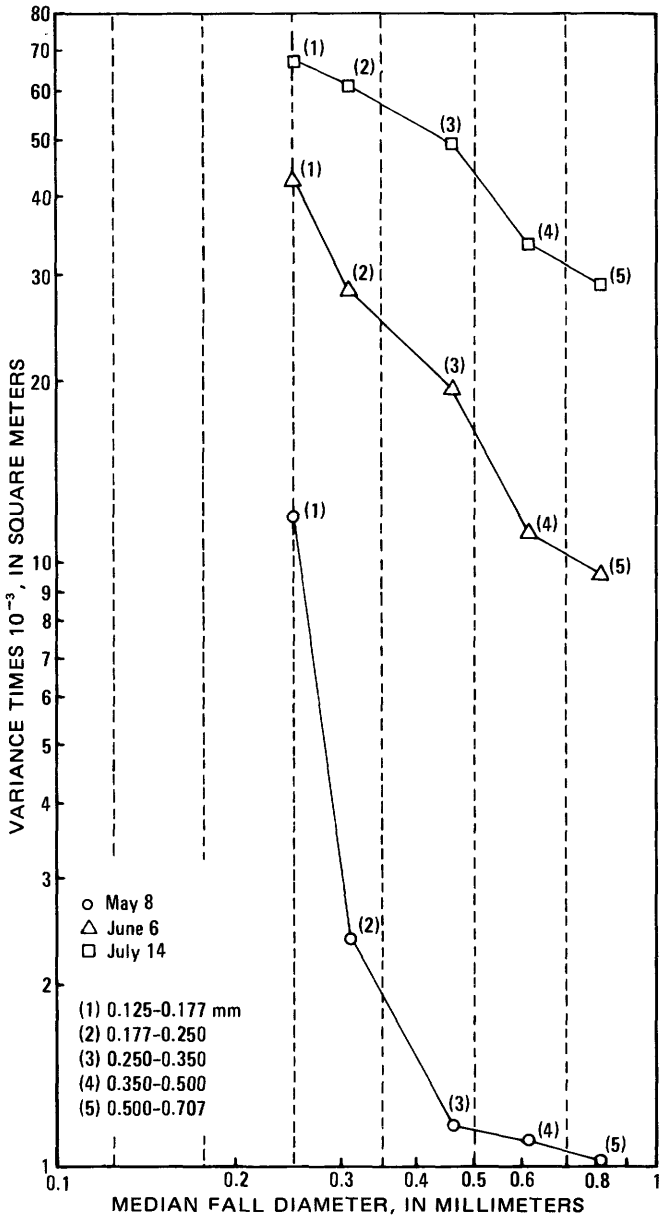

FIGURE 47. — Variation with fall diameter in the variances of the longitudinal distributions of the monazite tracers as defined by core samples collected on May 8, June 6, and July 14.

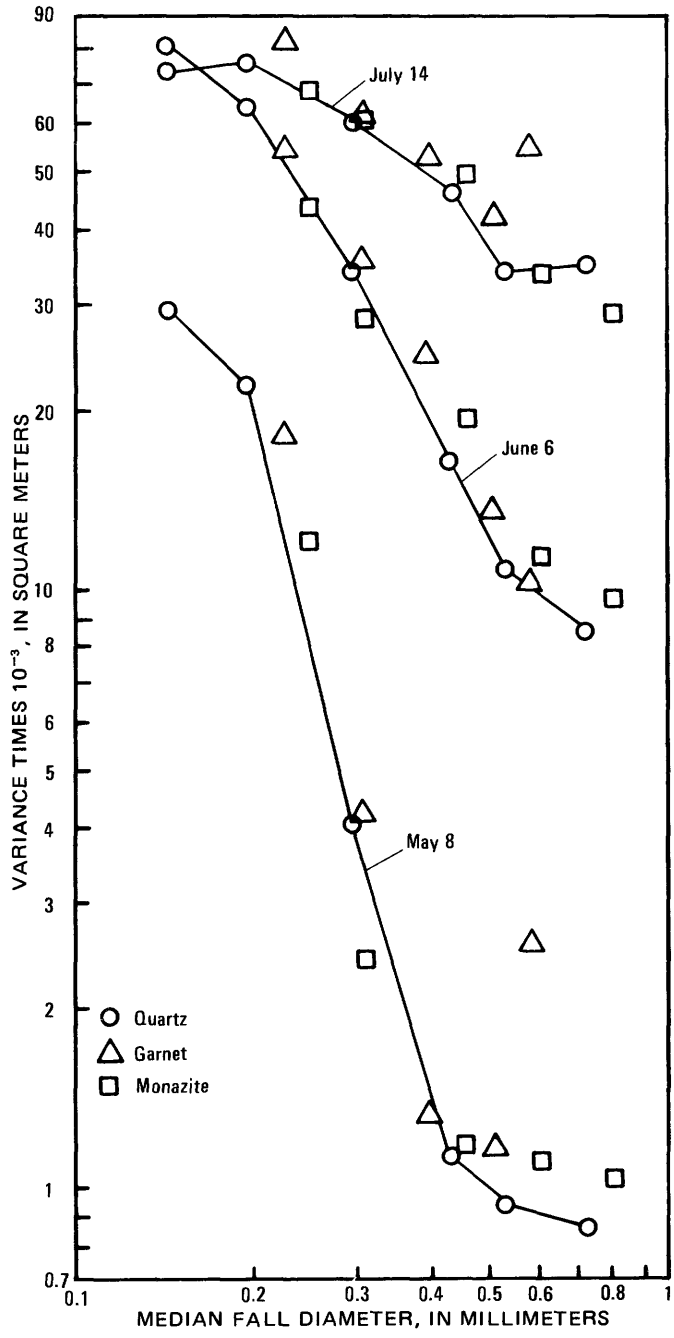

FIGURE 48. — Variation with fall diameter in the variances of the longitudinal distributions of quartz, garnet, and monazite tracers as defined by core samples collected on May 8, June 6, and July 14.

small. This was true, as figure 45 shows the calculated σ_x^2 value for the 0.125- to 0.177-mm sieve class for July 14 was actually less than the value for June 6, and the June 6 value for the 0.177- to 0.250-mm sieve class approximated the July 14 value.

Hence, in the determination of the longitudinal dispersion coefficient, k_x, by equation 36, the σ_x^2 values for the 0.125- to 0.177-mm and 0.177- to 0.250-mm sieve classes of quartz were estimated by extrapolating the general trend of the curve to be 133 and 82.7 m^2 (1430 and 890 ft^2), respectively, for July 14. Also, the values for the 0.707- to 1.00-mm sieve class of quartz and the 0.500- to 0.707-mm sieve class of garnet for July 14 were estimated as 25.1 and 36.2 m^2 (270 and 390 ft^2), respectively. Least-squares lines were calculated for the σ_x^2 versus time data, and the slopes were used to compute k_x from equation 36. The k_x values are presented in table 55. The values of k_x decreased with increase in particle size, supporting the previous conclusion that the small particles dispersed downstream faster than the large particles. The k_x values presented

TABLE 55. — *Longitudinal dispersion coefficients determined from distributions of fluorescent tracers defined by core samples collected on May 8, June 6, and July 14*

Mineral	Sieve class (mm)	k_x (m^2/h)
Quartz	0.125–0.177	32.0
	0.177–0.250	18.4
	0.250–0.350	17.5
	0.350–0.500	14.2
	0.500–0.707	10.4
	0.707–1.00	7.62
Garnet	0.125–0.177	19.8
	0.177–0.250	18.0
	0.250–0.350	16.1
	0.350–0.500	13.0
	0.500–0.707	10.7
Monazite	0.125–0.177	17.1
	0.177–0.250	18.3
	0.250–0.350	15.0
	0.350–0.500	10.2
	0.500–0.707	8.77

in table 55 should be considered approximate because they were determined from only three sets of σ_x^2 versus t data.

Comparison of the k_x values in table 55 with the lateral dispersion coefficient, k_z, values presented previously in table 45 shows that the k_x values are from 286 to 1300 times larger than the corresponding k_z value.

EVALUATION OF THE FLUORESCENT TRACER TECHNIQUE

Both the steady-dilution and spatial-integration procedures gave values of the total transport rate of bed material that were in good agreement with total transport rates calculated by the modified Einstein procedure. Agreement of the transport rates for the individual sieve classes was not as good but was satisfactory in most instances. The two tracer techniques, however, have different characteristics and requirements for their application. The steady-dilution procedure is analogous to the Eulerian technique of classical fluid mechanics — that is, one cross section of the channel is monitored as the tracer particles move through the channel. The spatial-integration procedure, on the other hand, is Lagrangian in the sense that the movement of the tracer particles is followed throughout the study reach. Thus, the differences in characteristics and requirements will influence the selection of the technique to be used in a particular study. The advantages and disadvantages of each are discussed in the following paragraphs.

The steady-dilution procedure requires samples only at the measurement cross section. Samples as a function of time at enough points in the cross section to define a mean concentration for the cross section are necessary; also, enough samples must be obtained to insure that plateau concentrations are achieved for all sieve classes of interest. The results of the present study showed that samples of the material moving along the surface of the dune bed are sufficient, provided the injection of tracers has been long enough to permit establishment of equilibrium with respect to mixing in the dune bed. An advantage of the steady-dilution procedure is that at the critical time for estimating the sediment transport rate, the samples all have relatively large concentrations of tracers; hence, the counting statistics are excellent, and small errors in the particle counts do not significantly affect the results. A disadvantage of the steady-dilution procedure is that a decision as to when plateau concentrations have been achieved must be made on the basis of a qualitative analysis of the samples under field conditions. Single concentrations are used in the steady-dilution procedure — that is, ratios of concentrations are not involved (eq 2) — and, hence, the number of fluorescent particles per gram of fluorescent material must be accurately known for each sieve class.

The steady-dilution procedure, as the name implies, requires a continuous injection of tracers until, under ideal conditions, a steady-state concentration that is uniform across the channel is obtained at the measurement cross section. An acceptable alternative is a distribution of tracer concentrations that is not changing appreciably with time at some downstream cross section. This alternative requires that the sediment transport rate be approximately uniform across the channel. For a low-sediment-velocity dune-bed condition such as existed in the present study, a long injection period and a large quantity of tracer are needed to allow sufficient time for such a steady-state distribution to develop. A long injection period requires constant attention by project personnel and the injection rate of each sieve class of tracer must be accurately known. Another requirement of the steady-dilution procedure is that the sediment transport rate and, hence, that the hydraulic conditions in the reach be reasonably constant during the injection period. This is particularly important for low sediment velocities because the concentrations at the measurement cross section would take a very long time to respond to changing conditions.

Two variations of the steady-dilution procedure, although not used in the present study, would appear to have advantages when there is a large range of particle velocities, such as was true for the dune-bed form of the present study. The first variation would be to have several measurement cross sections at varying distances downstream from the injection point. These cross sections would be located according to the mixing and dispersion characteristics of the different sizes of tracer particles. Locations of these cross sections could

be estimated by using the lateral dispersion parameters presented in table 37. Thus, the slower moving, rapidly dispersing large particles would be sampled at an upstream cross section and the faster moving, slowly dispersing small particles would be sampled at a downstream cross section. This procedure would reduce the total sampling time required to obtain information on a range of particle sizes.

The second variation would be to sample at one cross section until a plateau concentration was obtained for the smaller sizes of tracer particles. Determination of when a plateau concentration was obtained would have to be on the basis of a qualitative examination of samples in the field. After the plateau was established, samples would be collected in the upstream direction to determine the points at which plateau concentrations were established for the larger particles. The cross section should be located about twice the distance downstream at which significant quantities of the small tracer particles reach the banks of the channel. This distance can be estimated using the lateral dispersion information presented in table 37. This second variation probably would require fewer samples than the first variation or the basic steady-dilution procedure as used in the present study.

The spatial-integration procedure requires a one-time slug injection of the tracers and determination of the complete spatial distributions of the tracers within the study reach for at least two different times. Hence, the advantage of the simple injection process is offset by the need to collect and analyze many more samples than are necessary for the steady-dilution procedure. The spatial distributions should be determined in a quasi-instantaneous manner, that is, the change in the position of the centroid during the sample collection period should be negligible relative to the change in position between the determinations of the distributions. This was not a problem in the present study where the sediment transport rates were small. The mean value of the depth of mixing must be determined for the spatial-integration procedure; thus, core samples, analyzed in several separate segments, must be obtained. The velocities of the centroids of the tracer masses must be determined, and this determination requires the measurement of the very small concentrations out on the leading edges of the tracer distributions. If the bed material and the corresponding tracers contain a range of particle sizes, then sorting with respect to size in the downstream direction, such as occurred in the present study, requires that a very long reach be sampled.

The spatial-integration procedure required two somewhat arbitrary decisions in the present study because of the extreme sensitivity of the fluorescent tracer procedure. The first was deciding where to truncate the leading edges of the longitudinal distributions; the point selected was that at which the concentration decreased to 1.0 percent of the maximum concentration of the distribution. The point selected affects the determination of the centroid velocity and has even greater significance in the determination of the variances of the longitudinal distributions. The second was deciding what constituted the lower limit of mixing in the core samples. This decision was complicated by the general irregularity of the distributions of tracers among the segments of the core samples. The procedure decided upon was to neglect bottom segments when two or more consecutive segments contained very small concentrations of tracers.

The spatial-integration procedure can in theory be used for changing flow conditions, and it has been suggested (Crickmore, 1967, p. 179) that the procedure automatically integrates the effects of changing conditions between the times at which the spatial distributions are determined. On the other hand, Hubbell and Sayre (1965) pointed out that the centroid velocity, the channel width, and the depth of mixing all may vary with both time and position in the reach for changing hydraulic and sediment transport conditions, thus complicating the interpretation of the results. An additional problem associated with decreasing flow and transport conditions is the trapping of tracers near the lower limit of the zone of movement. These tracers, although no longer in motion, are still sampled by the core sampler. This apparently occurred in the present study and affected the mean values of the centroid depth, the centroid velocities, and consequently the transport rates calculated by the spatial-integration procedure. Such a problem, however, does not occur if the flow and transport conditions are constant or increasing with time. On the other hand, it would still be necessary to know how V, $\bar{d}_m$, and B are changing with time (Hubbell and Sayre, 1965).

The steady-dilution and spatial-integration procedures can be used to calculate the total transport rates of bed material, provided the tracer material covers the entire range of sizes present in the moving bed material. In the present study, however, the analysis for fluorescent particles was limited to particles larger than 0.125 mm because of the difficulty of distinguishing between actual particles and chips or flakes of dye from large particles. The 0.062- to 0.088-mm and 0.088- to 0.125-mm sieve classes may contribute substantially to the total transport rates of many channels. If these size classes are important, then it is suggested that a different color of dye be used for each of them. This procedure was not possible in the present study because the other colors of dyes were

used on the garnet, monazite, and lead, and experience has shown that the human eye can distinguish easily at most four colors of dye on small sand particles. Some difficulty was experienced with the green dye because the bed material of the Atrisco Feeder Canal contained natural material that fluoresced under the ultraviolet light with a very light green color. The difficulties with the blue dye used on the lead particles were discussed previously.

In many streams, it may be unnecessary to use the tracer technique for measurement of the 0.062- to 0.088-mm and 0.088- to 0.125-mm sieve classes because there is enough turbulence that sampling of suspended sediment by standard methods is sufficiently accurate.

The comparison of results ($\bar{z}$, σ_x^2, $d\sigma_z^2/dx$ and k_z) determined from the "dustpan" samples and the core samples obtained on May 8 showed no significant differences. This result suggests that samples of the bed material moving along the surface of the bed and the accompanying tracers are sufficient to define the dispersion and mixing properties of the dune bed, when the tracers are mixed throughout the depth of mixing of the dune bed. The only apparent requirements are that a continuous injection of tracers be used and that sufficient time be allowed for the tracers to establish equilibrium with respect to the depth of mixing.

There are, as discussed previously, three basic methods for estimating the mean value of the depth of mixing. Hubbell and Sayre (1964) used all three procedures with radioactive tracers in two laboratory studies and one field study. They obtained comparable results with all procedures except in one laboratory study where they attributed the lack of agreement to an insufficient number of core samples. They concluded (Hubbell and Sayre, 1965) that the procedure based on the analysis of sonic depth-sounding records was probably the most reliable. De Vries (1966) also used this method in his flume study with fluorescent tracers. He suggested that the core sample procedure was very laborious and that a very large number of core samples had to be analyzed to get an acceptable average because of the irregularity of the bed forms. He believed that the procedure based on the mass continuity of the tracers was apt to give uncertain results if part of the tracers were temporarily buried; also the small concentrations in the tail region of the distribution are important in the calculation of the integral. De Vries (1966) suggested one possible disadvantage of the depth-sounding record procedure — that is, one deep trough gives a very large contribution to the computation of the mean value of the depth of mixing. It would seem, however, that such a trough would give an incorrect $\bar{d}_m$ only if it did not persist through the study reach. If this occurred, then it is apparent that several profiles should have been obtained at different times throughout the study to determine the effect of time on $\bar{d}_m$. De Vries (1966) observed one situation in which a deep trough existed, and he concluded that a better estimate of $\bar{d}_m$ for this run was 0.5 $\bar{H}$, where $\bar{H}$ is the mean dune height.

Crickmore (1967) used the core sample method and a somewhat arbitrary modification of the mass conservation method in his field study with radioactive tracers. Because of the generally irregular distributions of tracers in the segments of the core samples, he computed the depth of mixing from

$$d_c = \frac{\Delta y(r_1 + r_2 + r_3 \ldots)}{r_{MAX}}, \tag{38}$$

where Δy is the thickness of the core sample segment, r_1, r_2, r_3, ... are the activities in segments 1, 2, 3, ... and r_{MAX} is the maximum activity in any segment. In the application of equation 38, the observed vertical distributions of tracers were arbitrarily adjusted to produce either uniform distributions or distributions that decreased continuously with depth in the core sample. Using this procedure, the computed depth of mixing for a uniform distribution corresponds to the lower limit of activity in the core sample; for distributions that decrease with depth, the computed depth of mixing lies between the centroid of the vertical distribution of the tracer and the lower limit of the distribution. It would seem, then, that depths of mixing computed by this procedure in general will be less than the true depth of mixing that should be used in equation 28. This conclusion is supported by the results of Crickmore (1967) who found that depths of mixing computed from equation 38 were about 20 percent less than the depths of mixing computed on the basis of mass continuity of the tracers.

However, the phenomenon of the presence of tracers, both radioactive and fluorescent, at depths in the bed much deeper than would be expected on the basis of the dune heights has been noted and discussed previously by Grigg (1969). In a laboratory study using single radioactive tracers, he found that the particles tended to deposit more frequently below the mean bed-surface elevation than above; thus, the particles moved deeper and deeper into the bed. To check this observation, he used three sizes of fluorescent particles, allowing them to recirculate several times through the system until equilibrium was established. From an analysis of core samples, he found significant concentrations of tracers at as many as six standard deviations below the mean bed-surface elevation. The bed-surface elevation of a dune bed is generally considered to be approximately normally distributed about the mean bed elevation (Crickmore and Lean 1962; Yang, 1968; Nordin, 1971). Grigg (1969) pointed out that the probability of exposing a bed-surface elevation five standard deviations

below the mean bed-surface elevation was less than 0.01 percent. Because this was an extremely unlikely event, he sought another explanation for the phenomenon.

Grigg (1969) considered the core sample data of Sayre and Hubbell (1965) and Yang (1968) and concluded that the phenomenon was present in the data of Yang but not in that of Sayre and Hubbell. He attributed the difference to the fact that Yang was sampling with a small-diameter sampler in clean uniform sand in a laboratory flume, whereas Sayre and Hubbell were sampling with a large-diameter sampler in natural river sand containing fine sand and clay. A reconsideration of the data of Sayre and Hubbell (1965), however, suggests that the phenomenon may have been present in their data as well. They analyzed 19 core samples and found that the "average depth to which tracer particles extended below the bed surface was 1.45 feet (0.442 metres)." This $\bar{d}_m$ value was in good agreement with $\bar{d}_m$ values determined by the other two procedures. If samples are collected at random positions on a dune bed, then the mean bed-surface elevation of the points at which samples are collected approaches the true mean bed-surface elevation as the number of samples becomes large. However, Sayre and Hubbell (1965, p. C12) restricted their sampling largely to the troughs of the dunes; hence, the 0.442 m (1.45 ft) is more correctly relative to the mean trough elevation than to the mean elevation of the bed. This conclusion is supported by the fact that the mean depth of flow at the 19 sample points (Sayre and Hubbell, 1965, figs. 25–29) was 0.762 m (2.50 ft) compared with a mean flow depth of 0.646 m (2.12 ft) for the reach. The mean dune height was about 0.305 to 0.457 m (1.0 to 1.5 ft) (Hubbell and Sayre, 1965, p. C20); hence, the depth of mixing, relative to the mean bed-surface elevation, probably is at least 0.442 + 0.15 or about 0.60 m (1.45 + 0.5 or about 2.0 ft). Nordin (1971) found that the standard deviation of the bed elevation is approximately 0.1 the mean flow depth; thus, $\sigma_y \cong 0.06$ m (0.2 ft) for the study reach of Hubbell and Sayre. This means then that the lower limit of the zone of movement was approximately 10 standard deviations below the mean bed-surface elevation; the probability of exposing a point this many standard deviations below the mean bed-surface elevation is very small.

Grigg (1969) suggested two possible explanations for this phenomenon — (1) migration of the tracer particles downward in the bed, and (2) a basic error associated with the core sampling technique. He concluded that the core sampling technique was the most likely explanation and suggested two ways in which the technique could produce the phenomenon. First, pushing the sampler into the bed could compress the loosely formed dune bed at the sample point; and second, mixing could occur in the sampler when it was rotated upward to prevent loss of the bottom part of the sample. A third possibility exists, however, and that is drag at the inside surface of the sampler and subsequent smearing downward of the tracers as the barrel of the sampler is pushed into the bed. This problem and the resultant effect on cores of marine sediments was discussed by Igarashi, Ridlon, Campbell, and Allman (1970).

This discussion of the depth of mixing indicates that further study of this parameter is needed. It enters directly into the calculation of the transport rate of bed material by the spatial-integration procedure (eq 28) and into the calculation of the areas under the longitudinal distribution curves through the calculation of the concentrations. On the other hand, the effect of the depth of mixing on the dispersion parameters, the velocities of the centroids, and the recovery ratios tends to cancel because ratios of concentrations are involved in the compution of these quantities.

SUMMARY AND CONCLUSIONS

A tracer technique, in which mineral particles were coated with fluorescent dyes, was used to study the transport and dispersion of sediment particles of various diameters and specific gravities under dune-bed conditions in an alluvial channel. The experiment was conducted in the Atrisco Feeder Canal near Bernalillo, N. Mex., from May 1 to July 14, 1967. Samples of the bed material in transport and the accompanying tracers moving along the surface of the dune bed were obtained periodically during the study with "dustpan" samplers especially designed for fluorescent tracer studies. In addition, the spatial distributions of the tracers in the bed were determined three times during the study by core sampling.

Principal conclusions are —

1. The total transport rate of bed material measured by the steady dilution procedure was within the range of total transport rates computed by the modified Einstein procedure. When the measured and computed transport rates were compared by sieve classes, agreement was good for the small sizes but was poor for the large sizes. The steady-dilution procedure gave rates for the large particles that were too large because plateau concentrations for these particles were not achieved during the injection period.
2. The total transport rate of bed material measured by the spatial-integration procedure for the period from May 1 to May 8 corresponded closely to the rates computed by the modified Einstein procedure for this period. Qualitative comparisons of the same type for the second and third periods from May 8 to June 6 and from June 6 to July 14 showed that the rate for the spatial-integration procedure agreed well with

the computed rate for the second period but that the spatial-integration result for the third period was too small. This discrepancy was attributed to the trapping of tracer particles in immobile layers of the bed during the decreasing flow conditions in the latter part of the study, and to transport of large numbers of the small tracer particles beyond the study reach.

3. The steady-dilution procedure has the advantage that information on tracer concentrations need be collected at only one cross section; however, the sampling or monitoring must be sufficiently comprehensive to identify when plateau concentrations are achieved for all sieve classes of interest and also to define mean concentrations for the cross section. Disadvantages of the procedure are (a) a very long injection period may be necessary to obtain plateau concentrations if the sediment velocities are small, as they were in the present study; (b) the injection rates of the tracers and the number of fluorescent particles per gram of fluorescent material must be known accurately; and (c) the requirement of constant hydraulic and sediment transport conditions is likely to be violated. The injection period can be shortened by having two (or more) measurement cross sections, one near the injection point for the slower-moving, rapidly dispersing large particles and the other farther downstream for the faster moving, slowly dispersing small particles.
4. The spatial-integration procedure has the advantage that an instantaneous slug injection of tracers may be used. Disadvantages of the procedure are (a) much more information on tracer concentrations is necessary than for the steady-dilution procedure because complete spatial distributions of the tracers in the study reach must be determined at least twice; (b) determination of the mean velocities of the tracer particles involves measuring the small concentrations on the leading and trailing edges of the tracer distributions; and (c) required information on the depth of mixing and the vertical distributions of the tracers ordinarily must be obtained by analyzing segments of core samples. Also, the quantity of tracers injected for each sieve class must be known; however, the number of fluorescent particles per gram of fluorescent material need not be known. The spatial-integration procedure in theory integrates the effects of changing flow conditions. However, results of the present study suggest that the procedure is not applicable to a dune-bed condition when the rate of transport decreases with time and bed material previously in transport is deposited on the bed.
5. "Dustpan" samples showed that the velocities of the leading edges of the tracer masses at cross section 90 for the small tracer particles were inversely proportional to the 0.86 power of the fall diameter. The change in the dependence of the velocity on the particle fall diameter seemed to occur at a diameter between 0.25 and 0.30 mm, which is just slightly larger than the median diameter of the bed material of the canal.
6. "Dustpan" samples showed that both the variance of the lateral distributions of tracer concentrations at a particular cross section and the rate of change of the variance with distance downstream increased with the size of the tracer particles. This indicates that lateral dispersion increases with particle size. The lateral dispersion coefficient, defined analogously to the dispersion coefficient for a dissolved dispersant, showed a large dependence on particle size for the small particles and relatively little dependence for the large particles.
7. Further study of the depth of mixing parameter is needed. Tracers were found at larger depths in the dune bed than would be expected on the basis of the sizes of the dunes in the channel, in agreement with earlier studies described in the literature. However, only the calculation of the transport rate of bed material by the spatial-integration procedure and the calculation of the areas under the longitudinal distribution curves are affected by an incorrect depth of mixing; the effect of an incorrect value of the depth of mixing on the calculation of the dispersion parameters, the centroid velocities, and the recovery ratios of the tracers tends to cancel because ratios of concentrations are involved.
8. The mean values of the depth of mixing increased between May 8 and June 6 and changed very little between June 6 and July 14. Depth of mixing values for the largest particle sizes of the quartz and monazite tracers were significantly smaller than values for other sizes of these tracers. Depth of mixing values for the four sieve classes of lead tracer were significantly smaller than values for comparable sieve-diameter sizes of the other tracers.
9. The mean values of the centroid depth increased with time throughout the experiment, in contrast to the depth of mixing. The difference in behavior was attributed to trapping of some of the tracers in immobile layers near the lower limit of the zone of movement as flow decreased during the latter part of the study.

10. The ratio of the centroid depth to the depth of mixing, which is indicative of the vertical concentration gradient, in general, increased with time during the study. The ratio values indicated that the large and heavy particles tended to be more concentrated toward the bottom of the zone of movement. Conversely, the mean values of the depth of mixing showed that the zones of movement for these particles tended to be thinner than for the smaller and less dense particles.

11. The variances of the lateral distributions of concentration determined from the core samples showed the same characteristics as those for the "dustpan" samples — that is, the variances increased with particle size at a particular cross section and the rate of change of the variance with distance downstream increased with particle size. Comparison of the mean lateral positions, variances, rates of change of variance with distance downstream, and lateral dispersion coefficients for the lateral concentration distributions determined from the "dustpan" samples and from the core samples obtained at the end of the injection period showed that the results were approximately the same. Hence, it would appear that samples of the material moving along the surface of the bed are sufficient to define the lateral dispersion characteristics of sediment particles for a dune-bed form. The only apparent requirements when "dustpan" samples are used are a continuous injection of tracers and sufficient time to permit establishment of equilibrium with respect to mixing in the dune bed.

12. The velocities of the centroids of the tracer masses determined from the core samples were inversely proportional to the 1.1 power of the median fall diameter of the sieve class. The velocities were smaller than the velocities based on first arrival times at cross section 90 as determined from the "dustpan" samples. The differences apparently result from the fact that the centroid velocities are for particles moving throughout the complete zone of movement, whereas the first-arrival-time velocities are primarily for the smaller particles sizes within each sieve class, which spend a greater than average amount of time moving in suspension and by saltation.

13. Recovery ratios for the tracers, which indicate how closely the sample collection and analysis procedures approximate perfect conditions, were satisfactory with the exception of the ratios for the two smallest sizes and the largest size of quartz tracer and the four sieve classes of lead tracer. The ratios for the small quartz tracers were too small because of the movement of large quantities of these tracers out of the study reach. Ratios for the lead tracers were generally inconsistent because of problems in determining sample concentrations accurately.

14. The variances of the longitudinal distributions of mean cross-sectional concentrations determined from the core samples decreased as particle size increased. The longitudinal dispersion coefficient, defined analogously to the dispersion coefficient for a dissolved dispersant, also decreased as the particle size increased.

15. The lead tracer particles moved so slowly that only qualitative evaluations of their rates of movement and dispersion were possible. Some of the lead tracer particles moved about 90 m (300 ft) downstream during the extent of the study.

16. Mean particle velocities, variances of the concentration distributions, and rates of change of the variances with distance and (or) time determined from both the "dustpan" and core samples were comparable for tracer particles having the same fall diameter but different specific gravities. It appeared that the smaller tracer particles which moved predominantly in suspension were more nearly hydraulically equivalent than were the large particles which moved predominantly by surface creep. However, the scatter of the data precluded any definite conclusions regarding the hydraulic equivalence of the tracer particles.

17. The highly variable concentrations of tracer particles within the segments of a particular core sample and between adjacent core samples downstream from the injection point strongly indicate that dune movement does not result in a uniform mixing of the sediment in transport as might be expected. This observation, plus the apparently anomalous depth of mixing, suggests that there is much to be learned about the specifics of particle movement in the dune-bed regime.

18. The fluorescent tracer technique is an excellent tool for following the movement of particles of various sizes and specific gravities for the dune-bed condition of alluvial-channel flow. The steady-dilution procedure is preferred when the bed form is dunes because the number of samples required to establish dispersion characteristics, particles velocities, and transport rates is less than for the spatial-integration pro-

cedure. Improvements in methods for injecting the tracer particles, determining tracer concentrations, and other procedures are needed, however.

REFERENCES CITED

Bennett, C. A., and Franklin, N. L., 1954, Statistical analysis in chemistry and the chemical industry: New York, John Wiley & Sons, 724 p.

Brady, L. L., and Jobson, H. E., 1973, An experimental study of heavy-mineral segregation under alluvial-flow conditions: U.S. Geol. Survey Prof. Paper 562–K, 38 p.

Colby, B. R., 1964, Discharge of sands and mean-velocity relationships in sand-bed streams: U.S. Geol. Survey Prof. Paper 462–A, 47 p.

Colby, B. R., and Hembree, C. H., 1955, Computations of total sediment discharge Niobrara River near Cody, Nebraska: U.S. Geol. Survey Water-Supply Paper 1357, 187 p.

Colby, B. R., and Hubbell, D. W., 1961, Simplified methods for computing total sediment discharge with the modified Einstein procedure: U.S. Geol. Survey Water-Supply Paper 1593, 17 p.

Courtois, G., and Sauzay, G., 1966, The count rate balance methods of measuring sediment mass flows by radioactive tracers: La Houille Blanche, v. 21, no. 3, p. 279–290.

Crickmore, M. J., 1967, Measurement of sand transport in rivers with special reference to tracer methods: Sedimentology, v. 8, p. 175–228.

Crickmore, M. J., and Lean, G. H., 1962, The measurement of sand transport by the time-integration method with radioactive tracers: Royal Soc. [London] Proc., v. A270, p. 27–47.

De Vries, M., 1966, Applications of luminophores in sand transport studies: Delft, Netherlands, Delft Hydraulics Lab. Pub. 39, 86 p.

Fischer, H. B., 1966, A note on the one-dimensional dispersion model: Internat. Jour. Air and Water Pollution, v. 10, p. 443–452.

_____1967, Transverse mixing in a sand-bed channel, *in* Geological Survey research 1967: U.S. Geol. Survey Prof. Paper 575–D, p. D267–D272.

Gottschalk, L. C., 1964, Reservoir sedimentation, *in* Ven Te Chow, ed., Handbook of applied hydrology: New York, McGraw-Hill Book Co., p. 17–17.

Grigg, N. S., 1969, Motion of single particles in sand channels: U.S. Geol. Survey open-file rept., 142 p.

_____1970, Motion of single particles in alluvial channels: Am. Soc. Civil Engineers Proc., Jour. Hydraulics Div., v. 96, no. HY 12, p. 2501–2518.

Guy, H. P., Simons, D. B., and Richardson, E. V., 1966, Summary of alluvial channel data from flume experiments, 1956–61: U.S. Geol. Survey Prof. Paper 462–I, 96 p.

Hubbell, D. W., and Matejka, D. Q., 1959, Investigations of sediment transportation Middle Loup River at Dunning, Nebraska: U.S. Geol. Survey Water-Supply Paper 1476, 123 p.

Hubbell, D. W., and Sayre, W. W., 1964, Sand transport studies with radioactive tracers: Am. Soc. Civil Engineers Proc., Jour. Hydraulics Div., v. 90, no. HY 3, p. 39–68.

_____1965, Closure to Sand transport studies with radioactive tracers: Am. Soc. Civil Engineers Proc., Jour. Hydraulics Div., v. 91, no. HY 5, p. 139–149.

Igarashi, Y., Ridlon, J. B., Campbell, J. R., and Allman, R. L., 1970, Note on a mode of piston core disturbance: Jour. Sed. Petrology, v. 40, no. 4, p. 1351–1355.

Karaki, S. S., Gray, E. E., and Collins, J., 1961, Dual channel stream monitor: Am. Soc. Civil Engineers Proc., v. 87, no. HY 6, p. 1–16.

Kennedy, V. C., and Kouba, D. L., 1970, Fluorescent sand as a tracer of fluvial sediment: U.S. Geol. Survey Prof. Paper 562–E, 13 p.

Lean, G. H., and Crickmore, M. J., 1966, Dilution methods of measuring transport of sand from a point source: Jour. Geophys. Research, v. 71, no. 24, p. 5843–5855.

Maddock, Thomas, Jr., 1972, Closure to indeterminate hydraulics of alluvial channels: Am. Soc. Civil Engineers Proc., Jour. Hydraulics Div., v. 98, no. HY 3, p. 555–567.

Nordin, C. F., Jr., 1971, Statistical properties of dune profiles: U.S. Geol. Survey Prof. Paper 562–F, 41 p.

Rathbun, R. E., Kennedy, V. C., and Culbertson, J. K., 1971, Transport and dispersion of fluorescent tracer particles for the flat-bed condition, Rio Grande conveyance channel, near Bernardo, New Mexico: U.S. Geol. Survey Prof. Paper 562–I, 56 p.

Rittenhouse, G., 1943, Transportation and deposition of heavy minerals: Geol. Soc. America Bull., v. 54, p. 1725–1780.

Rubey, W. W., 1933, The size-distribution of heavy minerals within a water-laid sandstone: Jour. Sed. Petrology, v. 3, no. 1, p. 3–29.

Sayre, W. W., and Chang, F. M., 1968, A laboratory investigation of open-channel dispersion processes for dissolved, suspended, and floating dispersants: U.S. Geol. Survey Prof. Paper 433–E, 71 p.

Sayre, W. W., and Hubbell, D. W., 1965, Transport and dispersion of labeled bed material North Loup River, Nebraska: U.S. Geol. Survey Prof. Paper 433–C, 48 p.

Simons, D. B., and Richardson, E. V., 1966, Resistance to flow in alluvial channels: U.S. Geol. Survey Prof. Paper 422–J, 61 p.

Task Committee for the Preparation of the Sedimentation Manual, 1971, Sediment discharge formulas: Am. Soc. Civil Engineers Proc., Jour. Hydraulics Div., v. 97, no. HY 4, p. 523–567.

Troxell, G. E., and Davis, H. E., 1956, Composition and properties of concrete: New York, McGraw-Hill Book Co., 434 p.

U.S. Inter-Agency Committee on Water Resources, 1957a, The development and calibration of the visual-accumulation tube, *in* A study of methods used in measurement and analysis of sediment loads in streams: Washington, U.S. Govt. Printing Office, Rept. 11, 109 p.

_____ 1957b, Some fundamentals of particle-size analysis, *in* A study of methods used in measurement and analysis of sediment loads in streams: Washington, U.S. Govt. Printing Office, Rept. 12, 55 p.

Yang, Tsung, 1968, Sand dispersion in a laboratory flume: Fort Collins, Colo., Colorado State Univ., Dept. Civil Eng., unpub. Ph. D. dissert., 162 p.

SUPPLEMENTAL DATA

TABLES 12 – 31 AND 46 – 48

TABLE 12. — *Concentration of quartz tracers in the 0.125- to 0.177-mm sieve class in "dustpan" samples collected at cross section 90*

[Leaders (. . .) indicate no sample collected at that time and lateral position; (*) indicates sample was misplaced]

Hours from injection (h)	Left edge of water (m)	Concentration times 10^5, at indicated lateral position (in m)										
		1.5	3.0	4.5	6.0	7.5	9.0	10.5	12	13.5	15	16.5
0.067	1.1	. . .	. . .	. . .	1.75	(*)	2.48	3.62	1.24	0.849	. . .	. . .
.270	1.1	. . .	. . .	0.0610	1.85	3.88	4.10	1.38	1.38	1.63	. . .	. . .
.500	1.1	. . .	0.271	.217	1.43	3.80	(*)	2.50	1.92	.721	.203	0.200
1.13	1.1	. . .	1.07	.227	4.18	12.2	1.41	3.91	6.41	1.64	2.12	..337
2.00	1.1	. . .	.620	.594	4.01	9.47	6.51	6.79	6.06	2.38	.766	(*)
3.09	1.1	. . .	.278	1.35	3.15	16.2	8.44	7.58	5.06	3.10	.664	.133
4.05	1.1	. . .	1.81	1.07	6.50	23.2	8.34	25.3	16.2	3.12	2.10	.0681
5.06	1.1	. . .	.604	2.97	4.44	15.6	10.8	29.5	6.61	6.70	.551	.158
6.00	1.1	. . .	5.20	1.52	8.75	26.2	10.4	9.06	21.9	2.57	1.76	.305
8.06	1.1	. . .	.759	3.08	5.55	30.8	(*)	18.8	7.44	4.75	1.35	.434
10.0	1.1	. . .	.630	3.52	13.5	25.8	17.7	14.9	13.2	3.93	2.84	1.41
12.0	1.1	. . .	.382	4.16	16.1	18.1	30.5	19.4	34.1	.824	2.30	.320
22.0	1.1	. . .	4.20	8.48	17.9	61.0	17.9	47.0	22.2	8.24	5.11	.328
34.0	1.1	. . .	5.38	8.20	33.8	97.1	25.2	54.4	11.8	4.32	(*)	.281
47.0	1.1	1.21	6.12	5.03	16.6	137	25.6	11.5	4.21	9.29	1.25	.180
59.8	1.1	1.99	4.35	30.0	11.5	72.3	27.0	20.7	5.79	4.86	.909	.387
70.7	1.1	1.73	4.80	24.5	65.5	24.0	29.5	58.8	23.0	2.81	2.37	.326
83.5	1.1	.550	5.36	8.04	96.7	59.0	92.4	7.83	13.3	1.62	.833	.106
95.1	1.1	.790	11.4	6.99	28.0	126	76.8	104	7.93	2.31	.274	.116
108	1.1	3.21	3.60	35.0	41.8	154	42.8	14.4	20.4	4.63	1.49	.553
118	1.1	2.44	13.9	51.5	90.1	133	47.1	44.2	18.2	1.91	.892	.756
124	1.1	2.38	17.0	63.5	105	117	67.7	1.03	15.5	.848	1.52	1.20
132	1.1	4.45	18.6	15.3	81.5	120	88.7	19.9	19.9	6.09	(*)	.675
138	1.1	4.15	1.42	8.42	61.6	145	62.4	70.1	7.62	3.00	2.12	.309
143	1.1	(*)	(*)	79.4	37.1	139	49.9	4.25	48.7	2.10	.964	.270
149	1.1	.326	4.35	13.2	74.0	86.7	75.8	55.2	(*)	5.87	1.76	.663
162	1.1	(*)	6.55	8.60	69.3	104	137.	22.8	27.9	11.4	2.50	.740
193	1.5	1.40	3.75	12.7	9.31	6.77	23.3	11.0	9.29	3.87	1.38	.360
238	.5	1.86	5.57	3.65	8.94	10.4	8.21	1.85	.536	.764	.124	. . .
285	.5	.588	.743	2.21	2.58	4.92	5.51	1.44	.916	.0714	.513	. . .
339	.5	.273	.698	1.06	1.71	1.71	.221	.411	.119	.103	.187	. . .
356	.3	0	.338	.0790	.809	1.22	.632	.655	.248	.154	.161	. . .
429	.3	7.20	37.0	4.29	107	1.18	.0810	12.2	52.6	5.69	11.2	. . .
525	.3	.0950	.568	1.50	.666	2.94	1.17	.750	.250	.163	.0434	. . .
597	.3	.790	.760	.230	1.43	.103	(*)	.294	.790	0	.450	. . .

TABLE 13. — *Concentration of quartz tracers in the 0.177- to 0.250-mm sieve class in "dustpan" samples collected at cross section 90*

[Leaders (. . .) indicate no sample collected at that time and lateral position; (*) indicates sample was misplaced]

Hours from injection (h)	Left edge of water (m)	Concentration times 10^5, at indicated lateral position (in m)										
		1.5	3.0	4.5	6.0	7.5	9.0	10.5	12	13.5	15	16.5
0.067	1.1	. . .	. . .	. . .	0.129	(*)	(*)	0.368	1.61	0.321	. . .	. . .
.270	1.1	. . .	. . .	0.0274	.764	0.330	0.0900	.249	.312	.502	. . .	. . .
.500	1.1	. . .	0.232	.126	.0965	.594	.791	.699	.190	.189	0.0856	0.228
1.13	1.1	. . .	.935	.192	1.40	1.79	.0900	.448	1.46	1.45	1.52	.482
2.00	1.1	. . .	.805	.368	.616	2.52	(*)	.783	1.96	.240	.594	(*)
3.09	1.1	. . .	.126	.225	.656	2.22	1.10	.860	1.24	.262	.176	.204
4.05	1.1	. . .	.936	.0702	1.21	4.33	.559	4.13	3.47	.567	2.32	.148
5.06	1.1	. . .	.264	.601	.690	3.38	.936	6.12	1.34	2.93	.241	.126
6.00	1.1	. . .	1.15	.180	3.17	9.84	.270	4.42	5.06	.892	1.19	.346
8.06	1.1	. . .	.121	.845	.383	11.2	(*)	6.72	2.26	2.33	.177	.204
10.0	1.1	. . .	1.51	.738	2.40	2.55	2.59	4.43	3.18	1.13	.168	2.45
12.0	1.1	. . .	.173	1.19	3.66	2.98	(*)	8.26	10.7	.445	.638	.0572
22.0	1.1	. . .	2.06	3.46	11.7	26.9	5.28	35.4	8.16	6.32	2.12	.184
34.0	1.1	. . .	3.27	6.60	25.4	69.4	13.8	62.4	7.42	2.26	(*)	.114
47.0	1.1	1.48	7.94	6.26	10.8	40.5	11.1	12.2	7.16	9.22	3.35	1.37
59.8	1.1	4.13	7.56	21.5	16.5	31.8	17.1	14.8	8.30	8.74	1.83	.693
70.7	1.1	3.48	5.70	29.4	77.0	14.5	18.0	60.1	33.2	4.34	3.30	.667
83.5	1.1	3.20	7.96	8.84	95.3	30.2	21.2	9.43	11.9	1.90	1.20	.137
95.1	1.1	2.78	22.4	9.16	17.5	114	26.4	103	7.98	4.26	.686	.269
108	1.1	8.02	5.97	54.6	29.4	153	24.8	16.9	13.0	4.88	1.77	.861

TABLE 13. — *Concentration of quartz tracers in the 0.177- to 0.250-mm sieve class in "dustpan" samples collected at cross section 90* — Continued

Hours from injection	Left edge of water	Concentration times 10^5, at indicated lateral position (in m)										
(h)	(m)	1.5	3.0	4.5	6.0	7.5	9.0	10.5	12	13.5	15	16.5
118	1.1	8.29	6.06	44.1	96.6	94.2	29.4	53.6	27.0	2.82	1.85	1.71
124	1.1	7.65	34.6	65.7	118	111	31.4	.345	23.0	.642	4.12	1.82
132	1.1	8.66	35.9	20.0	86.8	99.4	93.4	23.4	23.8	5.16	(*)	1.13
138	1.1	8.50	6.97	11.9	72.2	84.4	39.4	83.1	9.25	5.60	3.30	1.21
143	1.1	(*)	(*)	97.0	54.6	167	35.8	4.12	79.8	4.01	1.76	1.04
149	1.1	.550	8.15	25.6	58.1	132	46.3	74.4	(*)	9.40	1.82	1.71
162	1.1	(*)	5.32	14.9	39.4	191	158	31.3	24.8	15.6	3.87	1.25
193	1.5	4.41	18.7	44.3	55.9	36.2	17.6	48.1	28.1	11.2	1.59	1.46
238	.5	3.31	13.7	8.84	15.6	33.4	20.6	11.7	4.56	3.02	.408	...
285	.5	2.26	2.53	3.51	4.10	19.9	1.69	3.38	2.59	.640	.743	...
339	.5	.644	3.54	2.37	6.51	7.33	2.19	4.09	.383	.420	.0675	...
356	.3	.256	1.56	1.12	4.49	3.18	2.74	.925	.368	.546	.116	...
429	.3	.876	2.25	.630	3.08	.0182	12.2	2.58	2.58	.780	1.02	...
525	.3	1.53	2.54	4.16	2.38	7.85	1.91	1.69	1.06	.128	.0636	...
597	.3	4.69	4.34	2.62	3.75	1.27	(*)	.488	.701	.318	.666	...

TABLE 14. — *Concentration of quartz tracers in the 0.250- to 0.350-mm sieve class in "dustpan" samples collected at cross section 90*

[Leaders (. . .) indicate no sample collected at that time and lateral position; (*) indicates sample was misplaced]

Hours from injection	Left edge of water	Concentration times 10^5, at indicated lateral position (in m)										
(h)	(m)	1.5	3.0	4.5	6.0	7.5	9.0	10.5	12	13.5	15	16.5
0.067	1.1	...	...	...	0.0	(*)	(*)	0.305	0.0	0.210	...	...
.270	1.1	...	...	0.146	.600	0.098	0.0	0.323	.297	.455	...	...
.500	1.1	...	0.241	.075	.119	.203	0	.350	.177	0	0.126	0.683
1.13	1.1	...	.847	.175	.944	.117	0	0	1.10	2.29	.623	.096
2.00	1.1	...	.189	.305	0	.188	.523	.143	1.28	.176	1.64	(*)
3.09	1.1	...	0	.337	0	.062	.471	.138	0	.060	0	.631
4.05	1.1	...	2.37	.150	.472	.282	.210	1.12	.390	.221	1.03	.179
5.06	1.1	...	0	.471	0	.229	.157	.210	0	6.23	0	.484
6.00	1.1	...	.902	.170	.175	.413	.105	.474	2.04	.349	.246	.104
8.06	1.1	...	.250	.232	.085	1.02	(*)	1.10	.084	5.37	.063	.119
10.0	1.1	...	.031	.258	.100	.194	.210	.393	.318	.144	0	0
12.0	1.1	...	.260	.132	.374	.481	.157	.923	1.57	.253	.999	0
22.0	1.1	...	.605	.722	3.41	3.55	3.35	2.16	2.51	1.56	.173	.160
34.0	1.1	...	1.42	1.14	4.50	8.19	10.5	12.7	2.44	.149	(*)	.201
47.0	1.1	0.777	4.80	4.30	14.6	14.7	14.6	12.2	8.95	6.21	2.01	1.12
59.8	1.1	4.80	12.3	13.9	18.5	28.4	23.5	26.6	14.6	11.7	2.22	1.03
70.7	1.1	8.95	11.2	38.0	50.7	23.4	34.4	34.7	22.3	6.54	3.53	1.07
83.5	1.1	14.2	16.9	16.9	86.8	41.8	43.1	19.6	13.5	4.40	2.30	.868
95.1	1.1	15.4	37.0	24.9	38.7	84.0	57.3	350	20.5	12.6	1.80	1.12
108	1.1	20.2	17.1	73.6	47.5	153	77.0	31.0	23.7	6.36	3.19	1.49
118	1.1	38.0	20.8	72.9	112	133	90.9	66.6	35.7	7.84	5.64	5.48
124	1.1	33.9	76.3	106	160	90.9	84.7	.418	30.2	.228	9.78	4.09
132	1.1	28.2	69.4	43.3	88.1	119	96.5	24.6	33.5	14.4	(*)	3.50
138	1.1	43.9	31.7	28.0	136	122	51.3	96.5	21.4	13.7	9.30	5.01
143	1.1	(*)	(*)	141	93.0	165	51.6	16.2	36.9	11.9	7.91	5.25
149	1.1	3.92	42.8	67.9	129	205	103	85.4	(*)	21.2	6.61	6.86
162	1.1	(*)	22.3	38.9	61.6	192	170	52.8	39.1	28.9	13.6	5.71
193	1.5	17.0	55.0	117	158	159	105	79.1	51.2	28.2	12.7	8.54
238	.5	26.0	54.9	39.9	60.9	146	103	40.3	24.6	29.1	6.40	...
285	.5	18.3	18.3	30.3	35.0	94.4	72.9	33.7	19.8	14.9	14.4	...
339	.5	11.1	34.9	22.3	27.5	43.6	22.8	38.9	17.1	1.23	1.60	...
356	.3	11.7	16.1	14.5	43.8	24.6	30.9	14.9	8.33	3.50	1.32	...
429	.3	1.50	2.21	1.76	12.9	7.56	15.4	21.5	13.6	6.93	2.21	...
525	.3	5.36	9.51	14.0	13.9	14.2	13.7	9.16	6.36	.729	.668	...
597	.3	2.35	15.1	9.92	11.2	11.0	(*)	1.76	1.32	1.22	.847	...

TABLE 15. — *Concentration of quartz tracers in the 0.350- to 0.500-mm sieve class in "dustpan" samples collected at cross section 90*

[Leaders (. . .) indicate no sample collected at that time and lateral position; (*) indicates sample was misplaced]

Hours from injection (h)	Left edge of water (m)	Concentration times 10^5, at indicated lateral position (in m)										
		1.5	3.0	4.5	6.0	7.5	9.0	10.5	12	13.5	15	16.5
0.067	1.1	. . .	. . .	. . .	0.0	(*)	(*)	0.233	0.0	1.48	. . .	. . .
.270	1.1	. . .	. . .	0.0	1.87	0.0	0.0	.831	.411	0	. . .	. . .
.500	1.1	. . .	0.560	.956	0	0	0	1.21	0	.538	0.0	0.0
1.13	1.1	. . .	0	.640	0	.258	0	0	0	3.97	.865	0
2.00	1.1	. . .	0	2.61	0	.558	0	0	.533	.316	0	(*)
3.09	1.1	. . .	0	0	0	.714	(*)	0	0	.700	0	.549
4.05	1.1	. . .	0	0	.574	.765	1.18	.527	.614	0	.773	.213
5.06	1.1	. . .	0	2.67	0	.248	0.	.318	0	25.3	0	.480
6.00	1.1	. . .	2.54	.852	0	.243	0.	.460	0	0	0	0
8.06	1.1	. . .	0	0	.158	.611	(*)	1.28	0	9.63	0	2.26
10.0	1.1	. . .	0	0	0	0	.296	0	.721	.420	0	0
12.0	1.1	. . .	0	0	0	.586	.296	.661	1.19	0	0	0
22.0	1.1	. . .	1.38	0	.825	.350	.443	.776	.592	.402	.459	.424
34.0	1.1	. . .	0	.535	.399	1.13	1.48	1.88	.385	0	(*)	1.32
47.0	1.1	0.180	.740	.182	.926	2.05	1.48	2.09	2.05	2.44	.381	.940
59.8	1.1	2.05	5.32	4.04	2.90	5.61	5.91	5.30	2.86	6.52	2.99	.849
70.7	1.1	6.59	7.28	19.5	21.4	6.24	18.9	15.1	11.7	3.62	.926	.781
83.5	1.1	16.5	12.3	14.9	66.6	51.5	24.2	17.7	10.1	3.28	0	3.04
95.1	1.1	38.4	53.6	42.5	68.8	122	67.1	54.5	25.9	22.2	.776	3.73
108	1.1	39.7	54.3	114	61.3	159	127.	72.9	68.8	12.7	6.41	8.11
118	1.1	149	154	143	178	226	181	125.	68.7	23.8	18.3	17.2
124	1.1	136	265	194	248	141	234	0	70.9	0	19.8	12.6
132	1.1	191	257	102	165	220	179	95.8	71.6	46.4	(*)	17.3
138	1.1	307	105	73.4	266	238	112	169.	66.5	29.0	38.5	20.0
143	1.1	(*)	(*)	325	186	286	122	47.1	142	32.3	24.0	28.3
149	1.1	64.9	260	298	346	414	234	179	(*)	65.4	32.8	26.3
162	1.1	(*)	135	210	244	460	346	150	77.1	85.9	27.8	29.3
193	1.5	171.	399	448	518	453	382	359	115	107	53.7	58.0
238	.5	91.0	281	157	239	573	380	114	73.7	180	50.4	. . .
285	.5	83.3	178	189	176	540	575	202	166	93.1	83.5	. . .
339	.5	82.5	277	97.4	155	450	144	463	121	175	43.6	. . .
356	.3	74.1	110	75.6	368	138	312	119	85.0	41.4	41.9	. . .
429	.3	25.2	47.5	48.2	216	156	256	186	107	64.1	43.4	. . .
525	.3	65.0	57.5	105	84.2	192	. . .	96.1	109	39.6	12.4	. . .
597	.3	81.0	86.0	140	49.9	11.6	(*)	22.6	11.3	7.77	2.91	. . .

TABLE 16. — *Concentration of quartz tracers in the 0.500- to 0.707-mm sieve class in "dustpan" samples collected at cross section 90*

[Leaders (. . .) indicate no sample collected at that time and lateral position; (*) indicates sample was misplaced]

Hours from injection (h)	Left edge of water (m)	Concentration times 10^5, at indicated lateral position (in m)										
		1.5	3.0	4.5	6.0	7.5	9.0	10.5	12	13.5	15	16.5
0.067	1.1	. . .	. . .	. . .	0.0	(*)	(*)	0.0	0.0	0.0	. . .	. . .
.270	1.1	. . .	. . .	0.0	0	0.0	0.0	2.33	1.45	0	. . .	. . .
.500	1.1	. . .	0.0	0	0	0	0	0	0	0	0.0	0.0
1.13	1.1	. . .	0	0	0	0	0	3.07	0	2.42	0	0
2.00	1.1	. . .	0	0	0	0	(*)	0	0	0	0	(*)
3.09	1.1	. . .	0	0	0	0	0	0	0	0	0	0
4.05	1.1	. . .	0	0	0	0	0	0	0	0	0	0
5.06	1.1	. . .	0	0	0	2.84	0	0	0	54.4	0	0
6.00	1.1	. . .	0	9.06	0	0	0	0	0	0	0	0
8.06	1.1	. . .	0	0	0	0	(*)	4.08	0	20.4	0	2.90
10.0	1.1	. . .	0	0	0	0	0	0	0	2.79	0	5.79
12.0	1.1	. . .	0	0	0	3.56	0	1.58	0	0	0	0
22.0	1.1	. . .	0	0	0	0	0	1.81	0	0	0	3.82
34.0	1.1	. . .	0	0	0	1.04	0	0	0	0	(*)	0
47.0	1.1	0.0	3.18	0	0	0	0	0	0	0	2.11	0
59.8	1.1	0	0	0	2.25	0	1.45	0	0	0	6.26	0
70.7	1.1	0	0	2.11	0	3.53	1.45	0	0	2.44	5.95	0

TABLE 16. — *Concentration of quartz tracers in the 0.500- to 0.707-mm sieve class in "dustpan samples collected at cross section 90* — Continued

Hours from injection (h)	Left edge of water (m)	Concentration times 10^5, at indicated lateral position (in m)										
		1.5	3.0	4.5	6.0	7.5	9.0	10.5	12	13.5	15	16.5
83.5	1.1	0	3.29	0	21.4	3.62	3.62	0	9.53	0	0	0
95.1	1.1	18.1	3.41	13.4	3.59	30.8	17.8	2.43	2.01	20.3	2.42	0
108	1.1	43.2	26.8	30.0	24.8	63.2	54.8	48.5	57.6	6.59	9.06	36.5
118	1.1	139	78.1	43.1	53.9	15.0	89.2	125	16.5	30.2	34.5	12.5
124	1.1	101	179	124	180	62.3	208	0	79.4	0	14.7	25.0
132	1.1	109	188	151	120	181	172	103	126	29.9	(*)	0
138	1.1	454	179	157	223	151	152	146	104	21.0	42.2	60.3
143	1.1	(*)	.(*)	341	120	247	266	60.9	270	46.4	57.6	73.0
149	1.1	181	358	315	252	314	204	137	(*)	105	58.0	67.3
162	1.1	(*)	322	422	554	552	288	265	74.7	121	51.4	65.5
193	1.5	846	1510	851	971	817	(*)	418	166	147	133	184
238	.5	367	584	529	959	1150	439	420	243	356	285	...
285	.5	364	441	426	636	1400	1130	761	754	423	273	...
339	.5	298	739	258	622	1110	621	1560	775	683	290	...
356	.3	240	386	490	877	547	1100	731	447	755	222	...
429	.3	127	96.7	393	795	492	1010	609	384	311	278	...
525	.3	346	290	354	444	506	511	456	382	222	96.7	...
597	.3	246	255	254	253	467	(*)	99.7	56.5	20.4	27.9	...

TABLE 17. — *Concentration of quartz tracers in the 0.707- to 1.00-mm sieve class in "dustpan" samples collected at cross section 90*

[Leaders (. . .) indicate no sample collected at that time and lateral position; (*) indicates sample was misplaced]

Hours from injection (h)	Left edge of water (m)	Concentration times 10^5, at indicated lateral position (in m)										
		1.5	3.0	4.5	6.0	7.5	9.0	10.5	12	13.5	15	16.5
0.067	1.1	...	...	...	0.0	(*)	(*)	0.0	0.0	0.0	...	...
.270	1.1	...	...	0.0	0	0.0	0.0	0	0	0	...	...
.500	1.1	...	0.0	0	0	0	0	0	0	0	0.0	0.0
1.13	1.1	...	0	0	0	0	0	0	0	0	0	0
2.00	1.1	...	0	0	0	0	(*)	0	0	0	0	(*)
3.09	1.1	...	0	0	0	0	0	0	0	0	0	0
4.05	1.1	..	0	0	0	0	0	0	0	0	0	0
5.06	1.1	...	0	0	0	0	0	0	0	0	0	0
6.00	1.1	...	0	0	0	0	0	0	0	0	0	0
8.06	1.1	...	0	0	0	0	(*)	0	0	0	0	0
10.0	1.1	...	0	0	0	0	0	0	0	0	0	0
12.0	1.1	...	0	0	0	0	0	0	0	0	0	0
22.0	1.1	...	0	0	0	0	0	0	0	0	0	0
34.0	1.1	...	0	0	0	0	0	0	0	0	(*)	0
47.0	1.1	0.0	0	0	0	0	0	0	0	0	0	0
59.8	1.1	0	0	0	0	0	0	0	0	0	0	0
70.7	1.1	0	0	0	0	0	0	0	0	0	0	0
83.5	1.1	0	0	0	0	0	0	0	0	0	0	0
95.1	1.1	0	0	0	0	0	0	0	0	0	0	0
108	1.1	0	0	10.1	0	0	0	0	0	0	0	0
118	1.1	0	7.45	0	0	0	12.0	0	0	0	0	0
124	1.1	0	0	0	0	0	36.8	0	22.1	0	0	0
132	1.1	0	17.1	23.5	0	0	0	7.61	47.1	0	(*)	0
138	1.1	0	26.9	8.76	0	19.3	0	30.5	37.7	13.0	0	0
143	1.1	(*)	(*)	54.7	25.5	0	0	0	0	16.9	0	0
149	1.1	0	2.59	0	10.4	0	0	12.3	(*)	0	0	0
162	1.1	(*)	72.2	40.7	37.7	27.9	18.8	0	0	0	40.1	41.8
193	1.5	0	49.1	99.4	128	70.3	61.0	36.4	0	0	15.4	37.6
238	.5	200	79.2	104	83.6	147	26.3	48.9	73.2	63.8	150.	...
285	.5	132	114	113	322	312	183	349	119	215	47.0	...
339	.5	133	129	67.6	376	172	338	423	637	150	188	...
356	.3	136	194	125	122	216	207	230	157	83.6	282	...
429	.3	0	0	37.6	75.1	54.4	250	76.8	60.2	37.6	83.5	...
525	.3	75.1	167	36.2	104	83.6	33.9	0	41.7	75.2	75.2	...
597	.3	18.4	30.2	150	61.6	80.2	(*)	0	0	0	0	...

TABLE 18. — *Concentration of garnet tracers in the 0.125- to 0.177-mm sieve class in "dustpan" samples collected at cross section 90*

[Leaders (. . .) indicate no sample collected at that time and lateral position; (*) indicates sample was misplaced]

Hours from injection (h)	Left edge of water (m)	Concentration times 10^5, at indicated lateral position (in m)										
		1.5	3.0	4.5	6.0	7.5	9.0	10.5	12	13.5	15	16.5
0.067	1.1	. . .	. . .	. . .	1.96	(*)	0.152	0.0	0.0	0.0724	. . .	. . .
.270	1.1	. . .	. . .	0.0	.394	0.0	.268	.0804	0	.656	. . .	. . .
.500	1.1	. . .	0.109	0	.124	0	(*)	.116	0	.057	0.0	0.0
1.13	1.1	. . .	0	.0589	0	.0575	0	0	.0701	.262	0	0
2.00	1.1	. . .	0	.316	.275	0	.0408	0	0	.124	0	(*)
3.09	1.1	. . .	0	0	0	.0965	.118	0	0	.322	0	.0480
4.05	1.1	. . .	.134	0	.245	.115	.0680	.624	.151	0	.309	0
5.06	1.1	. . .	0	0	0	.175	.0680	1.24	.114	.335	0.	.0716
6.00	1.1	. . .	.659	0	.305	.236	.149	0	.880	.169	.266	.475
8.06	1.1	. . .	0	.682	.288	0	(*)	.404	.322	.239	(*)	.790
10.0	1.1	. . .	0	.128	1.40	0	.177	.320	.430	.327	.151	.0533
12.0	1.1	. . .	0	.371	1.66	.155	7.94	1.00	1.99	.0712	.126	0
22.0	1.1	. . .	.624	0	.970	.464	.503	5.88	2.40	7.63	1.57	0
34.0	1.1	. . .	.460	.252	2.13	1.92	1.52	5.95	1.10	.347	0	0
47.0	1.1	0.0713	.475	.217	.288	1.87	1.56	.157	0	2.66	.103	.0935
59.8	1.1	.148	1.35	2.84	.495	27.2	3.42	3.45	.831	2.88	0	.108
70.7	1.1	0	.288	7.17	11.8	1.33	3.40	6.49	6.83	1.13	.226	.0845
83.5	1.1	.996	3.33	2.27	44.6	3.23	4.92	1.41	3.59	0	.595	0
95.1	1.1	1.65	9.33	1.96	15.9	29.0	13.5	27.8	1.27	.744	.0621	.105
108	1.1	2.94	1.65	4.66	21.2	45.5	17.7	1.10	8.04	.309	.245	.0627
118	1.1	1.82	9.61	4.55	13.0	25.2	12.5	7.55	5.51	.397	.860	.358
124	1.1	4.94	24.8	22.2	46.6	6.46	19.5	0	6.03	.384	1.35	.561
132	1.1	3.35	14.4	5.74	21.0	5.45	31.5	29.9	5.40	.607	(*)	.687
138	1.1	4.85	3.63	1.01	17.2	22.0	24.5	24.6	.886	.380	.769	.112
143	1.1	*)	(*)	19.8	9.30	9.79	25.0	.815	12.8	1.08	.964	.368
149	1.1	.0715	3.83	11.1	23.6	37.1	12.8	21.8	(*)	4.94	1.53	1.80
162	1.1	(*)	8.89	18.8	16.9	60.9	42.4	4.54	6.17	7.29	1.31	.703
193	1.5	.800	7.56	35.1	21.6	5.81	22.2	4.62	4.83	1.46	1.85	2.59
238	.5	1.23	6.11	9.84	19.8	38.5	14.7	9.30	5.93	.815	.169	. . .
285	.5	2.66	2.83	7.85	3.12	6.69	17.0	3.12	1.82	1.04	2.09	. . .
339	.5	.804	10.3	1.92	12.9	8.70	3.68	10.1	.969	.994	.135	. . .
356	.3	2.69	2.04	1.43	8.62	2.58	5.82	2.28	1.44	.374	.146	. . .
429	.3	0	.238	0	2.78	3.04	8.95	5.35	2.89	0	1.94	. . .
525	.3	3.78	4.31	3.18	1.87	7.29	.907	.628	.625	.197	0	. . .
597	.3	2.45	3.44	2.22	2.76	.656	(*)	.314	.055	.111	.272	. . .

TABLE 19. — *Concentration of garnet tracers in the 0.177- to 0.250-mm sieve class in "dustpan" samples collected at cross section 90*

[Leaders (. . .) indicate no sample collected at that time and lateral position; (*) indicates sample was misplaced]

Hours from injection (h)	Left edge of water (m)	Concentration times 10^5, at indicated lateral position (in m)										
		1.5	3.0	4.5	6.0	7.5	9.0	10.5	12	13.5	15	16.5
0.067	1.1	. . .	. . .	. . .	0.121	(*)	(*)	0.314	0.379	0.139	. . .	. . .
.270	1.1	. . .	. . .	0.0	.0574	0.0326	0.0	0	.0838	.404	. . .	. . .
.500	1.1	. . .	0.0725	0	.121	.0386	.0340	.0785	0	.257	0.0	0.131
1.13	1.1	. . .	0	0.0719	.141	.0212	0	0	0	.167	.121	.151
2.00	1.1	. . .	0	.0691	.0827	.218	(*)	.0735	.108	.0676	.0531	(*)
3.09	1.1	. . .	0	.141	.0685	0	.135	0	0	.110	0	.115
4.05	1.1	. . .	.167	0	.0672	.205	0	.351	0	.188	.325	.232
5.06	1.1	. . .	0	.167	0	.185	.372	.0746	0	.459	0	.238
6.00	1.1	. . .	0	0	.173	.229	0	0	.675	.181	0	.477
8.06	1.1	. . .	.0756	.184	0	.0526	(*)	.0675	.220	.307	(*)	.154
10.0	1.1	. . .	.929	0	.348	.113	.440	.0564	.149	.304	0	1.30
12.0	1.1	. . .	0	.167	.574	0	(*)	.115	.612	0	0	.0691
22.0	1.1	. . .	.281	.153	.476	.271	.270	1.88	.430	1.71	.246	.0345

TABLE 19. — *Concentration of garnet tracers in the 0.177- to 0.250-mm sieve class in "dustpan" samples collected at cross section 90* — Continued

Hours from injection (h)	Left edge of water (m)	Concentration times 10^5, at indicated lateral position (in m)										
		1.5	3.0	4.5	6.0	7.5	9.0	10.5	12	13.5	15	16.5
34.0	1.1	...	.181	.0676	.876	1.22	.879	2.56	1.09	.869	.0475	0
47.0	1.1	0.0	1.03	.189	.418	.695	1.62	.156	.248	2.25	.515	.222
59.8	1.1	1.11	1.80	3.72	.854	8.25	.980	1.89	.247	2.48	.0436	.310
70.7	1.1	.402	.262	5.65	18.9	1.02	2.44	8.01	6.16	.245	.943	.272
83.5	1.1	.939	3.00	2.15	41.0	5.43	1.32	.971	3.44	.108	.458	.0734
95.1	1.1	3.13	18.1	3.46	4.37	18.3	.777	12.0	.991	2.77	.0299	.101
108	1.1	13.3	1.32	9.77	11.8	22.8	5.27	.911	8.23	.431	.529	.104
118	1.1	9.91	.948	12.5	10.7	46.4	5.51	17.5	12.5	.631	1.90	1.61
124	1.1	13.2	53.2	26.9	73.6	6.26	4.97	0	7.94	.232	2.96	1.02
132	1.1	28.0	20.8	6.82	18.8	4.51	52.6	11.7	9.70	1.10	(*)	.384
138	1.1	26.0	3.96	2.71	58.1	14.2	7.32	60.5	1.69	5.70	2.14	1.33
143	1.1	(*)	(*)	55.5	17.2	14.8	17.5	1.24	15.5	.628	1.37	3.05
149	1.1	.176	10.5	28.0	18.9	52.9	17.1	41.5	(*)	4.65	1.64	3.65
162	1.1	(*)	8.41	10.2	7.49	132.	45.6	3.11	11.0	18.1	2.61	1.88
193	1.5	4.14	20.8	38.6	40.7	14.1	3.62	28.6	10.0	4.82	1.56	7.53
238	.5	2.53	7.19	19.0	11.4	79.1	8.62	31.8	10.0	3.08	1.24	...
285	.5	6.24	3.77	7.89	4.84	31.8	18.5	5.57	3.19	4.25	1.34	...
339	.5	1.68	40.4	1.81	17.8	29.0	9.40	1.69	5.32	6.99	.0845	...
356	.3	4.60	2.46	2.45	25.8	8.98	19.7	1.95	1.34	1.79	.272	...
429	.3	.0748	.815	.118	5.10	.136	5.44	16.2	1.51	2.04	1.56	...
525	.3	5.66	5.29	7.76	3.88	18.0	1.76	1.42	2.58	.0964	0	...
597	.3	16.7	12.3	3.04	5.00	1.24	(*)	0	1.97	.0579	.704	...

TABLE 20. — *Concentration of garnet tracers in the 0.250- to 0.350-mm sieve class in "dustpan" samples collected at cross section 90*

[Leaders (. . .) indicate no sample collected at that time and lateral position; (*) indicates sample was misplaced]

Hours from injection (h)	Left edge of water (m)	Concentration times 10^5, at indicated lateral position (in m)										
		1.5	3.0	4.5	6.0	7.5	9.0	10.5	12	13.5	15	16.5
0.067	1.1	...	...	...	0.0	(*)	(*)	0.409	0.0	0.562	...	...
.270	1.1	...	...	0.410	0	0.0	0.0	1.41	.314	1.46	...	...
.500	1.1	...	0.0646	0	0	.0544	0	.358	0	.260	0.102	1.46
1.13	1.1	...	0	0	.108	0	0	0	0	1.39	0	.461
2.00	1.1	...	0	1.07	0	.0336	0	0	0	.161	0	
3.09	1.1	...	0	.840	0	0	0	0	0	.192	0	.291
4.05	1.1	...	.0976	.0603	.0819	.113	0	.284	0	.124	0	.575
5.06	1.1	...	0	.496	0	0	0	.474	0	1.69	0	1.43
6.00	1.1	...	.241	0	0	.189	0	0	.393	.161	0	.668
8.06	1.1	...	.100	.745	.0289	.161	(*)	.785	0	2.18	(*)	.573
10.0	1.1	...	0	.118	.0537	0	0	0	0	.116	0	0
12.0	1.1	...	0	.212	.0860	.0595	0	0	.0934	.0815	0	0
22.0	1.1	...	0	.105	.518	.0971	.505	.231	.403	.407	0	.257
34.0	1.1	...	.0603	.174	.0602	.491	.252	1.15	.549	.786	0	0
47.0	1.1	0.156	1.11	.197	.540	.570	.756	.548	.228	1.71	1.03	.406
59.8	1.1	1.05	1.01	1.68	.157	1.67	.0841	.296	.173	.904	.0650	.824
70.7	1.1	.483	.390	4.83	5.92	.578	.336	2.03	2.61	.337	1.49	.164
83.5	1.1	.423	1.43	.898	4.49	2.46	1.68	.366	.929	.336	.0925	0
95.1	1.1	1.23	5.92	1.99	1.79	8.62	2.02	31.7	.825	1.14	.115	.0785
108	1.1	27.4	6.85	10.9	6.21	38.2	2.95	2.05	3.88	.246	.556	0
118	1.1	29.8	2.55	11.6	11.2	71.3	23.0	21.9	8.92	1.95	4.09	2.96
124	1.1	23.9	70.1	32.5	73.9	9.28	3.52	.0841	5.72	.0735	5.48	.918
132	1.1	101	44.5	6.14	7.95	31.8	23.2	2.88	5.75	2.26	(*)	.293
138	1.1	88.6	9.21	4.34	104	22.6	8.27	48.0	2.58	1.08	2.87	3.44
143	1.1	(*)	(*)	64.6	22.8	21.2	8.61	.571	2.89	.312	.773	4.22
149	1.1	2.72	16.6	34.9	32.2	166	31.9	22.5	(*)	8.99	2.22	6.22
162	1.1	(*)	20.7	25.6	20.1	179	59.5	2.30	17.8	30.2	6.15	5.33
193	1.5	19.4	55.6	102	31.8	44.3	11.0	6.00	16.7	29.7	3.41	13.9
238	.5	1.69	14.5	25.5	20.6	83.0	7.74	57.6	9.42	9.56	2.35	...
285	.5	11.0	7.04	10.3	7.89	70.4	9.60	12.4	5.34	15.0	2.76	...
339	.5	5.21	69.2	1.93	19.4	8.31	11.0	118	24.0	13.7	.387	...
356	.3	11.7	3.53	8.27	73.8	11.6	83.2	2.85	4.84	6.41	.529	...
429	.3	0	4.96	.651	28.8	6.23	34.2	60.9	1.24	5.46	1.66	...
525	.3	13.5	7.12	10.5	8.10	33.6	3.28	9.11	12.2	.318	.602	...
597	.3	9.52	23.2	4.19	5.98	5.42	(*)	.153	3.70	.400	1.64	...

TABLE 21. — *Concentration of garnet tracers in the 0.350- to 0.500-mm sieve class in "dustpan" samples collected at cross section 90*

[Leaders (. . .) indicate no sample collected at that time and lateral position; (*) indicates sample was misplaced]

Hours from injection (h)	Left edge of water (m)	Concentration times 10^5, at indicated lateral position (in m)										
		1.5	3.0	4.5	6.0	7.5	9.0	10.5	12	13.5	15	16.5
0.067	1.1	...	...	...	0.0	(*)	(*)	1.73	0.0	1.83	...	...
.270	1.1	...	...	0.497	0	0.0	0.0	1.37	1.29	0	...	...
.500	1.1	...	0.0	0	0	0	0	.374	0	0	0.0	0.437
1.13	1.1	...	0	0	0	0	0	0	0	4.26	0	.883
2.00	1.1	...	0	0	0	.230	0	0	0	0	0	(*)
3.09	1.1	...	0	3.27	0	0	(*)	0	0	.520	0.	.681
4.05	1.1	...	0	0	0	0	0	0	0	0	.497	.264
5.06	1.1	...	0	2.46	0	.154	0	1.18	0	4.47	0	.594
6.00	1.1	...	0	0	0	0	0	0	0	0	0	.835
8.06	1.1	...	0	3.99	0	0	(*)	.529	0	5.15	(*)	0
10.0	1.1	...	0	0	0	0	0	0	0	.520	0	0
12.0	1.1	...	0	0	0	0	.183	0	0	0	0	0
22.0	1.1	...	0	0	0	0	.336	.384	0	.497	0	.525
34.0	1.1	...	0	.331	0	0	0	.466	0	.358	0	0
47.0	1.1	0.0	.306	0	0	0	0	0	.636	0	0	0
59.8	1.1	2.54	.732	0	0	0	.183	0	1.18	.368	0	5.25
70.7	1.1	0	.376	0	1.19	.350	.366	1.09	.383	0	1.15	0
83.5	1.1	2.04	.424	0	1.61	4.08	0	0	0	0	0	0
95.1	1.1	1.06	1.52	.560	1.23	1.43	2.56	.595	.254	0	0	.924
108	1.1	17.8	7.29	8.80	1.30	12.3	35.1	1.35	6.38	0	0	0
118	1.1	28.0	17.8	6.38	16.7	31.8	28.9	18.3	5.11	0	9.08	4.60
124	1.1	47.3	54.0	20.2	37.9	4.06	79.0	0	9.60	0	0	.782
132	1.1	221	84.3	0	5.10	13.6	27.8	2.28	3.15	1.17	(*)	0
138	1.1	143	8.58	2.45	86.9	25.6	8.90	34.8	3.43	1.66	5.47	8.84
143	1.1	(*)	(*)	63.8	23.1	9.87	4.51	.921	15.5	1.39	1.75	5.01
149	1.1	44.0	38.0	44.6	94.2	170	32.7	17.2	(*)	10.4	3.66	8.69
162	1.1	(*)	42.8	59.6	23.6	199	37.7	2.53	12.2	35.4	.259	5.99
193	1.5	89.5	115	178	112	11.2	41.1	15.7	16.9	43.6	7.49	26.9
238	.5	7.52	54.6	46.0	87.7	68.2	19.6	40.4	6.92	14.1	8.65	...
285	.5	13.3	8.36	23.3	11.6	63.6	9.60	11.1	24.5	31.9	7.00	...
339	.5	5.67	24.4	5.76	41.4	26.1	34.0	167	83.7	160.	3.14	...
356	.3	21.8	25.6	15.6	102	29.2	142	7.20	7.49	17.8	2.47	...
429	.3	3.05	19.3	2.62	66.7	35.9	314	123	7.79	13.1	4.04	...
525	.3	28.4	10.2	24.0	7.68	57.5	(*)	4.91	33.0	0	1.81	...
597	.3	57.2	40.4	79.7	8.13	25.9	(*)	.181	1.37	0	2.88	...

TABLE 22. — *Concentration of garnet tracers in the 0.500- to 0.707-mm sieve class in "dustpan" samples collected at cross section 90*

[Leaders (. . .) indicate no sample collected at that time and lateral position; (*) indicates sample was misplaced]

Hours from injection (h)	Left edge of water (m)	Concentration times 10^5, at indicated lateral position (in m)										
		1.5	3.0	4.5	6.0	7.5	9.0	10.5	12	13.5	15	16.5
0.067	1.1	...	...	...	0.0	(*)	(*)	0.0	0.0	0.0	...	...
.270	1.1	...	...	0.0	0	0.0	0.0	1.97	1.19	0	...	...
.500	1.1	...	0.0	0	0	0	0	0	0	3.34	0.0	2.72
1.13	1.1	...	0	0	0	0	(*)	0	0	1.59	0	0
2.00	1.1	...	0	0	0	0	(*)	0	0	0	0	(*)
3.09	1.1	...	0	0	0	0	(*)	0	0	.348	0	0
4.05	1.1	...	0	0	0	11.0	0	0	0	.993	0	0
5.06	1.1	...	0	0	0	0	0	2.58	0	29.7	0	0
6.00	1.1	...	0	0	0	0	(*)	0	0	0	0	0
8.06	1.1	...	0	0	0	0	(*)	0	0	8.18	0	0
10.0	1.1	...	0	0	0	0	0	0	0	0	0	0
12.0	1.1	...	0	0	0	0	(*)	0	0	0	0	0
22.0	1.1	...	0	0	0	0	0	0	0	0	0	0
34.0	1.1	...	0	0	0	0	0	0	0	1.39	(*)	0
47.0	1.1	0.0	0	0	0	0	0	0	0	0	0	0
59.8	1.1	0	0	0	0	0	0	0	0	0	0	0
70.7	1.1	0	0	0	0	0	0	0	0	0	0	0
83.5	1.1	0	0	0	0	0	.891	0	0	0	0	0

TABLE 22. — *Concentration of garnet tracers in the 0.500- to 0.707-mm sieve class in "dustpan" samples collected at cross section 90* — Continued

Hours from injection (h)	Left edge of water (m)	Concentration times 10^5, at indicated lateral position (in m)										
		1.5	3.0	4.5	6.0	7.5	9.0	10.5	12	13.5	15	16.5
95.1	1.1	0	0	0	0	1.26	3.56	0	0	0	0	0
108	1.1	0	0	0	0	0	2.67	0	0	0	0	0
118	1.1	1.00	1.12	0	0	0	0.	0	0	0	0	0
124	1.1	3.28	11.1	2.22	2.52	0	9.50	0	2.82	0	0	0
132	1.1	6.14	8.79	0	1.43	0	3.30	2.29	0	0	(*)	0
138	1.1	3.48	1.27	0	17.3	2.13	0	1.36	2.38	2.22	0	0
143	1.1	(*)	(*)	6.75	0	2.71	0	0	0	0	0	2.06
149	1.1	0	13.8	9.01	0	15.1	0	0	(*)	0	0	0
162	1.1	(*)	6.44	14.5	0	41.1	0	2.77	0	13.2	0	3.58
193	1.5	2.30	20.9	33.9	10.6	.86	(*)	4.02	12.4	0	0	2.32
238	.5	3.30	35.4	8.56	26.2	4.65	2.67	4.76	3.06	3.43	0	...
285	.5	3.29	0	9.38	10.0	20.1	4.16	21.7	0	42.9	0	...
339	.5	0	15.4	1.30	17.2	1.69	14.6	83.6	90.5	42.5	6.06	...
356	.3	10.7	5.66	25.1	12.7	11.3	26.4	1.72	4.95	164.	4.79	...
429	.3	0	0	0	6.86	11.0	85.0	11.3	2.16	0	13.8	...
525	.3	10.2	1.83	1.49	11.1	5.82	7.12	0	16.2	8.25	0	...
597	.3	6.86	14.1	1.75	3.09	4.23	(*)	0	0	0	0	...

TABLE 23. — *Concentration of monazite tracers in the 0.125- to 0.177-mm sieve class in "dustpan" samples collected at cross section 90*

[Leaders (. . .) indicate no sample collected at that time and lateral position; (*) indicates sample was misplaced]

Hours from injection (h)	Left edge of water (m)	Concentration times 10^5, at indicated lateral position (in m)										
		1.5	3.0	4.5	6.0	7.5	9.0	10.5	12	13.5	15	16.5
0.067	1.1	...	...	...	0 146	(*)	0.147	0.109	0.0	0.209	...	...
.270	1.1	...	...	0.0	.285	0.114	.129	0	.172	.316	...	...
.500	1.1	...	0.0	0	.119	.358	(*)	0	0	.110	0.0	0.0
1.13	1.1	...	0	.0568	.168	.895	.0655	.388	.270	.0504	.0950	0
2.00	1.1	...	0	.244	.925	1.13	.956	.0824	.336	.120	.265	(*)
3.09	1.1	...	0	.244	0	1.11	.916	.771	.257	.543	0	0
4.05	1.1	...	0	.0779	.590	1.33	1.85	1.80	1.46	.382	0	.0799
5.06	1.1	...	0	.452	.431	2.71	2.33	1.72	.220	.859	0	.138
6.00	1.1	...	0	0	.235	1.83	2.46	.324	2.79	.285	0	.0762
8.06	1.1	...	.441	.304	.830	6.94	(*)	2.08	.414	.507	0	0
10.0	1.1	...	0	.0616	.416	1.57	2.45	.771	.580	.504	.292	.154
12.0	1.1	...	.889	1.07	.659	2.02	7.99	2.01	12.3	0	0	0
22.0	1.1	...	.240	1.42	6.16	13.8	9.89	20.1	4.40	46.9	.151	.0573
34.0	1.1	...	2.26	5.75	3.87	18.9	27.8	23.4	1.22	.802	(*)	0
47.0	1.1	0.137	10.0	1.33	8.53	42.2	22.0	7.73	3.12	15.3	2.68	.676
59.8	1.1	1.07	6.24	22.2	10.4	140	32.6	20.9	5.46	32.1	.264	1.47
70.7	1.1	3.92	7.49	45.0	94.3	19.9	104	48.3	42.0	2.15	3.82	.978
83.5	1.1	2.88	13.4	16.6	324	41.4	79.5	7.17	10.9	.835	1.25	.185
95.1	1.1	12.9	55.2	8.13	156	171	112	113	10.9	15.9	.0599	.0508
108	1.1	30.7	8.72	19.2	77.5	326	128	15.1	47.0	2.76	1.30	.362
118	1.1	15.0	66.3	18.1	23.8	441	147	64.5	21.0	1.62	6.39	1.44
124	1.1	17.4	96.5	87.3	209	225	154	0	18.2	.148	9.66	1.35
132	1.1	42.6	79.4	16.4	55.1	115	124	92.5	18.8	8.66	(*)	1.40
138	1.1	51.8	29.4	17.4	131	220	68.4	129	13.2	4.33	7.32	3.94
143	1.1	(*)	(*)	83.5	74.8	176	100	5.50	49.0	9.55	4.08	5.54
149	1.1	.595	50.0	63.0	108	380	58.7	168	(*)	9.88	19.1	6.66
162	1.1	(*)	26.2	39.3	188	749	138	14.7	36.3	52.9	6.89	7.82
193	1.5	15.8	49.7	257	169	130	109	112.	47.8	15.9	7.34	13.9
238	.5	12.4	31.4	44.5	94.2	292	107	27.8	19.6	4.47	3.37	...
285	.5	14.5	11.5	28.1	14.5	113	82.9	12.9	3.73	10.4	2.80	...
339	.5	3.33	92.9	3.71	35.5	50.9	12.9	66.0	5.90	5.50	.0652	...
356	.3	15.5	6.90	12.4	45.7	10.1	38.7	6.35	2.43	4.40	.565	...
429	.3	.131	1.73	.434	14.7	24.3	71.9	47.6	2.52	7.31	5.93	...
525	.3	15.9	38.2	21.5	10.8	61.5	5.40	4.94	4.04	.190	.0757	...
597	.3	22.0	27.4	10.3	16.1	15.4	(*)	.857	1.10	.644	.436	...

TABLE 24. — *Concentration of monazite tracers in the 0.177- to 0.250-mm sieve class in "dustpan" samples collected at cross section 90*

[Leaders (. . .) indicate no sample collected at that time and lateral position; (*) indicates sample was misplaced]

Hours from injection (h)	Left edge of water (m)	Concentration times 10^5, at indicated lateral position (in m)										
		1.5	3.0	4.5	6.0	7.5	9.0	10.5	12	13.5	15	16.5
0.067	1.1	. . .	. . .	. . .	0.0	(*)	(*)	0.0	0.0	0.0	. . .	. . .
.270	1.1	. . .	. . .	0.0476	.0532	0.0	0.0	0	0	0	. . .	. . .
.500	1.1	. . .	0.0	.0311	0	.221	.0313	0	0	0	0.0	0.0
1.13	1.1	. . .	0	0	.0870	.0979	0	0	.0358	.0324	0	0
2.00	1.1	. . .	.133	0	0	.121	(*)	0	.100	.167	.0491	(*)
3.09	1.1	. . .	0	0	0	0	.0940	0	0	0	.153	.0356
4.05	1.1	. . .	0	0	.124	.128	.0626	.0466	0	.0580	.151	.0860
5.06	1.1	. . .	0	0	.114	.0287	.0940	.0691	.0764	.340	0	0
6.00	1.1	. . .	.0803	0	.0806	.382	0	.0439	.248	.240	.0824	0
8.06	1.1	. . .	.490	.113	.0606	.292	(*)	.0902	.220	.189	0	.213
10.0	1.1	. . .	0	0	0	0	.0940	.156	.0693	0	.0581	.142
12.0	1.1	. . .	.200	.0516	0	.0749	(*)	.159	.243	0	.0529	.0320
22.0	1.1	. . .	.209	.0707	.588	1.43	.439	1.20	.266	2.80	.0380	.0320
34.0	1.1	. . .	.139	.188	.609	2.54	4.79	4.47	.254	0	(*)	0
47.0	1.1	0.0624	.914	.342	1.12	4.56	0	1.01	.316	1.63	.106	.358
59.8	1.1	.586	1.71	1.78	3.28	9.76	2.54	2.47	1.65	4.47	.161	.488
70.7	1.1	.858	1.57	6.05	20.1	3.41	6.41	8.62	7.13	.282	.765	.504
83.5	1.1	1.04	2.85	3.69	49.7	10.2	4.64	3.52	3.91	1.20	.359	.112
95.1	1.1	8.65	20.8	4.82	17.7	51.0	8.30	12.3	5.17	8.22	.0764	0
108.	1.1	20.3	7.08	6.94	19.2	45.6	42.1	6.64	10.7	.732	.666	.145
118.	1.1	11.0	4.05	6.16	8.08	232.	40.6	16.2	13.0	.365	2.15	.727
124.	1.1	12.3	62.6	27.3	69.2	44.1	35.8	0.	5.19	0	4.05	.548
132.	1.1	37.9	24.3	13.3	17.4	54.8	59.1	10.4	7.85	1.92	(*)	.499
138.	1.1	38.0	9.26	8.08	47.4	104.	20.5	65.0	6.45	1.45	2.51	1.33
143.	1.1	(*)	(*)	42.3	21.5	66.9	20.4	2.14	22.2	1.74	1.44	2.98
149.	1.1	.767	18.3	37.2	21.8	85.0	17.6	49.2	(*)	3.52	1.10	3.43
162.	1.1	(*)	10.6	12.9	29.6	286.	43.5	4.33	9.96	24.4	3.31	2.63
193.	1.5	11.9	27.8	66.1	130.	141.	32.5	94.8	22.2	8.34	2.37	9.80
238.	.5	4.79	6.29	20.7	19.1	162.	21.0	31.2	11.6	2.46	2.16	. . .
285.	.5	8.98	4.54	10.1	6.53	41.7	41.1	6.79	1.96	8.22	1.74	. . .
339.	.5	2.72	36.1	1.72	13.5	28.2	11.8	43.6	6.91	8.46	.274	. . .
356.	.3	6.04	4.60	5.52	27.0	6.22	22.1	1.76	1.77	2.14	.100	. . .
429.	.3	0.276	1.16	.219	6.75	7.12	13.2	25.5	2.48	1.53	1.22	. . .
525.	.3	7.06	13.9	18.7	5.98	25.0	2.13	1.40	3.32	.0446	0	. . .
597.	.3	5.09	15.6	3.98	6.01	4.57	(*)	.318	.870	.165	.507	. . .

TABLE 25. — *Concentration of monazite tracers in the 0.250- to 0.350-mm sieve class in "dustpan" samples collected at cross section 90*

[Leaders (. . .) indicate no sample collected at that time and lateral position. (*) indicates sample was misplaced.]

Hours from injection (h)	Left edge of water (m)	Concentration times 10^5, at indicated lateral position (in m)										
		1.5	3.0	4.5	6.0	7.5	9.0	10.5	12	13.5	15	16.5
0.067	1.1	. . .	. . .	. . .	0.0	(*)	(*)	0.0980	0.0	0.0	. . .	. . .
.270	1.1	. . .	. . .	0.210	0	0.0631	0.0	.177	0	.438	. . .	. . .
.500	1.1	. . .	0.0	0	.114	0	0	0	0	0	0.0	0.146
1.13	1.1	. . .	0	0	0	.0281	0	0	0	.286	0	0
2.00	1.1	. . .	0	0	0	.0401	.100	0	0	.0483	0	(*)
3.09	1.1	. . .	0	0	0	0	0	0	0	.230	0	0
4.05	1.1	. . .	.234	0	.0980	0	0	.453	0	0	0	.0688
5.06	1.1	. . .	0	0	0	0	0	0	0	0	0	.311
6.00	1.1	. . .	0	0	0	.170	0	0	0	0	0	0
8.06	1.1	. . .	.120	.0743	0	.0772	(*)	.117	0	.208	0	.228
10.0	1.1	. . .	0	0	0	.0621	0	.0840	0	.138	0	0
12.0	1.1	. . .	0	0	0	0	0	0	0	0	.550	0
22.0	1.1	. . .	0	0	.124	0	0	0	0	.244	0	0
34.0	1.1	. . .	0	0	.0720	.220	0	.106	.109	0	(*)	0
47.0	1.1	0.0	.221	0	0	.546	0	.220	.182	.256	.0945	0
59.8	1.1	0	.161	.530	.0938	.802	.100	.236	0	.360	0	0
70.7	1.1	.434	.389	1.52	2.06	.794	1.11	.914	.380	.100	.170	.392
83.5	1.1	0	.465	.293	3.45	.654	.805	.525	.929	0	.111	0

TABLE 25. — *Concentration of monazite tracers in the 0.250- to 0.350-mm sieve class in "dustpan" samples collected at cross section 90* — Continued

Hours from injection (h)	Left edge of water (m)	Concentration times 10^5, at indicated lateral position (in m)										
		1.5	3.0	4.5	6.0	7.5	9.0	10.5	12	13.5	15	16.5
95.1	1.1	2.30	2.77	2.16	3.58	8.44	9.85	6.32	1.56	1.43	.0692	0
108	1.1	9.45	8.49	2.82	5.17	12.9	36.9	1.44	5.10	.359	.133	0
118	1.1	9.50	4.74	3.49	5.36	123	34.7	11.3	5.69	0	2.05	.637
124	1.1	15.4	42.9	14.9	24.9	9.15	49.6	0	3.57	0	1.81	.458
132	1.1	47.1	15.5	6.83	3.31	30.0	10.8	2.92	4.72	1.95	(*)	.177
138	1.1	40.5	13.1	4.00	37.4	43.5	12.6	18.8	4.83	1.19	1.68	.858
143	1.1	(*)	(*)	20.3	10.1	35.6	8.66	1.27	2.95	.467	.694	3.11
149	1.1	2.52	12.1	19.4	38.6	121	11.0	23.0	(*)	3.55	.880	2.85
162	1.1	(*)	20.2	21.8	27.8	125	14.6	1.25	7.47	16.7	1.95	3.71
193	1.5	33.8	18.2	45.2	7.67	64.8	14.7	29.4	11.9	18.0	1.05	7.11
238	.5	1.31	4.77	19.4	15.1	57.5	14.4	30.8	9.09	6.03	2.13	...
285	.5	10.0	3.45	17.6	5.16	30.6	10.6	12.1	3.84	13.4	2.00	...
339	.5	3.40	27.5	1.70	11.1	20.1	8.80	50.0	14.5	19.5	.386	...
356	.3	6.35	4.97	7.41	34.1	14.5	31.7	1.40	2.02	3.40	0	...
429	.3	.152	1.34	.425	10.9	9.10	59.1	33.9	.989	2.99	1.28	...
525	.3	5.49	7.70	10.7	3.16	3.32	2.92	2.00	5.07	.255	.0801	...
597	.3	14.3	13.2	2.80	4.90	7.11	(*)	0	.170	0	.368	

TABLE 26. — *Concentration of monazite tracers in the 0.350- to 0.500-mm sieve class in "dustpan" samples collected at cross section 90*

[Leaders (. . .) indicate no sample collected at that time and lateral position; (*) indicates sample was misplaced]

Hours from injection (h)	Left edge of water (m)	Concentration times 10^5, at indicated lateral position (in m)										
		1.5	3.0	4.5	6.0	7.5	9.0	10.5	12	13.5	15	16.5
0.067	1.1	...	...	...	0.0	(*)	(*)	0.0	0.0	0.0	...	...
.270	1.1	...	...	0.0	0	0.0	0.0	0	0	0	...	...
.500	1.1	...	0.0	0	0	0	0	0	0	0	0.0	0.726
1.13	1.1	...	0	0	0	0	0	0	0	.221	0	0
2.00	1.1	...	0	2.69	0	0	0	0	0	.325	0	(*)
3.09	1.1	...	0	0	0	0	(*)	0	0	1.73	0	0
4.05	1.1	...	0	0	0	0	0	0	0	.597	0	.440
5.06	1.1	...	0	0	0	0	0	.328	0	0	0	0
6.00	1.1	...	0	0	0	0	0	0	0	0	0	0
8.06	1.1	...	0	1.32	0	0	(*)	0	0	.535	0	0
10.0	1.1	...	0	0	0	0	0	0	0	0	0	0
12.0	1.1	...	0	0	0	0	0	0	0	0	0	0
22.0	1.1	...	0	0	0	0	.609	0	0	0	0	0
34.0	1.1	...	0	0	0	0	0	0	0	0	(*)	0
47.0	1.1	0.0	.509	0	0	.264	0	0	0	0	0	0
59.8	1.1	4.23	0	0	0	0	.304	0	0	0	1.03	0
70.7	1.1	0	0	0	1.32	0	0	0	0	0	0	0
83.5	1.1	0	0	.460	1.08	0	0	0	0	0	0	0
95.1	1.1	2.93	1.81	0	5.44	11.3	3.35	1.97	0	2.33	0	0
108	1.1	6.80	22.9	5.27	8.64	9.04	49.2	5.05	3.03	0	0	0
118	1.1	15.5	28.3	10.6	20.1	66.5	42.3	15.9	5.66	0	3.78	3.82
124	1.1	61.6	74.6	16.9	34.0	9.54	128	0	12.4	0	3.20	0
132	1.1	209	66.0	5.49	5.08	27.3	26.7	10.9	6.07	7.77	(*)	1.02
138	1.1	155	3.77	5.00	51.2	48.4	46.2	24.8	13.3	2.06	7.44	4.40
143	1.1	(*)	(*)	51.3	24.5	20.0	20.0	2.04	9.96	2.62	4.36	7.54
149	1.1	12.2	32.6	82.5	42.7	204	36.9	12.2	(*)	16.2	8.69	2.85
162	1.1	(*)	131.	166.	79.6	224	27.5	3.36	18.3	38.7	.430	3.12
193	1.5	182	92.3	105.	290.	14.5	33.2	57.2	16.4	51.1	2.77	19.9
238	.5	13.4	26.0	71.0	81.2	20.4	18.2	52.4	15.7	13.4	16.5	...
285	.5	17.5	21.7	45.2	11.9	22.4	14.3	29.1	20.4	40.1	19.7	...
339	.5	14.5	15.4	10.4	37.4	54.8	57.1	104	105	86.2	1.05	...
356	.3	38.8	36.8	50.2	48.7	55.2	120.	5.71	10.5	19.7	4.11	...
429	.3	0	6.11	1.74	44.8	60.6	28.2	92.5	1.85	14.8	6.71	...
525	.3	20.2	19.0	30.4	12.8	24.2	(*)	28.6	25.2	1.32	3.01	...
597	.3	35.1	25.9	53.6	19.9	23.5	(*)	.664	0	0	0	...

TABLE 27. — *Concentration of monazite tracers in the 0.500- to 0.707-mm sieve class in "dustpan" samples collected at cross section 90*

[Leaders (. . .) indicate no sample collected at that time and lateral position; (*) indicates sample was misplaced]

Hours from injection (h)	Left edge of water (m)	Concentration times 10^5, at indicated lateral position (in m)										
		1.5	3.0	4.5	6.0	7.5	9.0	10.5	12	13.5	15	16.5
0.067	1.1	. . .	. . .	. .	0.0	(*)	0.0	0.0	0.0	0.0	. . .	. . .
.270	1.1	. . .	. . .	0.0	0	0.0	0	0	0	0	. . .	. . .
.500	1.1	. . .	0.0	0	0	0	0	0	0	0	0.0	0.0
1.13	1.1	. . .	0	0	0	0	0	0	0	0	0	0
2.00	1.1	. . .	0	0	0	0	0	0	0	0	0	(*)
3.09	1.1	. . .	0	0	0	0	0	0	0	.677	0	0
4.05	1.1	. . .	0	0	0	0	0	0	0	0	0	0
5.06	1.1	. . .	0	0	0	0	0	2.52	0	0	0	0
6.00	1.1	. . .	0	0	0	0	0	0	0	0	0	0
8.06	1.1	. . .	0	0	0	0	(*)	0	0	0	0	0
10.0	1.1	. . .	0	0	0	0	0	0	0	0	0	0
12.0	1.1	. . .	0	0	0	0	0	0	0	0	0	0
22.0	1.1	. . .	0	0	0	0	0	0	0	0	0	0
34.0	1.1	. . .	0	0	0	0	0	0	0	0	(*)	0
47.0	1.1	0.0	0	0	0	0	0	0	0	0	0	0
59.8	1.1	0	0	0	0	0	0	0	0	0	0	0
70.7	1.1	0	0	0	0	0	0	0	0	0	0	0
83.5	1.1	0	0	0	0	0	1.73	0	0	0	0	0
95.1	1.1	0	0	2.37	5.71	4.89	2.88	0	0	0	0	0
108	1.1	0	64.1	3.41	3.03	3.86	5.30	0	9.14	0	0	0
118	1.1	44.4	19.6	6.41	9.77	15.2	3.40	0	6.55	0	0	0
124	1.1	48.0	112	0	58.6	3.54	160	0	5.49	0	0	19.9
132	1.1	230	81.1	0	1.39	21.8	32.0	8.91	12.5	20.4	(*)	13.1
138	1.1	230	69.3	12.6	62.5	31.0	18.6	26.4	13.0	0	0	0
143	1.1	(*)	(*)	50.6	19.1	33.2	41.5	2.77	0	2.73	0	0
149	1.1	0	0	114	25.7	185	16.2	3.74	(*)	0	0	41.2
162	1.1	(*)	189	120	73.4	305	56.0	5.39	0.	6.42	0	34.7
193	1.5	576	148	122	550	64.0	(*)	50.8	24.0	77.8	4.71	31.5
238	.5	51.3	77.4	216	272	27.1	10.9	46.3	41.6	34.8	94.5	. . .
285	.5	51.3	37.6	81.9	9.68	44.6	16.1	77.3	93.8	134	57.2	. . .
339	.5	39.0	52.2	7.14	118.	56.0	89.5	330	440	206	23.6	. . .
356	.3	49.4	101	260	58.5	20.4	146	23.2	57.6	212	9.30	. . .
429	.3	0	19.2	0	60.0	35.6	666	110.	8.42	54.9	53.6	. . .
525	.3	26.4	10.7	0	7.20	31.0	12.1	149.	40.5	16.0	0	. . .
597	.3	35.4	32.2	74.6	36.1	49.4	(*)	0	0	0	0	. . .

TABLE 28. — *Concentration of lead tracers in the 0.125- to 0.177-mm sieve class in "dustpan" samples collected at cross section 90*

[Leaders (. . .) indicate no sample collected at that time and lateral position; (*) indicates sample was misplaced]

Hours from injection (h)	Left edge of water (m)	Concentration times 10^5, at indicated lateral position (in m)										
		1.5	3.0	4.5	6.0	7.5	9.0	10.5	12	13.5	15	16.5
0.067	1.1	. . .	. . .	. . .	0.424	(*)	0.0	0.0	0.0	0.0	. . .	. . .
.270	1.1	. . .	. . .	0.0	0	0.0	0	0	0	0	. . .	. . .
.500	1.1	. . .	0.0	0	0	0	(*)	.652	0	0	0.0	0.0
1.13	1.1	. . .	0	0	0	0	0	0	0	1.17	0	0
2.00	1.1	. . .	0	0	0	0	0	0	0	0	0	(*)
3.09	1.1	. . .	0	0	0	0	0	0	0	0	0	0
4.05	1.1	. . .	0	0.227	0	0	0	0	0	0	0	0
5.06	1.1	. . .	0	0	0	0	0	.385	0	2.10	0	0
6.00	1.1	. . .	0	0	0	0	0	0	0	0	0	0
8.06	1.1	. . .	0	0	0	0	(*)	.377	0	.403	0	0
10.0	1.1	. . .	0	0	0	0	0	0	0	0	0	1.64
12.0	1.1	. . .	0	0	0	0	0	0	0	0	0	0
22.0	1.1	. . .	0	0	0	0	0	0	0	0	0	0
34.0	1.1	. . .	0	0	0	0	0	0	0	0	(*)	0
47.0	1.1	0.199	0	0	0	0	0	0	0	.266	0	0
59.8	1.1	0	0	0	0	.846	0	0	0	0	0	0
70.7	1.1	0	0	0	0	0	0	0	0	0	0	.711
83.5	1.1	.465	0	0	0	0	0	0	0	0	0	0

TABLE 28. — *Concentration of lead tracers in the 0.125- to 0.177-mm sieve class in "dustpan" samples collected at cross section 90* — Continued

Hours from injection (h)	Left edge of water (m)	Concentration times 10^6, at indicated lateral position (in m)										
		1.5	3.0	4.5	6.0	7.5	9.0	10.5	12	13.5	15	16.5
95.1	1.1	0	0	0	0	0	0	0	0	0	0	0
108	1.1	0	0	0	0	7.06	0	0	0	0	0	0
118	1.1	0	0	0	0	0	0	0	0	0	0	0
124	1.1	.476	6.10	0	0	0	0	0	0	0	0	0
132	1.1	0	0	0	0	0	0	3.70	0	0	0	0
138	1.1	0	0	0	0	0	.618	0	0	.177	0	0
143	1.1	(*)	(*)	0	.984	0	0	.254	0	0	0	0
149	1.1	0	0	.363	.846	0	1.33	0	(*)	.425	0	0
162	1.1	(*)	0	0	0	26.6	1.67	0	0	0	0	0
193	1.5	.372	2.47	1.69	0	0	.501	0	32.0	148.	11.9	67.1
238	.5	0	0	0	.597	0	1.27	0	.544	0	0	...
285	.5	0	0	0	0	0	.459	0	0	0	0	...
339	.5	0	2.22	.317	0	0	0	0	0	0	.189	...
356	.3	0	0	.200	0	0	0	0	0	0	0	...
429	.3	0	0	0	0	0	2.05	10.2	0	0	0	...
525	.3	0	0	0	.169	0	0	0	0	0	0	...
597	.3	0	0	0	.258	0	(*)	0	0	.312	0	...

TABLE 29. — *Concentration of lead tracers in the 0.177- to 0.250-mm sieve class in "dustpan" samples collected at cross section 90*

[Leaders (. . .) indicate no sample collected at that time and lateral position; (*) indicates sample was misplaced]

Hours from injection (h)	Left edge of water (m)	Concentration times 10^6, at indicated lateral position (in m)										
		1.5	3.0	4.5	6.0	7.5	9.0	10.5	12	13.5	15	16.5
0.067	1.1	...	...	...	0.0	(*)	(*)	0.0	0.0	0.0	...	...
.270	1.1	...	...	0.0	0	0.0	0.0	0	0	0	...	
.500	1.1	...	0.0	0	0	0	0	0	0	0	0.0	0.0
1.13	1.1	...	0	0	0	0	0	0	0	.358	0	0
2.00	1.1	...	0	0	0	0	0	0	0	0	0	(*)
3.09	1.1	...	0	0	0	0	0	0	0	0	0	0
4.05	1.1	...	0	0	0	0	0	0	0	0	0	0
5.06	1.1	...	0	0	0	0	0	0	0	.944	0	0
6.00	1.1	...	0	0	0	0	0	0	0	0	0	0
8.06	1.1	...	0	0	0	0	(*)	0	0	.395	0	0
10.0	1.1	...	0	0	0	0	0	0	0	0	0	.493
12.0	1.1	...	0	0	0	0	0	0	0	0	0	0
22.0	1.1	...	0	0	0	0	0	0	0	0	0	0
34.0	1.1	...	0	0	0	0	0	0	0	0	(*)	0
47.0	1.1	0.0	0	0	0	0	0	0	0	0	0	0
59.8	1.1	0	0	0	0	0	0	0	0	0	0	0
70.7	1.1	0	0	0	0	0	0	0	0	0	0	0
83.5	1.1	0	0	0	0	0	0	.109	0	0	0	0
95.1	1.1	.141	0	0	0	0	0	0	0	0	0	0
108	1.1	0	.110	.536	0	0	0	0	0	0	0	0
118	1.1	(*)	0	0	0	0	0	0	0	0	0	0
124	1.1	0	9.09	0	0	0	0	0	0	0	0	0
132	1.1	0	0	0	.967	0	0	0	0	0	0	0
138	1.1	.249	0	0	0	0	0	0	0	0	0	0
143	1.1	(*)	(*)	0	0	0	0	0	0	0	0	0
149	1.1	0	0	0	0	0	.489	0	(*)	.119	0	0
162	1.1	(*)	0	0	0	16.0	0	0	0	0	0	0
193	1.5	0	33.2	4.73	0	0	0	0	434.	12.0	87.5	4.85
238	.5	0	0	0	0	3.83	0	0	0	0	0	...
285	.5	0	0	0	0	7.49	6.00	0	0	0	0	...
339	.5	0	2.00	0	.167	.584	.136	0	0	0	0	...
356	.3	0	0	0	0	0	0	0	0	0	0	...
429	.3	0	0	0	0	0	0	1.68	0	0	0	...
525	.3	0	.105	0	0	.498	.260	0	0	0	0	...
597	.3	0	0	0	0	0	(*)	0	0	0	0	...

TABLE 30. — *Concentration of lead tracers in the 0.250- to 0.350-mm sieve class in "dustpan" samples collected at cross section 90*

[Leaders (. . .) indicate no sample collected at that time and lateral position; (*) indicates sample was misplaced]

Hours from injection (h)	Left edge of water (m)	Concentration times 10^5, at indicated lateral position (in m)										
		1.5	3.0	4.5	6.0	7.5	9.0	10.5	12	13.5	15	16.5
0.067	1.1	. . .	. . .	. . .	0.0	(*)	(*)	0.0	0.0	0.0	. . .	. . .
.270	1.1	. . .	. . .	0.0	0	0.0	0.0	0	0	0	. . .	. . .
.500	1.1	. . .	0.0	0	0	0	0	0	0	0	0.0	0.0
1.13	1.1	. . .	0	0	0	0	0	0	0	.334	0	0
2.00	1.1	. . .	0	0	0	0	0	0	0	0	0	(*)
3.09	1.1	. . .	0	0	0	0	0	0	0	0	0	0
4.05	1.1	. . .	0	0	0	0	0	0	0	0	0	0
5.06	1.1	. . .	0	0	0	0	0	0	0	.785	0	0
6.00	1.1	. . .	0	0	0	0	0	0	0	0	0	0
8.06	1.1	. . .	0	0	0	0	. . .	0	0	.134	0	0
10.0	1.1	. . .	0	0	0	0	0	0	0	0	0	.276
12.0	1.1	. . .	0	0	0	0	0	0	0	0	0	0
22.0	1.1	. . .	0	0	0	0	0	0	0	0	0	0
34.0	1.1	. . .	.140	0	0	0	0	0	0	0	(*)	0
47.0	1.1	0.0	0	0	0	0	0	.143	0	0	0	0
59.8	1.1	0	0	0	0	0	0	0	0	0	0	0
70.7	1.1	0	0	0	0	0	0	0	0	0	0	0
83.5	1.1	0	0	0	0	0	0	0	0	0	0	0
95.1	1.1	0	0	0	0	0	.196	0	0	0	0	0
108	1.1	0	0	0	0	0	.391	0	0	0	0	0
118	1.1	0	0	0	0	0	.391	0	0	0	0	0
124	1.1	0	0	0	0	0	1.56	0	0	0	0	0
132	1.1	0	0	0	0	0	0	0	0	0	0	0
138	1.1	0	0	0	0	0	0	0	0	0	0	0
143	1.1	(*)	(*)	0	0	0	0	0	0	0	0	0
149	1.1	0	0	0	0	0	0	0	(*)	0	0	0
162	1.1	(*)	0	0	0	37.0	0	0	0	0	0	0
193	1.5	0	2.05	6.19	0	0	.586	0	2.62	218	.510	16.6
238	.5	0	0	0	0	0	1.37	.352	0	0	0	. . .
285	.5	0	0	0	0.	4.37	0	0	0	0	0	. . .
339	.5	0	0	0	0	0	0	1.90	0	.243	0	. . .
356	.3	0	0	0	0	.440	0	0	.156	.339	0	. . .
429	.3	0	0	.137	0	0	7.24	7.74	.480	0	0	. . .
525	.3	0	0	0	0	3.70	0	0	0	0	0	. . .
597	.3	0	0	0	0	0	(*)	0	0	0	0	. . .

TABLE 31. — *Concentration of lead tracers in the 0.350- to 0.500-mm sieve class in "dustpan" samples collected at cross section 90*

[Leaders (. . .) indicate no sample collected at that time and lateral position; (*) indicates sample was misplaced]

Hours from injection (h)	Left edge of water (m)	Concentration times 10^5, at indicated lateral position (in m)										
		1.5	3.0	4.5	6.0	7.5	9.0	10.5	12	13.5	15	16.5
0.067	1.1	. . .	. . .	. . .	0.0	(*)	(*)	0.0	0.0	0.0	. . .	. . .
.270	1.1	. . .	. . .	0.0	0	0.0	0.0	0	0	0	. . .	. . .
.500	1.1	. . .	0.0	0	0	0	0	0	0	0	0.0	0.0
1.13	1.1	. . .	0	0	0	0	0	0	0	.749	0	0
2.00	1.1	. . .	0	0	0	0	0	0	0	0	0	(*)
3.09	1.1	. . .	0	0	0	0	(*)	0	0	0	0	0
4.05	1.1	. . .	0	0	0	0	0	0	0	0	0	0
5.06	1.1	. . .	0	0	0	0.	0	0	0	4.18	0	0
6.00	1.1	. . .	0	0	0	0	0	0	0	0	0	0
8.06	1.1	. . .	0	0	0	0	(*)	0	0	0	0	0
10.0	1.1	. . .	0	0	0	0	0	0	0	0	0	0
12.0	1.1	. . .	0	0	0	0	0	0	0	0	0	0
22.0	1.1	. . .	0	0	0	0	0	0	0	0	0	0
34.0	1.1	. . .	0	0	0	0	0	0	0	0	(*)	0
47.0	1.1	0.0	0	0	0	0	0	0	0	0	0	0
59.8	1.1	0	0	0	0	0	0	0	0	0	0	0
70.7	1.1	0	0	0	0	0	0	0	0	0	0	0
83.5	1.1	0	0	0	0	0	0	0	0	0	0	0

TABLE 31. — *Concentration of lead tracers in the 0.350- to 0.500-mm sieve class in "dustpan" samples collected at cross section 90* — Continued

Hours from injection (h)	Left edge of water (m)	Concentration times 10^5, at indicated lateral position (in m)										
		1.5	3.0	4.5	6.0	7.5	9.0	10.5	12	13.5	15	16.5
95.1	1.1	0	0	0	0	0	0	0	0	0	0	0
108	1.1	0	0	0	0.	0	1.03	0	0	0	0	0
118	1.1	0	0	0	0	0	0	0	0	0	0	0
124	1.1	0	0	0.	0	0	1.37	0	0	0	0	0
132	1.1	0	0	0	0	0	1.02	0	0	0	0	0
138	1.1	0	0	0	0	0	0	0	0	0	0	0
143	1.1	(*)	(*)	0	0	0	0	0	0	0	0	0
149	1.1	0	0	0	0	0	0	0	(*)	0	0	0
162	1.1	(*)	0	1.33	0	0	0	0	0	0	0	0
193	1.5	0	4.53	15.1	0	0	0	0	5.28	260	0	13.7
238	.5	0	0	0	0	6.56	0	0	0	0	0	...
285	.5	0	0	0	0	C	.304	0	0	0	0	...
339	.5	0	1.58	0	0	0	0	0	1.17	0	0	...
356	.3	0	0	0	0	.750	0	0	0	0	0	...
429	.3	0	0	0	0	0	17.8	4.17	0	0	0	...
525	.3	0	0	0	0	2.00	(*)	0	5.85	0	0	...
597	.3	0	0	0	0	0	(*)	0	0	0	0	...

TABLE 46. — *Concentrations of fluorescent tracers for different minerals and sieve classes in core samples collected on May 8*

[Leaders (...) indicate no sample collected at that time and lateral position. (*) indicates sample was misplaced.]

Cross section (m)	Concentration times 10^5									
	Quartz						Lead			
	0.125 - 0.177	0.177 - 0.250	0.250 - 0.350	0.350 - 0.500	0.500 - 0.707	0.707 - 1.00	0.125 - 0.177	0.177 - 0.250	0.250 - 0.350	0.350 - 0.500
7.5	17.5	26.7	70.1	439	1140	411	165	38.4	28.7	41.0
15	27.0	33.9	68.7	320	783	200	131	33.6	19.1	20.7
30	17.8	28.3	60.6	249	719	124	32.6	10.9	5.94	4.75
60	20.6	23.8	45.5	155	294	74.0	5.88	2.57	3.76	1.20
90	22.1	33.4	39.0	92.6	117	16.9	1.15	.478	1.15	.411
180	18.4	20.0	14.3	1.62	1.22	0	.489	.142	.107	.0602
270	16.8	12.4	1.64	.340	.140	.592	.172	.240	.0666	.0282
360	15.1	9.82	.676	.621	.650	.927	.959	.314	.171	.333
450	15.4	8.52	.390	.372	.964	.369	.210	.220	.0973	.130
540	14.0	3.17	.605	.713	.385	.878	.140	.0832	.0378	.0383

Cross section (m)	Concentration times 10^5									
	Garnet					Monazite				
	0.125 - 0.177	0.177 - 0.250	0.250 - 0.350	0.350 - 0.500	0.500 - 0.707	0.125- 0.177	0.177- 0.250	0.250- 0.350	0.350- 0.500	0.500- 0.707
7.5	11.7	33.3	67.2	134	25.9	91.2	41.3	27.6	102	88.9
15	15.7	36.8	74.9	93.1	28.5	82.3	40.7	31.3	76.0	68.4
30	10.2	28.4	34.2	46.2	13.2	68.4	38.0	16.8	40.0	52.1
60	12.4	17.0	29.6	31.2	5.71	55.0	23.3	14.5	32.0	35.7
90	6.91	12.1	21.0	17.1	2.64	33.0	14.0	16.6	15.1	15.0
180	2.92	2.62	.912	.139	.343	14.4	3.01	.191	.0902	.114
270	1.19	.519	.349	.223	.319	4.25	.399	.109	.0956	0
360	2.12	.402	.255	.294	.243	3.47	.495	.653	.294	1.17
450	.418	.342	.284	.233	.996	1.41	.258	.790	.922	.158
540	.448	.344	.515	.744	.670	1.70	1.36	.187	.859	.502

TABLE 47. — *Concentrations of fluorescent tracers for different minerals and sieve classes in core samples collected on June 6*

Cross section (m)	Concentration times 10^5									
	Quartz						Lead			
	0.125-0.177	0.177-0.250	0.250-0.350	0.350-0.500	0.500-0.707	0.707-1.00	0.125-0.177	0.177-0.250	0.250-0.350	0.350-0.500
30	4.95	4.12	3.64	12.0	52.2	10.2	139	309	101	72.7
60	1.59	2.06	3.84	24.4	107	36.8	58.3	38.2	10.1	6.05
90	6.37	4.82	5.52	30.8	99.2	26.5	10.4	4.99	2.62	1.64
120	3.18	2.46	4.66	29.5	102	19.1	3.20	.260	.293	.446
150	2.76	4.60	9.92	72.0	267	58.8	1.67	1.00	.338	1.03
180	4.03	3.47	7.84	60.5	185	59.9	1.79	1.05	1.36	.618
210	.759	2.22	9.44	74.0	176	34.2	.128	1.20	2.01	1.58
240	.629	1.64	8.68	51.5	156	24.4	.415	.0629	.0258	.0228
270	1.08	2.32	13.3	82.4	183	41.6	.305	.113	.0365	.319
300	1.16	2.19	11.1	72.1	130	25.7	.309	.154	.143	.0803
330	1.90	3.45	13.9	72.7	99.2	12.1	.277	.130	.0573	0
360	2.78	3.67	14.7	48.2	63.1	5.10	.394	.0576	.0295	0
390	.874	2.80	15.5	51.8	58.3	8.40	.284	.0116	.0285	.195
420	2.19	4.20	15.5	42.7	24.3	3.02	.0348	.0102	0	0
450	1.18	4.40	18.7	39.9	45.5	1.22	.339	.106	.0572	.0360
480	1.42	4.19	13.1	14.5	4.83	.870	.254	.0431	0	.0446
510	1.56	6.19	12.8	9.60	2.52	0	.303	.0536	.117	0
540	1.37	3.96	12.5	18.4	.877	0	.103	.156	0	0
570	2.21	6.14	10.1	10.7	.325	0	.0570	0	.0609	0
600	2.02	3.32	6.56	2.41	.660	0	.269	.0357	.0742	0
630	2.57	4.51	4.68	1.82	.960	0	.0888	.0335	0	.0919
660	2.70	5.79	5.64	.457	.559	0	.0728	.0104	.0145	.0525
690	1.25	4.57	3.88	.300	.181	0	.124	.0208	0	.0370
720	2.49	3.39	2.57	.223	1.66	1.59	.0815	.0332	.0158	0
750	1.40	4.56	2.80	.535	.385	0	.0463	.111	0	0
780	1.72	8.07	3.24	.268	.295	0	.0337	.646	0	0
810	1.44	3.54	2.25	.478	.440	0	.0590	.0431	.0958	.0368
840	1.35	3.49	1.50	.370	.447	0	.0408	0	0	0
870	1.41	3.02	.923	.194	.183	0	.0874	.0118	0	0

Cross section (m)	Concentration times 10^5									
	Garnet					Monazite				
	0.125-0.177	0.177-0.250	0.250-0.350	0.350-0.500	0.500-0.707	0.125-0.177	0.177-0.250	0.250-0.350	0.350-0.500	0.500-0.707
30	1.70	2.75	6.47	9.18	2.47	8.13	6.37	5.48	14.7	13.1
60	1.69	3.91	5.86	15.1	4.95	17.0	8.08	5.14	21.3	31.1
90	4.13	7.98	10.1	18.0	3.63	26.6	11.6	7.01	16.6	20.6
120	1.70	2.75	5.91	13.6	3.43	12.9	5.57	3.33	12.8	11.1
150	2.54	6.03	11.7	30.7	12.7	22.4	10.8	8.55	27.4	38.2
180	2.95	7.78	17.2	27.5	8.99	18.9	12.9	10.9	25.8	
210	2.86	8.00	16.7	30.2	4.94	23.5	11.9	10.3	24.3	24.4
240	1.43	4.16	4.62	10.7	11.1	11.4	7.49	5.20	10.7	19.2
270	1.98	4.25	8.92	13.0	1.94	15.5	7.26	4.30	8.93	14.1
300	1.17	3.29	7.17	9.94	2.90	11.2	5.60	4.18	11.0	6.39
330	2.12	5.86	8.49	8.69	.406	15.1	8.51	6.08	9.08	4.46
360	1.95	5.61	9.04	8.51	.224	18.5	9.22	4.80	8.58	7.68
390	2.04	4.96	6.88	5.88	.476	12.2	6.52	3.33	4.62	1.53
420	3.76	7.82	8.22	4.31	.458	23.1	8.74	2.93	2.92	2.66
450	2.44	4.50	4.90	2.50	3.44	14.9	5.36	2.32	1.41	2.51
480	1.71	2.25	2.08	1.85	.214	9.72	3.62	.866	.398	.627
510	2.88	2.18	4.28	.669	.166	9.20	2.68	4.80	.543	.322
540	1.64	2.26	2.09	.965	0	11.3	3.25	.626	.150	.275
570	2.34	1.39	1.28	1.68	0	9.56	2.16	.606	.298	0
600	.958	1.06	.630	.436	0	4.38	.834	.144	.129	.902
630	1.83	1.49	.877	.666	.134	7.30	1.74	.0974	.142	.260
660	1.76	.981	.890	.304	.109	5.79	.981	.142	.0746	0
690	.786	.660	.352	.0716	.0889	4.36	.654	.0369	.0794	0
720	.942	.451	.379	.106	.437	3.03	.309	.122	0	.203
750	.983	.890	.593	.364	0	2.49	.416	.0879	.177	0

TABLE 47. — *Concentrations of fluorescent tracers for different minerals and sieve classes in core samples collected on June 6* — Continued

Cross section (m)	Concentration times 10^5									
	Garnet					Monazite				
	0.125-0.177	0.177-0.250	0.250-0.350	0.350-0.500	0.500-0.707	0.125-0.177	0.177-0.250	0.250-0.350	0.350-0.500	0.500-0.707
780	1.20	.753	.443	0	.228	4.20	.646	.0580	0	.442
810	1.49	.515	.407	.279	.438	5.18	.266	.108	.0398	.851
840	1.41	.685	.274	.0679	0	2.14	.216	.0373	.0183	0
870	.386	.723	.112	.0363	0	1.31	.172	.0177	0	0

TABLE 48. — *Concentrations of fluorescent tracers for different minerals and sieve classes in core samples collected on July 14*

Cross section (m)	Concentration times 10^5									
	Quartz						Lead			
	0.125-0.177	0.177-0.250	0.250-0.350	0.350-0.500	0.500-0.707	0.707-1.00	0.125-0.177	0.177-0.250	0.250-0.350	0.350-0.500
30	1.03	1.59	2.54	17.0	70.0	18.8	30.3	10.7	1.94	0.562
90	.867	1.42	4.28	24.2	67.8	19.1	14.8	6.37	2.93	1.45
150	.502	.805	2.17	12.4	48.6	20.0	.178	.105	.0758	.144
210	1.60	3.40	8.05	19.2	61.6	13.9	.545	.392	.853	.679
270	.369	1.14	3.94	34.3	113	28.6	.218	.0618	.0815	.0653
330	.359	.597	4.64	40.7	122	24.3	.0578	.115	0	.0484
390	1.37	1.00	5.84	49.8	154	40.8	.493	.115	.0665	.0398
450	.415	.796	4.50	43.8	133	17.7	.207	.160	.155	.354
510	.688	2.17	8.26	48.0	95.0	18.6	.390	.130	.102	.128
570	.559	2.05	9.72	51.0	96.5	17.6	.245	.255	.478	0
630	.559	1.57	7.56	34.8	45.8	6.49	.416	.118	.0660	.132
690	.285	1.59	7.84	30.9	24.8	6.82	.112	.0071	.0684	.197
750	1.30	3.06	14.8	30.8	19.1	1.97	.856	.347	.534	.305
810	.356	2.27	10.7	17.7	10.3	2.72	.0523	.0545	.0255	.0313
870	.615	1.71	6.63	9.92	3.51	.585	.0333	.0303	.0853	.0363

Cross section (m)	Concentration times 10									
	Garnet					Monazite				
	0.125-0.177	0.177-0.250	0.250-0.350	0.350-0.500	0.500-0.707	0.125-0.177	0.177-0.250	0.250-0.350	0.350-0.500	0.500-0.707
30	4.23	3.39	4.98	7.92	8.24	6.25	3.13	2.23	5.05	9.95
90	1.66	3.89	9.64	14.6	2.86	15.4	5.91	5.73	14.1	19.0
150	.450	1.07	2.52	4.99	.942	3.36	1.83	1.54	5.48	7.97
210	1.13	2.74	5.56	14.8	4.17	6.37	4.11	3.74	12.0	8.22
270	1.36	4.40	7.81	15.2	4.94	13.4	5.17	4.36	11.8	18.4
330	.848	2.03	5.58	11.5	2.59	9.33	3.43	3.63	10.7	9.98
390	1.43	3.34	7.81	13.2	1.94	12.1	4.57	4.25	8.69	12.6
450	.915	3.14	6.64	14.4	3.62	9.19	5.01	4.77	12.3	11.9
510	1.44	3.48	4.48	7.47	2.98	8.46	3.18	2.02	4.93	4.47
570	1.40	3.72	6.35	8.12	1.39	8.38	3.92	2.56	4.20	4.31
630	.832	1.53	2.10	3.56	1.46	4.87	2.17	1.40	2.47	.782
690	.884	2.74	3.47	3.50	.416	7.81	3.07	1.39	1.38	.875
750	2.68	4.94	4.83	6.24	1.74	14.8	5.57	2.22	1.69	.252
810	1.16	2.29	2.04	1.14	.0895	7.36	2.40	.992	.746	.899
870	.791	1.24	1.23	1.17	1.30	6.40	1.10	.668	.281	0

★U.S. Government Printing Office: 1978-777-102/25